



## REMERCIEMENTS

L'achèvement de ce travail mené sur plusieurs années m'a procuré une grande satisfaction. Il est l'occasion de se remémorer les différentes embûches qu'il a fallu surmonter mais surtout les personnes qui m'ont permis d'en arriver là, ma gratitude et mes remerciements vont :

A mon promoteur le Professeur Frédéric Vanden Eynden, pour son soutien et son aide. Je suis ravi de travailler en sa compagnie car outre son appui scientifique, il a toujours été présent pour me soutenir et me conseiller au cours de l'élaboration de cette thèse.

A mon co-promoteur, le Professeur Phillippe van de Borne pour sa disponibilité, sa rigueur et sa précision dans ce travail.

A ma présidente du comité d'accompagnement, La Professeur Kathleen Mc Entee qui m'a ouvert les portes du royaume de son laboratoire.

Au Professeur Guido Van Nooten avec qui j'ai commencé mes travaux de recherches.

Aux membres du jury qui ont accepté de juger ce travail de thèse.

Aux donateurs : le Fonds pour la chirurgie cardiaque, la Fondation Emile Saucez-René Van Poucke, ayant permis la réalisation de ce projet.

Aux collaborateurs scientifiques qui ont contribué à cet effort au travers de discussions, d'aide techniques, de dosages biologique, et par leur soutien : Professeur Laurence Dewachter, Docteur Constantin Stefanidis, Docteur Géraldine Hubesch, Docteur Antoine Herpain, Docteur Filippo Anoni, Madame Pascale Jaspers et le Professeur Christian Mélot.

A mes très chers parents, pour leur amour.

A mon épouse Nana, à mes filles Yasmine, Line et Rama pour leurs encouragements, soutiens inconditionnels tout au long de ce périple et cela malgré les difficultés.

## GLOSSARY

AHF	Acute Heart Failure
AR	Aortic regurgitation
Ca <sup>2+</sup>	Calcium
CO	Cardiac Output
DBP	Diastolic Blood Pressure
DT	Diastolic Time
EF	Ejection Fraction
FS	Fractional Shortening
HF	Heart Failure
O <sub>2</sub>	Oxygen
OM	Omecamtiv Mecarbil
PEP	Pre-ejection Period
PHT	Pressure Half Time
PWT	Posterior Wall Thickness
RAS	Renin Angiotensin System
ROS	Reactive Oxygen Species
RWT	Relative Wall Thickness
SBP	Systolic Blood Pressure
ST	Systolic Time
SWT	Septal Wall Thickness
SV	Stroke Volume
LV	Left Ventricle
LVEF	Left Ventricular Ejection Fraction
LVEDV	Left Ventricle End Diastolic Volume
LVESV	Left Ventricle End Systolic Volume
LVESD	Left Ventricle End Systolic Diameter
LVEDD	Left Ventricle End Diastolic Diameter
LVET	Left Ventricle Ejection Time

# TABLE OF CONTENTS

<b>GLOSSARY</b> .....	<b>3</b>
<b>RESUME</b> .....	<b>7</b>
<b>ABSTRACT</b> .....	<b>9</b>
<b>LIST OF FIGURES</b> .....	<b>10</b>
<b>LIST OF TABLES</b> .....	<b>13</b>
<b>1. INTRODUCTION</b> .....	<b>14</b>
1.1 AORTIC VALVE .....	14
1.1.1 <i>Anatomy structure and function</i> .....	14
1.1.2 <i>Aortic valve regurgitation</i> .....	15
1.1.2.1 Definition .....	15
1.1.2.2 Epidemiology .....	16
1.1.2.3 Etiology .....	17
1.1.2.4 Pathophysiology .....	18
1.1.2.5 Natural history and treatments .....	20
1.1.2.6 Treatments .....	21
1.2 EXPERIMENTAL AORTIC REGURGITATION .....	23
1.3 OMECANTIV MECARBIL .....	25
1.3.1 <i>Background</i> .....	25
1.3.2 <i>Pharmacodynamics and pharmacokinetics</i> .....	28
1.3.3 <i>Bioenergetic aspects</i> .....	30
1.3.4 <i>Clinical efficacy</i> .....	31
1.4 CARDIAC BIOMARKERS .....	33
1.4.1 <i>N-terminal pro-B-type natriuretic peptide (NT-proBNP)</i> .....	33
1.4.2 <i>Soluble suppression of tumorigenicity 2 (also called interleukin 1 receptor-like 1; sST2)</i> .....	33
1.5 LEFT VENTRICULAR GENE EXPRESSION PROFILE .....	35
1.5.1 <i>Apoptosis and oxidative stress determinants</i> .....	35
1.5.1.1 Mitochondrial members Bax and Bcl-2 .....	35
1.5.1.2 Biomarkers of oxidative stress .....	35
1.5.2 <i>Molecules implicated in energy substrate use</i> .....	36
1.5.2.1 AMPK, PPAR $\alpha$ , and PPAR $\gamma$ .....	36
1.5.2.2 Glucose transporters Glut1 and Glut4 .....	37
1.5.2.3 PDK4 and CPT1 .....	38
1.5.2.4 CD36, Lox 1, and ALOX15 .....	39
1.5.3 <i>Vasoactive determinants</i> .....	40
1.5.3.1 Angiotensin receptors AT1 and AT2 .....	40
1.5.3.2 ACE1 and ACE2 .....	41
1.5.3.3 eNOS and iNOS .....	41
1.5.3.4 Kallikrein-kinin signalling .....	42
1.5.3.5 Bradykinin receptors .....	43
1.5.3.6 Calcium-dependent myocardial contraction .....	44
<b>2. GENERAL HYPOTHESIS AND AIMS OF THE RESEARCH WORK</b> .....	<b>46</b>
<b>3. METHODS</b> .....	<b>49</b>
3.1 EFFECTS OF OMECANTIV MECARBIL ON CARDIAC FUNCTION, AORTIC REGURGITATION AND LV WALL STRESS IN AN EXPERIMENTAL RAT'S MODEL .....	49
3.1.1 <i>Experimental animals</i> .....	49

3.1.2 Anesthesia and surgical procedure.....	50
3.1.3 Cardiac measurements.....	50
3.1.4 Calculation of wall stress variables.....	52
3.1.5 Invasive blood pressure measurement.....	52
3.1.6 Experimental design.....	53
3.1.7 Statistical analyses.....	53
3.2 EFFECTS OF OMECAMTIV MECARBIL AND AORTIC REGURGITATION ON CARDIAC BIOMARKERS IN AN EXPERIMENTAL RAT MODEL.....	54
3.2.1 Study protocol.....	54
3.2.2 Study Design.....	54
3.2.3 Measurements of plasma levels of sST2 and NT-proBNP.....	55
3.2.4 Statistical analysis.....	56
3.3 EFFECTS OF OMECAMTIV MECARBIL AND AORTIC REGURGITATION ON LEFT VENTRICLE IN AN EXPERIMENTAL RAT'S MODEL.....	56
3.3.1 Protocol and experimental design.....	57
3.3.2 Real-time quantitative polymerase chain reaction (RTq-PCR).....	57
3.3.3 Statistical analysis.....	63
<b>4. RESULTS.....</b>	<b>64</b>
4.1 EFFECTS OF AR ON RATS LEFT VENTRICLE, CARDIAC BIOMARKERS AND LV GENES EXPRESSION.....	64
4.1.1 AR and LV measurements.....	64
4.1.2 AR effects on wall stress and blood pressure.....	67
4.1.3 Effects of AR on cardiac biomarkers.....	67
4.1.3.1 Plasma NT-proBNP levels in rats with AR.....	67
4.1.3.2 Plasma sST2 levels in rats with AR.....	68
4.1.4 Effects of AR in rats LV genes expression.....	71
4.1.4.1 AR and LV expression of genes regulating apoptosis and oxidative stress.....	71
4.1.4.2 AR impacted LV expression profile of key determinants of cardiac energy substrate use.....	73
4.1.4.3 AR altered LV expression of genes implicated in cardiac contractility.....	75
4.2 EFFECTS OF OM AND PLACEBO ON LV RATS WITH AR.....	76
4.2.1 Effects of placebo in rats with AR.....	76
4.2.2 Effects of OM rat with AR.....	79
4.2.3 Effects of OM compared with placebo rats with AR.....	80
4.2.4 effects of OM in sham-operated rats.....	84
4.3 EFFECTS OF OM AND PLACEBO ON CARDIAC BIOMARKERS.....	85
4.3.1 Effects of OM and placebo on plasma NT-proBNP levels.....	85
4.3.2 Effects of OM and placebo on plasma sST2 levels.....	86
4.4 OM AND LV GENES EXPRESSION.....	87
4.4.1 OM and LV Expression of Genes Regulating Apoptosis and Oxidative Stress.....	87
4.4.2 OM and LV Expression of genes determinants of Cardiac Energy Substrate Use.....	88
4.4.3 OM and LV Expression of Genes Implicated in Cardiac Contractility.....	91
<b>5. GENERAL DISCUSSION.....</b>	<b>93</b>
5.1 EFFECT OF AR ON CARDIAC FUNCTION.....	93
5.2 EFFECT OF OM ON AR AND WALL STRESS.....	95
5.3 EFFECT OF OM ON CARDIAC FUNCTION.....	96
5.4 THE DIFFERENTIAL RESPONSE OF CARDIO BIOMARKERS TO OM IN EXPERIMENTAL MODEL OF AR.....	99
5.5 OM AND LV RAT'S GENE EXPRESSION.....	102
5.6 COMBINED VOLUME AND PRESSURE OVERLOAD AND LV RAT'S GENE EXPRESSION.....	107
5.7 LIMITATIONS OF THE STUDIES AND PERSPECTIVES.....	110
<b>6. CONCLUSION.....</b>	<b>111</b>

<b>7. REFERENCES .....</b>	<b>112</b>
<b>8. APPENDIX A.....</b>	<b>142</b>
.....	143
.....	145
.....	146
<b>9. APPENDIX B.....</b>	<b>151</b>
.....	152
.....	153
.....	154
.....	155
.....	156
.....	157
<b>10. APPENDIX C.....</b>	<b>161</b>
.....	162
.....	164
.....	166
.....	167
<b>11. APPENDIX D.....</b>	<b>169</b>
.....	171
.....	173
.....	174
.....	177
.....	179
.....	180
.....	181
<b>12. APPENDIX E.....</b>	<b>184</b>
<b>LIST OF PUBLICATIONS .....</b>	<b>209</b>

## RESUME

La régurgitation aortique est une pathologie valvulaire caractérisée par une mal coaptation d'une ou de plusieurs cuspidés aortiques. Le résultat est un reflux du sang de l'aorte vers le ventricule gauche avec une surcharge de volume et de pression. En phase aiguë en présence d'une fuite aortique massive, le ventricule gauche évolue rapidement vers une défaillance terminale. Cependant en présence d'une fuite sévère, le ventricule s'adapte chroniquement par une série de mécanismes compensatoires : par l'augmentation de sa masse, du diamètre de la chambre de chasse et par une hypertrophie ventriculaire gauche. Cette dernière facilite la réduction de la tension pariétale résultante de la surcharge en pression et en volume afin finalement de réduire la consommation en oxygène. L'évolution est marquée par une détérioration progressive de la fonction ventriculaire qui en l'absence de traitement évolue vers l'insuffisance cardiaque. Le seul traitement actuel de la régurgitation aortique est le traitement chirurgical. À l'heure actuelle, il y a plusieurs drogues utilisées dans le traitement de l'insuffisance cardiaque mais leur point commun est la modification de l'homéostasie calcique, l'augmentation de la consommation d'oxygène avec un risque d'augmenter les arythmies, la morbidité et la mortalité. L'omecantiv mecarbil est un activateur sélectif de la myosine cardiaque et est une nouvelle drogue en phase d'études cliniques pour son potentiel rôle dans le traitement l'insuffisance cardiaque systolique. Il active spécifiquement l'ATPase myocardique et améliore l'utilisation de l'énergie cardiaque. Il augmente le taux de libération de phosphate de la myosine, une fois que la myosine est liée à l'actine, elle reste liée beaucoup plus longtemps en présence d'omecantiv mecarbil. Le résultat est une amélioration de la fonction systolique en augmentant la durée d'éjection systolique sans consommer plus d'énergie d'ATP, d'oxygène ou altérer les niveaux de calcium intracellulaire entraînant une amélioration globale de l'efficacité cardiaque. Nous avons évalué les effets de l'omecantiv mecarbil sur le ventricule gauche des rats avec ou sans régurgitation aortique (régurgitation aortique créée chirurgicalement) ainsi que les effets de la régurgitation aortique sur le ventricule gauche en mesurant différents marqueurs de la fonction cardiaque tels que les paramètres échocardiographiques, les paramètres hémodynamiques et électrocardiographiques, les dosages de biomarqueurs sériques, l'analyse tissulaire au niveau du ventricule gauche de l'expressions des gènes impliqués dans le stress oxydatif, l'apoptose, le métabolisme énergétique ainsi que dans l'homéostasie calcique impliquée dans la contractilité cardiaque. Ces paramètres ont été investigués chez des rats mâles adultes de type Wistar qui ont reçu de l'omecantiv mecarbil par voie intraveineuse fémorale et de rats qui ont reçu du placebo dans des séries randomisées. Nos données de recherche ont montré que l'omecantiv mecarbil prolonge le temps de l'éjection systolique chez les rats mais ne réduit pas la régurgitation aortique. Il réduit la tension pariétale liée à la régurgitation aortique. On a observé que l'omecantiv mecarbil influence différemment la libération des biomarqueurs de l'étirement des fibres myocardiques chez le rat avec régurgitation aortique, ce qui n'est pas le cas avec l'administration du placebo (solution saline). Dans le ventricule gauche des rats sans régurgitation aortique, l'omecantiv mecarbil augmente l'expression des gènes à action anti-apoptotique et antioxydante. L'expression des gènes favorisant l'utilisation d'acide gras comme source majeur d'énergie était augmentée, sans altérer l'expression des gènes impliqués dans la contraction cardiaque calcium-dépendante. Nos données ont également montré que la

réurgitation aortique augmente l'expression des gènes à action pro-apoptique et pro-oxydatif. Les gènes favorisant l'utilisation de glucose comme source majeure d'énergie au niveau cardiaque et l'expression des gènes impliqués dans la dysfonction ventriculaire. D'autres études seront nécessaires pour mieux comprendre les mécanismes d'action de l'omecamtiv mecarbil, ainsi que son effet à des doses et des stades différents de la pathologie aortique pour définir s'il a une place dans le traitement de la réurgitation aortique.



## ABSTRACT

Aortic regurgitation (AR) is a pathology characterized by insufficient coaptation of one or more of the leaflets of the aortic valve. AR can lead to the reflux of blood from the aorta into the left ventricle (LV) followed by both pressure and volume overload. During the acute phase, massive aortic reflux into the LV evolves rapidly toward terminal heart failure (HF). By contrast, the LV can adapt to chronic reflux via a series of compensatory mechanisms including increased muscle mass and chamber diameter. These mechanisms, which ultimately lead to ventricular hypertrophy, facilitate reductions in the LV tension that results from pressure and volume overload and will ultimately reduce oxygen consumption. However, these structural changes may also lead to progressive functional deterioration and ultimately HF in the absence of treatment. Surgical intervention is currently the only treatment available for AR and must be performed at a comparatively early stage of the disease. While several drugs can be used to treat HF, many of them alter calcium homeostasis and increase oxygen consumption and the risk of developing arrhythmias, leading to increased morbidity and mortality. Omecamtiv mecarbil (OM) is a selective cardiac myosin activator that is currently tested in clinical trials for the treatment of systolic HF. OM specifically targets and activates the myocardial ATPase, improves energy utilization, increases the rate of phosphate release from myosin, and results in prolonged myosin-actin binding. Collectively, these mechanisms lead to improved systolic function and cardiac efficiency by increasing the systolic ejection time without consuming more ATP or oxygen or altering intracellular calcium levels. In this study, we evaluated the impact of OM in an experimental rat model of surgically-induced AR by measuring various markers of cardiac function. We evaluated echocardiographic and hemodynamic parameters, serum biomarkers, and expression of genes involved in oxidative stress, apoptosis, cardiac energy metabolism, and calcium homeostasis. OM or placebo was delivered via femoral vein injection to adult male Wistar rats that were randomized into 2 groups. Our data revealed that the administration of OM increased the systolic ejection time and decreased wall stress in rats with AR but did not reduce the extent of AR. Administration of OM also resulted in the differential release of biomarkers of myocardial fiber stretch in rats with AR compared to placebo-treated control rats. LV tissues from OM-treated control rats (i.e., those without AR) exhibited increased expression of genes associated with anti-apoptotic and anti-oxidant pathways as well as those involved in the shift to fatty acids (FAs) use as a major energy source; by contrast, no changes in the expression of genes implicated in calcium homeostasis were observed. Our data also revealed that induction of AR led to the increased expression of pro-apoptotic and pro-oxidant genes as well as those associated with the metabolic shift to glucose use as a major energy source. Our results also revealed increased expression of genes implicated in ventricular dysfunction. Additional studies will be needed to provide a better understanding of the action of OM and to determine its impact when administered at different doses and at different stages of the disease. This information will be necessary for future consideration of OM as a potential novel treatment for AR.

## LIST OF FIGURES

Figure 1. Anatomy of the heart valves

Figure 2. Different stages of AR

Figure 3. Right common carotid artery dissection. From El Oumeiri personal picture

Figure 4. Rat circulatory system from  
[https://www.biologycorner.com/worksheets/rat\\_circulatory.html](https://www.biologycorner.com/worksheets/rat_circulatory.html)

Figure 5. Myocyte structure

Figure 6. Cardiomyocyte contractile cycle

Figure 7. The mechanochemical cycle of myosin

Figure 8. Overview of RAS

Figure 9. Hemodynamic effects of aortic regurgitation (AR) induced in rats

Figure 10. Plasma NT-proBNP levels in adult male rats (n = 18) at baseline and 60 days after induction of AR (day 60)

Figure 11. Plasma sST2 levels in adult male rats (n = 18) at baseline and 60 days after the induction of AR induction

Figure 12. (A) Correlations between plasma NT-proBNP and sST2 levels and body weight (n=18 rats) at baseline and 60days after the induction of AR (p <0.01).

(B) Correlations between plasma NT-proBNP and sST2 levels and PWTd (n=18 rats) at baseline and 60 days after the induction of AR

Figure 13. Myocardial left ventricular relative expression of genes implicated in:

(A) apoptosis (Bax, Bcl2) and

(B) oxidative stress (Gpx, Sod1, Sod2) processes seven days after placebo (AR; n = 10; black bars) versus placebo (n = 8; grey bars) infusion.

Figure 14. Myocardial left ventricular relative expression of genes implicated in cardiac metabolism, including:

(A) cellular energy sensors such as Ampk, Ppar  $\alpha$ , and Ppar  $\gamma$ ;

(B) glucose transporters Glut1 and Glut4;

(C) mitochondrial metabolic regulators contributing to glucose to fatty acids shift as cardiac major energy fuel, such as Pdk4 and

(D) Cpt1; and

(E) fatty acid metabolism regulators such as Cd36, Lox-1, and Alox-15, seven days after omecamtiv mecarbil (OM; n = 6; black bars) versus placebo (n = 8; grey bars) infusion.

Figure 15. Myocardial left ventricular relative expression of genes controlling myocardial contractility including:

(A) AT1 and AT2 angiotensin II receptors

(B) ACE1 and ACE2 angiotensin-converting enzymes

(C) endothelial (eNos or Nos3) and inducible (iNos or Nos2) nitric oxide synthases

(D) major cardiac actors of kallikrein (Klk8, Klk10, Klk1c2, and Klk1c12)

(E) bradykinin (Bdkrb1 and Bdkrb2) system and of

(F) Ca<sup>2+</sup>-dependent excitation–contraction Atp2a, Ryr2, Cacna1c, Slc8a1, and Camk2d seven days after omecamtiv mecarbil (OM; n = 6; black bars) versus placebo (n = 8; grey bars) infusion.

Figure 16. Hemodynamic effects of aortic regurgitation (AR) induced in rats at baseline, 2 months after induction of AR (pre-infusion), and following infusion (I) of omecamtiv mecarbil (OM) or placebo (0.9% NaCl)

Figure 17. Illustrative examples of M-mode echocardiography recordings in 2 Wistar rats during the entire study

Figure 18. Two-way ANOVA with Bonferroni corrections for multiple comparisons on the effects of OM versus placebo on FS (p = 0.014) and EF (p = 0.012) after 2 months of AR

Figure 19. Plasma NT-proBNP levels

Figure 20. Plasma sST2 levels

Figure 21. Myocardial left ventricular relative expression of genes implicated in (A) apoptosis (Bax, Bcl2) and (B) oxidative stress (Gpx, Gsr, Sod1, Sod2) processes seven days after omecamtiv mecarbil (OM; n = 6; black bars) versus placebo (n = 8; grey bars) infusion

Figure 22. Myocardial left ventricular relative expression of genes implicated in cardiac metabolism, including:

(A) cellular energy sensors such as Ampk, Ppar  $\alpha$ , and Ppar  $\gamma$

(B) glucose transporters Glut1 and Glut4; and

(C) fatty acid metabolism regulators such as Cd36, Lox-1, and Alox-15, seven days after placebo (AR; n = 10; black bars) versus placebo (n = 8; grey bars) infusion

Figure 23. Myocardial left ventricular relative expression of genes controlling myocardial contractility including:

(A) Ca<sup>2+</sup>-dependent excitation–contraction Cacna1c, Ryr2, serca2a;

(B) cardiac actors of kallikrein (Klk8, Klk10) - bradykinin (Bdkrb1 and Bdkrb2) system and of seven days after placebo (AR; n = 10; black bars) versus placebo (n = 8; grey bars) infusion

## LIST OF TABLES

Table 1. Prevalence of AR in the Framingham Offspring Study.

Table 2. Primers used for real-time quantitative polymerase chain reaction (RTq-PCR) in rat left ventricular (LV) myocardial tissue.

Table 3. Primers used for real-time quantitative polymerase chain reaction (RTq-PCR) in rat with AR left ventricular (LV) myocardial tissue.

Table 4. Two-way ANOVA statistics with Bonferroni correction at base (T1), before injection (T2) and after injection (T3) for all sham animals (n = 4).

Table 5. Echocardiographic measurements in rats (n = 18) at baseline and 60 days after induction of AR. Correlations of plasma NT-proBNP and sST2 levels with echocardiographic variables and invasive arterial pressure measurements at baseline and two months (60 days) after the induction of AR.

Table 6. Two-tailed T-test before and after Placebo infusion on LV function after 2 months of AR in a rat model (n = 5).

Table 7. Two-tailed T-test before and after OM infusion on LV function after 2 months of AR in a rat model (n = 7).

Table 8. Two-way ANOVA statistics with Bonferroni correction at base (T1), before injection (T2) and after injection (T3) for all animals (n = 12).

Table 9. Echocardiographic measurements in rats (n = 6) at baseline and 30 min after OM infusion.

Table 10. Hemodynamic effects of aortic regurgitation (AR) induced in rats at baseline, 2 months after induction of AR (pre-infusion), and following infusion of omecantiv mecarbil (OM) or placebo (0.9% NaCl) and sham-operated rats 2 months after operation.

## 1. Introduction

### 1.1 Aortic valve

#### 1.1.1 Anatomy structure and function

Heart valves are specialized structures that prevent the backflow of blood into the chambers of the heart. The aortic valve is present in the hearts of humans and most other animals, and is located between the left ventricle (LV) and the aorta (Fig. 1). It is one of the four valves of the heart and one of the two semilunar valves, the other of which is the pulmonary valve. The aortic valve normally has three cusps or leaflets, although 1–2% of the population congenitally has two leaflets (1).

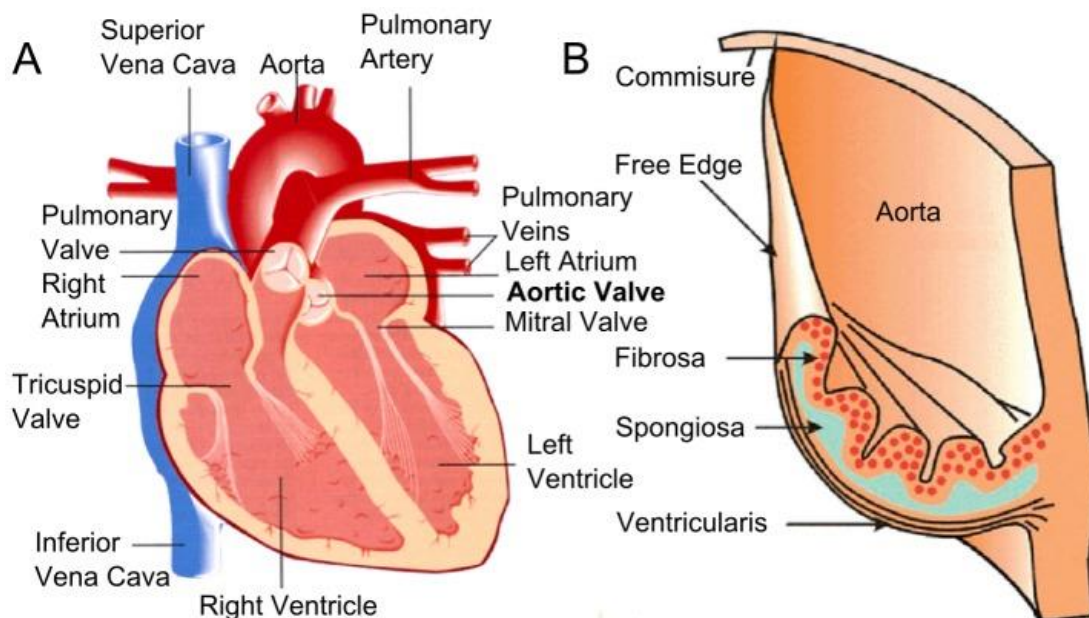


**Figure 1.** Anatomy of heart valves. A) The arrangement of the valves in the heart. B) The structures and layers of an aortic valve leaflet. From Rock et al. (2).

The aortic valve comprises three leaflets identified according to the presence of two coronary artery ostioles: a left coronary leaflet, a right coronary leaflet, and a non-coronary leaflet. Current anatomic texts simply describe the leaflet as comprising three layers (Fig. 1). On the aortic side, the fibrosa comprises an arrangement of collagen sheets and large collagen fiber bundles. On the ventricular side, a thin ventricularis layer is present. Between these outer layers is the spongiosa, a layer rich in proteoglycans. The layered structure (determined largely from inspection and analysis of histological specimens) has been described as an adaptation to the multiple functional requirements for a frequent flexion duty cycle, durability, high shear compliance, and high aortic hemodynamic pressure (3,4,5). This simple model is useful as a basic representation of valve anatomy. However, the valve material and biomechanical properties are well known to vary among leaflets and even within individual leaflets (6,7,8).

### 1.1.2 Aortic valve regurgitation

#### *1.1.2.1 Definition*

Aortic regurgitation (AR) is characterized by diastolic reflux of blood from the aorta into the LV because of malcoaptation of the aortic cusps. Its clinical presentation varies and depends on a complex interplay among several factors, including the acuity of onset, aortic and LV compliance, hemodynamic conditions, and lesion severity. Although chronic AR can be generally well tolerated for many years; acute AR can lead to rapid cardiac failure and, if untreated, to early death (9).

### 1.1.2.2 Epidemiology

The prevalence of chronic AR and the incidence of acute AR are not precisely known. Singh et al. (10) have reported the prevalence of chronic AR, detected by color Doppler echocardiography, in a large unselected adult population in the Framingham Offspring Study. The overall prevalence of AR in men was 13%, and that in women 8.5%. However, most of the AR in this population was trace or mild in severity, whereas moderate or severe AR was rare (Table 1). Multiple logistic regression analysis revealed that age and male sex were predictors of AR. Interestingly, hypertension did not predict AR in multivariate analysis, thus confirming the results of earlier studies indicating that hypertension is associated with modest increases in aortic root size, but not AR, when age is included in the model (11,12). The Strong Heart Study (13) has indicated an overall AR prevalence of 10% in a Native American population. Most cases were mild, and age and aortic root diameter, but not sex, were found to be independent predictors of AR.

	Age, y				
	26–39	40–49	50–59	60–69	70–83
According to multivariate analysis, only age and sex predicted AR prevalence. Adapted from Singh et al. <sup>2</sup>					
Men	(n=91)	(n=352)	(n=433)	(n=359)	(n=91)
None	96.7%	95.4%	91.1%	74.3%	75.6%
Trace	3.3%	2.9%	4.7%	13.0%	10.0%
Mild	0%	1.4%	3.7%	12.1%	12.2%
≥Moderate	0%	0.3%	0.5%	0.6%	2.2%
Women	(n=93)	(n=451)	(n=515)	(n=390)	(n=90)
None	98.9%	96.6%	92.4%	86.9%	73.0%
Trace	1.1%	2.7%	5.5%	6.3%	10.1%
Mild	0%	0.7%	1.9%	6.0%	14.6%
≥Moderate	0%	0%	0.2%	0.8%	2.3%

TABLE 1. Prevalence of AR in the Framingham Offspring Study. Adapted from Singh et al. (10)



### *1.1.2.3 Etiology*

Pure AR has multiple causes, many of which arise from primary abnormalities in the aortic valve leaflets. The most frequent causes include congenital abnormalities of the aortic valve most notably the bicuspid valves, but also the unicuspid, tricuspid, and quadricuspid valves rheumatic disease, infective endocarditis, calcific degeneration, and myxomatous degeneration. Other common causes of AR include diseases of the aorta without direct involvement of the aortic valve, such as systemic hypertension idiopathic annulo-aortic ectasia, aortic dissection, and Marfan syndrome (14,15). Less common causes of AR include traumatic injuries to the aortic valve, aortitis occurring in ankylosing spondylitis, syphilitic infection, rheumatoid arthritis, osteogenesis imperfecta, giant cell aortitis, Takayasu disease, Ehlers Danlos syndrome, and Reiter syndrome. AR can also occur in people with discrete subaortic stenosis in the presence of a ventricular septal defect with prolapse of an aortic cusp, ruptured aneurysms of the sinuses of Valsalva, or fenestrated aortic cusps (16). AR has also been described as a complication associated with balloon aortic valvuloplasty (17), and anorectic drugs have been reported to cause AR (18). However, in many people with AR, the precise etiology is unclear. In a pathologic study of a surgical series of excised aortic valves, as many as 34% cases of pure AR were considered to have unclear etiology (15). Most of these lesions produce chronic AR, with slow, insidious LV dilatation and a prolonged asymptomatic phase.

Other lesions, particularly infective endocarditis, aortic dissection, and trauma, often produce acute severe AR with sudden elevation of LV filling pressure, pulmonary edema, and decreased cardiac output (CO).

#### 1.1.2.4 Pathophysiology

Chronic severe AR imposes a combined volume and pressure overload on the LV. The volume overload is a consequence of the regurgitant volume itself and is therefore directly related to the severity of the leak. Thus, whereas mild AR produces only minimal volume overload, severe AR can produce massive LV volume overload and progressive chamber dilation. The pressure overload results from systolic hypertension, which occurs as a result of increased total aortic stroke volume, because both the regurgitant volume and the forward stroke volume is ejected into the aorta during systole (19). Systolic hypertension can contribute to a cycle of progressive dilation of the aortic root and subsequent worsening of AR. In early, compensated severe AR, the LV adapts to the volume overload through eccentric hypertrophy, in which sarcomeres are laid down in series, and myofibers are elongated (20,21).

Eccentric hypertrophy preserves LV diastolic compliance, such that LV filling pressures remain normal or mildly elevated despite a large regurgitant volume. In addition, eccentric hypertrophy increases LV mass, such that the LV volume/mass ratio is normal, and the LV ejection fraction (LVEF) is maintained by the increased preload. The slope of the LV pressure volume relationship (elastance or  $E_{max}$ ), a load-independent measure of myocardial function, is normal (22). Over time, progressive LV dilation and systolic hypertension increase wall stress and the volume/mass ratio. During this process, a phase occurs during which the LVEF remains normal, but  $E_{max}$  decreases, thereby indicating early myocardial dysfunction that is largely masked by the increased preload. At this stage, LVEF still increases after successful valve replacement (27).

Eventually, the increase in wall stress leads to overt LV systolic dysfunction, manifested as a decline in LVEF and severely diminished  $E_{max}$ . In chronic severe AR, the end-systolic wall stress can be as high as that in aortic stenosis (23). Marked LV hypertrophy (*cor bovinum*)

develops with elevated LV volume and mass and spherical geometry (24). In decompensated severe AR, LV systolic dysfunction is accompanied by a decrease in LV diastolic compliance as a result of hypertrophy and fibrosis, thus leading to high filling pressure and heart failure symptoms. Exertional dyspnea is the most common manifestation, but angina can also occur because of a decrease in coronary flow reserve with predominantly systolic coronary flow (25,26). In experimental animals, the transition from a compliant (chronic compensated AR) to a stiff (decompensated AR) LV chamber appears to involve upregulation of several cardiac fibroblast genes (27,28). Acute AR leads to rapid decompensation due to low forward cardiac output and pulmonary congestion. The time is insufficient for compensatory LV dilation to occur, and severe hypotension occurs rather than the systolic hypertension that characterizes chronic severe AR. The different stages of AR are shown in Figure 2.

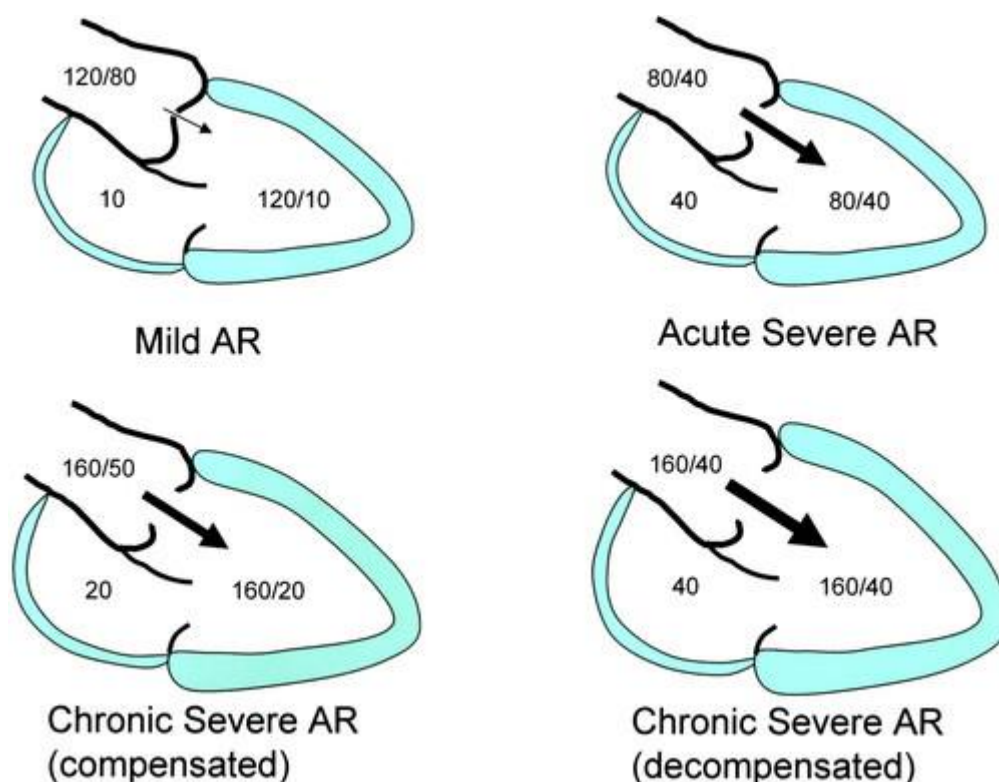


Figure 2. Stages of AR. Top left: In mild AR, LV size, function, and hemodynamics are normal. Top right: In acute severe AR, equilibration of aortic and LV pressures (80/40 mm Hg in this example) is observed. The left atrial pressure is elevated, thus leading to pulmonary edema. Bottom left: In chronic severe compensated AR, the LV may begin to dilate, but LVEF is often maintained in a normal range

by an increased preload. Systolic arterial hypertension and a wide pulse pressure are observed. However, LV filling pressures are normal or only slightly elevated, such that dyspnea is absent. Bottom right: In decompensated chronic severe AR, the LV is dilated and hypertrophied, and LV function is often depressed as a result of afterload excess. Forward output decreases, thus leading to fatigue and other low-output symptoms. Fibrosis and hypertrophy decrease LV compliance, thereby leading to increased filling pressures and dyspnea. From Bekeredjian et al. (29).

#### *1.1.2.5 Natural history and treatments*

No information is available regarding the natural history of mild AR. Natural history data for asymptomatic patients with severe AR and normal LV systolic function have been analyzed in the American College of Cardiology (ACC)/American Heart Association (AHA) guidelines on valvular heart disease (30), which included a review of nine published series in a total of 593 such patients (31,32,33). These studies have consistently shown that patients can remain asymptomatic with preserved LV function for a considerable period of time. The rate of progression to symptoms and/or LV dysfunction averaged 4.3% per year. Sudden death occurred in 7 of the 593 patients, and the average mortality rate was less than 0.2% per year. The available data have also indicated that the rate of development of LV dysfunction, defined as an ejection fraction (EF) at rest below normal, occurs at a rate of 1.2% per year. Despite the low likelihood of patients developing asymptomatic LV dysfunction, more than one-quarter of patients in these series experienced this condition before the onset of warning symptoms. Thus, in the serial evaluation of patients, assessing symptomatic status alone is insufficient, and quantitative assessment of LV size and function is essential. Natural history studies have also defined variables that predict the development of symptoms or LV dysfunction. These variables are age, LV end-diastolic dimension or volume, LV end-systolic dimension or volume, and LVEF during exercise (31,34,35,36). A tenth study of asymptomatic patients with normal LV systolic function, published after the 2006 ACC/AHA guidelines, has reported a higher clinical event rate and a higher mortality rate (37). That study, in which quantitative measurement of

severity of AR was obtained with Doppler echocardiography, has reported that patients with severe AR have a much higher mortality risk and a higher likelihood of AVR than patients with less severe AR. The measures of AR severity are stronger predictors of outcomes than LVEF or any measures of LV dilatation. Importantly, the annual mortality rate in this 10th study of patients with initially normal EF was 2.2%, a percentage 10-fold higher than the average 0.2% per year mortality rate in the previous nine studies (30). This higher mortality rate may be explained by the more advanced age of the patients in the 10<sup>th</sup> study (60 years), which is more than 20 years older than the average age of patients in the other studies (39 years). This finding suggests that severe AR in older patients, who have stiffer arteries and stiffer LVs, may be more poorly tolerated than AR in younger patients.

Data for asymptomatic patients with depressed LV function are limited, but the average rate of symptom onset in such patients has been estimated to exceed 25% per year (38,39). Symptoms caused by AR are strong predictors of clinical outcomes (40). Data have indicated that patients with dyspnea, angina, or overt heart failure have poor outcomes after medical therapy, with annual mortality rates greater than 10% in those with angina and 20% in those with heart failure (41,42,43).

#### *1.1.2.6 Treatments*

Current ACC/AHA guidelines provide three potential indications for vasodilators in severe chronic AR (43). The first is long-term treatment of patients with symptoms and/or LV dysfunction who has a very high surgical risk because of additional cardiac or noncardiac factors. The second is short-term therapy to improve the hemodynamic profiles of patients with severe heart failure symptoms and severe LV dysfunction before proceeding to valve surgery.

The third is to preserve LV function and possibly delay the need for AVR in asymptomatic patients with chronic AR.

This indication received a class Ia recommendation by the 1998 ACC/AHA Task Force (44), but has since been downgraded to class IIb level by the 2006 ACC/AHA Task Force, which has been maintained in the current guidelines. This change reflects uncertainty regarding the evidence supporting the use of vasodilators for chronic asymptomatic AR. The 2007 European Society of Cardiology (ESC) Valvular Guideline recommendations are similar (45). In asymptomatic patients with chronic severe AR and hypertension, vasodilators such as ACE inhibitors or dihydropyridine calcium-channel blockers are warranted. However, the ESC guidelines have also concluded that the role of vasodilators in delaying surgery in patients with asymptomatic AR without hypertension is insufficiently supported. Vasodilators evaluated in aortic regurgitation include the dihydropyridine calcium antagonist nifedipine; the ACE inhibitors enalapril and captopril; and hydralazine. Vasodilators decrease peripheral vascular resistance and blood pressure. In addition, these actions decrease afterload with no change in regurgitant volume. Diminished regurgitant volume would be expected to decrease ventricular filling pressure, LV end-systolic volume (LVESV), and LVEDV indexes (29).

Diminished afterload would also be expected to improve forward stroke volume and decrease LV hypertrophy. These effects might translate into improved clinical outcomes during long term treatment. Furthermore, ACE inhibitors target the RAAS, thus potentially providing a theoretical advantage over other vasodilators in asymptomatic chronic AR. However, whether vasodilatory agents have favorable effects on LV remodeling or improve clinical outcomes remains controversial (46). In addition, the possibility of adverse effects of treatment must be considered. For example, a decrease in an already low aortic diastolic blood pressure with vasodilator treatment could potentially adversely affect coronary perfusion. Currently, evidence indicating favorable and or unfavorable clinical effects of vasodilator treatments is lacking (46).

While vasodilators have several theoretical advantages in patients with severe asymptomatic aortic regurgitation, the clinical studies evaluating their effects in chronic AR have not enabled a reliable evaluation of their overall benefits and risks.

In acute AR, immediate surgical intervention is necessary, because the acute volume overload results in life-threatening hypotension and pulmonary edema (47). Symptom onset is an indication for surgery, regardless of LV function (30,48), when the symptoms are mild, such as in NYHA class II dyspnea, clinical judgment is necessary, and in this setting, exercise testing is valuable. In symptomatic patients with decreased LV systolic function (subnormal EF), surgery is indicated (30,48). Surgery should also be considered for asymptomatic patients with severe AR and impaired LV function at rest, defined by a resting EF less than 50% and/or extreme degrees of LV dilatation ( $LVEDD \geq 70$  to  $75$  mm and  $LVEDD \geq 50$  to  $55$  mm) (49,50).

## 1.2 Experimental aortic regurgitation

Several animal models of AR have been developed in the past, and in small animals such as rats and rabbits, experimental AR can be induced by retrograde aortic leaflet perforation using a rigid catheter inserted via the right carotid artery (24,320) without thoracotomy (Figures 3 and 4). This model has the advantage of being relatively non-invasive. Rats and rabbits are good subjects to evaluate the response of the LV to severe AR since they develop LV abnormalities in a relatively short period of time (weeks) compared with humans, who can tolerate this condition without LV dysfunction for decades (31,32,33). In the past, experimental AR has been performed in rats under hemodynamic guidance. That is, the investigator relied solely on a popping sensation that occurred when a leaflet was perforated, accompanied by an acute fall in aortic diastolic pressure of  $>30\%$  during the procedure, to determine whether significant AR had been induced (320). The insertion of electromagnetic probes around the ascending aorta of

rabbits to quantitate AR has been used in many protocols, but this requires a thoracotomy. As a consequence, the procedure becomes invasive and more complicated (320), with high intraoperative and perioperative mortality rate in small animals. AR was found to be induced more precisely, easily and safely under echocardiographic guidance, with concomitant gradation of the severity of the regurgitation and evaluation of LV function (Figure 11), complications can be quickly identified and treated whenever is possible (217,221,299). Consequently, homogenous group of animals can be obtained with a pure valvular disease thereby improving the validity of research protocols. Experimental AR rats showed a LV hypertrophy characterized by clear chamber dilatation (increased LVEDD and decreased RWT), and moderate loss of function.

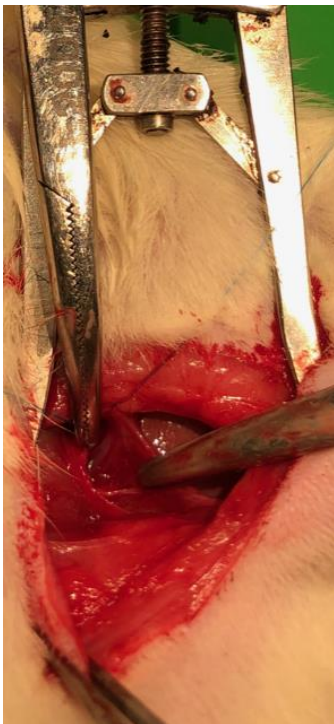


Figure 3. Right common carotid artery dissection. From El Oumeiri personal picture



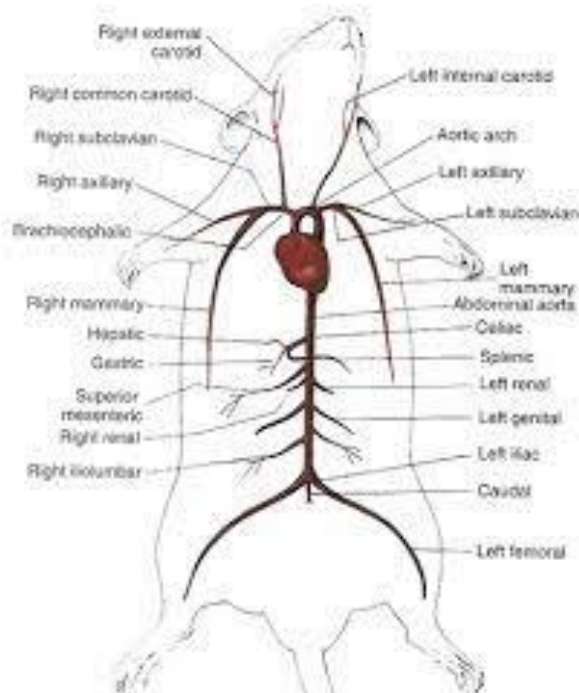


Figure 4. Rat circulatory system from:

[https://www.biologycorner.com/worksheets/rat\\_circulatory.html](https://www.biologycorner.com/worksheets/rat_circulatory.html)

### 1.3 Omecamtiv mecarbil

#### 1.3.1 Background

Myocardial contraction results from the remarkable transduction of chemical energy into mechanical energy, as regulated on a beat-to-beat basis by inter-associated signaling pathways acting on the sarcomeres, the contractile units of myocytes (51). Sarcomeres have a complicated structure, wherein the main force-generating unit consists of actin, myosin, and multiple regulatory proteins (such as troponin and tropomyosin) (Figure 5).

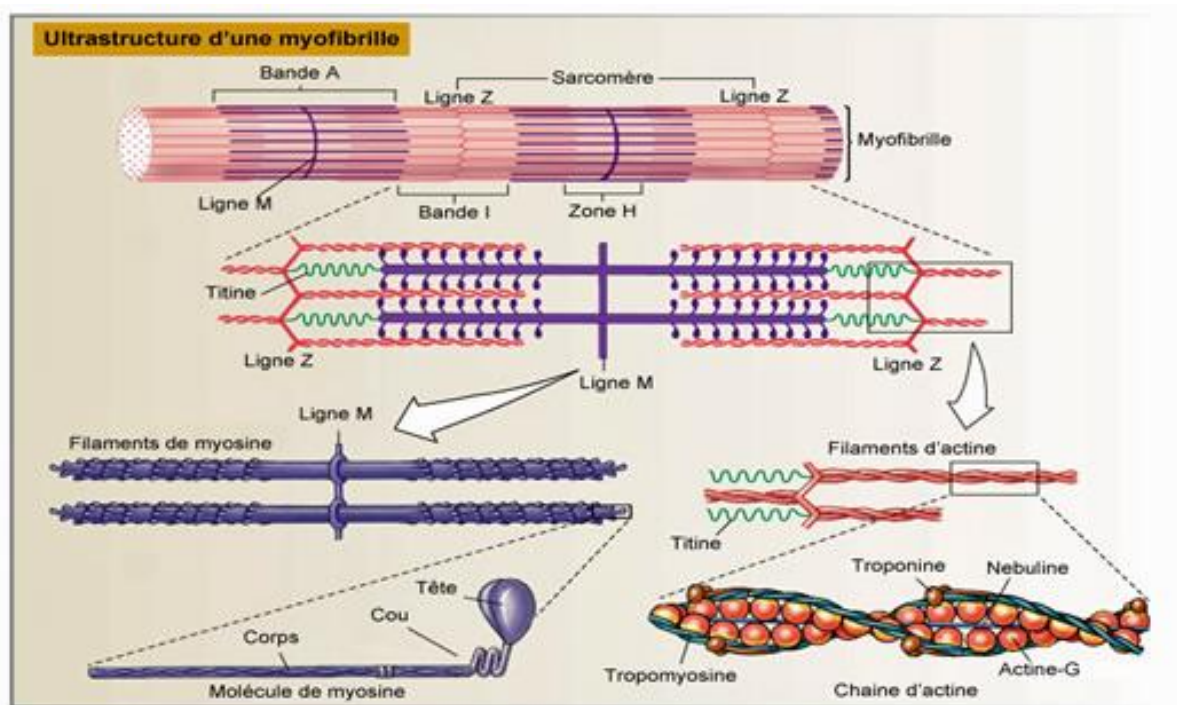


Figure 5. Myocyte structure from Marieb et al. (52).

The myosin complex consists of two myosin heavy chains and two pairs of myosin light chains. The myosin heavy chain has a globular head containing an ATPase domain [which cleaves adenosine triphosphate (ATP) and consequently produces energy], as well as an actin-binding site, through which contractile force is transduced. Cardiac troponin (TnC) and tropomyosin form a complex that regulates the interaction of myosin with actin in a calcium sensitive manner (53). In the resting state, calcium concentrations in myocytes are low, and the troponin–tropomyosin complex blocks cross-bridge formation between actin and myosin. Myocyte depolarization triggers calcium release from the sarcoplasmic reticulum (SR), thereby increasing sarcomeric concentrations of calcium and resulting in calcium binding to TnC and a shift in tropomyosin, such that it no longer blocks actin–myosin cross-bridge formation. Subsequently, myosin binds actin and, using energy released through the hydrolysis of ATP to ADP, produces a force-generating conformational change and shortening of the sarcomere. Calcium is actively transported back into the SR in a highly energy-intensive process, where it

awaits release again after the next depolarization event. This cycle repeats for the lifetime of the organism. The cardiac actin–myosin cycle (54,55) is central to this process of myocardial force generation (Figure 6).

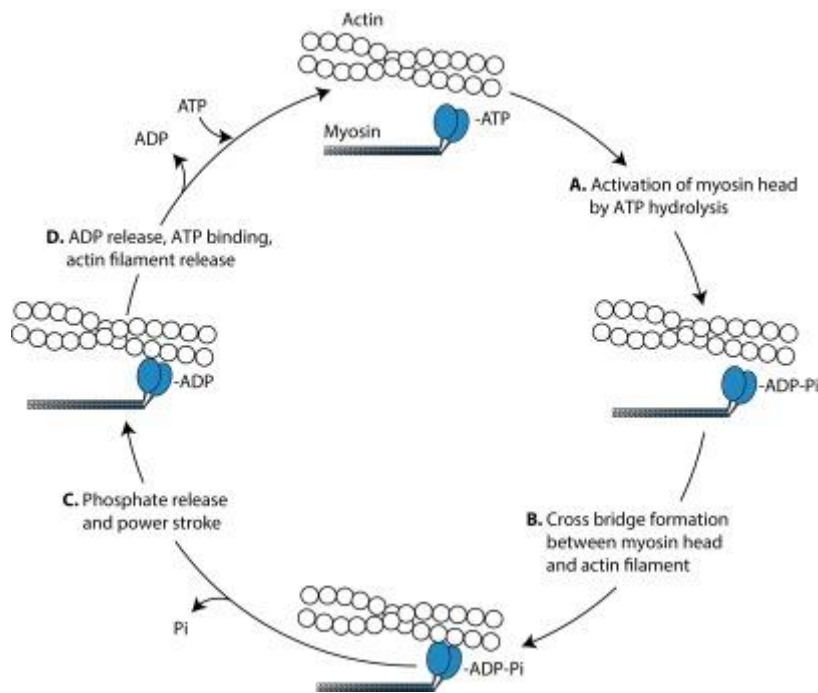


Figure 6. Cardiomyocyte contractile cycle. from Edgardo et al. (56). Calcium binds TnC (inhibiting TnI), thus inducing a conformational change that displaces tropomyosin from binding sites and exposes active sites between actin and myosin. Myosin head activation occurs through ATP hydrolysis (ADP+Pi) which is no longer inhibited (TnI), thereby enabling cross-bridge formation between myosin heads and active sites on actin (A/B). Release of Pi reinforces these interactions (myosin and actin) thus triggering the “power stroke,” another conformational change that firmly pulls myosin against actin in a highly stable force-generating association (B/C). The myosin-ADP-actin complex dissociates when an ATP molecule binds myosin heads, thereby liberating ADP and releasing actin filaments (D). Calcium dissociation from troponin occurs when its cytosolic levels decrease, and tropomyosin returns to its original state (blocking actin binding sites). ADP, adenosine diphosphate; ATP, adenosine triphosphate; Pi, inorganic phosphate; TnC, troponin C; TnI, troponin I.

Omecamtiv mecarbil (OM) (formerly known as CK-1827452 or AMG 423) (57) is a cardiac myosin activator that selectively activates the S1 domain of cardiac myosin but not other muscle myosins. OM binds the catalytic domain of myosin, thus stabilizing the pre-power-stroke state (58), increasing the transition rate of myosin into the strongly actin-bound force-generating

state (Figure 7) (57), and consequently increasing cardiac contractility. The cycle time of myosin is similar to the duration of systole, thus enabling more myosin heads to enter the force-generating state and resulting in more hands pulling on the rope and greater force production. The rate of ADP release is unaffected: with more myosin heads bound to the actin filaments; the thin filament remains activated longer as calcium levels fall, thus prolonging myocyte contraction (57). OM increases the rate of ATP turnover only when cardiac myosin S1 is present, regardless of the thin filament source (troponin-tropomyosin-regulated actin), and not when fast skeletal or smooth myosin are present (57).

### 1.3.2 Pharmacodynamics and pharmacokinetics

The pharmacodynamic signature of OM is an increase in the systolic ejection time (SET), as a consequence of the increase in the number of myosin heads interacting with actin filaments, thereby facilitating a longer duration of systole, even as  $[Ca^{2+}]_c$  decays. OM prolongs the time and increases the amplitude, but not the rate of cell shortening, and does not interfere with  $[Ca^{2+}]_c$  transients (Figure 5) (57). In healthy men and people with stable HF with comparable increases in SET, the net increases in SV and cardiac output, and the subsequent decreases in heart rate, have been found to be smaller overall than those observed in preclinical studies, thus perhaps reflecting the broad range of baseline conditions across human studies. In these early studies, OM was examined over a broad range of plasma concentrations, in some cases exceeding 1200 ng/mL. Increases in SET have been observed at plasma concentrations as low as 100–200 ng/mL, whereas the effect on SV appears to plateau at 400–500 ng/mL. In some patients, myocardial ischemia develops with chest pain, ECG changes and/or troponin increases at plasma concentrations beyond 1200 ng/mL (59,60). This finding may be explained by an excessive increase in SET, thus prolonging cardiac contraction, and progressively shortening

diastole (during which coronary perfusion occurs). (59,60). However, in a trial of patients with ischemic cardiomyopathy and angina in daily life, OM at target plasma concentrations of 295 ng/mL and 550 ng/mL has not been found to affect symptom-limited exercise capacity in treadmill tests or plasma troponin I levels (61). Subsequent trials have focused on dose regimens constraining exposure to less than 1000 ng/mL.

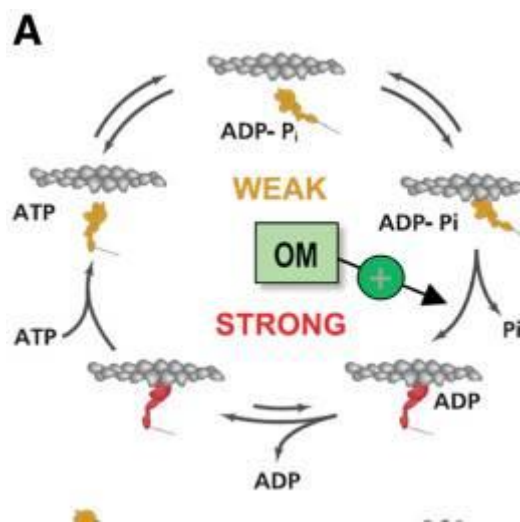


Figure 7. The mechanochemical cycle of myosin. from Malik et al. (57). Yellow indicates myosin weakly bound to actin, whereas red indicates myosin strongly bound to actin. Omecamtiv mecarbil (OM) accelerates the transition rate of myosin into the strongly actin-bound force-generating state.

OM pharmacokinetics has been clinically investigated in healthy volunteers (60) and in patients with heart failure (59). Vu et al. (62) have aggregated the results from the studies by Teerlink et al. (60), Cleland et al. (59), and a study with oral dosing (62), and analyzed the population pharmacokinetics of OM, and the relationship between OM plasma levels and SET and LV outflow tract stroke volume. The absolute bioavailability of the oral formulation was assessed, and 90% maximal concentration was reached after approximately 1 hour. The elimination half-life was approximately 18.5 hours, and systemic clearance occurred within 11.9 L/h, with an apparent volume of distribution of 298 L. These findings were consistent with the data from the individual studies (59,60). The first human study (60) was a randomized, double blind, placebo-

controlled trial in which OM or placebo was administered intravenously in healthy men at doses ranging from 0.005 to mg/kg per hour for 6 hours. The percentage of plasma protein binding of OM was approximately 81.5%. OM was found to be extensively metabolized, mainly through decarbamylation. Only 8% of the parent compound was recovered unchanged in the urine, during collection for as many as 336 hours (60). In a recent study by Chen et al. (63), in a total of 4346 healthy participants or patients with HF and decreased EF who received intravenous or oral doses of 25 mg, 37.5 mg, and 50 mg twice daily, OM was found to have a clearance of 11.7 L/h (0.701% relative standard error) and a central volume distribution of 275 L (2.12% relative standard error). The estimated half-life of OM was 33 hours. Body weight and estimated glomerular filtration rate were significant covariates, but their effects on exposure were modest and lacked clinical relevance. Additional covariates, including sex, race, bilirubin, albumin, concomitant medications, New York Heart Association functional classification, N-terminal-pro hormone B-type natriuretic peptide, troponin I, creatine kinase MB, serum hemoglobin, tablet formulation, aspartate aminotransferase, and serum urea, were tested and found to have no effect on OM exposures (63).

### 1.3.3 Bioenergetic aspects

In a canine model of HF, OM has not been found to increase O<sub>2</sub> consumption (64), although in a post-ischemic pig model, O<sub>2</sub> consumption has been found to tend to increase (65). In isolated mouse hearts, OM has been observed to impair myocardial efficacy by increasing O<sub>2</sub> consumption in working hearts and during basal (resting) metabolism, but these effects are abolished by a myosin-ATPase inhibitor (65). These data suggest that OM increases (tonic) myosin-ATPase activity (66) and thereby O<sub>2</sub> consumption, in contrast with the effect of OM in inhibiting the basal ATPase activity of myosin in vitro (67). In skinned rat cardiac myocytes, OM shifts the pCa/force relationship to the left, thus indicating sensitization of myofilaments

to  $\text{Ca}^{2+}$  (68). In the human myocardium, OM increases the myosin duty ratio, thereby enhancing  $\text{Ca}^{2+}$  sensitivity but slowing force development (69). In a mouse model of dilated cardiomyopathy with diminished myofilament  $\text{Ca}^{2+}$  sensitivity, OM has been observed to resensitize myofilaments toward control levels (70). However, in most patients with HF, the  $\text{Ca}^{2+}$  affinity of myofilaments is elevated rather than diminished (71,72,73,74). In the LV myocardium in patients with terminal HF, increased diastolic tension consumes as much ATP and  $\text{O}_2$  as systolic tension, and elevated diastolic tension is a substantial energetic burden in failing hearts, particularly at higher heart rates (75).

#### 1.3.4 Clinical efficacy

In the ATOMIC-AHF study on patients with AHF and an LVEF  $\leq 40\%$ , the primary endpoint of dyspnea relief was not reached after three ascending intravenous infusion doses of OM versus placebo (76). However, in the highest dose group ( $n = 202$ ), more patients experienced dyspnea relief with OM (51%) than placebo (37%;  $P = 0.034$ ) treatment. In an echocardiographic substudy, OM has been found to prolong SET and decrease LV end-systolic dimension, without increasing LV stroke volume (76). Additionally, slight decreases in heart rate ( $-2$  b.p.m.) and increases in systolic blood pressure were observed. In the COSMIC-HF trial, oral OM at either a fixed dose (25 mg twice daily) or dosing based on a pharmacokinetic titration protocol was tested against placebo in patients with stable (not acute) systolic HF receiving standard of care therapy (77). After 20 weeks, moderate increases in SET and SV and a slight decrease in heart rate were observed in the pharmacokinetic titration group. This effect might reflect slightly diminished endogenous sympathetic activity (78). Furthermore, the LV end-diastolic volume were 11 mL lower, and the N-terminal pro-B-type natriuretic peptide (NT-proBNP) levels were 970 pg/mL lower than those in the placebo group. As in ATOMIC-AHF (76), a small increase was observed in cardiac troponin I, which did not correlate with OM plasma concentrations

(59,60). The frequency of deaths, arrhythmias, hospital admissions, or adverse events did not differ between groups, thus suggesting the safety of the treatment. Overall, the hemodynamic profile of OM appears promising within its therapeutic range. The increase in cardiac contractility and subsequent prolongation of SET increases LV stroke volume in patients with chronic HF; consequently, blood pressure initially rises and may decrease endogenous sympathetic activation, as indicated by the slight, consistent lowering of heart rate observed in human and animal studies. Consequently, cardiac output in humans appears to be largely unchanged despite the modest decrease in heart rate, thereby suggesting improved cardiac efficiency. Furthermore, the decrease in LV filling pressure, as indicated by the decrease in NT-proBNP in COSMIC-HF, and the decrease in LV end-diastolic pressures in acute studies in dogs, suggests that LV unloading may facilitate reverse remodeling of the LV. In the GALACTIC-HF trial (79), more than 8,000 patients with chronic symptomatic (New York Heart Association functional class II to IV) HF, left ventricular EF  $\leq$ 35%, elevated natriuretic peptides, and either current hospitalization for HF or history of hospitalization or emergency department visit for HF within a year of screening were randomized to either oral placebo or OM. The preclinical and clinical data suggest that OM improves cardiac function, decreases ventricular wall stress, reverses ventricular remodeling, and promotes sympathetic withdrawal (79). In a post hoc analysis (80) of data from the GALACTIC-HF clinical trial, OM therapy was found to be well tolerated in patients with severe HF, and no significant differences in blood pressure, kidney function, or potassium level were observed between the OM and placebo groups (80). These data support a potential role of OM therapy in patients for whom current treatment options are limited (80).



## 1.4 Cardiac biomarkers

### 1.4.1 N-terminal pro-B-type natriuretic peptide (NT-proBNP)

NT-proBNP is a corin-catalyzed cleavage product of proBNP that is synthesized in, and secreted from, primarily the ventricular myocardium (81,82). The circulating levels of these peptides are elevated in response to increased cardiac wall stress and myocardial hypertrophy in states of pressure and/or volume overload (83,84). In patients with congestive HF, BNP and NT-proBNP are elevated, and this response is correlated with clinical presentation and hemodynamic changes (85). Both markers have also been found to be independent predictors of prognosis in patients with heart failure, acute coronary syndrome, and pulmonary embolism (86,87,88). Gerber et al. have reported an association of NT-proBNP and BNP with symptoms and left ventricular function in 40 patients with AR (89). NT-proBNP can be used as a biomarker reflecting hemodynamic stress due to volume overload caused by AR (90). Furthermore, NT-proBNP provides prognostic information for the assessment of clinical outcomes in patients with isolated AR, particularly in those treated conservatively (90). NT-proBNP levels might better reflect changes in LVMI caused by volume overload rather than by pressure overload. In chronic severe AR, higher preoperative NT-proBNP levels are predictive of LV reverse remodeling early after surgery in aortic valve disease (91).

### 1.4.2 Soluble suppression of tumorigenicity 2 (also called interleukin 1 receptor-like 1; sST2)

Suppression of tumorigenicity (ST2) is a member of the interleukin-1 (IL-1) receptor/Toll-like superfamily. ST2 is an interleukin-1 receptor-like 1 (IL1RL-1) protein that was considered an “orphan” receptor when it was first described in 1989. (92) Interleukin-33 (IL-33), a member

of the IL-1 family of cytokines, was described as a ligand for suppression of tumorigenicity 2 in 2005 (93). The discovery of IL-33 aided in understanding of the signaling axis of IL-33 and ST2. ST2L, after IL-33 binding, inhibits the inflammatory response associated with Th2 lymphocytes. Suppression of tumorigenicity 2 participates in inflammatory processes and functions in relation to immune diseases. According to current knowledge, ST2 has four isoforms: the two main isoforms are membrane-bound receptor (ST2L) and soluble (sST2) forms, whereas the other two are ST2V (94) and ST2LV (95). Differences in their structures and quantities result from a dual promoter system to drive differential mRNA expression (96). The ST2L membrane protein consists of three extracellular domains, a single transmembrane domain, and an intracellular domain (96). Because sST2 lacks the transmembrane and intracellular domains, it circulates freely in the blood. Interleukin-33, after tissue damage or necrosis, is released into the extracellular space, where it binds the ST2 receptor and subsequently recruits IL-1 receptor accessory protein (IL-1RAcP), thereby leading to the activation of the nuclear factor kappa-light-chain-enhancer of activated B cells (NF- $\kappa$ B) signaling pathway (97). The soluble form of ST2, after binding IL-33, inhibits the inflammatory response associated with Th2 lymphocytes, thereby blocking the protective effect of IL-33. IL-33 is biologically active and is released by living cells; it can additionally be released by necrotic cells after tissue damage, thereby acting as an endogenous danger signal (98). Multiple organs and cell types in humans express IL-33 (93). Together with ST2, IL-33 is involved in many inflammatory and allergic diseases, including asthma (99), rheumatoid arthritis (100), and inflammatory bowel disease (101); moreover, it participates in cardiovascular pathophysiology. Weinberg et al. have described the expression of ST2 in cardiac cells as a “response” to myocardial stress and biomechanical overload (102). This discovery resulted in research focusing on the role of ST2 in the cardiovascular system. Further studies have revealed that in cardiac diseases, the main source of sST2 may be vascular endothelial cells rather than

myocardium (103). The interaction of IL-33 and ST2L is part of the cardioprotective pathway that prevents fibrosis and inhibits the inflammatory response, hypertrophy, and apoptosis of cardiomyocytes. The prognostic value of circulating sST2 levels has been confirmed in acute dyspnea, acute coronary syndrome, and acute and chronic heart failure (104).

## 1.5 Left ventricular gene expression profile

### 1.5.1 Apoptosis and oxidative stress determinants

#### *1.5.1.1 Mitochondrial members Bax and Bcl-2*

Apoptosis, or programmed cell death, is a process of ordered, active, non-inflammatory cell death. Bcl-2 is a member of a family of genes that are divided into two categories according to their effects on apoptosis. One group, including Bax, promotes apoptosis, whereas the other group, including Bcl-2, inhibits cell death pathways (105,106). Of these proteins, Bcl-2, Bax, and Bcl-XL are the best characterized members of the Bcl-2 family (107). In the presence of stress, Bcl-2 family proteins congregate at the outer mitochondrial membrane and regulate apoptosis. Pro-apoptotic Bax undergoes conformational changes, then translocates from the cytosol to the mitochondria via homo-oligomerization with cell stress signaling proteins (108). The Bax/Bcl-2 ratio is a measure of cell vulnerability to apoptosis: a higher Bax/Bcl-2 ratio is associated with greater vulnerability to apoptotic activation, and up-regulation of the Bax/Bcl-2 ratio indicates greater apoptotic activity (109,110).

#### *1.5.1.2 Biomarkers of oxidative stress*

The main function of antioxidant enzymes (GPXs, GR, and SOD) is to protect cells against various reactive oxygen species (ROS), such as hydroperoxides through scavenging reactions

(111). Oxidative stress develops because of an imbalance between free radical production, which is often increased in the presence of dysfunctional mitochondria, and decreased antioxidant defenses (112,113). The mitochondrial electron transport chain is a major source of ROS (114). Oxidative stress is involved in the development and progression of clinical and experimental heart failure (115,116,117). Glutathione peroxidase (GPx) is the general name of an enzyme family with peroxidase activity, whose main biological role is to protect organisms from oxidative damage (118). The biochemical function of GPX is to reduce lipid hydroperoxides to their corresponding alcohols and to reduce free hydrogen peroxide to water (119). Superoxide dismutase (SOD) is an enzyme that catalyzes the dismutation of the superoxide ( $O_2^-$ ) radical into ordinary molecular oxygen ( $O_2$ ) and hydrogen peroxide ( $H_2O_2$ ) (120). Superoxide is produced as a by-product of oxygen metabolism and, if not regulated, causes many types of cell damage. SOD1 is located in the cytoplasm, whereas SOD2 is located in the mitochondria (121). Glutathione reductase catalyzes the reduction of glutathione disulfide (GSSG) to the sulfhydryl form glutathione (GSH), a critical molecule in resisting oxidative stress and maintaining the reducing environment of the cell (122). The ratio of GSSG/GSH present in cells is a key factor in properly maintaining cellular oxidative balance (i.e., maintaining high levels of reduced glutathione and low levels of oxidized glutathione disulfide). This narrow balance is maintained by glutathione reductase, which catalyzes the reduction of GSSG to GSH (123).

### *1.5.2 Molecules implicated in energy substrate use*

#### *1.5.2.1 AMPK, PPAR $\alpha$ , and PPAR $\gamma$*

Adenosine monophosphate-activated protein kinase (AMPK) is a serine/threonine protein kinase widely found in eukaryotic organisms; its major role in the myocardium is regulation of energy metabolism (124,125). The activation of AMPK is beneficial to the heart through the

activation of energy-producing pathways and inhibition of energy expenditure. AMPK regulates fatty acid metabolism via promoting fatty acid uptake, transport, and oxidation; moreover, it regulates glucose metabolism through promoting glucose uptake and glycolysis, and inhibiting glycogen synthesis (126).

Peroxisome proliferator-activated receptor alpha (PPAR $\alpha$ ) is a nuclear receptor protein functioning as a transcription factor (127). PPAR $\alpha$  is regulated by free fatty acids (128), and is involved in modulating myocardial metabolism under basal conditions and in response to physiologic stressors (129). Activation of PPAR $\alpha$  promotes the uptake, utilization, and catabolism of fatty acids through the upregulation of genes involved in fatty acid transport, fatty acid binding and activation, and peroxisomal and mitochondrial fatty acid  $\beta$ -oxidation (130). PPAR $\alpha$  activation also inhibits glycolysis and glycogen synthesis (128). PPAR $\alpha$  is the pharmaceutical target of fibrates used as hypolipidemic drugs (130).

Peroxisome proliferator-activated receptor gamma (PPAR $\gamma$ ) is a nuclear receptor functioning as a transcription factor present primarily in adipose tissue (131). PPAR $\gamma$  regulates fatty acid storage and glucose metabolism (132). The genes activated by PPAR $\gamma$  stimulate lipid uptake and adipogenesis by fat cells: PPAR $\gamma$  increases insulin sensitivity by enhancing the storage of fatty acids in fat cells, and is itself activated by free fatty acids and eicosanoids (133).

#### *1.5.2.2 Glucose transporters Glut1 and Glut4*

Glucose is transported into cells by members of the family of facilitative glucose transporters (GLUTs). The predominant glucose isoforms expressed in the heart are GLUT1 and GLUT4. The GLUT1/GLUT4 ratio in rat hearts varies from 0.1 to 0.6 (134). GLUT translocation to the plasma membrane is an important mechanism through which the net flux of glucose into cells are regulated. Fasting is associated with a decline in GLUT1 expression (135). After 48 hours

of fasting, basal glucose uptake and GLUT1 expression decrease by 90% and 60%, respectively, in rat hearts. However, GLUT4 expression and insulin mediated glucose uptake do not change, thus indicating that GLUT4 is the major regulator of insulin stimulated glucose uptake in the heart (134). Chronic left ventricular hypertrophy (LVH) in rats is associated with increased total GLUT1, decreased total GLUT4, increased distribution of both transporters to the plasma membrane and AMPK activity (136). In severely failing human hearts, GLUT1, GLUT4, and muscle carnitine palmitate transferase-1 (mCPT-1) are downregulated (137). Chronic or intermittent myocardial ischemia is also associated with increased expression of GLUT1 in the heart (138). In most models of diabetes (type 1 or type 2), diminished expression of GLUT1 and GLUT4 in the heart is consistently observed (139).

#### *1.5.2.3 PDK4 and CPT1*

Pyruvate dehydrogenase kinase isozyme 4 (PDK4), an enzyme located in the matrix of the mitochondria, inhibits the pyruvate dehydrogenase complex by phosphorylating one of its subunits, thereby decreasing the conversion of pyruvate, which is produced from the oxidation of glucose and amino acids, to acetyl-CoA, and contributing to the regulation of glucose metabolism. Expression of this gene is regulated by glucocorticoids, retinoic acid, and insulin (140). PPAR $\alpha$  upregulates PDK4 mRNA, whereas PPAR $\gamma$  activation downregulates PDK4 expression (141). PDK4 is downregulated in cardiac muscle tissue during HF (142).

CPT1 is an outer mitochondrial membrane enzyme (143). Membrane-impermeant long chain acyl-CoA requires CPT1A and CPT1B to enter mitochondria and undergo  $\beta$ -oxidation. Malonyl-CoA, the product of the first committed step in fatty acid synthesis, is usually derived from glucose. Malonyl-CoA physiologically inhibits CPT1A and CPT1B, thereby resulting in

strong control of fatty acid oxidation (FAO) flux. The increased levels of malonyl-CoA caused by hyperglycemia and hyperinsulinemia inhibit CPT1 (144,145).

#### *1.5.2.4 CD36, Lox 1, and ALOX15*

CD36 is a high affinity membrane scavenger receptor for long chain fatty acid that has been shown to facilitate net fatty acid uptake into muscle and adipose tissues in rodents and humans (146). CD36 contributes to the metabolic adjustments of muscle fatty acid uptake, whereas its deletion abolishes the muscle's metabolic flexibility and ability to adapt to fasting (147). In insulin resistant human muscle, CD36 trafficking is disrupted with chronic relocation of CD36 to the sarcolemma (148), which is associated with fatty acid accumulation. CD36 modulates myocardial Ca<sup>2+</sup> metabolism and fatty acid cycling into phospholipids (149).

Lectin-type oxidized LDL receptor 1 (Lox1) is a membrane scavenger receptor involved in internalization of oxidized LDL by endothelial cells. Lox1 has been found to be localized to endothelial cells (150), macrophages, platelets, cardiomyocyte and smooth muscle cells. Accumulating evidence supports its involvement not only in oxidized LDL internalization, but also in endothelial dysfunction, atherosclerosis, plaque instability, thrombogenesis, and innate immune responses (151). Lox1 expression increases when endothelial cells are exposed to shear stress (152). Lox1 activation by oxidized LDL contributes to the progression of fibrosis and cardiac dysfunction after ischemic insult or induced cardiomyopathy; consequently, drugs that block Lox1 might potentially be effective cardioprotective treatments of these diseases (153). Arachidonic acid lipoxygenase (ALOX15) is a lipid-peroxidizing enzyme (154). ALOX15 and its metabolites have both pro- and anti-inflammatory effects, and differential effects of the same metabolite may arise from their differential levels (155).

Moreover, 12/15-LOX is expressed in various cell types and organs of the body and has been implicated in a variety of diseases, including atherosclerosis, hypertension, diabetes, obesity, and neurodegenerative disorders. No specific LOX inhibitors are currently available (155).

### *1.5.3 Vasoactive determinants*

#### *1.5.3.1 Angiotensin receptors AT1 and AT2*

The renin-angiotensin system (RAS) is considered the major regulator of blood pressure and fluid homeostasis. The main effector molecule of the RAS, angiotensin (Ang) II, is produced from the substrate angiotensinogen through sequential enzymatic cleavages by renin and angiotensin converting enzyme (ACE). Renin cleaves angiotensinogen, thus forming Ang I, which in turn is converted to Ang II by ACE (Fig. 1). ACE is a circulating enzyme found in endothelial cells of the lungs, vascular endothelium, and cell membranes of the kidneys, heart, and brain. ACE also degrades bradykinin into inactive fragments and decreases the serum levels of endogenous vasodilators (156). Ang II increases systemic and local blood pressure via its vasoconstrictive effect, influences renal tubule retention of sodium and water, and stimulates aldosterone release from the adrenal glands (157). Beyond being a potent vasoconstrictor, Ang II exerts several prominent nonhemodynamic effects including proliferative, proinflammatory, and profibrotic activities (158). The binding of Ang II to Ang receptor type II (AT2) activates vasorelaxation of conduit and resistant arteries, improves resistance artery remodeling, promotes cardiovascular protection against ischemia-reperfusion injury and acute myocardial infarction, inhibits cardiac fibrosis, and protects the kidneys from ischemic injury (159).



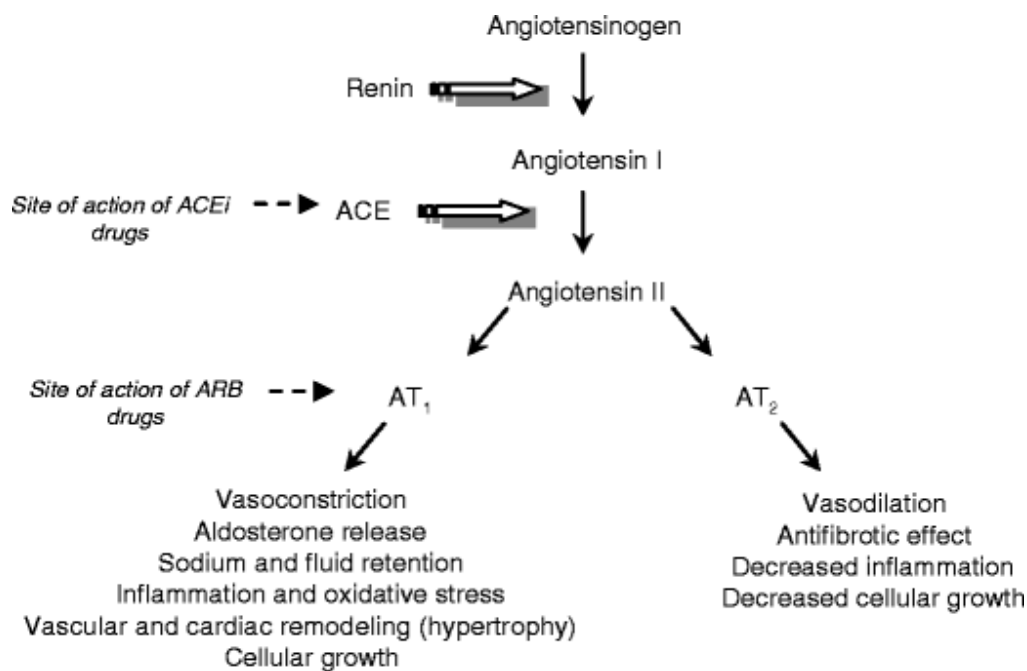


Figure 8. Overview of the renin-angiotensin system RAS. from Cassis et al. (160). ACE angiotensin converting enzyme; AT1R angiotensin type 1 receptor; AT2R angiotensin type 2 receptor; ARB angiotensin II receptor blockers.

### 1.5.3.2 ACE1 and ACE2

Angiotensin-converting enzymes 1 (ACE1) and 2 (ACE2) are central components of the RAS, which controls blood pressure by regulating the volume of fluids in the body, and converts the angiotensin I into the active vasoconstrictor angiotensin II (160). ACE participates to the kinin-kallikrein system, in which it degrades bradykinin, a potent vasodilator, and other vasoactive peptides (161). The ACE gene encodes two isozymes. A negative correlation between the ACE1 D-allele frequency and the prevalence and mortality of COVID-19 has been established (162).

### 1.5.3.3 eNOS and iNOS

Nitric oxide (NO) is a soluble gas endogenously produced by nitric oxide synthase (NOS) enzymes. In the heart, three NOS isoforms are present: neuronal NOS (nNOS or NOS1),

endothelial NOS (eNOS or NOS3), and inducible NOS (iNOS or NOS2). NOS1 and NOS3 are constitutively present, and their enzymatic activity is  $\text{Ca}^{2+}$ -dependent (163). NOS2 or iNOS is absent in healthy hearts, but its expression is induced by inflammation (164). In physiological conditions, NO exerts several functions in the myocardium, such as acceleration of relaxation (165). This effect is attributed to cGMP-dependent, protein kinase G (PKG)-mediated phosphorylation of troponin I, thereby leading to a decrease in myofilament  $\text{Ca}^{2+}$  sensitivity (166). Thus, sarcolemma-bound NOS3 or eNOS inhibits L-type  $\text{Ca}^{2+}$  channels and attenuates the  $\beta$ -adrenergic receptor-stimulated increase in myocardial contractility (167). eNOS has been reported to increase the ryanodine receptor (RyR) open probability ( $P_o$ ) and the amplitude of the  $\text{Ca}^{2+}$  transients under conditions of sustained myocardial stretch via a cGMP-independent mechanism (168). ACE inhibitors have been shown to enhance eNOS expression and NO bioavailability (169). eNOS expression levels have been shown to be diminished in HF (170). iNOS is now widely considered to be involved in various pathophysiological conditions of the myocardium, such as ischemia-reperfusion injury (171), aging (172), infarction (173), and HF (174). NOS2 has been found to contribute to contractile dysfunction (174). In contrast, studies have also found beneficial effects of NOS2 expression (175). This discrepancy may depend on which pathway is activated (cGMP-dependent or independent) and/or the end targets, which in turn may be dependent on the ROS levels in the heart (176).

#### *1.5.3.4 Kallikrein-kinin signalling*

The tissue kallikrein-associated peptidase family (KLK) is a group of trypsin- and chymotrypsin-like serine proteases with homology to parent tissue kallikrein (KLK1) (177). Kininogen is a well-known substrate of KLK members. Low-molecular weight kininogen is cleaved by KLK1, thus leading to the release of the vasoactive peptide kinin (178). Kinin in turn interacts with kinin receptors and exerts broad biological effects, such as vasodilation

(179), non-vascular smooth muscle contraction (180), and inflammation (181). Kinins have protective effects against myocardial ischemia/reperfusion insult or hypertrophy by interacting with two specific receptors: kinin B1 receptor (B1R) and B2 receptor (B2R) (182). Abnormalities in the KLK1–kinin system (KKS) are associated with cardiac hypertrophy (178). KLK8 induces cardiac hypertrophy but not through releasing kinin peptides (183).

#### *1.5.3.5 Bradykinin receptors*

Bradykinin B1 and B2 receptors (B1R and B2R) are transmembrane receptors belonging to the rhodopsin-like G protein-coupled receptor (GPCR) superfamily (184). The signaling of bradykinin receptors are mediated by kinins (185), which are produced when kininogens are cleaved by serine proteases in the KKS (186). B1R is generally absent in healthy tissues, and its expression is induced by injury and inflammation (187). In contrast, B2R is ubiquitously expressed throughout the body and is involved in vasodilation, osmoregulation, smooth muscle contraction, and nociceptor activation (184). B2R is more associated with cardiovascular disorders (184). The activation of B2R by kinins can induce vasodilatation, plasma extravasation, and cardioprotective effects (anti-hypertrophic, anti-proliferative, and anti-atherosclerotic action) (188). In contrast, B2R activation is associated with inflammation. In this context, B2R antagonists can effectively treat inflammation-associated cardiovascular diseases (184). The activation of B1R confers protection against cardiac ischemia (184); however, proinflammatory cytokines stimulate B1R in leukocyte recruitment and/or activation, which is involved in disorders such as atherosclerosis (189). B1R expression is also associated with hypertension and HF (190).

### 1.5.3.6 Calcium-dependent myocardial contraction

Sarcoplasmic/endoplasmic reticulum (SR) ATPase (SERCA, SR Ca<sup>2+</sup>-pump ATPase) plays a major role in Ca<sup>2+</sup> signaling (191) and is involved in various aspects of cell function (192), such as transcription (193), apoptosis, exocytosis, signal transduction (194), and cell motility (195). SERCA is responsible for the movement of Ca<sup>2+</sup> against the concentration gradient between the SR and the cytosol. The SR membrane contains Ca<sup>2+</sup>-pump ATPases that pump Ca<sup>2+</sup> ions into the tubular network. This active transport is required because Ca<sup>2+</sup> ions from the cytoplasm cannot passively enter the SR (196). The major component of the longitudinal SR is SERCA (197). The SERCA2a isoform is expressed in cardiac muscle, and pressure overload decreases SERCA2a mRNA levels (198). Ryanodin receptor (RyR), another major protein in the SR membrane, is responsible for the release of Ca<sup>2+</sup> from the intracellular stores during excitation-contraction (199). Mutations in isoform RyR2, the predominant form in the heart muscle, are associated with human disorders such as polymorphic ventricular tachycardia (200). Thus, SR Ca<sup>2+</sup>-release plays a critical role in inducing cardiac contraction, and alterations in its signaling and function are also considered to be involved in the genesis of cardiac arrhythmias and fibrillation (201). The main role of RyR2 is Ca<sup>2+</sup>-release for the generation of cardiac contractile force (202). The sensitivity of RyR has been shown to govern the stability and synchrony of Ca<sup>2+</sup>-release during excitation-contraction coupling in the heart (203). SR Ca<sup>2+</sup>-release is not only regulated by phosphorylation and dephosphorylation (204), but also modulated by glycation and oxidation (205). The L-type Ca<sup>2+</sup> channel  $\alpha$ 1C-subunit gene (*Cacna1c*) plays an essential role in cardiac excitation-contraction coupling (206). This protein is localized in the T-tubule sarcolemma adjacent to RyR2, where it controls Ca<sup>2+</sup> influx from the extracellular milieu into the cytosol and thus serves as a major determinant of cardiac function. Beta-adrenergic receptor stimulation increases the number of L-type channels at the sarcolemma,

thereby enhancing  $\text{Ca}^{2+}$  influx and amplifying excitation-contraction coupling (207). Prolonged AT1 signaling via decreased L-type  $\text{Ca}^{2+}$  channels result in a negative inotropic effect (207).

The SLC8A1 gene encodes the  $\text{Na}^+/\text{Ca}^{2+}$  exchanger (NCX1) (208). The plasma membrane (PM)  $\text{Ca}^{2+}$  ATPase and  $\text{Na}^+/\text{Ca}^{2+}$  exchanger are two major systems that extrude  $\text{Ca}^{2+}$  from cells (209). Because NCX mediates an electrogenic ion-exchange stoichiometry ( $3\text{Na}^+ : \text{Ca}^{2+}$ ), it can operate in either forward ( $\text{Ca}^{2+}$ -extrusion) or reverse ( $\text{Ca}^{2+}$ -entry) mode, depending on intracellular and extracellular  $\text{Na}^+$  and  $\text{Ca}^{2+}$  concentrations and the membrane potential (210). In steady-state conditions, forward mode NCX removes nearly all  $\text{Ca}^{2+}$  that has entered cells during depolarization (211). Under normal conditions,  $\text{Ca}^{2+}$  release from the SR is triggered by  $\text{Ca}^{2+}$  entry into cells through the L-type  $\text{Ca}^{2+}$  current, whereas under abnormal conditions,  $\text{Ca}^{2+}$  is released spontaneously from the SR as a  $\text{Ca}^{2+}$  wave (212) after the SR  $\text{Ca}^{2+}$  content exceeds a threshold level (213). These  $\text{Ca}^{2+}$  waves activate electrogenic  $\text{Na}^+/\text{Ca}^{2+}$  exchange, and the resulting current has been implicated in cardiac arrhythmias (211). Heart muscle cells adapt to both acute and chronic changes in the circulatory demands of the body. Short-term adaptation is mediated by phosphorylation and de-phosphorylation of cytosolic proteins involved in contraction, excitability, and signaling. Over the long term, these same kinases and phosphatases modulate the cardiac phenotype through the activation of a myriad of transcription factors. A central pathway is mediated by  $\text{Ca}^{2+}$ -calmodulin-dependent protein kinase II (CaMKII), which translates changes in  $[\text{Ca}^{2+}]_i$  into corresponding levels of kinase activity. In cardiac muscle cells, CaMKII phosphorylates cytosolic targets, such as L-type  $\text{Ca}^{2+}$  channels (LTCCs), RyRs, and the SERCA-regulating protein phospholamban, thus establishing positive feedback between the cardiomyocyte beating rate and  $\text{Ca}^{2+}$  signaling through  $\text{Ca}^{2+}$ -dependent facilitation of plasmalemmal calcium flux and enhanced SR  $\text{Ca}^{2+}$  dynamics (214).

However, under excessive cytosolic CaMKII activity, this physiological feedback becomes maladaptive. In the presence of acute overexpression of cytosolic CaMKII, excessive

phosphorylation of CaMKII target proteins alters cardiomyocyte calcium signaling to a profile similar to that seen in cardiac failure models (215). Furthermore, long-term potentiation of CaMKII activity by transgenic overexpression of cytosolic CaMKII leads to cardiac hypertrophy and failure (216).

## 2. General hypothesis and Aims of the research work

AR is a valvular heart disease associated with higher morbidity and mortality than that in the general population (30,37,38,41,42,43). Chronic severe AR imposes a combined LV volume and pressure overload. Volume increase is a direct consequence of the regurgitant volume itself, whereas pressure overload results from increased parietal stress and systolic hypertension (19). In early compensated severe AR, the LV adapts to the volume overload via eccentric hypertrophy (20). Over time, progressive LV dilation and systolic hypertension increase wall stress, and the volume/mass ratio of the LV (29), thereby impairing LV systolic function, leading to clinical signs of heart failure, and finally becoming irreversible and lethal (31,32). Rats have been found to develop progressive LV dilatation and eccentric hypertrophy after chronic LV volume overload, as well as progressive irreversible LV systolic dysfunction, thus closely mimicking the progression of the disease that occurs over a much longer time span in humans (217). OM is a cardiac myosin activator that increases the proportion of myosin heads bound to actin, thereby creating a force-producing state that is not associated with cytosolic calcium accumulation and has no effect on  $\text{Ca}^{2+}$  homeostasis (57). OM accelerates the transition of myosin from the weakly actin-bound state to the strongly actin-bound state, as measured by the release of hydrolyzed phosphate (Pi).

OM appears to shift the equilibrium toward myosin ATP hydrolysis without affecting the rate of hydrolysis, in addition to accelerating the rate of Pi release. OM decreases the rate of Pi release when actin is removed. This decrease in actin-independent ATP hydrolysis potentially

increases the overall energetic efficiency of the system by decreasing ATP utilization not associated with mechanical work (57). Consequently, OM increases the systolic ejection duration without changing the rate of left ventricular pressure development (57,64). In two different canine models of pacing-induced systolic heart failure after myocardial infarction, and in the presence of left ventricular hypertrophy (64), OM increases the systolic ejection time, improves global cardiac function and cardiac myocyte fractional shortening, and does not significantly increase LV myocardial oxygen consumption or myocyte intracellular calcium (64). A major determinant of myocardial oxygen consumption is peak systolic wall stress (218). Resting LV myocardial oxygen consumption and wall stress also exhibit a linear relationship, in which a doubling of the wall tension approximately doubles LV oxygen consumption (219).

**Regarding these data on OM and AR, we tested the hypothesis that cardiac myosin activation with OM might improve LV function in a rat-model of chronic severe AR. Given that OM increases systolic ejection time and cardiac function, we sought to determine whether AR severity and LV wall stress might be affected by OM.** To test our hypothesis, we examined cardiac measurements and hemodynamic parameters in AR and sham rats receiving OM infusion, and AR rats receiving placebo infusion. AR increases LV wall stress (29,31,32); subsequently, cardiac fibroblasts and cardiomyocytes release sST2 in response to stress and overload, and circulating levels of this protein reflects the degree of myocardial stress, ventricular remodeling, and fibrosis (102). Moreover, the release of NT-proBNP indicates increases in ventricular wall stress and myocardial hypertrophy in states of pressure and/or volume overload (83). The effects of AR on sST2 and NT-proBNP, as well as the effects of OM-mediated increases in cardiac contraction strength on these parameters, are unknown in rodents. **We tested the hypothesis that severe chronic AR increased NT-proBNP and sST2 in rats in relation to changes in LV morphology and function. In addition, we anticipated that OM administration in AR might exert differential effects on**

**sST2 and NT-proBNP, given the importance of myocardial stress in sST2 release.** To test our hypothesis, in AR and sham rats receiving OM infusion, and AR rats receiving placebo infusion, cardiac measurements, hemodynamic parameters, and sST2 and NT-pro-BNP plasma levels were examined. As described above, OM increased the systolic ejection time, and improved global cardiac function and cardiac myocyte fractional shortening, but did not significantly increase LV myocardial oxygen consumption or myocyte intracellular calcium (64). In contrast, the administration of OM has been found to increase myocardial oxygen consumption in a pig model of HF (65). Although the data suggested that the administration of OM may increase O<sub>2</sub> consumption, the findings were not fully consistent with the OM-mediated inhibition of baseline myosin ATPase activity observed in vitro (67). Similarly, Nagy et al. (68) have reported that OM-treated myofilaments are sensitized to Ca<sup>2+</sup> in an exposed rat myocyte model, whereas Utter et al. (70) have found that OM re-sensitized myofilaments exhibit diminished Ca<sup>2+</sup> sensitivity in a mouse model of dilated cardiomyopathy. Gene expression profiles have been established in several animal models of AR, including a rat model in early (2 week) and late stages of the disease (220,221). **We tested the hypothesis that OM and AR mediated changes in gene expression in the adult rat myocardium, with a particular emphasis on the pathways associated with apoptosis, oxidative stress, energy substrate metabolism, and Ca<sup>2+</sup>-mediated cardiac contractility.** To test our hypothesis, OM or placebo were infused in rats with or without AR. Cardiac measurements, hemodynamic parameters, and LV myocardial gene expression were then examined.



### 3. Methods

#### 3.1 Effects of omecamtiv mecarbil on cardiac function, aortic regurgitation and LV wall stress in an experimental rat's model

This paragraph describes the material and methods used for the 2 first randomized, interventional studies, conducted on healthy adult Wistar rats. The first study evaluated the effects of OM on the LV and on the degree of AR in rats with severe chronic AR (229); the second study evaluated the effects of OM on LV wall stress and the degree of AR, with a different anesthesia technique and a more accurate measurement of AR (230). The experimental procedure and measurements will be explained in details in the following chapters. Both experimental studies were approved by the Institutional Animal Care and Use Committee of the *Université Libre de Bruxelles (644N)*. Studies were conducted in accordance with the Guide for the Care and Use of Laboratory Animals published by the National Institutes of Health (NIH Publication No. 85–23, revised 1996).

##### 3.1.1 Experimental animals

In the first study, twenty-four male adult Wistar rats ( $401 \pm 90$  g body weight) were randomized to a sham intervention ( $n = 4$ ) or to AR creation ( $n = 20$ ). Rats that survived the acute phase ( $n = 12$ ) was randomized into an OM group ( $n = 7$ ) or a placebo group ( $n = 5$ ). The 4 rats (two in the OM group and two in the placebo group) who underwent a sham operation served as control for the effect of time and measurement repetition on the parameters investigated.

For the second study, forty male adult Wistar rats ( $486 \pm 49$  g body weight) were separated into two groups: sham intervention ( $n = 6$ ) or AR induction ( $n = 34$ ). Rats that survived AR induction

or the acute phase (n = 18) were randomized into the OM (n = 8) or placebo (n = 10) groups. Rats that underwent the sham intervention (n = 6) also received OM and served as controls to assess the effect of time and repeated measurements on the variables investigated in the study.

### 3.1.2 Anesthesia and surgical procedure

In the first study, the animals were anesthetized with an intraperitoneal injection of 75 mg/kg of ketamine and 0.25 mg/kg of medetomidine. In the second study, the animals were anesthetized using 1.5% inhaled isoflurane. The same surgical procedure was performed in the both studies. The right internal carotid artery was surgically exposed and ligated distally; subsequently, a transverse arteriotomy was performed, through which a fixed-core wire guide (0.025-inch diameter; Cook Inc, IN, USA) was advanced toward the aortic valve in a retrograde manner to tear the valve leaflets and induce AR. The following echocardiographic criteria after achieving a popping sensation at the time of surgery were used to include animals in the study: (1) a jet extent greater than 30% of the length of the LV, and (2) a color-Doppler ratio of regurgitant jet width to LV outflow tract diameter greater than 50% (222). The six sham-operated animals underwent cannulation of the right carotid artery without aortic valve puncture. Animals were closely observed during the first hours and days after surgery for any sign of respiratory distress suggestive of acute HF. Pre- and post-surgery analgesia was administered.

### 3.1.3 Cardiac measurements

Heart rate (HR) and rhythm were monitored via limb leads throughout the procedure. Transthoracic 2D, M-mode and Doppler echocardiography were performed under general

anesthesia with an ultrasound unit (Vivid-7, GE Healthcare, US) equipped with a 10-Mhz surgical transducer in the first study and (Vivid-E90, GE Healthcare) equipped with a 12-MHz phased-array transducer (GE 12S-D, GE Healthcare) in the second study.

Rats were placed in the right and left lateral recumbent positions and their electrocardiogram was monitored via limb leads throughout the procedure. All measurements were made according to the recommendations of the American Society of Echocardiography currently applied to humans (222). Standard right parasternal (long and short axis) and left apical parasternal views were used for data acquisition. Left atrial size was assessed in right parasternal short axis at the level of the aorta. Diastolic (d) and systolic (s), septal wall thickness (SWT), posterior wall thickness (PWT) and LV diameters (LVEDD, LVESD) were measured in M-mode from a LV short axis view at the level of chordae tendinae and fractional shortening (FS) was calculated. Ejection fraction (EF) were derived using the Teicholz formula. Left ventricle mass was calculated using the American Society of Echocardiography recommended formula:  $LV\ mass = 0.8 \times \{1.04[(LVEDD + PWTd + SWTd)^3 - (LVEDD)^3]\} + 0.6\ g$ . Aortic diameter was measured from the right long axis parasternal view. Aortic flow was measured from the left apical view to calculate forward stroke volume (SV) and cardiac output and to measure pre-ejection period (PEP: delay from Q wave of QRS to aortic opening, msec), LV ejection time (LVET: interval from beginning to termination of aortic flow, msec), and inter-beat interval (RR). Systolic time was determined as PEP + LVET (msec). Diastolic time (msec) consists in RR interval (msec) - systolic time (msec). PEP/LVET ratio was also calculated. PEP/LVET is a more useful index of overall LV performance (223). This ratio is better correlated with other LV performance measurements than either PEP or LVET, and is considered independent of HR (224).

In the first study, severity of the regurgitant aortic jet was subjectively graded (1 to 4). In the second study, the severity of the regurgitated aortic jet was objectively evaluated by measuring

the pressure half-time (PHT) of the AR jet using a continuous-wave Doppler. A PHT of <200 msec was considered indicative of severe AR. Relative wall thickness (RWT) was calculated using the formula  $RWT = 2 \cdot PWTd / LVEDD$ , where PWTd is the posterior wall thickness at end-diastole (mm).

#### 3.1.4 Calculation of wall stress variables

Wall stress was calculated based on Laplace's law ( $\sigma = P \times r / 2w$ , where  $\sigma$  is the wall stress, P is the left intraventricular pressure, r is the LV diameter, and w is the wall thickness.) Wall stress—the true measure of LV afterload—decreases during ejection and is twice as high in protosystole as in telesystole. The calculation of maximum stress ( $\sigma_{max}$ ) must be performed at maximum systolic pressure using the telediastolic diameter, which is that of protosystole before it shortens during ejection as follows:  $\sigma_{max} = (P_{smax} \cdot Dtd) / 2w$ , where P is the maximum systolic pressure, D is the LVEDD, and w is the end-diastolic wall thickness. End-systolic wall stress ( $\sigma_{es}$ ) is calculated using the formula  $\sigma_{es} = P_{es} \cdot Dts / 2w$ , where  $P_{es}$  is the end-systolic pressure, Dts is the LVESD, and w is the end-systolic wall thickness. Wall stress on diastole ( $\sigma_d$ ) was also calculated:  $\sigma_d = P_d \cdot Dtd / 2w$ , where  $P_d$  is the diastolic pressure.

#### 3.1.5 Invasive blood pressure measurement

Invasive arterial pressures were measured with a micro manometer (rodent catheter 1.6 F, Transonic Systems Inc.) inserted in the right common carotid artery before and after the induction of AR (only once in sham-operated rats) and the left femoral artery for all rats before and after injection of OM or placebo (2 months after induction of AR). The micro manometer

was connected to a data acquisition system (ADV500PV system, Transonic Systems Inc.) to capture hemodynamic measurements.

### 3.1.6 Experimental design

Doppler echocardiography was performed before AR induction (corresponding to baseline time) during surgery to confirm the presence and the severity of AR. Doppler echocardiography was performed again 2 months after the induction of AR, both before and after the infusion of OM (1.2 mg/kg/hour) or placebo (0.9% NaCl). In the treatment groups, animals received equal volumes (12 mL/kg) of placebo or OM through a femoral vein perfusion for 30 min. This procedure allowed to achieve a plasma concentration of around 400 ng/mL of OM in a previous study (225). Doppler echocardiography was performed immediately after the 30-min infusion. All the animals remained alive during these experimental sessions. Five rats with placebo infusion and 7 rats with OM infusion were included in the first study. In the second study, there were 10 rats with placebo infusion and 8 rats with OM infusion.

### 3.1.7 Statistical analyses

Statistical analyses are described hereafter for published article.

#### *Part 1: El Oumeiri et al (229)*

Results are expressed as mean  $\pm$  standard deviation (SD). A 2-factor ANOVA for repeated measures followed by post-hoc Bonferroni corrections for multiple comparisons was used to assess the effects of OM *versus* placebo, and any interaction between them, after 2 months of AR in the 16 animals. All other statistical analysis consisted of paired-t tests between variables. Significance was set at a p-value less than 0.05. Statistical analysis was performed with the SPSS 23.0 program (IBM, Chicago, Ill, USA).

#### *Part 2: El Oumeiri B et al (230)*

Results are expressed as mean  $\pm$  standard deviation (SD). Data were analyzed using a two-

factor analysis of variance (ANOVA) for repeated measures. Inter-group differences were tested using two-way ANOVA. If the F ratio of the ANOVA reached the threshold p-value of <0.05, further comparisons were made using the parametric Student's t test. A p-value of <0.05 was considered to be significant (SPSS 23.0, IBM Corp.).

### 3.2 Effects of omecamtiv mecarbil and aortic regurgitation on cardiac biomarkers in an experimental rat model

#### 3.2.1 Study protocol

In this part of the study, circulating plasma levels of cardiac biomarkers, sST2 and NT-proBNP, were measured in rats 2 months after the creation of AR with or without OM infusion. The experimental protocol was approved by the Institutional Animal Care and Use Committee of the *Université Libre de Bruxelles (644N)*. Experiments were conducted in accordance with the Guide for the Care and Use of Laboratory Animals published by the National Institutes of Health (NIH Publication No. 85-23; revised 1996). This part of the study included 24 male adult Wistar rats (weighting  $482 \pm 57$  g). Six rats were assigned to a sham intervention and 18 rats underwent induction of AR. The 18 rats that were subjected to AR induction, were randomly assigned to OM (n = 8) or placebo (n = 10) treatment. AR was induced under general anesthesia (1.5% inhaled isoflurane) by retrograde puncture of the aortic valve leaflet as described above the six rats assigned to the sham group underwent cannulation of the right carotid artery under general anesthesia without aortic valve puncture. Cardiac measurements were similar as those described above.

#### 3.2.2 Study Design

Doppler-echocardiography was performed before the induction of AR induction (at baseline time) and during the surgical procedure to confirm the presence and severity of the lesion. Doppler echocardiography was performed again 60 days after the experimental induction of

AR in these rats. Rats with AR in the OM treatment (n = 8) and placebo (n = 10) groups received equal volumes (12 mL/kg body weight) of OM (1.2 mg/kg/hr) or placebo 0.9% NaCl, respectively, via a 30-min infusion through the femoral vein. Rats that underwent the sham intervention (n = 6) received the same dose of OM.

### 3.2.3 Measurements of plasma levels of sST2 and NT-proBNP

Blood samples were obtained from each rat by venipuncture under general anesthesia (1.5% inhaled isoflurane) on the day of the surgery immediately before (baseline) and two months after the induction of AR (or sham procedure, i.e., before infusion of OM or placebo), and 1, 2, and 7 days thereafter. Samples were collected into vacuum blood collection tubes (BD Vacutainer, Plymouth, UK) with ethylenediaminetetraacetic acid (EDTA) as the anticoagulant. Tubes were centrifuged immediately after collection at 3000 rpm and 4°C for 15 min to obtain plasma, which was separated in multiple aliquots and stored at -80°C until analysis. Plasma levels of sST2 were measured using a rat ST2 ELISA Kit (MYBIOSOURCE, San Diego, CA, USA). The detection range for sST2 assay kit was 62.5-2000 pg/mL. Plasma levels of NT-proBNP were measured using a rat NT-proBNP ELISA Kit (MYBIOSOURCE, San Diego, CA, USA). Plasma levels of sST2 and NT-proBNP were measured using electrochemiluminescence immunoassay GLOMAX multi detection system (Promega Corporation, Madison, WI, USA). The lower limit of detection for the NT-proBNP assay kit was 5 pg/mL, with a functional sensitivity of <50 pg/mL and working range (imprecision profile  $\leq 10\%$  coefficient of variation) that extended to ~35 000 pg/mL. The assays were carried out as per the manufacturer's instructions. Results were presented as the mean value of duplicated experiments. Laboratory technicians were blinded as to the specific characteristics of each sample.

### 3.2.4 Statistical analysis

Statistical analyses are described hereafter for the published article.

*El Oumeiri et al (231)*

Results are presented as mean  $\pm$  SD. Data were analyzed using a two-factor analysis of variance (ANOVA) for repeated measures. Inter-group differences were tested using a two-way ANOVA. If the F ratio of the ANOVA reached the threshold p-value of  $<0.05$ , further comparisons were made using the parametric Student's t-test. A p-value of  $<0.05$  was considered to be significant (SPSS 23.0, IBM Corp., Armonk, NY). Correlations were analyzed parametrically by Pearson's rank correlation.

### 3.3 Effects of omecamtiv mecarbil and aortic regurgitation on left ventricle in an experimental rat's model

Here, we described materials and methods used for the realization of two studies evaluating myocardial changes in gene expression profile in adult rats with a particular emphasis on pathways associated with apoptosis, oxidative stress, energy substrate metabolism, and  $\text{Ca}^{2+}$ -mediated cardiac contractility, 1) after OM infusion and 2) induced by AR. Both studies were approved by the Institutional Animal Care and Use Committee of the Faculty of Medicine of the *Université Libre de Bruxelles* (ULB; Brussels, Belgium; protocol acceptance number: 644N). Experiments were conducted in accordance with the Guide for the Care and Use of Laboratory Animals published by the United States National Institutes of Health (NIH Publication No. 85-23; revised 1996).



### 3.3.1 Protocol and experimental design

In the first study, fourteen adult male Wistar rats (Janvier, Le Genest-Saint-Isle, France) were randomly assigned to intravenous administration of OM (1.2 mg/kg/hour for 30 min via the femoral vein; n=6; mean body weight:  $553 \pm 38$  g) or placebo (n=8; mean body weight:  $536 \pm 39$  g) on day 0. Dose of OM was chosen to achieve peak plasma concentrations of  $\sim 400$  ng/mL, as previously reported (13). Seven days after OM infusion, OM- and placebo-treated rats were sacrificed by exsanguination via section of the abdominal aorta. The hearts were rapidly harvested and dissected to isolate the LV, which was snap-frozen in liquid nitrogen and stored at  $-80^{\circ}\text{C}$  for further biological analysis.

In the second study, 18 male adult Wistar rats (Janvier, Le Genest-Saint-Isle, France). Ten rats (mean body weight:  $577 \pm 24$  g) has aortic regurgitation (AR) created two months before AR was induced under general anesthesia (1.5% inhaled isoflurane) by retrograde puncture of the aortic valve leaflet as previously described. The other group (n=8) served as control group (mean body weight:  $536 \pm 39$  g). Rats with AR (n = 10) and the group control (n = 8) received equal volumes (12 ml/kg body weight) of 0.9% NaCl, respectively, via a 30 min infusion through the femoral vein. Seven days after saline infusion rats were sacrificed by exsanguination via section of the abdominal aorta. The hearts were rapidly harvested and dissected to isolate the LV, which was snap-frozen in liquid nitrogen and stored at  $-80^{\circ}\text{C}$  for further biological analysis. IN both studies Cardiac measurements are the same as described before.

### 3.3.2 Real-time quantitative polymerase chain reaction (RTq-PCR)

In both studies, total RNA was extracted from snap-frozen LV myocardial tissue using TRIzol reagent (Invitrogen, Merelbeke, Belgium) followed by a chloroform/ethanol extraction and a

final purification using QIAGEN RNeasy® Mini kit (QIAGEN, Hilden, Germany), according to manufacturer's instructions. RNA concentration was determined by standard spectrophotometric techniques, using a spectrophotometer Nanodrop® (ND-1000; Isogen Life Sciences, De Meern, The Netherlands) and RNA integrity was assessed by visual inspection of GelRed (Biotium, Hayward, California)-stained agarose gels. Reverse transcription was performed using random hexamer primers and Superscript II Reverse Transcriptase (Invitrogen, Merelbeke, Belgium) according to the manufacturer's instructions. Gene-specific sense and antisense primers for RTq-PCR (Table 2 and Table 3) were designed using the Primer3 program for *rattus norvegicus* gene sequences, including those for B-cell lymphoma 2 (Bcl2), Bcl2 associated X apoptosis regulator (Bax), glutathione peroxidase (Gpx), glutathione-disulfide reductase (Gsr), superoxide dismutases 1 and 2 (Sod1 and Sod2), AMP-activated protein kinase (Ampk), peroxisome proliferator-activated receptors alpha and gamma (Ppar alpha and gamma), solute carrier family 2 members 1 (Slc2a1, also known as Glut1) and 4 (Slc2a4 or Glut4), pyruvate dehydrogenase kinase (Pdk4), carnitine palmitoyltransferase1 (Cpt1), fatty acid transporter Cd36, oxidized low-density lipoprotein receptor 1 (Olr1, also known as Lox1), arachidonate 15-lipoxygenase (Alox15), angiotensin II receptor type 1a (Agtr1a, also known as AT1), angiotensin II receptor type 2 (Agtr2, also known as AT2), angiotensin converting enzymes 1 and 2 (ACE1 and ACE2), nitric oxide synthases 2 and 3 (Nos2, also called inducible NOS or iNOS and Nos3, also called endothelial NOS or eNOS), AT1, AT2, ACE1, ACE2, Nos2 and Nos3, kallikrein related-peptidases 8 and 10 (Klk8 and Klk10), kallikrein 1-related peptidases C2 and C12 (Klk1c2 and Klk1c12) only in the first study, bradykinin receptors B1 and B2 (Bdkrb1 and Bdkrb2), ATPase sarcoplasmic/endoplasmic reticulum Ca<sup>2+</sup> transporting 2 (Atp2a2, also called Serca2), ryanodine receptor 2 (Ryr2), calcium voltage-gated channel subunit alpha1C (Cacna1c), solute carrier family 8 member A1 (Slc8a1), Ca<sup>2+</sup>/calmodulin-dependent protein kinase II delta

(Camk2d) Slc8a1 and camk2d, glyceraldehyde-3-phosphate dehydrogenase (Gapdh) and hypoxanthine phosphoribosyltransferase 1 (Hprt1) used as housekeeping genes.

Intron-spanning primers were selected whenever possible to avoid inappropriate amplification of contaminant genomic DNA. Amplification reactions were performed in duplicate using SYBRGreen PCR Master Mix (Quanta Biosciences, Gaithersburg, MD, USA), specific primers, and diluted template cDNA. Analysis of the results was performed using an iCycler System (BioRad Laboratories, Hercules, CA, USA). Relative quantification was achieved using the Pfaffl method (226) by normalization with the housekeeping genes, Gapdh and Hprt1.

Genes		Primer Sequences
<b>Glycerol-3-phosphate dehydrogenase (GAPDH)</b>	<i>Sense</i>	5' – AAGATGGTGAAGGTCGGTGT – 3'
	<i>Antisense</i>	5' – ATGAAGGGGTCGTTGATGG – 3'
<b>Hypoxanthine guanine phosphoribosyl transferase (HPRT)</b>	<i>Sense</i>	5' – ACAGCCAGACTTTGTTGGA – 3'
	<i>Antisense</i>	5' – ATCCACTTTCGCTGATGACAC – 3'
<b>AMP-activated protein kinase (Ampk)</b>	<i>Sense</i>	5' – TTCGGGAAAGTGAAGGTGGG – 3'
	<i>Antisense</i>	5' – TCTCTGCGGATTTTCCCGAC – 3'
<b>Angiotensin converting enzyme 1 (ACE1)</b>	<i>Sense</i>	5' - AGTGGGTGCTGCTCTTCTA - 3'
	<i>Antisense</i>	5' - GGAGGCTGTGATGGTTATGG - 3'
<b>Angiotensin converting enzyme 2 (ACE2)</b>	<i>Sense</i>	5' - GCCTTGAAAATGTGGTAGG - 3'
	<i>Antisense</i>	5' - TTCAGCCAGACAAACAATGG - 3'
<b>Angiotensin II receptor type 1a (Agtr1a or AT1)</b>	<i>Sense</i>	5' – ACATTCTGGGCTTCGTGTTC – 3'
	<i>Antisense</i>	5' – CATCATTTCTTGGCGTGTTC – 3'
<b>Angiotensin II receptor type 2 (Agtr2 or AT2)</b>	<i>Sense</i>	5' – TGCTCTGACCTGGATGGGTA – 3'
	<i>Antisense</i>	5' – AGCTGTTTGGTGAATCCCAGG – 3'
<b>Arachidonate 15-lipoxygenase (Alox15)</b>	<i>Sense</i>	5' - GCACTCTCCGTCCATCTTG - 3'
	<i>Antisense</i>	5' - GCTTCTCCATTGTGCTTCCT - 3'
<b>ATPase sarcoplasmic/endoplasmic reticulum Ca<sup>2+</sup> transporting 2 (Atp2a2 or Serca2)</b>	<i>Sense</i>	5' – GCAGGTCAAGAAGCTCAAGG – 3'
	<i>Antisense</i>	5' – TCTCTGCGGATTTTCCCGAC – 3'
<b>Bcl2 associated X apoptosis regulator (Bax)</b>	<i>Sense</i>	5' - CGTGGTTGCCCTCTTCTACT - 3'
	<i>Antisense</i>	5' - TCACGGAGGAAGTCCAGTGT - 3'
<b>B-cell lymphoma 2 (Bcl2)</b>	<i>Sense</i>	5' - TTTCTCTGGCTGTCTCTGAA - 3'
	<i>Antisense</i>	5' - CATATTTGTTTGGGGCAGGT - 3'
<b>Bradykinin receptor B1 (Bdkrb1)</b>	<i>Sense</i>	5' - AAGCTACGTGCCTGCTCATC - 3'
	<i>Antisense</i>	5' - CGGGGACGACTTTAACAGAG - 3'
<b>Bradykinin receptor B2 (Bdkrb2)</b>	<i>Sense</i>	5' - GCTGTCGTGGAAGTGGCTAT - 3'
	<i>Antisense</i>	5' - AAGGTCCCCTTATGAGCAGA - 3'

<b>Ca<sup>2+</sup>/calmodulin-dependent protein kinase II delta (<i>Camk2d</i>)</b>	<i>Sense</i>	5' – ATCCACAACCCTGATGGAAA – 3'
	<i>Antisense</i>	5' – GCTTTCGTGTTTCACGTCT – 3'
<b>Ca<sup>2+</sup> voltage-gated channel subunit alpha1 C (<i>Cacna1c</i>)</b>	<i>Sense</i>	5' – CCTATTTCCGTGACCTGTGG – 3'
	<i>Antisense</i>	5' – GGAGGGACTTGATGGTGTGG – 3'
<b>Carnitine palmitoyltransferase 1 (<i>Cpt1</i>)</b>	<i>Sense</i>	5' – AAGAACACGAGCCAACAAGC – 3'
	<i>Antisense</i>	5' ACCATACCCAGTGCCATCAC – 3'
<b>CD36 fatty acid transporter (<i>Cd36</i>)</b>	<i>Sense</i>	5' - TTCTGCTTTCTCATCGCCG - 3'
	<i>Antisense</i>	5' - GGATGTGGAACCCATAACTGG - 3'
<b>Glutathione peroxidase (<i>Gpx</i>)</b>	<i>Sense</i>	5' - CCGACCCCAAGTACATCATT - 3'
	<i>Antisense</i>	5' - AACACCGTCTGGACCTACCA - 3'
<b>Glutathione-disulfide reductase (<i>Gsr</i>)</b>	<i>Sense</i>	5' - GCCGCCTGAACAACATCTAC - 3'
	<i>Antisense</i>	5' - CTTTTTCCCGTTGACTTCCA - 3'
<b>Kallikrein-related-peptidase 8 (<i>Klk8</i>)</b>	<i>Sense</i>	5' -CGGAGACAGATGGGTCCTAA - 3'
	<i>Antisense</i>	5' - ATCTCTTGCTCGGGCTCAT - 3'
<b>Kallikrein-related-peptidase 10 (<i>Klk10</i>)</b>	<i>Sense</i>	5' - GCAGGTCTCCCTCTCCATA - 3'
	<i>Antisense</i>	5' - CAGTGGCTTATTTCTCCAGCA - 3'
<b>Kallikrein 1-related peptidase C2 (<i>Klk1c2</i>)</b>	<i>Sense</i>	5'- CAGGAGAGATGGAAGGAGGA - 3'
	<i>Antisense</i>	5' - CGGTGTTTTGGGTTTAGCAC - 3'
<b>Kallikrein 1-related peptidase C12 (<i>Klk1c12</i>)</b>	<i>Sense</i>	5' - CATCAAAGCCCACACACAGAT - 3'
	<i>Antisense</i>	5' - AAGCACACCATCACAGAGGAG - 3'
<b>Nitric oxide synthase 2 (<i>NOS2</i> or <i>iNOS</i>)</b>	<i>Sense</i>	5' - GTTTCCTCCAGATCCTCACT - 3'
	<i>Antisense</i>	5' - CTCTCCATTGCCCCAGTTT - 3'
<b>Nitric oxide synthase 3 (<i>NOS3</i> or <i>eNOS</i>)</b>	<i>Sense</i>	5' - GGTATTTGATGCTCGGGACT - 3'
	<i>Antisense</i>	5' - TGATGGCTGAACGAAGATTG - 3'
<b>Oxidized low density lipoprotein receptor 1 (<i>Olr1</i> or <i>Lox1</i>)</b>	<i>Sense</i>	5' -CATTACCTCCCCATTTT - 3'
	<i>Antisense</i>	5' - GTAAAGAAACGCCCTGGT - 3'
<b>Peroxisome proliferator-activated receptor alpha (<i>Ppar alpha</i>)</b>	<i>Sense</i>	5' – TTAGAGGCGAGCCAAGACTG – 3'
	<i>Antisense</i>	5' – CAGAGCACCAATCTGTGATGA – 3'
<b>Peroxisome proliferator-activated receptor gamma (<i>Ppar gamma</i>)</b>	<i>Sense</i>	5'– GCGCTAAATTCATCTTAACTC – 3'
	<i>Antisense</i>	5' – CTGTGTCAACCATGGTAATTT – 3'
<b>Pyruvate dehydrogenase kinase 4 (<i>Pdk4</i>)</b>	<i>Sense</i>	5' - GAGCCTGATGGATTTAGTGGA - 3'
	<i>Antisense</i>	5' - CGAACTTTGACCAGCGTGT - 3'
<b>Ryanodine receptor 2 (<i>Ryr2</i>)</b>	<i>Sense</i>	5' – GGAACTGACGGAGGAAAGTG – 3'
	<i>Antisense</i>	5' – GAGACCAGCATTTGGGTTGT – 3'
<b>Solute carrier family 2 member 1 (<i>Slc2a1</i> or <i>Glut1</i>)</b>	<i>Sense</i>	5' - TCTTCGAGAAGGCAGGTGTG - 3'
	<i>Antisense</i>	5' - TCCACGACGAACAGCGAC - 3'
<b>Solute carrier family 2 member 4 (<i>Slc2a4</i> or <i>Glut4</i>)</b>	<i>Sense</i>	5' - AGGCCGGGACACTATACCC - 3'
	<i>Antisense</i>	5' - TCCCCATCTTCAGAGCCGAT -5'
<b>Solute carrier family 8 member A1 (<i>Slc8a1</i>)</b>	<i>Sense</i>	5' – GAGATTGGAGAACCCCGTCT – 3'
	<i>Antisense</i>	5' – AGTGGCTGCTTGTTCATCGTA – 3'
<b>Superoxide dismutase 1 (<i>Sod1</i>)</b>	<i>Sense</i>	5' - GGTCCACGAGAAACAAGATGA - 3'
	<i>Antisense</i>	5' - CAATCACACCACAAGCCAAG - 3'
<b>Superoxide dismutase 2 (<i>Sod2</i>)</b>	<i>Sense</i>	5' -AAGGAGCAAGGTCGCTTACA - 3'
	<i>Antisense</i>	5' - ACACATCAATCCCCAGCAGT - 3'

Table 2. Primers used for real-time quantitative polymerase chain reaction (RTq-PCR) in rat left ventricular (LV) myocardial tissue

<b>Genes</b>		<b>Primer Sequences</b>
<b>Glycerol-3-phosphate dehydrogenase (GAPDH)</b>	<i>Sense</i>	5' – AAGATGGTGAAGGTCGGTGT – 3'
	<i>Antisense</i>	5' – ATGAAGGGGTCGTTGATGG – 3'
<b>Hypoxanthine guanine phosphoribosyl transferase (HPRT)</b>	<i>Sense</i>	5' – ACAGGCCAGACTTTGTTGGA – 3'
	<i>Antisense</i>	5' – ATCCACTTTCGCTGATGACAC – 3'
<b>AMP-activated protein kinase (Ampk)</b>	<i>Sense</i>	5' – TTCGGGAAAGTGAAGGTGGG – 3'
	<i>Antisense</i>	5' – TCTCTGCGGATTTTCCCGAC – 3'
<b>Arachidonate 15-lipoxygenase (Alox15)</b>	<i>Sense</i>	5' - GCACTCTTCCGTCCATCTTG - 3'
	<i>Antisense</i>	5' - GCTTCTCCATTGTTGCTTCCT - 3'
<b>ATPase sarcoplasmic/endoplasmic reticulum Ca<sup>2+</sup> transporting 2 (Atp2a2 or Serca2)</b>	<i>Sense</i>	5' – GCAGGTCAAGAAGCTCAAGG – 3'
	<i>Antisense</i>	5' – TCTCTGCGGATTTTCCCGAC – 3'
<b>Bcl2 associated X apoptosis regulator (Bax)</b>	<i>Sense</i>	5' - CGTGGTTGCCCTCTTCTACT - 3'
	<i>Antisense</i>	5' - TCACGGAGGAAGTCCAGTGT - 3'
<b>B-cell lymphoma 2 (Bcl2)</b>	<i>Sense</i>	5' - TTTCTCCTGGCTGTCTCTGAA - 3'
	<i>Antisense</i>	5' - CATATTTGTTTGGGGCAGGT - 3'
<b>Bradykinin receptor B1 (Bdkrb1)</b>	<i>Sense</i>	5' -AAGCTACGTGCTGCTCATC - 3'
	<i>Antisense</i>	5' - CGGGGACGACTTTAACAGAG - 3'
<b>Bradykinin receptor B2 (Bdkrb2)</b>	<i>Sense</i>	5' - GCTGTCGTGGAAGTGGCTAT - 3'
	<i>Antisense</i>	5' - AAGGTCCCGTTATGAGCAGA - 3'
<b>Ca<sup>2+</sup> voltage-gated channel subunit alpha1 C (Cacna1c)</b>	<i>Sense</i>	5' – CCTATTTCCGTGACCTGTGG – 3'
	<i>Antisense</i>	5' – GGAGGGACTTGATGGTGTG – 3'
<b>CD36 fatty acid transporter (Cd36)</b>	<i>Sense</i>	5' - TTTCTGCTTTCTCATCGCCG - 3'
	<i>Antisense</i>	5' - GGATGTGGAACCCATAACTGG - 3'
<b>Glutathione peroxidase (Gpx)</b>	<i>Sense</i>	5' - CCGACCCCAAGTACATCATT - 3'
	<i>Antisense</i>	5' - AACACCGTCTGGACCTACCA - 3'
<b>Kallikrein-related-peptidase 8 (Klk8)</b>	<i>Sense</i>	5' -CGGAGACAGATGGGTCCTAA - 3'
	<i>Antisense</i>	5' - ATCTCTTGCTCGGGCTCAT - 3'
<b>Kallikrein-related-peptidase 10 (Klk10)</b>	<i>Sense</i>	5' - GCAGGTCTCCCTCTTCCATA - 3'
	<i>Antisense</i>	5' - CAGTGGCTTATTCTCCAGCA - 3'
<b>Oxidized low density lipoprotein receptor 1 (Olr1 or Lox1)</b>	<i>Sense</i>	5' -CATTACCTCCCCATTTT - 3'
	<i>Antisense</i>	5' - GTAAAGAAACGCCCTGGT - 3'
<b>Peroxisome proliferator-activated receptor alpha (Ppar alpha)</b>	<i>Sense</i>	5' – TTAGAGGCGAGCCAAGACTG – 3'
	<i>Antisense</i>	5' – CAGAGCACCAATCTGTGATGA – 3'
<b>Peroxisome proliferator-activated receptor gamma (Ppar gamma)</b>	<i>Sense</i>	5' – GCGCTAAATTCATCTTAACTC – 3'
	<i>Antisense</i>	5' – CTGTGTCAACCATGGTAATTT – 3'
<b>Ryanodine receptor 2 (Ryr2)</b>	<i>Sense</i>	5' – GGAAGTACGAGGAAAGTG – 3'
	<i>Antisense</i>	5' – GAGACCAGCATTTGGGTTGT – 3'
<b>Solute carrier family 2 member 1 (Slc2a1 or Glut1)</b>	<i>Sense</i>	5' - TCTTCGAGAAGGCAGGTGTG - 3'
	<i>Antisense</i>	5' - TCCACGACGAACAGCGAC - 3'
<b>Solute carrier family 2 member 4 (Slc2a4 or Glut4)</b>	<i>Sense</i>	5' - AGGCCGGGACACTATACCC - 3'
	<i>Antisense</i>	5' - TCCCCATCTTCAGAGCCGAT -5'
<b>Superoxide dismutase 1 (Sod1)</b>	<i>Sense</i>	5' - GGTCACGAGAAACAAGATGA - 3'
	<i>Antisense</i>	5' - CAATCACACCACAAGCCAAG - 3'

<b>Superoxide dismutase 2 (<i>Sod2</i>)</b>	<i>Sense</i>	5' -AAGGAGCAAGGTCGCTTACA - 3'
	<i>Antisense</i>	5' - ACACATCAATCCCCAGCAGT - 3'

Table 3. Primers used for real-time quantitative polymerase chain reaction (RTq-PCR) in rat with AR left ventricular (LV) myocardial tissue

### 3.3.3 Statistical analysis

Statistical analyses are described hereafter for published article and submitted article.

*El Oumeiri et al. (227)*

Results are presented as mean  $\pm$  standard deviation (SD) with “n” representing the number of individual data points. The echocardiographic data were compared using Student’s t-test for repeated measures (n = 6) before and after OM perfusion. The RTq-PCR data evaluating LV gene expression, were compared using Student’s t-test for independent samples (with n = 8 in the control group and n=6 in the treated group). Statistical analyses were performed using StatView 5.0 Software. A p-value < 0.05 was considered statistically significant.

*El Oumeiri et al (submitted manuscript)*

Results are presented as mean  $\pm$  standard deviation (SD) with “n” representing the number of individual data points. The echocardiographic data were compared using Student’s t-test for repeated measures (n = 10) before and after saline perfusion. The RTq-PCR data evaluating LV gene expression, were compared using Student’s t-test for independent samples (with n = 8 in the control group and n=10 in the AR group). Statistical analyses were performed using StatView 5.0 Software. A p-value < 0.05 was considered statistically significant.

## 4. Results

### 4.1 Effects of AR on rats left ventricle, cardiac biomarkers and LV genes expression.

#### 4.1.1 AR and LV measurements

In the first study, AR was achieved in all 20 animals and confirmed by the presence of a regurgitant jet quantified as severe in all animals. Eight animals died of congestive HF within 2 months and were not included in the final analysis. After 2 months AR (graduated from 0 to 4) was achieved at  $3.67 \pm 0.44$  (Figure 11), and echocardiographic signs of volume overload and eccentric hypertrophy were present with increased left atrial diameter, LVEDD, LVEDV and LV mass ( $n = 12$ , all  $p < 0.05$ , paired t-tests). Load dependent indices of LV systolic function (FS and EF) was unchanged but LVESD were increased. SV and cardiac output were decreased ( $n = 12$ , both  $p < 0.01$ , paired t tests). As expected, no AR was detected in sham operated rats ( $n = 4$ ) with no modifications of LV function or dimension (Table 4).

In the second study, AR was achieved in all 34 rats, as confirmed by the presence of a regurgitant jet quantified as severe (PHT  $< 200$  msec). Sixteen rats died during the surgery or from congestive heart failure before the end of the 2-month follow-up and were thus excluded from the final analysis. After 2 months, AR (PHT  $< 200$  msec) was confirmed, and the presence of volume overload and eccentric hypertrophy were established echocardiographically by significant increases in LVEDD, LVESD, and LV mass ( $n = 18$ , all  $p < 0.001$ , Figure 9). Load-dependent indices of LV systolic function (FS and EF) and RWT were significantly lower than baseline ( $p < 0.05$ ,  $n = 18$ ), whereas SV and CO were significantly higher than baseline ( $n = 18$ , both  $p < 0.001$ ). As expected, signs of AR were not present in the sham-operated rats ( $n = 6$ ), and thus no changes in LV functions or dimensions were observed in this group.



	<b>T1</b>	<b>T2</b>	<b>p</b>	<b>T3</b>	<b>p</b>
Heart Rate (beats/min)	258 ± 11	270 ± 7	0,756	193 ± 15	0,251
Left Atrium (mm)	4.6 ± 0.2	6.2 ± 0.3	0,872	5.5 ± 0.2	0,118
LVEDD (mm)	7.9 ± 0.5	11.1 ± 0.4	0,938	10.1 ± 0.5	0,209
LVESD (mm)	5.5 ± 0.4	7.6 ± 0.3	0,736	6.1 ± 0.4	0,072
FS (%)	31.5 ± 1.4	30.5 ± 1.0	0,937	35.4 ± 1.5	0,011
EF (%)	64.1 ± 2.0	63.9 ± 1.4	0,630	68.8 ± 2.5	0,032
Stroke Volume (ml)	0.34 ± 0.03	0.22 ± 0.18	0,448	0.30 ± 0.04	0,762
Cardiac Output (ml/min)	79.5 ± 9.3	52.0 ± 4.5	0,890	61.6 ± 8.6	0,393
SWTs (mm)	2.1 ± 0.1	2.3 ± 0.2	0,671	2.7 ± 0.2	0,457
SWTd (mm)	1.4 ± 0.1	1.7 ± 0.2	0,971	2.1 ± 0.2	0,092
Systolic time (ms)	126 ± 3.7	134 ± 2.6	0,245	135 ± 2.6	0,153
Diastolic time (ms)	139 ± 8.4	135 ± 8.3	0,207	157 ± 14.5	0,138
PEP (ms)	15.0 ± 1.6	25.4 ± 1.3	0,413	21.8 ± 1.0	0,308
LVET (ms)	110 ± 4.4	109 ± 2.8	0,310	113 ± 3.9	0,268
PEP/LVET	0.13 ± 0.02	0.23 ± 0.02	0,800	0.19 ± 0.01	0,968
Systolic time/RR	0.48 ± 0.02	0.50 ± 0.02	0,344	0.47 ± 0.02	0,370

Table 4. Two-way ANOVA statistics with Bonferroni correction at base (T1), before injection (T2) and after injection (T3) for all sham animals (n = 4). Values are mean ± SD. LVEDD Left ventricle end-diastolic diameter, LVEDV Left ventricle end-diastolic volume, LVESD Left ventricle end-systolic diameter, LVESD Left ventricle end-systolic volume, FS Fractional shortening, EF Ejection fraction, SV stroke volume, SWTs septal wall thickness at end-systole, SWTd septal wall thickness at end-diastole, PEP aortic pre-ejection period, LVET Left ventricular ejection time, RR inter-beat interval.

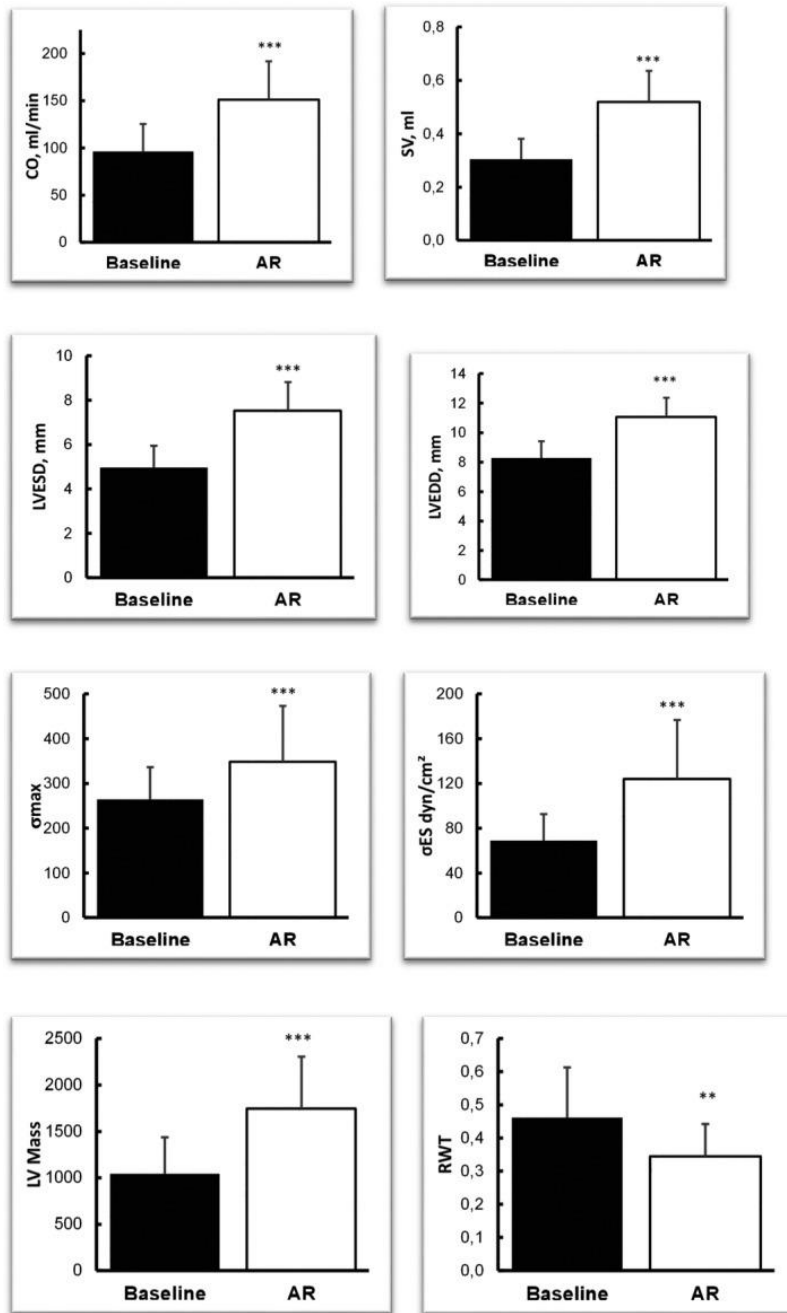


Figure.9 Hemodynamic effects of aortic regurgitation (AR) induced in rats (n = 18) at baseline and 2 months after induction of AR. Values are expressed as mean  $\pm$  SD. \* $p < 0.05$ ; \*\* $p < 0.01$ ; \*\*\* $p < 0.001$  (or other symbols; two-way analysis of variance). Comparisons: \* = within a group compared with baseline; \* between the same rats that had an AR 2 months before (n=18), before AR and 2 months after induction of AR. CO, cardiac output; LVEDD, left ventricle end-diastolic diameter; LVESD, left ventricle end-systolic diameter; RWT, relative wall thickness; SV, stroke volume;  $\sigma$ , max wall stress;  $\sigma_d$ , diastolic wall stress;  $\sigma_{es}$ , end-systolic wall stress

#### 4.1.2 AR effects on wall stress and blood pressure

As mentioned above, wall stress and invasive blood pressure measurements were only performed in the second study. Diastolic arterial blood pressure was significantly lower after the induction of AR ( $n = 18$ ,  $p < 0.001$ ). End-systolic and maximum wall stress were significantly higher in all rats with AR after induction ( $n = 18$ ,  $p < 0.05$ ). We detected no changes in  $\sigma$  max or arterial blood pressure in sham-operated rats ( $n = 6$ ).

#### 4.1.3 Effects of AR on cardiac biomarkers

##### *4.1.3.1 Plasma NT-proBNP levels in rats with AR*

The baseline levels of plasma NT-proBNP were  $244 \pm 48$  pg/mL in the 18 rats that were designated to undergo surgical induction of AR. About 60 days after the induction of AR, the plasma levels of NT-proBNP were not significantly different, i.e.,  $231 \pm 35$  pg/mL in this experimental cohort (Figure 13). We also detected no significant differences in plasma NT-proBNP levels among the six rats in the sham control group ( $235 \pm 37$  pg/mL at baseline *versus*  $280 \pm 66$  pg/mL measured 60 days later). We identified no correlations between plasma NT-proBNP levels and echocardiographic parameters, blood pressure, or body weight.

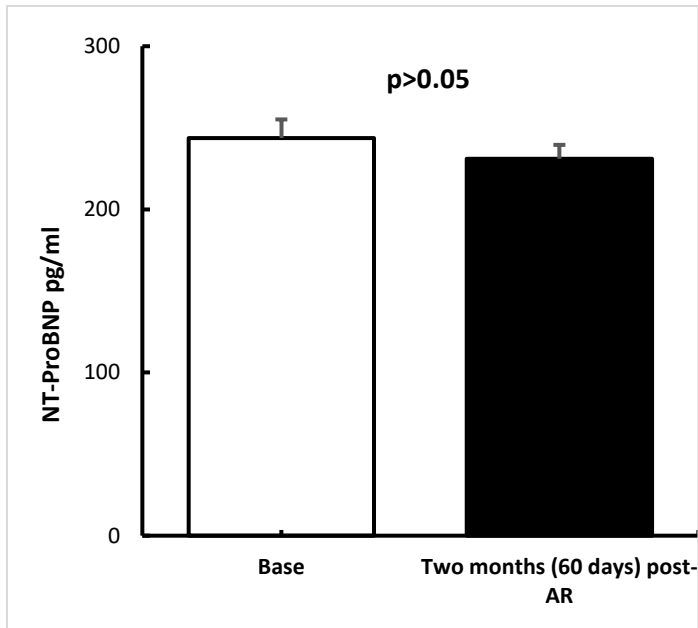


Figure 10. Plasma NT-proBNP levels in adult male rats (n = 18) at baseline and 60 days after induction of AR (day 60). Values shown (pg/mL) are means  $\pm$  SDs.

#### 4.1.3.2 Plasma sST2 levels in rats with AR

As shown in Figure 14, we detected no significant differences in plasma sST2 in rats when comparing levels detected before and 2 months after surgical induction of AR ( $583 \pm 514$  pg/mL vs.  $543 \pm 340$ ). We also detected no significant changes in the levels of plasma sST2 in rats in the sham group at these time points. However, we did identify significant correlations between plasma levels of sST2 and PWTd as determined by echocardiography ( $r=0.34$ ,  $p<0.05$ ). We also identified a significant correlation between plasma sST2 and body weight ( $r=0.45$ ,  $p<0.01$ ), as shown in Figure 15A and 15B.

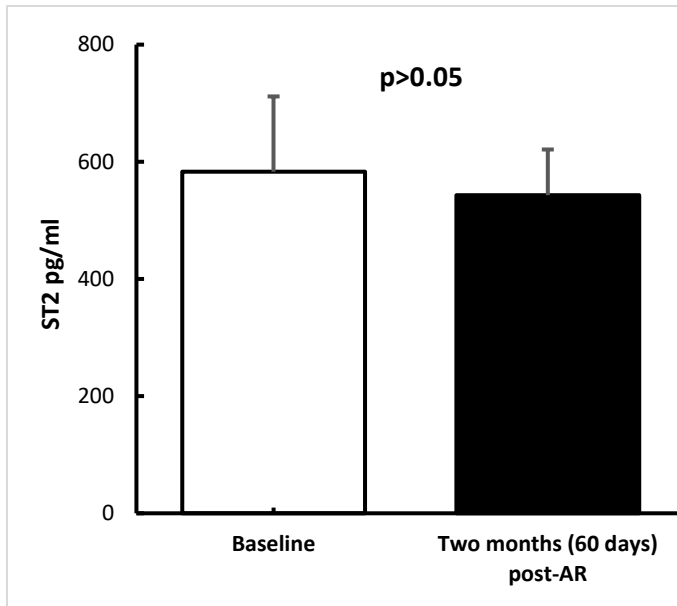
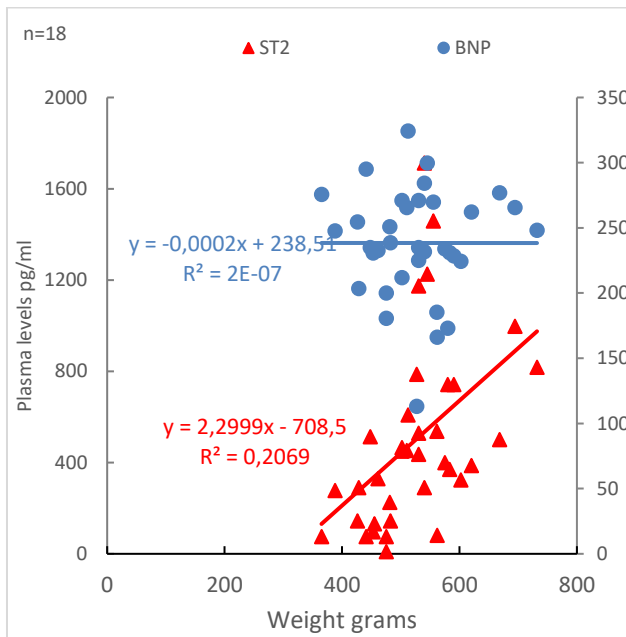


Figure 11. Plasma sT2 levels in adult male rats (n = 18) at baseline and 60 days after the induction of AR induction. Values shown (expressed in pg/mL) are means  $\pm$  SDs.

A.



B.

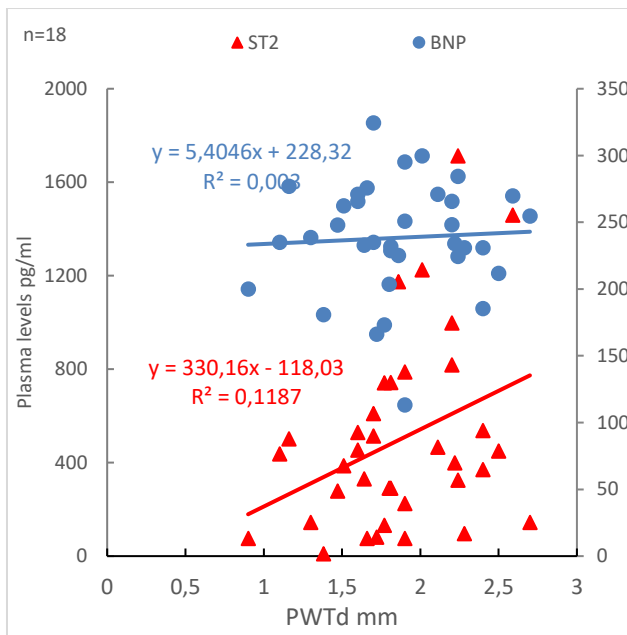


Figure 12. (A) Correlations between plasma NT-proBNP and sST2 levels and body weight (n=18) at baseline and 60days after the induction of AR ( $p < 0.01$ ). (B) Correlations between plasma NT-proBNP and sST2 levels and PWTd (n =18 rats) at baseline and 60 days after the induction of AR; \* $p < 0.05$ .

Parameter <sup>1</sup>	Baseline		Two months		r (NT-proBNP)	r (sST2)
	Value	Value	Value	Value		
FS, %	40 ± 6	32 ± 7 ***	0.014	0.12		
EF, %	75 ± 10	64 ± 12 ***	0.08	0.13		
SWTs, mm	2.72 ± 0.57	2.64 ± 0.59	0.017	0.04		
SWTd, mm	1.94 ± 0.53	2.11 ± 0.64	0.08	-0.065		
LVESD, mm	5.0 ± 1.0	7.5 ± 1.3 ***	-0.02	-0.06		
LVEDD, mm	8.3 ± 1.1	11.1 ± 1.3 ***	-0.033	-0.028		
HR, BPM	309 ± 50	291 ± 43	-0.096	-0.14		
LVOT, mm	2.48 ± 0.18	2.76 ± 0.18 ***	-0.14	0.12		
PWTs, mm	2.86 ± 0.46	2.87 ± 0.69	-0.083	0.21		
PWTd, mm	1.85 ± 0.45	1.87 ± 0.41	0.17	0.34*		
PEP, ms	24 ± 9	23 ± 13	0.014	0.08		
LVET, ms	78 ± 5	86 ± 8	0.08	0.2		
ST, ms	103 ± 13	108 ± 17	0.05	0.017		
DT, ms	99 ± 28	101 ± 30	0.06	0.1		
RR, ms	201 ± 30	208 ± 28	0.08	0.12		
PEP/LVET	0.30 ± 0.10	0.26 ± 0.15	-0.25	0.11		
ST/RR	0.53 ± 0.11	0.52 ± 0.10	0.03	-0.08		
ARPhT, ms		91 ± 25				
SV, ml	0.30 ± 0.08	0.52 ± 0.12 ***	-0.1	0.03		
CO, ml/min	96 ± 29	151 ± 41 ***	-0.08	0.02		

LVOT VTI, mm	65 ± 13	87 ± 15 ***	-0.081	-0.03
BP Sys, mmHg	116 ± 6	122 ± 15	-0.09	-0.05
BP Dia, mmHg	78 ± 7	60 ± 10 ***	0.05	-0.12
Weight, g	486 ± 76	562 ± 66 ***	-0.004	0.45**
LV mass	1042 ± 394	1747 ± 558 ***	0.047	0.02
$\sigma_d$ , dyn/cm <sup>2</sup>	88 ± 25	87 ± 30	-0.06	0.18
$\sigma_{max}$ , dyn/cm <sup>2</sup>	264 ± 72	348 ± 125 ***	-0.15	-0.014
$\sigma_{Es}$ , dyn/cm <sup>2</sup>	69 ± 24	124 ± 52 ***	-0.02	-0.02
RWT	0.46 ± 0.15	0.34 ± 0.10 **	0.08	0.24

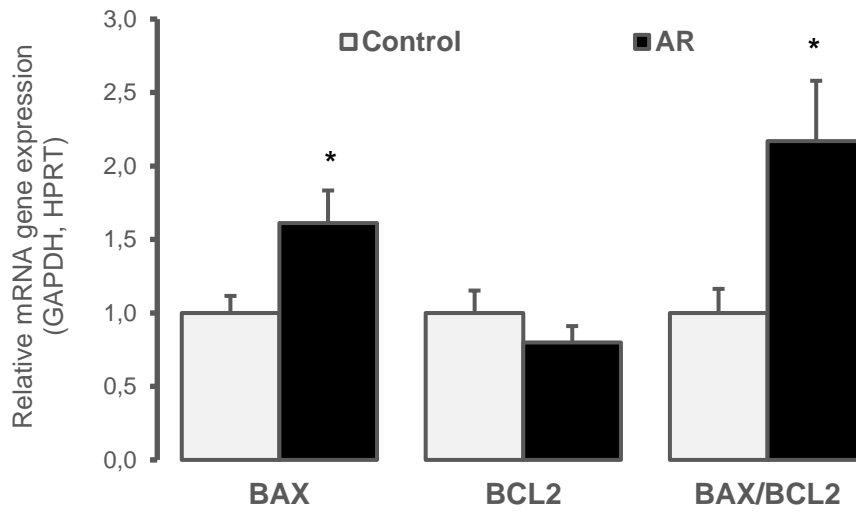
Table 5. El Oumeiri et al. (231). Echocardiographic measurements in rats (n = 18) at baseline and 60 days after induction of AR. Correlations of plasma NT-proBNP and sST2 levels with echocardiographic variables and invasive arterial pressure measurements at baseline and two months (60 days) after the induction of AR. Values presented are means ± SD; \*p < 0.05, \*\*p < 0.01, \*\*\*p < 0.001. <sup>1</sup>FS, fractional shortening; EF, ejection fraction; SWTs, septal wall thickness in systole; SWTd, septal wall thickness in diastole; LVESD, left ventricle end-systolic diameter; LVEDD, left ventricle end-diastolic diameter; HR, heart rate; LVOT, left ventricle outflow tract diameter; PWTs, posterior wall thickness in systole; PWTd, posterior wall thickness in diastole; PEP, pre-ejection period; LVET, left ventricular ejection time; ST, systolic time; DT, diastolic time; RR, interval between successive R waves; ARPht, aortic regurgitation pressure half-time; SV, stroke volume; CO, cardiac output; VTI, velocity-time integral; BP, blood pressure;  $\sigma$ , wall stress;  $\sigma_{max}$ , maximum wall stress;  $\sigma_d$ , end-diastolic wall stress;  $\sigma_{Es}$ , end-systolic wall stress; RWT, relative wall thickness.

#### 4.1.4 Effects of AR in rats LV genes expression

##### 4.1.4.1 AR and LV expression of genes regulating apoptosis and oxidative stress

Myocardial LV gene expression of pro-apoptotic Bax was significantly higher in rats with AR compared to control group, whereas no difference in gene expression of anti-apoptotic Bcl2 was observed (Figure 21A). The resulting pro-apoptotic Bax-to-Bcl2 ratio was increase in the LV of rats with AR (Figure 21A). We also examined differential expression of genes involved in oxidative stress regulation. Myocardial expression of Gpx, an anti-oxidant enzyme, increased in the LV rats with AR, decreased Sod2 gene expression whereas no changes in Sod1 gene expression were observed (Figure 21B).

A.



B.

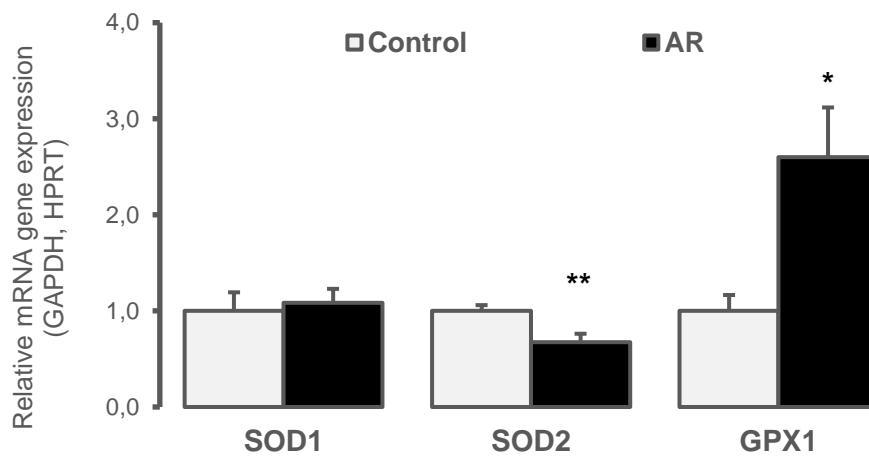


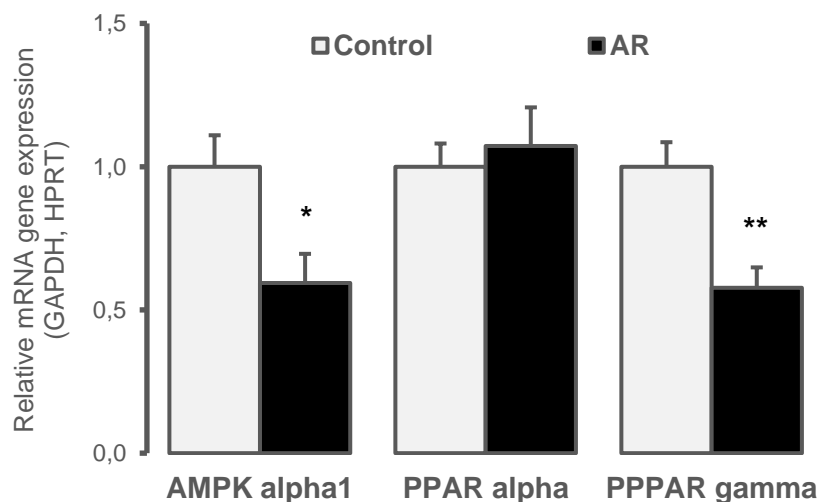
Figure 13. Myocardial left ventricular relative expression of genes implicated in (A) apoptosis (Bax, Bcl2) and (B) oxidative stress (Gpx, Sod1, Sod2) processes seven days after placebo (AR; n = 10; black bars) versus placebo (n = 8; grey bars) infusion. Values are presented as mean  $\pm$  SD; \* 0.01 < p < 0.05, \*\* 0.001 < p < 0.01, \*\*\* p < 0.001.



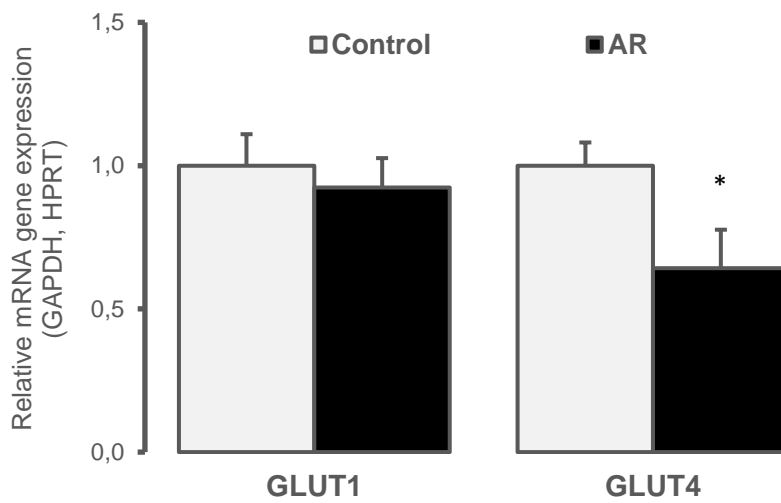
#### 4.1.4.2 AR impacted LV expression profile of key determinants of cardiac energy substrate use

To assess the effects of AR on basal myocardial energy metabolism, we evaluated gene expression profile of transcription factors and molecules regulating cardiac glucose and fatty acid metabolism. As illustrated in Figure 22A, myocardial LV gene expression of key energy sensors Ppar gamma and Ampk decreased. Myocardial LV expression of Slc2a1 (Glut1), the major myocardial glucose transporter remained unchanged in rats with AR, while gene expression of Slc2a4 (Glut4) decreased with AR (Figure 22B). As illustrated in Fig. 22C, AR increased LV expression of Alox15 encoding the 12/15 lipoxygenase enzyme implicated in polyunsaturated fatty acid metabolism, and of oxidized low-density lipoprotein receptor 1 (Olr1, also known as Lox1) encoding for a scavenger receptor mediating the uptake of oxidized lipoproteins into cells, whereas gene expression of fatty acid transporter Cd36 remained unchanged.

A.



B.



C.

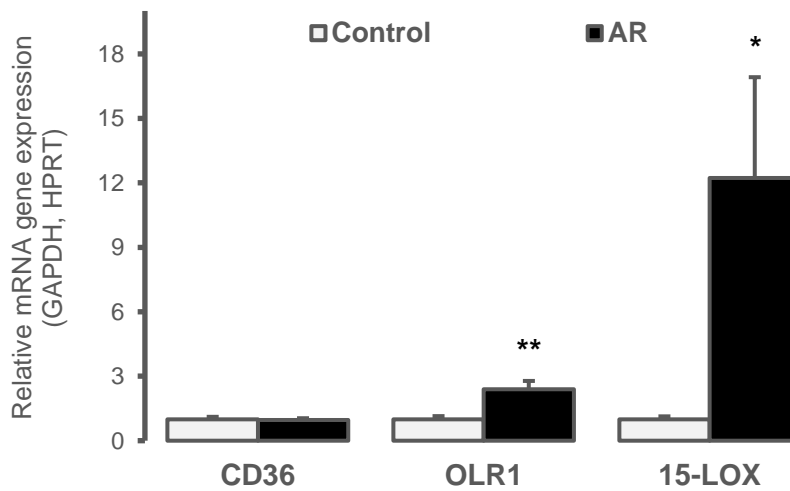
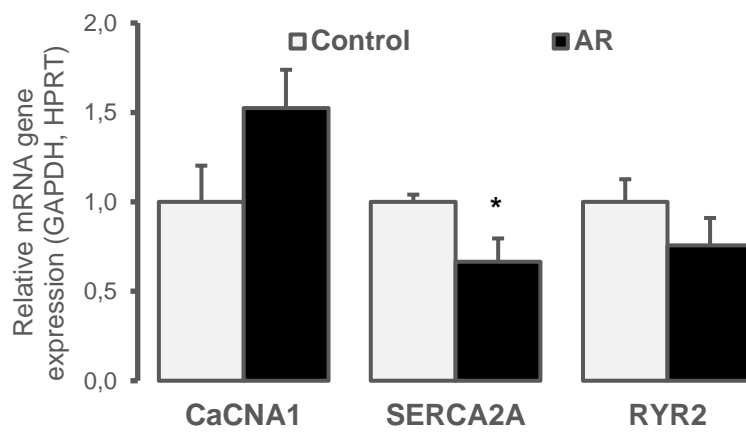


Figure 14. El Oumeiri et al. (228). Myocardial left ventricular relative expression of genes implicated in cardiac metabolism, including (A) cellular energy sensors such as Ampk, Ppar  $\alpha$ , and Ppar  $\gamma$ ; (B) glucose transporters Glut1 and Glut4; and (C) fatty acid metabolism regulators such as Cd36, Lox-1, and Alox-15, seven days after placebo (AR; n = 10; black bars) versus placebo (n = 8; grey bars) infusion. Values are presented as mean  $\pm$  SD; \*\* 0.001 < p < 0.01, \*\*\* p < 0.001.

#### 4.1.4.3 AR altered LV expression of genes implicated in cardiac contractility

As illustrated in Figure 3A, AR did not induce a major change in LV gene expression in kallikrein-bradykinin system except an increase in LV gene expression of KLK10. Again, after 2 months chronic severe AR did not induce major changes in gene expression of *Cacna1c* and RYR, except a decrease in LV gene expression of *Serca2* in response to AR (Figure 23B).

A.



B.

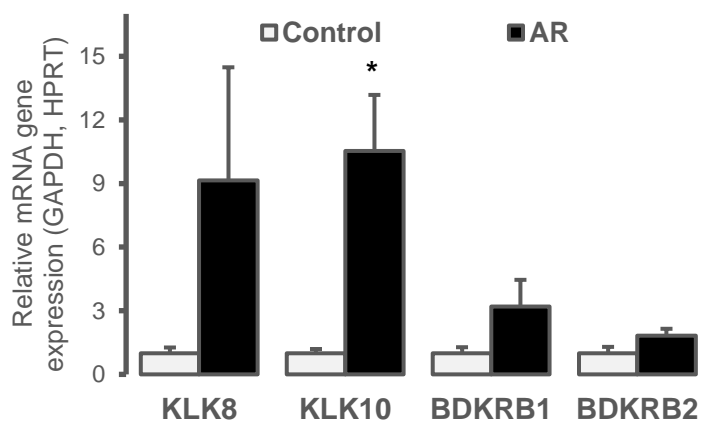


Figure 15. Myocardial left ventricular relative expression of genes controlling myocardial contractility including (A)  $Ca^{2+}$ -dependent excitation–contraction *Cacna1c*, *Ryr2*, *serca2a*; (B) cardiac actors of kallikrein (*Klk8*, *Klk10*) - bradykinin (*Bdkrb1* and *Bdkrb2*) system and of seven days after placebo (AR;  $n = 10$ ; black bars) versus placebo ( $n = 8$ ; grey bars) infusion. Values are presented as mean  $\pm$  SD; \*  $0.01 < p < 0.05$ , \*\*  $0.001 < p < 0.01$ , \*\*\*  $p < 0.001$ .

## 4.2 Effects of OM and placebo on LV rats with AR

### 4.2.1 Effects of placebo in rats with AR.

As illustrated in Table 5, in the first study before infusion, there was no difference in echocardiographic results between the 2 groups (Placebo *versus* OM). NaCl infusion affected none of the echocardiographic parameters of global and systolic cardiac function neither the indices of LV preload ( $n = 5$ ,  $p > 0.06$ , paired t tests).

In the second study, infusion with 0.9% NaCl (placebo group,  $n = 10$ ) affected some echocardiographic parameters in rats with AR (Figure 10 and table 9). FS was significantly higher ( $p < 0.05$ ), whereas LVESD, LVESDD, and end-systolic wall stress were significantly lower ( $p < 0.05$ ). Hemodynamically, NaCl infusion significantly increased systolic and diastolic blood pressures ( $p < 0.05$ ), as well as PWTs and the PEP/LVET ratio ( $p < 0.05$ ).

	Before infusion	After infusion	p-value
Heart Rate (beats/min)	249 ± 18	220 ± 41	0.437
Left Atrium (mm)	6.2 ± 0.8	5.8 ± 1.1	0.541
LVEDD (mm)	10.6 ± 0.8	12.24 ± 1.07	0.092
LVESD (mm)	7.5 ± 0.6	6.9 ± 0.84	0.341
FS (%)	28.8 ± 1.4	29.6 ± 5.2	0.706
EF (%)	60.8 ± 1.8	61.0 ± 8.4	0.968
Stroke Volume (ml)	0.24 ± 0.04	0.24 ± 0.08	0.890
Cardiac Output (ml/min)	60 ± 8	60 ± 12	0.369
SWTs (mm)	3.0 ± 0.16	2.9 ± 0.47	0.122
SWTd (mm)	1.6 ± 0.17	1.7 ± 0.29	0.281
Systolic time (ms)	136 ± 5	123 ± 17	0.340
Diastolic time (ms)	144 ± 24	173 ± 41	0.054
PEP (ms)	25.8 ± 4.6	21.2 ± 6.2	0.125
LVET (ms)	110 ± 8	102 ± 14	0.490
PEP/LVET	0.24 ± 0.05	0.20 ± 0.05	0.182
Systolic time/RR	0.49 ± 0.05	0.42 ± 0.05	0.047

Table 6. Two-tailed T-test before and after placebo infusion on LV function after 2 months of AR in a rat model (n = 5). Values are mean ± SD. Left ventricle end-diastolic diameter; LVEDV: Left ventricle end-diastolic volume; LVESD: Left ventricle end-systolic diameter; LVESD: Left ventricle end-systolic volume; FS: Fractional shortening; EF: Ejection fraction; SV: stroke volume; SWTs: septal wall thickness at end-systole; SWTd: septal wall thickness at end-diastole PEP: aortic pre-ejection period; LVET: Left ventricular ejection time; RR: inter-beat interval.

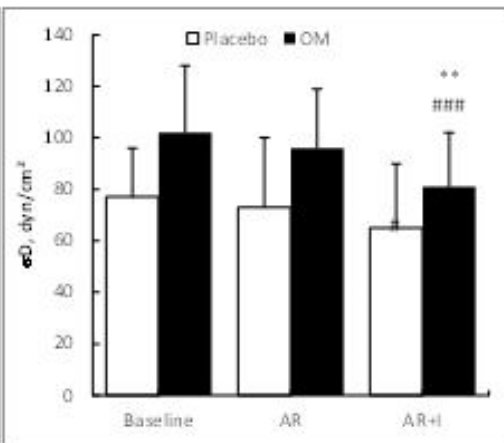
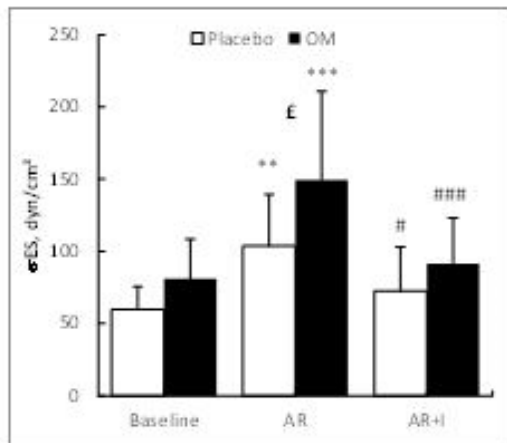
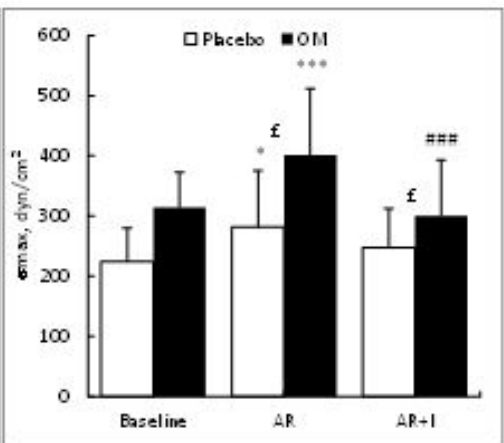
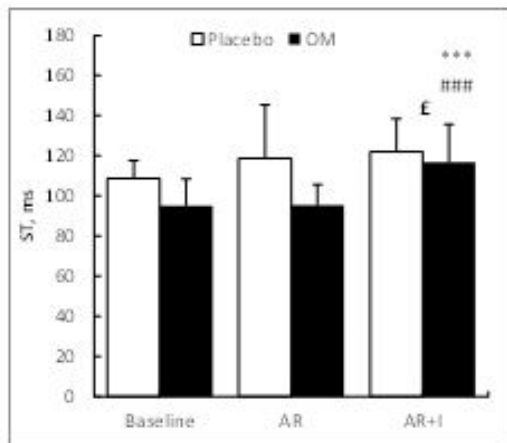
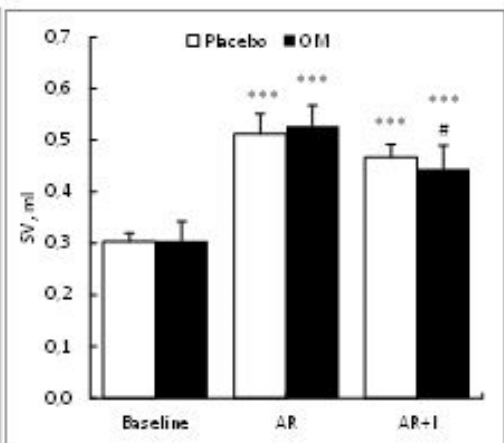
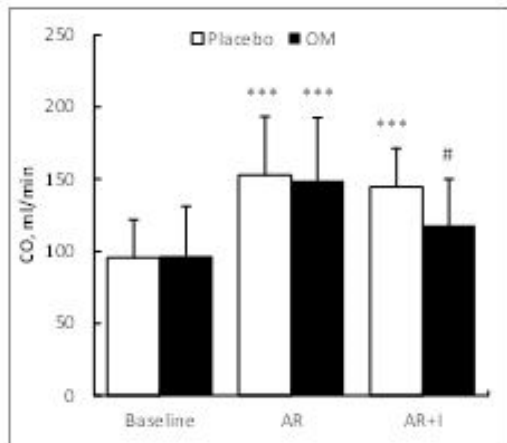
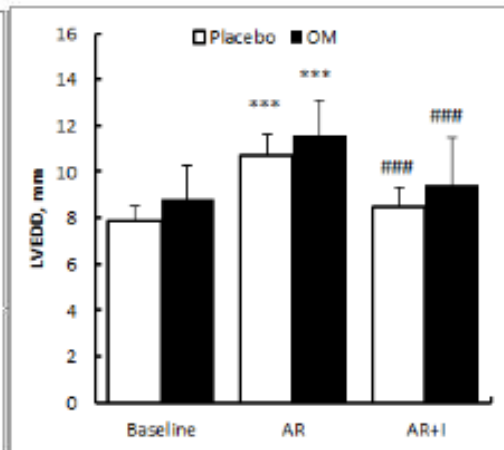
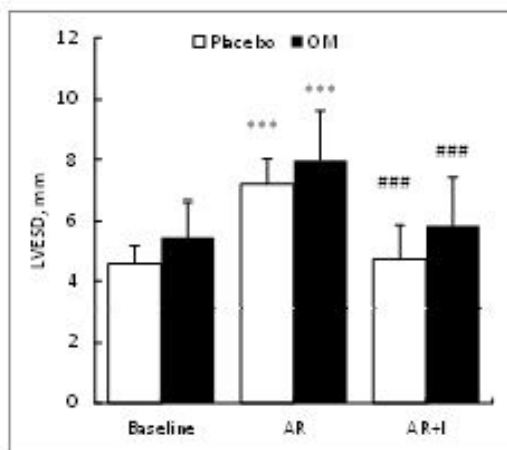


Figure 16. El umeiri et al. (230) Hemodynamic effects of aortic regurgitation (AR) induced in rats at baseline, 2 months after induction of AR (pre-infusion), and following infusion (I) of omecantiv mecarbil (OM) or placebo (0.9% NaCl)1. 1 Values are expressed as mean  $\pm$  SD. \* $p < 0.05$ ; \*\* $p < 0.01$ ; \*\*\* $p < 0.001$  (or other symbols; two-way analysis of variance). Comparisons: \* = within a group compared with baseline; # = within a group compared with 2 months (pre-infusion); £ = compared with placebo group at the same time point; # within the same group (placebo (n=10) or OM (n=8)) before and after infusion, the 2 group had a AR; ### is  $p < 0.001$  (in the same group placebo after 2 months before and after infusion of placebo n=10, or for the OM group (n=8) after 2 months before and after OM infusion). CO, cardiac output; LVEDD, left ventricle end-diastolic diameter; LVESD, left ventricle end-systolic diameter; ST, systolic time; SV, stroke volume;  $\sigma$  max, max wall stress;  $\sigma$  d, diastolic wall stress;  $\sigma$  es, end-systolic wall stress.

#### 4.2.2 Effects of OM rat with AR

OM increased indices of global cardiac function (SV, CO), decreased HR and increased systolic performance (FS, EF) (n = 7, all  $p < 0.05$ , paired t tests). These effects concurred with decreases in measures of LV preload (Left atrial diameter, LVEDD), and a decreased PEP/LVET ratio (n = 7, all  $p < 0.05$ , paired t tests). OM did not affect the severity score of the AR jet (Table 6). Infusion with OM (treatment group, n = 8; Figure 10, Table 9) significantly increased FS, ST, and LVET ( $p < 0.05$ ) and significantly decreased LVEDD and LVESD ( $p < 0.05$ ). In addition, OM treatment resulted in a significant decrease in the wall stress parameters  $\sigma$  max,  $\sigma$  es, and  $\sigma$  d ( $p < 0.05$ ). OM infusion also affected indices of global cardiac function, including significant decreases in SV and CO ( $p < 0.05$ ), but did not affect the severity of AR (PHT  $110 \pm 12$  ms vs.  $89 \pm 10$  ms before OM injection, P ns).

	Before infusion	After infusion	p-value
Heart Rate (beats/min)	253 ± 22	207 ± 35	0.091
Left Atrium (mm)	6.2 ± 0.8	5.5 ± 0.7	0.037
LVEDD (mm)	11.6 ± 1.09	9.0 ± 1.51	0.003
LVESD (mm)	7.8 ± 0.91	5.4 ± 1.30	0.009
FS (%)	32.1 ± 3.4	41.1 ± 5.3	0.004
EF (%)	65.0 ± 4.7	76.6 ± 5.8	0.002
Stroke Volume (ml)	0.19 ± 0.06	0.36 ± 0.11	0.011
Cardiac Output (ml/min)	44 ± 16	76 ± 14	0.027
SWTs (mm)	2.67 ± 0.48	3.33 ± 0.51	0.390
SWTd (mm)	1.6 ± 0.17	2.4 ± 0.39	0.274
Systolic time (ms)	133 ± 7	147 ± 8	0.003
Diastolic time (ms)	127 ± 16	141 ± 33	0.384
PEP (ms)	25.0 ± 2.3	22.4 ± 1.8	0.042
LVET (ms)	108 ± 6	125 ± 9	0.002
PEP/LVET	0.23 ± 0.02	0.18 ± 0.02	0.007
Systolic time/RR	0.51 ± 0.04	0.52 ± 0.06	0.735

Table 7. Two-tailed T-test before and after OM infusion on LV function after 2 months of AR in a rat model (n = 7). Values are mean ± SD. LVEDD Left ventricle end-diastolic diameter, LVEDV Left ventricle end-diastolic volume, LVESD Left ventricle end-systolic diameter, LVESD Left ventricle end-systolic volume, FS Fractional shortening, EF Ejection fraction, SV stroke volume, SWTs septal wall thickness at end-systole, SWTd septal wall thickness at end-diastole, PEP aortic pre-ejection period, LVET Left ventricular ejection time, RR inter-beat interval.

#### 4.2.3 Effects of OM compared with placebo rats with AR

Only FS and EF increased after OM as compared to placebo (p = 0.014 and p = 0.012, respectively; Table 7 and Figure 12). None of the other hemodynamic changes investigated in this study achieved the level of significance in this analysis.



In the second study, the effects of OM and placebo treatments in AR rats were compared by using two-way ANOVA (Table 9). In the comparison of OM *versus* placebo, values for PEP ( $p < 0.01$ ), the PEP/LVET ratio ( $p < 0.001$ ), the ST/RR ratio ( $p < 0.01$ ), and SWTs ( $p < 0.01$ ) were lower in rats infused with OM than those in the placebo group. Similarly, diastolic time (DT) was higher in rats of the OM group than in rats of the placebo group ( $p < 0.05$ ). No other echocardiographic or hemodynamic parameters investigated in this study exhibited significant differences between the OM and placebo groups.

	T1	T2	p	T3	p
Heart Rate (beats/min)	226 ± 23	228 ± 21	0.890	208 ± 28	0.113
Left Atrium (mm)	4.6 ± 0.2	6.2 ± 0.3	0.966	5.5 ± 0.2	0.277
LVEDD (mm)	7.9 ± 0.5	11.1 ± 0.4	0.235	10.1 ± 0.5	0.066
LVESD (mm)	5.5 ± 0.4	7.6 ± 0.3	0.871	6.1 ± 0.4	0.092
FS (%)	31.5 ± 1.4	30.5 ± 1.0	0.144	35.4 ± 1.5	0.014
EF (%)	64.1 ± 2.0	63.9 ± 1.4	0.173	68.8 ± 2.5	0.012
Stroke Volume (ml)	0.34 ± 0.03	0.22 ± 0.18	0.129	0.30 ± 0.04	0.135
Cardiac Output (ml/min)	79.5 ± 9.3	52.0 ± 4.5	0.098	61.6 ± 8.6	0.203
SWTs (mm)	2.1 ± 0.1	2.3 ± 0.2	0.597	2.7 ± 0.2	0.652
SWTd (mm)	1.4 ± 0.1	1.7 ± 0.2	0.439	2.1 ± 0.2	0.040
Systolic time (ms)	126 ± 3.7	134 ± 2.6	0.626	135 ± 2.6	0.293
Diastolic time (ms)	139 ± 8.4	135 ± 8.3	0.341	157 ± 14.5	0.293
PEP (ms)	15.0 ± 1.6	25.4 ± 1.3	0.771	21.8 ± 1.0	0.577
LVET (ms)	110 ± 4.4	109 ± 2.8	0.752	113 ± 3.9	0.180
PEP/LVET	0.13 ± 0.02	0.23 ± 0.02	0.811	0.19 ± 0.01	0.378
Systolic time/RR	0.48 ± 0.02	0.50 ± 0.02	0.567	0.47 ± 0.02	0.063

Table 8. Hemodynamic parameters at baseline (T1), before (T2) and after injection (T3) of OM in all animals ( $n = 12$ ) analyzed with a two-way ANOVA statistic test with Bonferroni correction. Values are expressed as mean ± SD. LVEDD means left ventricle end-diastolic diameter; LVEDV, left ventricle end-diastolic volume; LVESD, left ventricle end-systolic diameter; LVESD, left ventricle end-systolic volume; FS, fractional shortening; EF, ejection fraction; SV, stroke volume; SWTs, septal wall thickness at end-systole; SWTd, septal wall thickness at end-diastole; PEP, aortic pre-ejection period; LVET, left ventricular ejection time; RR, inter-beat interval.

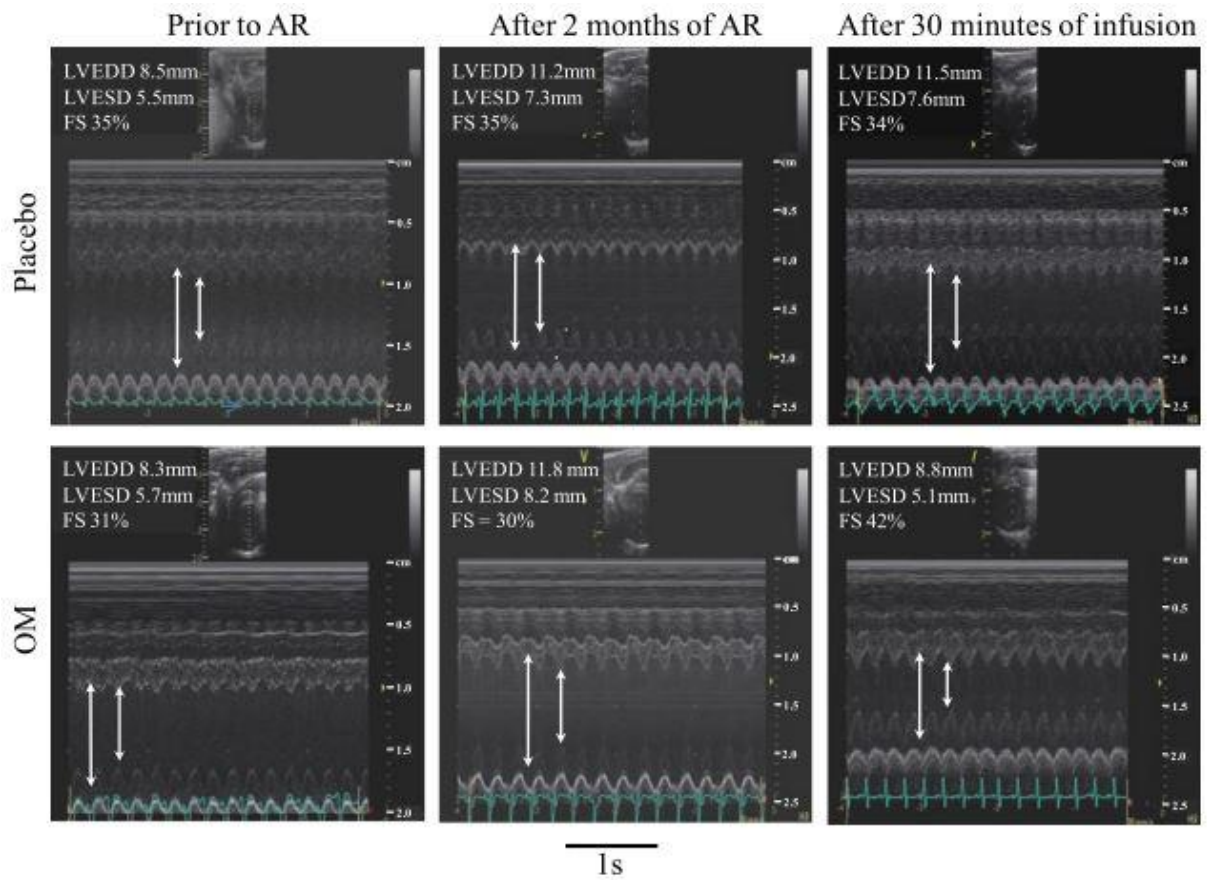


Figure 17. Illustrative examples of M-mode echocardiography recordings in 2 Wistar rats during the entire study. The figure displays left ventricular end diastolic diameter (LVEDD, mm) and fractional shortening (FS, %) prior to AR (left tracings), after 2 months of AR (middle tracings) and after 30 min of placebo (upper tracings) and OM infusions (lower tracings).

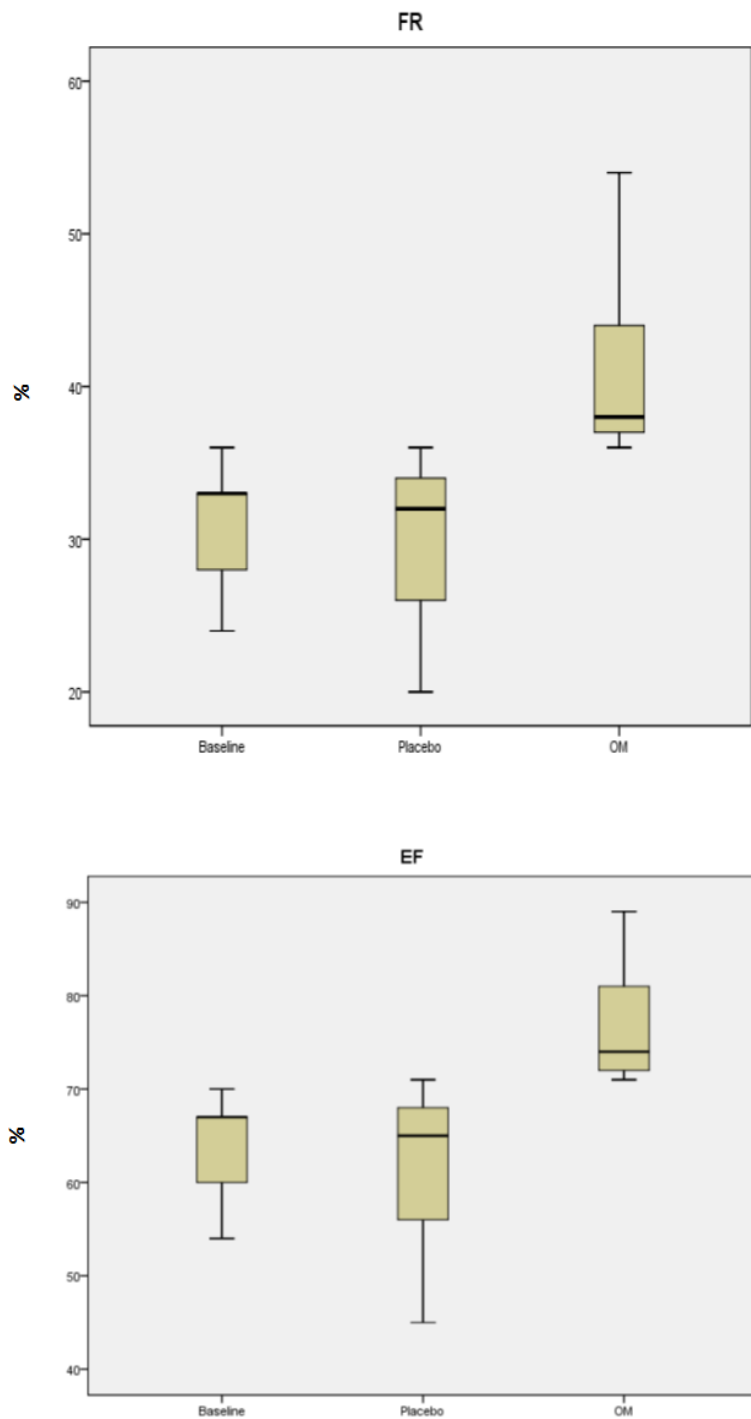


Figure 18. Two-way ANOVA with Bonferroni corrections for multiple comparisons on the effects of OM versus placebo on FS ( $p = 0.014$ ) and EF ( $p = 0.012$ ) after 2 months of AR. Box and Whisker plots before infusion, and after infusion of OM vs. placebo (median: horizontal band within the box, box top and bottom: upper and lower first quartiles, top and bottom whiskers: highest and lowest quartiles;  $n = 12$ ).

#### 4.2.4 effects of OM in sham-operated rats

No AR was detected in sham operated rats (n = 4) with no modifications of LV function or dimension in the placebo group while only FS and EF increased after injection of OM ( $p = 0.011$  and  $p = 0.032$ , respectively; Table 4). The effects of OM treatments in AR rats and sham-operated rats were compared by two-way ANOVA (Table 8). Infusion of OM in sham-operated rats (n = 6) resulted in significant increases in LVET, FS and decreases in  $\sigma d$ , the PEP/LVET ratio, and PEP (all  $p < 0.05$ ).

Parameters	Before OM Infusion	After OM Infusion
FS (%)	38.8 ± 3.6	44.1 ± 4.4 *
EF (%)	76.0 ± 4.4	80.6 ± 5.2
LVESD (mm)	5.5 ± 0.5	4.6 ± 0.9
LVEDD (mm)	9.0 ± 0.4	8.3 ± 0.9
HR (beats/min)	283 ± 57	303 ± 68
SBP (mmHg)	128 ± 9	128 ± 21
DBP (mmHg)	90 ± 10	88 ± 20
LVET (ms)	79 ± 6	89 ± 8 *
PEP (ms)	21 ± 5	14 ± 7 *
PEP/LVET	0.26 ± 0.06	0.15 ± 0.07 *
CO (mL/min)	90 ± 21	106 ± 22
SV (mL)	0.32 ± 0.06	0.35 ± 0.04
LA (mm)	5.8 ± 0.8	5.7 ± 0.5

Table 9. Echocardiographic measurements in rats (n = 6) at baseline and 30 min after OM infusion. Values presented are means ± SD; \*  $p < 0.05$ . FS, fractional shortening; EF, ejection fraction; LVESD, left ventricle end-systolic diameter; LVEDD, left ventricle end-diastolic diameter; HR, heart rate; PEP, pre-ejection period; LVET, left ventricular ejection time; SV, stroke volume; CO, cardiac output; SBP, systolic blood pressure; DBP, diastolic blood pressure; LA, left atrial diameter.

	SHAM (n=6)			Placebo (n=10)			Omecaptivmearcarbyl (n=8)		
	Base	2 Mois	2M+OM	Base	2 Mois	2M+placabo	IAO	2 Mois	2 Mois+OM
FR, %	40 ± 1	38.8 ± 3.6*	44.1 ± 4 *	42 ± 2	33 ± 1 *	44 ± 4 ###	38 ± 3	31 ± 4 *	38 ± 4 #
FE, %	74 ± 3	76 ± 2	81 ± 2	76 ± 3	65 ± 4 **	70 ± 3	73 ± 4	63 ± 5 *	68 ± 3
SIVs, mm	2.54 ± 0.11	2.56 ± 0.09	2.73 ± 0.13	3.03 ± 0.18	2.85 ± 0.22	3.20 ± 0.25	2.32 ± 0.09 ££	2.38 ± 0.11	2.51 ± 0.07 ££
SIVd, mm	1.65 ± 0.04	1.68 ± 0.07	1.77 ± 0.09	2.20 ± 0.18	2.38 ± 0.24 \$	2.42 ± 0.15 \$	1.62 ± 0.10	1.78 ± 0.05 £	1.87 ± 0.07
LVESD, mm	5.4 ± 0.2	5.5 ± 0.2	4.6 ± 0.4	4.6 ± 0.2	7.2 ± 0.3 \$\$\$**	4.7 ± 0.4 ###	5.4 ± 0.4	8.0 ± 0.6 \$\$\$**	5.9 ± 0.5 ###
LVEDD, mm	8.9 ± 0.2	9.0 ± 0.2	8.3 ± 0.4	7.9 ± 0.2	10.7 ± 0.3 \$\$\$**	8.5 ± 0.2 ###	8.8 ± 0.5	11.6 ± 0.6 \$\$\$**	9.4 ± 0.7 ###
FC, BPM	285 ± 19	283 ± 23	304 ± 28	315 ± 19	301 ± 15	313 ± 13	301 ± 13	279 ± 14	273 ± 16
LVOT, mm	2.37 ± 0.12	2.54 ± 0.08 *	2.59 ± 0.08 **	2.41 ± 0.06	2.82 ± 0.06 ***	2.85 ± 0.05 ***	2.58 ± 0.05	2.69 ± 0.05	2.69 ± 0.07
PVGs, mm	2.49 ± 0.05	2.63 ± 0.05	2.77 ± 0.09	3.00 ± 0.14	2.89 ± 0.24	3.45 ± 0.19 \$*#	2.69 ± 0.15	2.85 ± 0.23	2.93 ± 0.18
PVGd, mm	1.72 ± 0.05	1.64 ± 0.05	1.68 ± 0.04	1.88 ± 0.17	1.76 ± 0.15	2.35 ± 0.16	1.82 ± 0.12	2.01 ± 0.11	2.06 ± 0.15
PEP, ms	21 ± 3	21 ± 2	14 ± 3 *#	28 ± 2	31 ± 3	34 ± 3 \$\$\$**	20 ± 4	12 ± 2 ££**	15 ± 3 ££
LVET, ms	81 ± 3	79 ± 6	89 ± 8 *	81 ± 1	87 ± 3	88 ± 4	76 ± 2	84 ± 3	100 ± 10 \$\$\$**
ST, ms	103 ± 5	100 ± 3	102 ± 6	109 ± 3	119 ± 4	122 ± 6	95 ± 5	95 ± 4 £	117 ± 11 \$\$\$**
DT, ms	112 ± 9	114 ± 11	106 ± 18	88 ± 9	85 ± 8	72 ± 5 \$	112 ± 9	121 ± 7 £	115 ± 7 £
RR, ms	215 ± 14	214 ± 14	209 ± 23	197 ± 11	202 ± 9	194 ± 8	206 ± 9	216 ± 9	232 ± 14
PEP/LVET	0.25 ± 0.03	0.26 ± 0.03	0.15 ± 0.03 \$\$\$**	0.34 ± 0.02	0.36 ± 0.03	0.38 ± 0.03 ##	0.25 ± 0.04	0.13 ± 0.03 £££***	0.15 ± 0.02 £££**
ST/RR	0.48 ± 0.01	0.47 ± 0.02	0.50 ± 0.03	0.58 ± 0.04 \$	0.59 ± 0.02 \$\$	0.63 ± 0.02 \$\$	0.46 ± 0.02 ££	0.44 ± 0.01 £££	0.50 ± 0.03 ££
ARPht, ms					92 ± 7	123 ± 15 #		89 ± 10	110 ± 12
SV, ml	0.29 ± 0.03	0.32 ± 0.03	0.35 ± 0.02	0.30 ± 0.02	0.51 ± 0.04 \$\$\$**	0.47 ± 0.03 ***	0.31 ± 0.04	0.53 ± 0.04 \$\$\$**	0.44 ± 0.05 \$\$\$**
CO, ml/min	83 ± 10	90 ± 8	106 ± 9	96 ± 8	153 ± 12 \$\$\$**	145 ± 8 ***	97 ± 12	149 ± 15 \$\$\$**	118 ± 8 #
LVOT VTI, mm	67 ± 5	64 ± 4	67 ± 3	66 ± 4	81 ± 3	74 ± 4	63 ± 5	94 ± 6	77 ± 7
TA Sys Pré, mmHg	124 ± 8	128 ± 4	128 ± 9	119 ± 2	115 ± 2	135 ± 4 \$\$\$**	114 ± 2	131 ± 7 **	120 ± 4
TA Dia Pré, mmHg	88 ± 7	90 ± 4	88 ± 8	82 ± 1	59 ± 3 \$\$\$**	69 ± 4 \$*#	73 ± 3	62 ± 3 \$\$\$*	56 ± 3 \$\$\$**
TA Sys Post, mmHg				106 ± 3			97 ± 4		
TA Dia Post, mmHg				63 ± 3			51 ± 2		
Poids, g	479 ± 15	553 ± 16 ***		502 ± 27	577 ± 24 ***		466 ± 23	544 ± 18 ***	
LV Mass	756 ± 124	996 ± 69	883 ± 61	1094 ± 140	1750 ± 209 \$\$\$**	1453 ± 122 #	978 ± 121	1742 ± 156 \$\$\$**	1328 ± 204 *#
Laplace s	67 ± 7	68 ± 4	55 ± 6	46 ± 4	76 ± 7 **	53 ± 6 #	67 ± 8	120 ± 17 ££ \$\$\$**	71 ± 9 ##
Laplace d	119 ± 8	126 ± 12	104 ± 8 #	77 ± 6 \$	73 ± 9 \$\$	65 ± 8 \$	102 ± 9	96 ± 8 £	81 ± 7 \$\$\$**
omax	336 ± 21	343 ± 12	306 ± 29	224 ± 18 \$	282 ± 29 *	248 ± 20	314 ± 21 £	432 ± 39 ££***	309 ± 33 ###
Sigma Es	106 ± 11	110 ± 6	86 ± 9	60 ± 5 \$	104 ± 11 **	73 ± 10 #	81 ± 10	150 ± 22 £\$***	91 ± 11 ###
RWT	0.39 ± 0.02	0.36 ± 0.02	0.41 ± 0.02	0.49 ± 0.05	0.33 ± 0.03 **	0.56 ± 0.05 ##	0.43 ± 0.04	0.36 ± 0.04	0.46 ± 0.05

Table 10. Hemodynamic effects of aortic regurgitation (AR) induced in rats at baseline, 2 months after induction of AR (pre-infusion), and following infusion of omecamtiv mecarbil (OM) or placebo (0.9% NaCl) compared to sham-operated rats 2 months after operation. Values are expressed as mean ± SD. \*p < 0.05; \*\*p < 0.01; \*\*\*p < 0.001 (or other symbols; two-way ANOVA). Comparisons: \* = within a group compared with baseline; # = within a group compared with 2 months (pre-infusion); £ = compared with placebo group at the same time point. FS, fractional shortening; EF, ejection fraction; SWTs, septal wall thickness in systole; SWTd, septal wall thickness in diastole; LVESD, left ventricle end-systolic diameter; LVEDD, left ventricle end-diastolic diameter; HR, heart rate; LVOT, left ventricle outflow tract diameter; PWTs, posterior wall thickness in systole; PWTd, posterior wall thickness in diastole; PEP, pre-ejection period; LVET, left ventricle ejection time; ST, systolic time; DT, diastolic time; RR, interval between successive R; ARPht, aortic regurgitation pressure half-time; SV, stroke volume; CO, cardiac output; VTI, velocity-time integral; BP, blood pressure;  $\sigma$ d, diastolic wall stress;  $\sigma$ , max wall stress;  $\sigma$ Es, end-systolic wall stress; RWT, relative wall thickness.

### 4.3 Effects of OM and placebo on cardiac biomarkers

#### 4.3.1 Effects of OM and placebo on plasma NT-proBNP levels

The plasma NT-proBNP levels were measured on day 0 as well as on days 1, 2, and 7 after OM or placebo treatment (i.e., days 60, 61, 62, and 67 post-procedure) of rats with experimentally

induced AR and sham rats treated with OM (Figure 16). Interestingly, the plasma NT-proBNP levels increased significantly in the rats with surgically induced AR on day 7 after infusion of placebo ( $219 \pm 34$  pg/mL on day 0 vs.  $429 \pm 374$  pg/mL on day 7;  $p < 0.001$ ). We also observed significant increases in plasma NT-proBNP when comparing levels detected on day 1 and day 2 vs. day 7 ( $208 \pm 39$  pg/mL and  $220 \pm 57$  pg/mL, respectively vs.  $429 \pm 374$  pg/mL on day 7;  $p < 0.001$ ). We observed no significant changes when comparing levels detected on days 0, 1, and 2 (days 60, 61, and 62 post-procedure) to one another. Likewise, we observed no significant changes in plasma levels of NT-proBNP in either the sham ( $n=6$ ) or surgically induced AR group ( $n=8$ ) when comparing levels detected at day 0 to those on 1, 2, and 7 after infusion with OM.

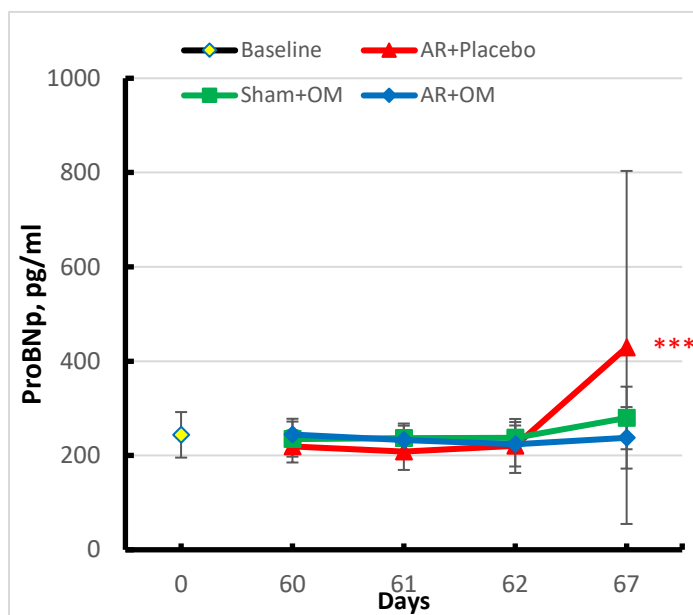


Figure 19. Plasma NT-proBNP levels at baseline (day 0) and at days 60, 61, 62, and 67 after induction of AR or sham procedure in response to administration of OM or placebo in rats with AR ( $n = 8$  or  $10$ , respectively) and OM infusion only in rats in the sham control group ( $n = 6$ ). Values shown are means  $\pm$  SD; \*\*\* $p < 0.001$ .

#### 4.3.2 Effects of OM and placebo on plasma sST2 levels

The plasma sST2 levels measured on day 0 and days 1, 2, and 7 after OM or placebo treatment (i.e., days 60, 61, 62, and 67 post-procedure) in rats with experimentally induced AR and sham

rats treated with OM were assessed (Figure 17). The plasma sST2 levels increased significantly on day 7 when compared to that on day 0 in rats with AR after infusion of placebo ( $543 \pm 154$  vs.  $1,457 \pm 1,248$  pg/mL,  $p < 0.01$ ). Significant increases in plasma sST2 were also observed when comparing results obtained on day 1 (day 61) and day 2 (day 62) vs. day 7 (day 67;  $498 \pm 225$  and  $625 \pm 393$  pg/mL, respectively, vs.  $1,457 \pm 1,248$  pg/mL,  $p < 0.01$ ). Among the rats with AR who were treated with OM, we detected significant increases in sST2 on day 7 after the infusion ( $543 \pm 483$  at day 0 vs.  $1,401 \pm 1,284$  pg/mL,  $p < 0.01$ ). However, we observed no significant differences in plasma sST2 when comparing levels detected on days 1 and 2 vs. day 7. No significant differences in plasma sST2 levels were detected in any of these comparisons in the sham group.

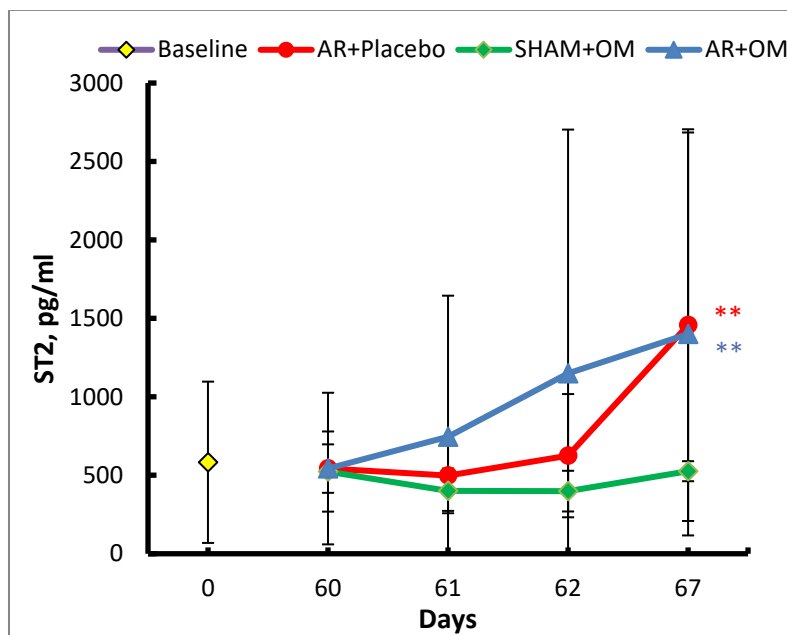


Figure 20. Plasma sST2 levels at baseline (day 0) and at days 60, 61, 62, and 67 after induction of AR or sham procedure in response to administration of OM or placebo in rats with AR ( $n = 8$  or  $10$ , respectively) and OM infusion only in rats in the sham control group ( $n = 6$ ). Values shown are means  $\pm$  SD; \*\* $p < 0.01$ .

#### 4.4 OM and LV genes expression

##### 4.4.1 OM and LV Expression of Genes Regulating Apoptosis and Oxidative Stress

Myocardial LV gene expression of anti-apoptotic Bcl2 was significantly higher in rats treated with OM, compared to placebo, whereas no difference in gene expression of pro-apoptotic Bax was observed (Figure 18A). The resulting pro-apoptotic Bax-to-Bcl2 ratio was reduced in the LV of rats that underwent OM infusion (Figure 18A). We also examined the differential expression of genes involved in oxidative stress regulation. The myocardial expression of Gpx, an antioxidant enzyme, increased in the LV after OM infusion, whereas no changes in Gsr, Sod1, or Sod2 gene expression were observed (Figure 18B).

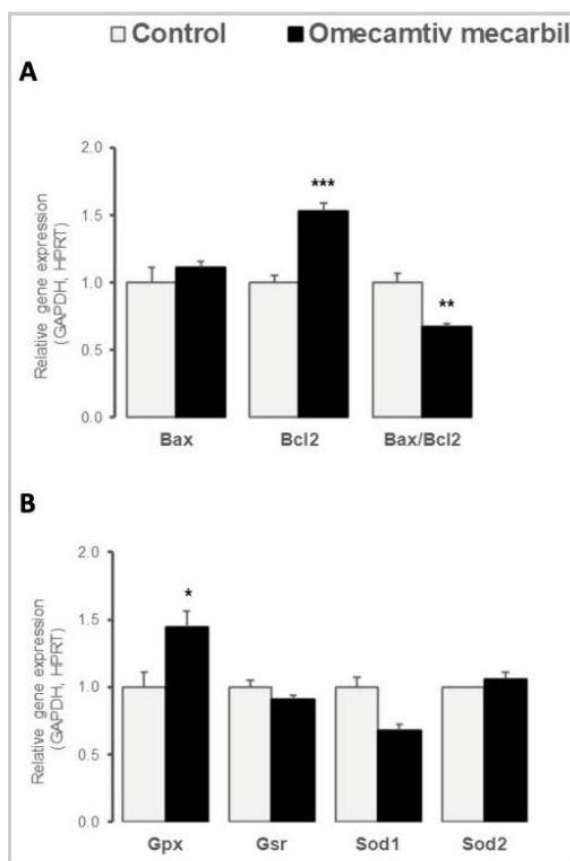


Figure 21. Myocardial left ventricular relative expression of genes implicated in (A) apoptosis (Bax, Bcl2) and (B) oxidative stress (Gpx, Gsr, Sod1, Sod2) processes seven days after omecamtiv mecarbil (OM; n = 6; black bars) versus placebo (n = 8; grey bars) infusion. Values are presented as mean  $\pm$  SD; \* 0.01 < p < 0.05, \*\* 0.001 < p < 0.01, \*\*\* p < 0.001.

#### 4.4.2 OM and LV Expression of genes determinants of Cardiac Energy Substrate Use

As illustrated in Figure 19A, myocardial LV gene expression of key energy sensors Ppar  $\alpha$  and  $\gamma$  and Ampk remained unchanged. Myocardial LV expression of Slc2a1 (Glut1), the major



myocardial glucose transporter, decreased after OM infusion, while gene expression of Slc2a4 (Glut4) remained unchanged (Figure 19B). In contrast, myocardial LV expression of Pdk4, a mitochondrial pyruvate dehydrogenase (PDH) regulator overarching metabolic shift between fatty acid oxidation and glycolysis as energy fuel, increased after OM infusion (Figure 19C), whereas the carnitine palmitoyltransferase1 (Cpt1) remained unchanged (Figure 19D). As illustrated in Figure 2E, the OM infusion increased the LV expression of Alox15 encoding the 12/15 lipoxygenase enzyme implicated in polyunsaturated fatty acid metabolism and of oxidized low-density lipoprotein receptor 1 (Olr1, also known as Lox1) encoding for a scavenger receptor mediating the uptake of oxidized lipoproteins into cells, whereas the gene expression of fatty acid transporter Cd36 remained unchanged.

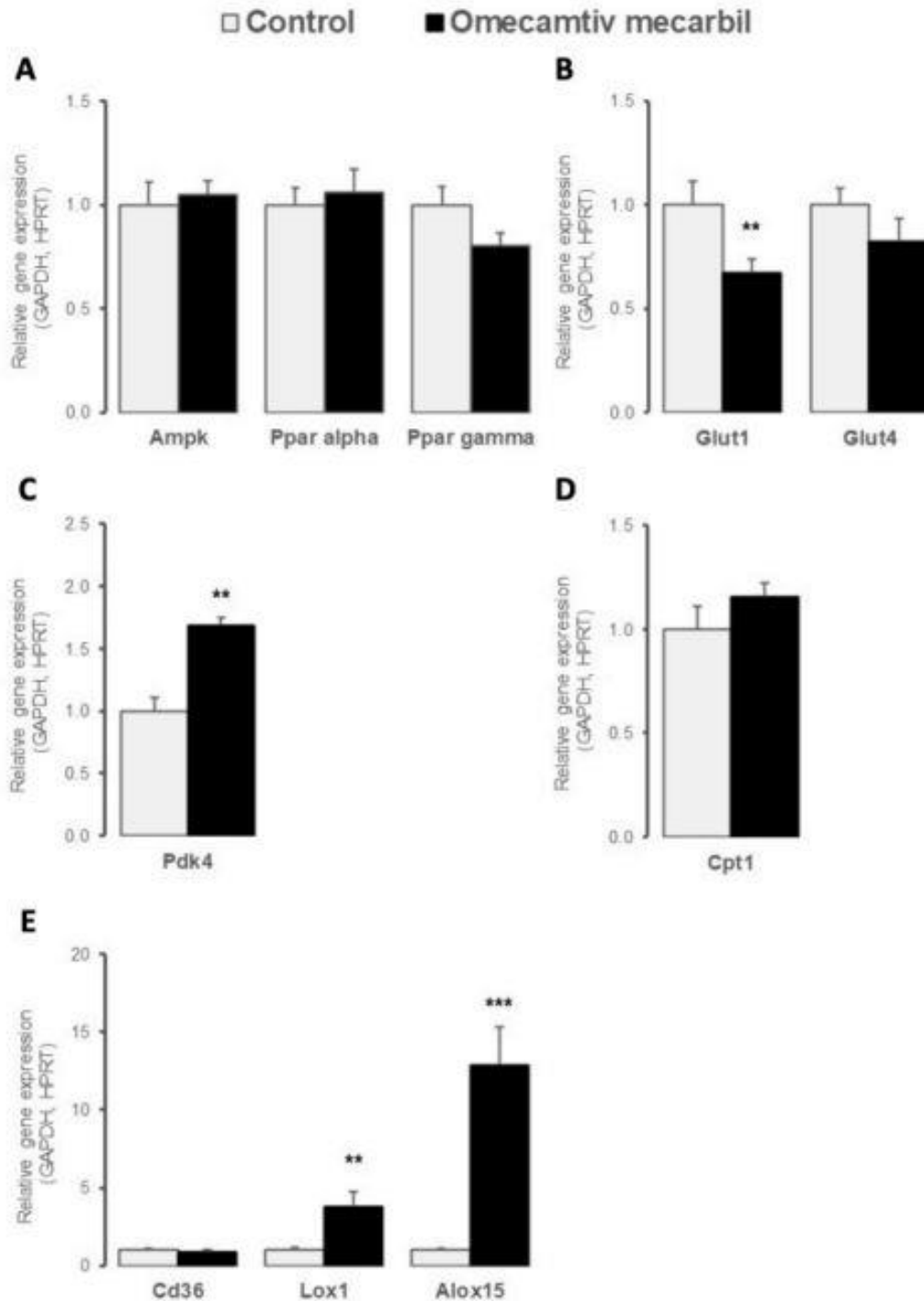


Figure 22. Myocardial left ventricular relative expression of genes implicated in cardiac metabolism, including (A) cellular energy sensors such as Ampk, Ppar  $\alpha$ , and Ppar  $\gamma$ ; (B) glucose transporters Glut1 and Glut4; (C) mitochondrial metabolic regulators contributing to glucose to fatty acids shift as cardiac major energy fuel, such as Pdk4 and (D) Cpt1; and (E) fatty acid metabolism regulators such as Cd36, Lox-1, and Alox-15, seven days after omecamtiv mecarbil (OM; n = 6; black bars) versus placebo (n = 8; grey bars) infusion. Values are presented as mean  $\pm$  SD; \*\* 0.001 < p < 0.01, \*\*\* p < 0.001.

#### 4.4.3 OM and LV Expression of Genes Implicated in Cardiac Contractility

Because OM is a myosin-specific activator that increases myocardial contractility independently of  $\text{Ca}^{2+}$  fluxes, we evaluated the OM-induced myocardial expression of different regulators of cardiac contraction. As illustrated in Figure 20A, OM infusion increased the myocardial LV gene expression of both angiotensin receptors AT1 and AT2, while the gene expression of angiotensin-converting enzymes ACE1 and ACE2 remained unchanged (Figure 20B). Myocardial LV expression of NO-synthase catalyzing the production of NO, a key modulator of myocardial function, was increased by OM infusion for the inducible iNOS isoform, while it remained stable for the constitutive eNOS isoform (Figure 20C). The kallikrein-bradykinin system was upregulated in the LV of rats after OM infusion, with the increased myocardial LV expression of genes encoding the serine proteases Klk8, Klk1c2, and Klk1c12 (Figure 20D), as well as the bradykinin receptors (Bdkr) B1 and B2 (Figure 20E), which are G-protein-coupled receptors mediating kinin actions. No change in myocardial gene expression in Klk10 was observed (Figure 20D). Finally, OM infusion did not induce any changes in the gene expression of major players involved in  $\text{Ca}^{2+}$ -dependent cardiac contraction, except for an increase in LV gene expression of *Cacna1c* in response to OM (Figure 20F).

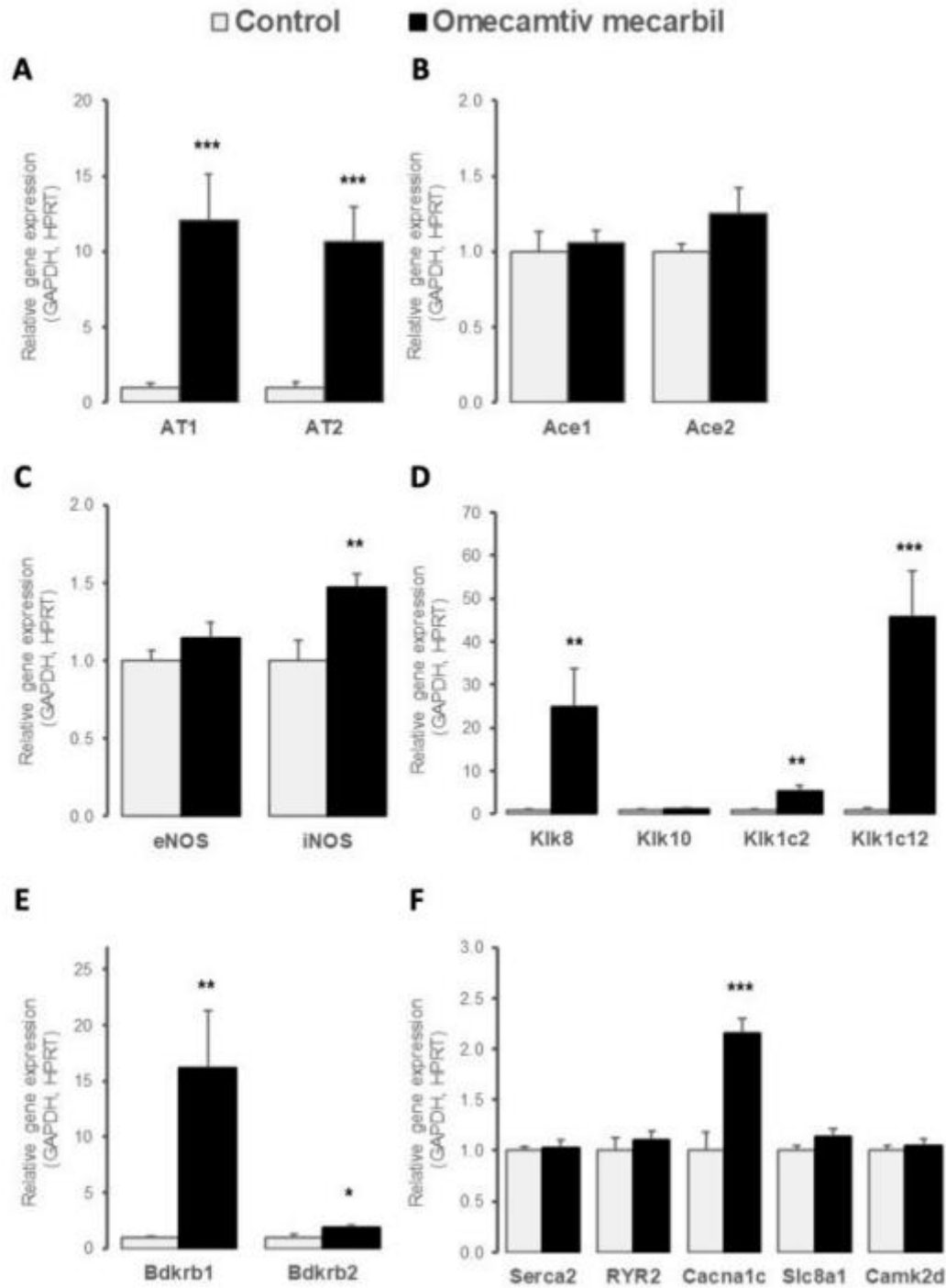


Figure 23. Myocardial left ventricular relative expression of genes controlling myocardial contractility including (A) AT1 and AT2 angiotensin II receptors; (B) ACE1 and ACE2 angiotensin-converting enzymes; (C) endothelial (eNos or Nos3) and inducible (iNos or Nos2) nitric oxide synthases; (D) major cardiac actors of kallikrein (Klk8, Klk10, Klk1c2, and Klk1c12)-(E) bradykinin (Bdkrb1 and Bdkrb2) system and of (F) Ca<sup>2+</sup>-dependent excitation–contraction Atp2a, Ryr2, Cacna1c, Slc8a1, and Camk2d seven days after omecamtiv mecarbil (OM; n = 6; black bars) versus placebo (n = 8; grey bars) infusion. Values are presented as mean ± SD; \* 0.01 < p < 0.05, \*\* 0.001 < p < 0.01, \*\*\* p < 0.001.

## 5. General Discussion

The main findings of the present original work can be summarized as follows:

A. In an experimental rat model of severe chronic AR, OM decreased volume overload, lessened LVEDD and LVESD, decreased LV wall stress parameters

associated with the prolongation of ejection time but did not affect the severity of AR. OM maintained the baseline global cardiac function in rats with severe chronic AR.

B. In this experimental model of AR, OM modified differently the plasma levels of pro-BNP and sST2, both biomarkers of stress and stretching of cardiomyocytes.

C. In the adult rat left ventricle, OM led to an altered gene expression profile in molecules implicated in the activation of apoptosis, oxidative stress, energy substrate metabolism, and induced a minor expression change in the genes involved in  $\text{Ca}^{2+}$  homeostasis and associated myocardial contraction.

D. AR led to an altered gene expression profile in adult rat left ventricle, mainly in genes implicated in myocardial apoptosis, with increased expression of molecules regulating the utilization of glucose as an energy source. This was accompanied by a change in the LV expression of the genes involved in  $\text{Ca}^{2+}$  homeostasis and its associated contraction.

### 5.1 Effect of AR on cardiac function

Chronic severe AR imposes a combined volume and pressure overload on the LV. The volume overload is a consequence of the regurgitant volume itself (29), whereas the pressure overload results from systolic hypertension, which occurs as a result of an increase in total aortic SV from both the regurgitant volume and the forward stroke volume that is ejected into the aorta during systole (29). This effect was observed in all rats (n=18) with induction of AR (Figure 9

in second study). In compensated severe AR, eccentric hypertrophy with combined concentric hypertrophy of the LV is an essential adaptive response to volume overload, which itself is a compensatory mechanism that permits the ventricle to normalize its afterload and maintain normal ejection performance (232). This effect was observed in our rat model, as demonstrated by an RWT value of  $0.34 \pm 0.02$  (n=18), with LV dilation, corresponding to physiologic hypertrophy (233), in agreement with the LV structural remodeling previously described (233) in humans. Sarcomeres are laid down in series, and myofibers are elongated (20), and eccentric hypertrophy preserves LV diastolic compliance and increases LV mass, such that the volume/mass ratio is normal, and LVEF is maintained by increased preload (29). Again, these effects were observed in our two study (increased left atrial diameter, LVEDD, LVEDV and LV mass (n = 12), all  $p < 0.05$ , Figure 9 in second study ).

LV dilatation and systolic hypertension increase wall stress and LV volume/mass ratio. LV wall stress was elevated in rats with AR, and EF was significantly lower than baseline, 2 months after the induction of AR (Figure9). Taniguchi et al. (234) reported an abnormal relationship between EF (depressed contractility) and LV wall stress in patients with chronic AR and advanced cellular hypertrophy which worsened with LV enlargement. Percy et al. (235) addressed the prognostic significance of LV wall stress in asymptomatic patients with AR, and concluded that elevated wall stress in chronic AR predicts a faster deterioration of LV function. Greenberg et al. (236) demonstrated associations between EF response and systolic wall stress and concluded that patients with EF decreased during exercise had elevated resting LV systolic wall stress. The groups studied had similar near-normal LV end-systolic dimensions and abnormal LV wall stress, suggesting that elevated wall stress in chronic AR predicts a poorer mechanical and clinical prognosis that may be independent of classical parameters such as LV dimensions and LV function.

In our first study (229) there is a decrease in stroke volume (SV) and cardiac output (CO) in this study we have no information regarding the hemodynamic conditions and as you know it is a of the determinants of cardiac output ( $DC=MAP/RTP$ , MAP=mean arterial pressure; RTP=total peripheral resistance), Figure 9 corresponds to the results of our second study (230) where there is an increase in these parameters (CO and SV), a second possible explanation the anesthesia technique is different depending on the study, Plante et al (322) reported Impact of anesthesia on echocardiographic evaluation of systolic and diastolic function in rats by comparing two groups of rats with RA, that the VES and DC is significantly lower in the group of rats anesthetized with Ketamine Xylazine intraperitoneally vs isoflurane, in our first study (229) the rats were anesthetized with Ketamine, medetomidine and the second (230) with isoflurane.

## 5.2 Effect of OM on AR and wall stress

In our two studies (229, 230), OM extended LVET and ST, as reported previously (67), without changes in DT. OM did not affect the severity of AR, as measured by AR PHT <200 msec (230). This finding was concordant with the results of our first study (229). However, in our first study, we subjectively graded the severity of the AR jet on a scale from 1 to 4, whereas in the second study, we used an objective quantification of AR to measure the effect of OM on AR more precisely. In mitigation, however, excessive prolongation the duration of systole might compromise myocardial blood flow, and thereby aggravate ischemia; even if studies with OM in patients with angina and ischemic cardiomyopathy seem reassuring in this regard (237). This stands in contrast with inotropic drugs that enhance the risk of ischemia, arrhythmias and death. Hence forth those risks have limited their utility in treating acute and chronic heart failure (238).

In our two studies (229,230), OM decreased volume overload induced by AR during the whole cardiac cycle, by lowering LVEDD. Moreover, by decreasing LVEDD and LVESD OM decreased wall stress in AR, our results showed that treatment with OM decreased maximum wall stress, end-systolic wall stress, and diastolic wall stress of the LV (Figure 8) in our rat model of AR. In our model, this effect was related to a decrease in LVEDD and a decrease in average maximum systolic pressure. End-systolic wall stress was significantly lower ( $p < 0.05$ ) in the placebo group ( $n = 10$ ), but to a lesser extent than in the OM group ( $n = 8$ ;  $p < 0.001$ ). Furthermore, decreases in LVEDD and end-diastolic pressure following OM have been reported in animal models of cardiac ischemia (65, 239).

Reducing ventricular wall stress is considered as a cornerstone in treating HF (240). In its simplest form, as described by Laplace's law, ventricular wall stress is directly proportional to the diameter of the ventricle and ventricular pressure and is inversely proportional to the wall thickness of the ventricle. It is widely believed that increased ventricular wall stress is responsible for the adverse remodeling process that eventually leads to HF (241). Increased wall stress is an independent predictor of subsequent LV remodeling (242). One of the main determinants of myocardial oxygen usage is peak systolic wall stress (243). Because the cavity decreases in size and the wall thickens increase during ejection, protosystolic stress is twice the telesystolic stress (244). This variation is greater than that of the pressures during systole; therefore, peripheral vascular resistance overestimates the overload losses secondary to vasodilatation but underestimates increase caused by vasoconstriction (245).

### 5.3 Effect of OM on cardiac function

OM decreased SV and CO without any effect on HR but were not inferior to baseline pump indices and with prolongation of LVET and ST (Table 9). In contrast, OM increased FS in a



similar manner to classic inotropes by improved emptying in systole. Furthermore, we did not observe any SV, CO, or HR changes in our all-placebo group (Table 5 and 9). The extended myocardial systole could have caused the reduced contractile efficiency observed in the OM group. The fact that LVEDD, and consequently the LV volume, decreased despite unchanged preload and HR suggest that OM induces myocardial constraint in late diastole. This is in line with a previous study that reported that OM slows relaxation and increases passive tension at rest in isolated rat cardiomyocytes (68).

Shen et al. (64) reported that OM significantly increases CO and SV. However, their study differed in several aspects from the present study. They used a canine model of ischemia, the animals were conscious, and the dose of OM and duration of infusion were different. All these factors could explain the difference in the effect of OM on cardiac function compared with our study. Nevertheless, OM significantly extended LVET in both studies. Because our AR model did not exhibit characteristics of diastolic dysfunction, the interpretation that OM impairs diastolic performance warrants caution. The impairment of diastolic function by OM was reported by Rønning et al. (239) in pigs with acute ischemic HF. OM failed to restore general pump indices such as SV, CO, and EF in the pig model. Likewise, they found no significant changes in SV and CO in the pig model of ischemia in response to OM treatment.

In our first study (229), OM increased SV and CO in rats with AR. In that study, the animals were anesthetized with an intraperitoneal injection of ketamine/medetomidine. Ketamine is a dissociative anesthetic agent with a cardiovascular effect resembling sympathetic nervous system stimulation, increasing HR and CO (246). Medetomidine improves muscle relaxation, potentiates the anesthetic action of ketamine, and compensates for the cardiac-stimulating effect of ketamine by decreasing HR and CO. Dexmedetomidine had no direct myocardial depressant effect in the rat heart in doses like those encountered in clinical conditions (247). Because the different animal groups were all anesthetized using the same regimen, the decrease in HR that

we observed can be attributed to OM in our previous study. However, we cannot predict whether this bradycardic effect of OM would also have occurred in conscious, non-sedated animals. In the second study (230), animals were anesthetized using 1.5% inhaled isoflurane. Current evidence suggests that isoflurane exerts a negative inotropic effect (248). This in contrast with the increase in SV during isoflurane anesthesia we observed in this study, possibly because the negative inotropic effects of isoflurane can be overridden by a decrease in systemic vascular resistance (249).

#### 5.4 The differential response of cardio biomarkers to OM in experimental model of AR

Our findings included several notable results. First, contrary to our initial hypothesis and despite the severity of cardiac dysfunction revealed by the echocardiographic findings (particularly those documenting changes in LV parameters), we detected no significant changes in plasma levels of NT-proBNP at two months after surgical induction of AR compared to baseline. As expected, we did not detect any significant correlations between echocardiographic parameters and plasma NT-proBNP levels. One explanation could be that compensatory mechanisms might develop in the LV in response to chronic severe AR. For example, the LV can adapt to volume overload by developing eccentric hypertrophy and increased mass. In this situation, the LV volume/mass ratio remains within normal limit values. In addition, the LVEF is maintained by increased preload, and, despite an increase in the end-systolic diameter and pressure early in the course of the disease, the end-systolic wall stress is maintained within the normal range of values by a compensatory increase in the wall thickness (29). In a previous study, Song et al. (250) reported that NT-proBNP levels may reflect time-dependent structural and/or functional changes in the LV. Similarly, Weber and colleagues (90) found that NT-proBNP levels were associated with clinical symptoms in patients with chronic AR, notably with dyspnea. Interestingly, none of the rats in our study developed dyspnea (231). Another possible explanation considers the long-time span between the induction of AR and the first biochemical assessment.

Given the biological half-life of NT-proBNP, plasma levels detected at two months after induction of AR may be significantly influenced by the number of cardiomyocytes available for and engaged in its production.

It is unlikely that the significant increase in NT-proBNP in the rats with AR treated with a placebo infusion can be explained by an increase in wall stress as a result of volume overload *per se* since the two groups of rats (AR and sham) treated with OM received the same volume of liquid. No modification of the plasma NT-proBNP levels was observed in the latter group.

However, volume overload not counteracted by concomitant OM administration in the presence of AR could explain this observation. This result is consistent with an OM-mediated reduction in myocardial wall stress in the AR group as reported in a previous study (230). Moreover, NT-proBNP expression is promoted not only by mechanical stretch, but also, by proinflammatory, oxidative, and trophic stimuli (251).

Our results also revealed that plasma sST2 levels underwent no significant change from baseline levels to 60 days after induction of AR despite the impact of this procedure on LV function. Najjar et al. (252) reported that there were no significant differences in sST2 levels when comparing healthy controls to subjects with HF with a preserved ejection fraction. This is in contrast to Weinberg et al. (102) who reported that sST2 levels increased significantly as early as one day after experimentally-induced myocardial infarction (MI). Interestingly, three days after MI, serum sST2 levels were similar to those of control mice. This group also reported a significant increase in sST2 levels detected in patients one day after experiencing a MI, compared to values obtained at two weeks and three months thereafter. These results suggest that elevations in circulating sST2 levels may represent a transient response to acute myocardial stress that diminishes over time and ultimately returns to baseline levels after several weeks to months.

In our study (231), we identified significant positive correlations between sST2 levels with body weight and PWTd. Interestingly, we observed no significant increases in PWTd two months after the induction of AR. The explanation for this observation is unclear given the overall absence of changes in sST2 after AR induction. We can only speculate that the stress imposed on cardiomyocytes, during diastole, secondary to overload associated to AR as described in humans, may play a role (101). The gene encoding sST2 is induced under conditions of myocardial overload associated with MI, as the myocardial tissue that remains viable is required to bear more stress.

In our model, we identified no associations between plasma sST2 levels and LV function and geometry, including LV volume and mass. This finding is consistent with results reported in

other recent studies that also demonstrated no specific associations between sST2 levels and LV function or geometry as assessed by echocardiography in humans (252,253).

Likewise, we observed a correlation between sST2 levels and weight only in the rats with surgically-induced AR. This correlation may reflect the impact of myocardial stress, ventricular remodeling, and/or fibrosis (102). It is also possible that surgical induction of AR results in a chronic inflammatory response. sST2 has been implicated in numerous inflammatory diseases (101), as well as in cardiovascular pathophysiology. No correlations between these parameters were detected in the sham group despite significant weight gain.

The significant increase in plasma sST2 levels observed in rats with AR in response to placebo administration may be directly related to acute cardiomyocyte stretch due to volume overload and mechanical stress (254). Volume overload in a setting of a fragilized hemodynamic status as a result of AR could conceivably induce similar changes in sST2 than those already discussed with NT-proBNP. In contrast, no changes in plasma sST2 levels were detected in the sham rats at days 1, 2, and 7 after OM administration. This could be explained by the fact that cardiomyocytes in control rats can support this acute volume overload. Changes in sST2 levels in rats with AR that present volume overload and were treated with OM, differ completely from those already discussed with NT-proBNP. We believe that this is an important finding of our study as it highlights a differential regulation of NT-proBNP and sST2 in AR. Rønning et al. (239) reported that administration of OM prolonged the systolic ejection time in LV dilated due to ischemia. This may be associated with

limited capacity of LV distensibility observed in diastole. Interestingly, OM had an opposite effect in animal models of cardiac ischemia. This is consistent with previous findings that suggest that OM reduces the rate of relaxation and increases passive tension in isolated cardiomyocytes at rest (68). This will limit the extent to which the cardiomyocytes can undergo additional stretch or distension, including that required to compensate for AR. NT-

proBNP remained unchanged, while sST2 increased markedly in our study (231) suggesting that passive muscle tension induced by OM has distinct and subtle deleterious effects in the setting of AR, not reliably assessed by modifications in circulating NT-proBNP levels.

### 5.5 OM and LV rat's gene expression

Our results show that a single 30-min infusion of myosin activator OM induced significant LV expression alterations in genes regulating apoptosis (with decreased pro-apoptotic Bax-to-Bcl2 ratio), oxidative stress (with increased antioxidant Gpx), cardiac metabolism (with decreased Glut1 and increased Lox1, Alox15, and Pdk4), and contraction (with increased AT1 and AT2, upregulation of kallikrein-bradykinin system, but no changes in molecules involved in Ca<sup>2+</sup>-dependent myocardial contraction) 7 days after OM infusion. The first set of gene expression profile focuses on the differential expression of the genes regulating apoptosis. Specifically, we examined the OM-induced gene expression of mitochondrial anti-apoptotic Bcl2, and pro-apoptotic Bax (255). Bcl2 is known to control the release of cytochrome c, preserve mitochondrial integrity, and protect against apoptosis (256). Our findings revealed a significant increase in Bcl2 expression, leading to a down-regulation of the Bax-to-Bcl2 ratio, in response to OM infusion. The Bax-to-Bcl2 ratio reflects an overall vulnerability to apoptosis; increases in the Bax-to-Bcl2 ratio suggest higher levels of apoptotic activity (257). In contrast to the response to the inotropic agent dobutamine, which partially activates the apoptosis processes in vivo (258), our results suggested that OM did not activate apoptotic processes and was even able to protect the LV against apoptosis. Gpx is one of three main antioxidant enzymes (259). Our findings revealed that OM infusion resulted in increased expression of Gpx, but had no impact on any other tested antioxidant genes.

Interestingly, these findings are contrasted with those reported for other inotropic drugs.

Indeed, levosimendan was shown to reduce oxidative stress through increased expression of genes encoding Sod and Gpx (260). In a recent publication, Rhoden et al. (261) reported that OM promoted the accumulation of mitochondrial reactive oxygen species (ROS) in both rat and human cardiac tissues. As ROS are known to promote the expression of Gpx (262), our results (227) suggested a link between OM and this critical antioxidant pathway. We also evaluated the effects of OM on cardiac metabolism via the evaluation of genes involved in the metabolism of fatty acids, glucose, and lactate and the production of high-energy phosphates (263). Glut1 is the major determinant of homeostatic glucose transport in cardiac muscle (264). Administration of OM resulted in decreased expression of Glut1 in rat LV, which may result in decreased glucose uptake. In contrast to the findings reported for dobutamine (264), the present results suggest that OM promoted a shift from glycolytic to oxidative metabolism (264). Fatty acid catabolism is coordinately regulated with glucose pathways to support homeostasis. In response to changes in energy supply or demand.

Reciprocal regulation in fatty acid and glucose metabolism involves both the PDH complex and the Cpt (265). PDH converts the pyruvate generated by glycolysis to acetyl-CoA and CO<sub>2</sub> via oxidative decarboxylation, while the Cpt contributes to fatty acid transport into mitochondria, where they undergo oxidation to generate acetyl-CoA (265). Pdk4 is an important regulator of PDH activity (266). Increased levels of Pdk4 promote the inactivation of PDH and, thus, act on the metabolic shift from glucose to fatty acid oxidation (267). In the present study, the administration of OM resulted in increased expression in Pdk4, which may be a marker of increased fatty acid oxidation in the LV (268).

Decreased glucose uptake and increased fatty acid oxidation may result in the production of higher levels of ATP and higher O<sub>2</sub> consumption. These findings are consistent with those reported by Bakkehaug et al. (65), who reported that the administration of OM resulted in increased myocardial oxygen consumption. Similarly, Lox1, which was originally identified as

a receptor for oxidatively-modified LDL (269), can be induced by numerous stimuli, including angiotensin II (270), shear stress (271), and ischemia-reperfusion injury (272). Alox15, which is a lipid-peroxidizing enzyme (273), has been implicated in the pathogenesis of atherosclerosis (268,269,274) diabetes, and neurodegenerative disease (273). The expression levels of both Lox1 and Alox15 were markedly increased in HF (274,275), and increased expression of Lox1 was detected in cases of diastolic dysfunction (262,276). OM-associated diastolic dysfunction and stiffness have also been reported (277,278). Here, we found increased LV expression in Lox1 and Alox15 in OM-infused rats. Because Lox1 expression has been related to diastolic dysfunction, the link between OM infusion, specific molecular determinants, and diastolic dysfunction should be further studied in future studies. Angiotensin II binding to AT1 induces vasoconstriction and promotes oxidative stress by activating NADPH oxidase and inducing eNOS uncoupling. This results in a switch from NO to the production of ROS, including superoxide. In contrast, binding to AT2 promotes vasorelaxation, protection against ischemia-reperfusion injury and myocardial infarction, and decreased inflammation (279). Thus, the activation of AT2-mediated pathways may counter-regulate those resulting from AT1 activation (280). Here, we found increased gene expression of both AT1 and AT2 in response to OM, with an observed AT2-to-AT1 ratio of 1.15. A high AT2-to-AT1 ratio has been associated with increased oxidative stress and cardiac cell apoptosis (281). The relatively low ratio observed in the present study is consistent with the absence of activation of apoptosis and oxidative stress. Nitric oxide synthase (NOS) catalyzes the conversion of L-arginine to L-citrulline and NO, which is a free radical involved in both homeostatic and immunological functions. iNOS is a Ca<sup>2+</sup>-independent enzyme that is expressed in cardiomyocytes, in response to environmental perturbation (e.g., cytokine release) (282). The activation of iNOS results in substantially higher levels of NO, compared to other forms of NOS (283). In the heart, iNOS contributes to a contractile dysfunction characteristic of ischemia-reperfusion injury,



infarction, and HF (284,285). In contrast, several studies have shown beneficial effects of iNOS in the normal, hypertrophied, transplanted, or cardiomyopathic human heart (286,287). Here, we found that the administration of OM resulted in increased iNOS expression, whose significance to OM mechanism of action has to be further determined.

KLK8 has been previously detected in the rat myocardium (288). Although its physiologic substrates remain largely unknown, the expression of Klk8 protects against acute ischemia-reperfusion injury and induces cardiac hypertrophy in rats (288,289), in response to pressure overload (288). Klk1c2 (also known as tonin) can catalyze the release of angiotensin II directly from angiotensinogen; thus, the activation of this enzyme may result in increased production of angiotensin II, independently of ACE activity (290). Klk1c2 may also induce cardiac hypertrophy (291). Klk1c2 perfusion in Wistar rats induced coronary vasoconstriction and simultaneously depressed myocardial contractility; the time to peak for cell shortening and half relaxation was significantly reduced. All these results suggest that  $Ca^{2+}$  handling is significantly accelerated by Klk1c2 (292). Direct interactions between Klk1c2 or Klk1 and the Kinin B2 receptor are critical factors responsible for cardioprotective responses. The activation of this pathway is known to inhibit oxidative stress, apoptosis, and inflammation, as well as cardiac hypertrophy and fibrosis (293). These ligand-receptor interactions result in improved cardiac function and lead to reduced blood pressure (293). In our study, OM administration resulted in an increased expression of Klk1, Klk1c2, and Klk8. In the present study, increases in all these three proteases may allow the heart to develop a combined adaptative response to OM (288). The bradykinin receptor family includes two G protein-coupled receptors (Bdkrb1 and Bkrbr2) that also mediate the biological effects of kinins (293).

Bdkrb1 is expressed and synthesized de novo, in response to tissue injury and inflammation (294). Bdkrb2 is the main receptor for bradykinin; it interacts directly with AT2 (294), as well as other receptors (293). While signaling, both Bdkrb1 and Bdkrb2 induce NO production

(293), and their overall physiological and pathophysiological significance remain unknown (293). Cardioprotective effects mediated by Bdkrb1 or Bdkrb2 alone via ACE-inhibition have been reported (293). Endothelial overexpression of Bdkrb1 in rat models has resulted in an expanded LV cavity and reduced function (295). Bradykinin-mediated upregulation of Bdkrb2 in the absence of Bdkrb1 did not provide full cardioprotection. Interestingly, the upregulation of Bdkrb1, in the absence of Bdkrb2, results in further tissue damage (296). In the present study, the administration of OM resulted in increased expression of both Bdkrb1 and Bdkrb2 and could, therefore, suggest potential cardioprotective effects. The L-type  $\text{Ca}^{2+}$  channel  $\alpha 1\text{C}$ -subunit gene (*Cacna1c*) plays an essential role in cardiac excitation–contraction coupling (297). This protein is localized in the T-tubule sarcolemma, adjacent to RYR2, where it controls  $\text{Ca}^{2+}$  influx from the extracellular milieu into the cytosol and, thus, serves as a major determinant of cardiac function.  $\beta$ -adrenergic receptor stimulation increases the number of L-type channels at the sarcolemma, which results in enhanced  $\text{Ca}^{2+}$  influx and amplification of excitation–contraction coupling (298). Prolonged AT1 signaling via reduced L-type  $\text{Ca}^{2+}$  channels result in a negative inotropic effect (299).  $\text{Ca}^{2+}$ -calmodulin-dependent protein kinase II (CaMKII) activity controls the expression of *Cacna1c* in isolated rat neonatal ventricular cardiomyocytes (276). In the present study, the administration of OM increased the expression of *Cacna1c*, although this resulted in no modification of the *Serca2*, RYR2, GLUT1, or *CamkII* expressions; these have been all implicated in maintaining  $\text{Ca}^{2+}$  homeostasis. In canine LV monocytes, OM has been recently shown to affect intracellular  $\text{Ca}^{2+}$  homeostasis by increasing the capacity of RYR2 to remain open, therefore impacting cardiomyocyte repolarization (299). However, it seems that *Cacna1c* would provide only minor contributions to intracellular  $\text{Ca}^{2+}$  release.

Administration of OM did not result in a significant increase in the concentration of cytosolic  $\text{Ca}^{2+}$ . The increase in *Cacna1c* expression in response to OM might, instead, be related to a diastolic  $\text{Ca}^{2+}$  leak from the sarcoplasmic reticulum (276). Low-level  $\text{Ca}^{2+}$  release induced by

Cav1.2  $\alpha 1$  may serve to restore and maintain  $\text{Ca}^{2+}$  levels that resulted from the leak in the SR (300). As previously reported (277), permeabilized human cardiomyocytes exhibited a marked reduction in the rate of force generation and relaxation once the  $\text{Ca}^{2+}$  concentration reached a steady state in permeabilized human cardiomyocytes. Collectively, these findings suggest the existence of a previously unidentified action of OM in promoting  $\text{Ca}^{2+}$  regulation at the actin-myosin complex.

### 5.6 Combined volume and pressure overload and LV rat's gene expression

The present experimental model of combined volume and pressure overload in rats induced significant LV expression alterations in genes regulating apoptosis (with increased pro-apoptotic Bax-to- Bcl2 ratio), oxidative stress (with decreased antioxidant Sod2), cardiac metabolism (with decreased Glut4, ampk4, ppar gamma and increased Lox1, Alox15), and contraction (with increase of kallikrein 10, and decreased SERCA2a involved in  $\text{Ca}^{2+}$ -dependent myocardial contraction) 7 days after placebo infusion in rats with AR.

In the present study, we evaluated the echocardiographic parameters and gene expression in the LV of rats with AR. As previously reported (230), the administration of placebo in rats with AR resulted in increased FS, cardiac output and stroke volume, and decreased LVESD, LVESDD, and end-systolic wall stress. Hemodynamically, placebo infusion significantly increased systolic and diastolic blood pressures. However, we did not observe significant increases in maximum wall stress, end-diastolic wall stress and EF.

The first set of gene expression profile focuses on the differential expression of the genes regulating apoptosis. We therefore examined the AR-induced gene expression of mitochondrial anti-apoptotic Bcl2, and pro-apoptotic Bax (255). Our findings revealed a significant increase in Bax expression, leading to an up-regulation of the Bax-to-Bcl2 ratio, in response to AR. As already mentioned above, the Bax-to-Bcl2 ratio reflects an overall vulnerability to apoptosis (257). Our findings revealed that AR also resulted in increased

expression of Gpx, and decreases SOD2. Gpx and SOD are antioxidant enzymes acting to protect cells against different hydroperoxides resulting from reactive oxygen species (ROS) through scavenging reactions (302). As ROS are known to promote the expression of Gpx (299), SOD2 clear mitochondrial reactive oxygen species (ROS) and, as a result, confer protection against cell death. (303), In animal models of hemodynamic overload leading to myocardial remodeling and failure, there is a chronic increase in myocardial oxidative stress (304), tonic mechanical stretch of rat papillary muscle increases the production of reactive oxygen species (ROS), which appear to be involved in mediating myocyte apoptosis in that model (305). Thus, our results suggest a link between AR and apoptotic activation.

We also evaluated the effects of AR on cardiac metabolism via the evaluation of genes involved in the metabolism of fatty acids and glucose. In the present study, AR was associated with decreased myocardial expression of GLUT4, while GLUT1 expression did not change. Both GLUT1 and GLUT4 are the main glucose transporters in the heart. Germ-line disruption of the GLUT4 gene resulted in striking cardiac hypertrophy, and impaired cardiac function. These mice were hyperinsulinemic and had profound alterations in cardiac substrate delivery, thus it was uncertain if the cardiac hypertrophy was a primary or secondary consequence of GLUT4 ablation (306). In the present study, cardiac expressions of different key energy sensors, including Ppar's and Ampk was also evaluated. Ampk detects intracellular ATP/AMP ratio and plays a pivotal role in intracellular adaptation to energy stress. Here, expression of Ampk was decreased after AR. Cardiac AMPK activation has been involved in cardiac protection, accelerating ATP generation and attenuating ATP depletion, protecting against cardiac dysfunction and cardiomyocyte apoptosis (307). Inactivation of Ampk has been linked to the activation of apoptotic processes in cardiomyocytes (308), while Ampk activation reduced cardiomyocyte apoptosis improved diabetic cardiomyopathy and can inhibit myocardial hypertrophy (309,310).

Ampk can regulate the fatty acid metabolism via promoting the fatty acid uptake, oxidation, it can regulate the glucose metabolism through promoting glucose uptake and glycolysis

(310). PPAR $\gamma$  regulates fatty acid storage by stimulate lipid uptake and adipogenesis by fat cells and glucose metabolism by increases insulin sensitivity (132), decreased of GLUT4, Ampk and PPAR $\gamma$  without alteration of GLUT1 expression suggest that AR switches myocardial energy source for oxidative energy from fatty acids to glucose.

Lox1 is a membrane scavenger receptor involved in internalization of oxLDL by endothelial cells (150). Myocardial ischemia enhances expression of Lox1, which, in turn, promotes cardiomyocyte apoptosis, local inflammation, and fibroblast activation, thereafter favoring myocardial fibrosis and loss of cardiac function (311). Similar results were also found when endothelial cells were exposed to shear stress, supporting a role of disturbed blood flow on Lox1 mechanotransduction (152), increased expression of Lox1 was detected in cases of diastolic dysfunction (300). Alox15, which is a lipid-peroxidizing enzyme (269), has been implicated in the pathogenesis of atherosclerosis (150), diabetes, and neurodegenerative disease (270). The expression levels of both Lox1 and Alox15 were markedly increased in HF (271, 272). AR is associated with diastolic dysfunction and shear stress who can explain at least partly the present results.

Sarcoplasmic reticulum ATPase (SERCA, SR Ca<sup>2+</sup>-pump ATPase) plays a major role in Ca<sup>2+</sup> signalling, and is involved in various aspects of cell function, such as transcription, apoptosis, exocytosis, signal transduction, and cell motility (312). SERCA is responsible for the movement of Ca<sup>2+</sup> against concentration gradient between the SR and the cytosol. It has been shown that SERCA 2 gene knockout disrupted SR function and this disruption was associated with HF in mice (313). It has been described in chronic overload, with decreased SERCA2a expression in both pressure (314) and volume overload (315), in our study SERCA2a decreased in rats' wit AR these results correlate with the literature data.

Klk10 is a member of the kallikrein-related peptidase 'KLK' family and was initially discovered as a potential tumor suppressor with its expression downregulated in breast, prostate, testicular, and lung cancer (316, 317). Klk10 inhibits endothelial inflammation,

endothelial barrier dysfunction, and reduces endothelial migration and tube formation, but not apoptosis or proliferation. It may serve as potential anti-atherogenic therapeutic targets (317). Our results show an increase in *klk10* in rats with AR. Only one study reported increased expression of *klk10* in a model of volume overload with aorta-cava fistula (318) but not in AR. It may be thus be related to the compensatory phase of AR, an adaptation mechanism to protect against ventricular dysfunction.

### 5.7 Limitations of the studies and perspectives

The present studies have several limitations. First the limited number of rats with chronic AR, that thus represented a narrow observational window into the natural course of this disease.

Further investigations with a larger sample size will be necessary for a more robust evaluation, interpretation, and corroboration of our findings.

Second, we did not measure plasma NT-proBNP and sST2 at all the time points between the induction of AR and the initiation of experimental OM infusions two months later. Thus, we do not have a clear kinetics of the events that may have occurred during this interval period.

Third, we did not perform echocardiographic or any invasive hemodynamic measurements on days 1, 2, and 7 after the OM or placebo infusions. Thus, we were unable to evaluate the relationships between these parameters and the changes in plasma sST2 and NT-proBNP concentrations observed. We used an ELISA kit marked “research use only” to assay plasma sST2 levels. There may be considerable differences between the results from this commercial assay and others currently in wide use (319).

Although the effects of OM are concentration-, time-, and species-dependent (298), only one set of experimental conditions was examined here. Indeed, we did not assess dose-dependent hemodynamic effects in our model of AR. Thus, caution is appropriate when extrapolating these data to humans. In addition, the evaluation was performed at gene level and may not correspond directly with protein expression and function levels *in vivo*. Future studies should be performed in experimental models with LV pathology to better understand the effects of

OM in this context. Finally, all the rats in the present study were male and we know that the expression of genes in the left ventricle related to AR can be different depending on the sex (320). The role of various signaling pathways controlling the gene expression in the AR should be more extensively explored.

## 6. Conclusion

In conclusion, the administration of OM led to a significant increase in the duration of left ventricular ejection time (LVET) and ST in the rat AR model; while it did not affect the duration of DT or the severity of AR. OM also significantly decreased LV wall stress in experimental rats with chronic severe AR. The mechanisms underlying these findings remain to be determined.

In terms of cardiac function, OM maintained general pump indices and baseline values of SV and CO. Increased and decreased plasma levels of cardiac biomarkers sST2 and NT-proBNP were observed in response to therapeutic OM infusions in rats with AR. These results may reflect ongoing AR-associated LV dysfunction in response to the administration of OM. We note that the mechanism of action of this drug has not been fully elucidated.

OM infusion in rats with normal LV function yielded gene expression profiles that suggested the preservation of myocardial LV tissue against induction of apoptosis and oxidative stress. The gene expression profiles also suggested an increase in fatty acid oxidation in the LV that may be compatible with an increased rate of oxygen consumption. Interestingly, OM administration had no impact on LV expression of genes involved in  $Ca^{2+}$  homeostasis or  $Ca^{2+}$ -mediated muscle contraction. Future studies based on these results may provide further insight into the precise mechanisms of action of OM. Plasma sST2 levels correlated positively with both PWTd (posterior wall thickness in diastole) and body weight in rats with chronic severe AR. LV gene expression profiles from these rats suggested increased myocardial LV apoptosis, oxidative stress, and glucose oxidation among other findings, thereby highlighting potential LV dysfunction.

## 7. REFERENCES

1. Bayne, Edward J (8 January 2016). "Bicuspid Aortic Valve: Background, Pathophysiology, Epidemiology". Medscape.
2. Rock CA, Han H, Doehring TC. Complex collagen fiber and membrane morphologies of the whole porcine aortic valve. *PLoS One*. 2014 Jan 21;9(1): e86087.
3. Butcher JT, Mahler GJ, Hockaday LA (2011) Aortic valve disease and treatment: the need for naturally engineered solutions. *Adv Drug Deliv Rev* 63: 242–268.
4. Gross L, Kugel MA (1931) Topographic Anatomy and Histology of the Valves in the Human Heart. *Am J Pathol* 7: 445–474 447.
5. Sacks MS, David Merryman W, Schmidt DE (2009) On the biomechanics of heart valve function. *J Biomech* 42: 1804–1824.
6. Balguid A, Driessen NJ, Mol A, Schmitz JP, Verheyen F, et al. (2008) Stress related collagen ultrastructure in human aortic valves—implications for tissue engineering. *J Biomech* 41: 2612–2617.
7. Gundiah N, Kam K, Matthews PB, Guccione J, Dwyer HA, et al. (2008) Asymmetric mechanical properties of porcine aortic sinuses. *Ann Thorac Surg* 85: 1631–1638.
8. Khan Z, Boughner DR, Lacefield JC (2008) Anisotropy of high-frequency integrated backscatter from aortic valve cusps. *Ultrasound Med Biol* 34: 1504–1512.
9. Cohn LH, Birjiniuk V. Therapy of acute aortic regurgitation. *Cardiol Clin*. 1991; 9: 339–352.
10. Singh JP, Evans JC, Levy D, Larson MG, Freed LA, Fuller DL, Lehman B, Benjamin EJ. Prevalence and clinical determinants of mitral, tricuspid, and aortic regurgitation (the Framingham Heart Study) [published correction appears in *Am J Cardiol*. 1999; 84:1143]. *Am J Cardiol*. 1999; 83: 897–902.
11. Kim M, Roman MJ, Cavallini MC, Schwartz JE, Pickering TG, Devereux RB. Effect of hypertension on aortic root size and prevalence of aortic regurgitation. *Hypertension*. 1996; 28: 47–52.



12. Vasan RS, Larson MG, Levy D, Larson MG, Freed LA, Fuller DL, Lehman B, Benjamin EJ. Determinants of echocardiographic aortic root size. *Circulation*. 1995; 91: 734–740.
13. Lebowitz NE, Bella JN, Roman MJ, Liu JE, Fishman DP, Paranicas M, Lee ET, Fabsitz RR, Welty TK, Howard BV, Devereux RB. Prevalence and correlates of aortic regurgitation in American Indians: The Strong Heart Study. *J Am Coll Cardiol*. 200; 36: 461–467.
14. Mills P, Leech G, Davies M, Leathan A. The natural history of a non-stenotic bicuspid aortic valve. *Br Heart J*. 1978 Sep;40(9):951-7.
15. Roberts WC. The congenitally bicuspid aortic valve. A study of 85 autopsy cases. *Am J Cardiol*. 1970 Jul;26(1):72-83.
16. Wauchope G. The clinical importance of variations in the number of cusps forming the aortic and pulmonary valves. *Q J Med* 1928; 21:383-399.
17. Smith DE, Matthews MB. Aortic valvular stenosis with coarctation of the aorta, with special reference to the development of aortic stenosis upon congenital bicuspid valves. *Br Heart J*. 1955 Apr;17(2):198-206.
18. Bacon AP, Matthews MB. Congenital bicuspid aortic valves and the aetiology of isolated aortic valvular stenosis. *Q J Med*. 1959 Oct; 28:545-60.
19. Carabello BA. Aortic regurgitation: a lesion with similarities to both aortic stenosis and mitral regurgitation. *Circulation*. 1990; 82: 1051–1053.
20. Ricci DR. Afterload mismatch and preload reserve in chronic aortic regurgitation. *Circulation*. 1982; 66: 826–834.
21. Ross J Jr, McCullagh WH. Nature of enhanced performance of the dilated left ventricle during chronic volume overloading. *Circ Res*. 1972; 30: 549–556.
22. Starling MR, Kirsh MM, Montgomery DG, Gross MD. Mechanism for left ventricular systolic dysfunction in aortic regurgitation: importance for predicting the functional response to aortic valve replacement. *J Am Coll Cardiol*. 1991; 17: 887–897.
23. Wisenbaugh T, Spann JF, Carabello BA. Differences in myocardial performance and load between patients with similar amounts of chronic aortic versus chronic mitral regurgitation. *J Am Coll Cardiol*. 1984; 3: 916–923.
24. Magid NM, Young MS, Wallerson DC, Goldweit RS, Carter JN, Devereux RB, Borer JS. Hypertrophic and functional response to experimental chronic aortic regurgitation. *J*

- Mol Cell Cardiol. 1988; 20: 239–246.
25. Nitenberg A, Foulst JM, Antony I, Blanchet F, Rahali M. Coronary flow and resistance reserve in patients with chronic aortic regurgitation, angina pectoris and normal coronary arteries. *J Am Coll Cardiol.* 1988; 11: 478–486.
  26. Ardehali A, Segal J, Cheitlin MD. Coronary blood flow reserve in acute aortic regurgitation. *J Am Coll Cardiol.* 1995; 25: 1387–1392.
  27. Borer JS, Truter S, Herrold EM, Falcone DJ, Pena M, Carter JN, Dumlao TF, Lee JA, Supino PG. Myocardial fibrosis in chronic aortic regurgitation: molecular and cellular responses to volume overload. *Circulation.* 2002; 105: 1837–1842.
  28. Truter SL, Goldin D, Kolesar J, Dumlao TF, Borer JS. Abnormal gene expression of cardiac fibroblasts in experimental aortic regurgitation. *Am J Ther.* 2000; 7: 237–243.
  29. Bekeredjian R, Grayburn PA. Valvular heart disease: aortic regurgitation. *Circulation* 2005 Jul 5;112(1):125-34.
  30. Bonow RO, Carabello BA, Chatterjee K, de Leon AC Jr, Faxon DP, Freed MD, Gaasch WH, Lytle BW, Nishimura RA, O’Gara PT, O’Rourke RA, Otto CM, Shah PM, Shanewise JS; 2006 Writing Committee Members; American College of Cardiology/American Heart Association Task Force. 2008 Focused update incorporated into the ACC/AHA 2006 guidelines for the management of patients with valvular heart disease: a report of the American College of Cardiology/American Heart Association Task Force on Practice Guidelines (Writing Committee to Revise the 1998 Guidelines for the Management of Patients With Valvular Heart Disease): endorsed by the Society of Cardiovascular Anesthesiologists, Society for Cardiovascular Angiography and Interventions, and Society of Thoracic Surgeons. *Circulation.* 2008 Oct 7;118(15):e523-661.
  31. Bonow RO, Lakatos E, Maron BJ, Epstein SE. Serial long-term assessment of the natural history of asymptomatic patients with chronic aortic regurgitation and normal left ventricular systolic function. *Circulation.* 1991 Oct;84(4):1625-35.
  32. Bonow RO, Rosing DR, McIntosh CL, Jones M, Maron BJ, Lan KK, Lakatos E, Bacharach SL, Green MV, Epstein SE. The natural history of asymptomatic patients with aortic regurgitation and normal left ventricular function. *Circulation.* 1983 Sep;68(3):509-17.
  33. Tarasoutchi F, Grinberg M, Spina GS, Sampaio RO, Cardoso Lu, Rossi EG, Pomerantzeff P, Laurindo F, da Luz PL, Ramires JA. Ten-year clinical laboratory follow-up after application of a symptom-based therapeutic strategy to patients with severe chronic aortic regurgitation of predominant rheumatic etiology. *J Am Coll*

Cardiol. 2003 Apr 16;41(8):1316-24.

34. Siemieniczuk D, Greenberg B, Morris C, Massie B, Wilson RA, Topic N, Bristow JD, Cheitlin M. Chronic aortic insufficiency: factors associated with progression to aortic valve replacement. *Ann Intern Med.* 1989 Apr 15;110(8):587-92.
35. Scognamiglio R, Rahimtoola SH, Fasoli G, Nistri S, Dalla Volta S. Nifedipine in asymptomatic patients with severe aortic regurgitation and normal left ventricular function. *N Engl J Med.* 1994 Sep 15;331(11):689-94.
36. Borer JS, Hochreiter C, Herrold EM, Supino P, Aschermann M, Wencker D, Devereux RB, Roman MJ, Szulc M, Kligfield P, Isom OW. Prediction of indications for valve replacement among asymptomatic or minimally symptomatic patients with chronic aortic regurgitation and normal left ventricular performance. *Circulation.* 1998 Feb 17;97(6):525-34.
37. Detaint D, Messika-Zeitoun D, Maalouf J, Tribouilloy C, Mahoney DW, Tajik AJ, Enriquez-Sarano M. Quantitative echocardiographic determinants of clinical outcome in asymptomatic patients with aortic regurgitation: a prospective study. *JACC Cardiovasc Imaging.* 2008 Jan;1(1):1-11.
38. Henry WL, Bonow RO, Rosing DR, Epstein SE. Observations on the optimum time for operative intervention for aortic regurgitation. II. Serial echocardiographic evaluation of asymptomatic patients. *Circulation.* 1980 Mar;61(3):484-92.
39. Bonow RO. Radionuclide angiography in the management of asymptomatic aortic regurgitation. *Circulation.* 1991 Sep;84(3 Suppl): I296-302.
40. Dujardin KS, Enriquez-Sarano M, Schaff HV, Bailey KR, Seward JB, Tajik AJ. Mortality and morbidity of aortic regurgitation in clinical practice. A long-term follow-up study. *Circulation.* 1999 Apr 13;99(14):1851-7.
41. Spagnuolo M, Kloth H, Taranta A, Doyle E, Pasternack B. Natural history of rheumatic aortic regurgitation. Criteria predictive of death, congestive heart failure, and angina in young patients. *Circulation.* 1971 Sep;44(3):368-80.
42. Hegglin R, Scheu H, Rothlin M. Aortic insufficiency. *Circulation.* 1968 Jul;38(1 Suppl):77-92.
43. American College of Cardiology/American Heart Association Task Force on Practice Guidelines. 2008 Focused update incorporated into the ACC/AHA 2006 guidelines for the management of patients with valvular heart disease: a report of the American College of Cardiology/American Heart Association Task Force on Practice Guidelines (Writing Committee to Revise the 1998 Guidelines for the Management of Patients with

Valvular Heart Disease), endorsed by the Society of Cardiovascular Anesthesiologists, Society for Cardiovascular Angiography and Interventions, and Society of Thoracic Surgeons. *Circulation* 118(15), e523–e661 (2008).

44. Guidelines for the management of patients with valvular heart disease executive summary. A Report of the American College of Cardiology/American Heart Association Task Force on Practice Guidelines (Committee on Management of Patients with Valvular Heart Disease). *Circulation* 98, 1949–1984 (1998).
45. Guidelines on the management of valvular heart disease: the Task Force on the Management of Valvular Heart Disease of the European Society of Cardiology. *Eur. Heart J.* 28, 230 (2007).
46. Lin A, Stewart R. Medical treatment of asymptomatic chronic aortic regurgitation. *Expert Rev Cardiovasc Ther.* 2011 Sep;9(9):1249-54.
47. Cohn LH, Birjiniuk V. Therapy of acute aortic regurgitation. *Cardiol Clin.* 1991 May;9(2):339-52.
48. Vahanian A, Baumgartner H, Bax J, Butchart E, Dion R, Filippatos G, Flachskampf F, Hall R, Iung B, Kasprzak J, Nataf P, Tornos P, Torracca L, Wenink A; Guidelines on the management of valvular heart disease: The Task Force on the Management of Valvular Heart Disease of the European Society of Cardiology. *Eur Heart J.* 2007 Jan;28(2):230-68.
49. Nishimura RA, McGoon MD, Schaff HV, Giuliani ER. Chronic aortic regurgitation: indications for operation--1988 *Mayo Clin Proc.* 1988 Mar;63(3):270-80.
50. Enriquez-Sarano M, Tajik AJ. Clinical practice. Aortic regurgitation. *N Engl J Med.* 2004 Oct 7;351(15):1539-46.
51. Hinken AC, Solaro RJ. A dominant role of cardiac molecular motors in the intrinsic regulation of ventricular ejection and relaxation. *Physiology (Bethesda, MD)* 2007;22:73–80.
52. Marieb, E.N. et Hoehn K., *Anatomie et Physiologie humaines*, 2e et 4e Ed. Éditions du Renouveau Pédagogique inc., 1999.
53. Solaro RJ, de Tombe PP. Review focus series : sarcomeric proteins as key elements in integrated control of cardiac function. *Cardiovasc Res.* 2008; 77:616–618.
54. Spudich JA. How molecular motors work. *Nature.* 1994; 372:515–518.

55. Vale RD, Milligan RA. The way things move: looking under the hood of molecular motor proteins. *Science*. 2000; 288:88–95.
56. Kaplinsky E, Mallarkey G. Cardiac myosin activators for heart failure therapy: focus on omecamtiv mecarbil. *Heart Fail Rev*. 2009 Dec;14(4):289-98.
57. Malik FI, Hartman JJ, Elias KA, Morgan BP, Rodriguez H, Brejc K, Anderson RL, Sueoka SH, Lee KH, Finer JT, Sakowicz R, Baliga R, Cox DR, Garard M, Godinez G, Kawas R, Kraynack E, Lenzi D, Lu PP, Muci A, Niu C, Qian X, Pierce DW, Pokrovskii M, Suehiro I, Sylvester S, Tochimoto T, Valdez C, Wang W, Katori T, Kass DA, Shen YT, Vatner SF, Morgans DJ. Cardiac myosin activation: a potential therapeutic approach for systolic heart failure. *Science* 2011; 331:1439–1443.
58. Planelles-Herrero VJ, Hartman JJ, Robert-Paganin J, Malik FI, Houdusse A. Mechanistic and structural basis for activation of cardiac myosin force production by omecamtiv mecarbil. *Nat Commun* 2017; 8:190.
59. Cleland JG, Teerlink JR, Senior R, Nifontov EM, Mc Murray JJ, Lang CC, Tsyrlin VA, Greenberg BH, Mayet J, Francis DP, Shaburishvili T, Monaghan M, Saltzberg M, Neyses L, Wasserman SM, Lee JH, Saikali KG, Clarke CP, Goldman JH, Wolff AA, Malik FI. The effects of the cardiac myosin activator, omecamtiv mecarbil, on cardiac function in systolic heart failure: a double-blind, placebo-controlled, crossover, dose-ranging phase 2 trial. *Lancet* 2011; 378:676–683.
60. Teerlink JR, Clarke CP, Saikali KG, Lee JH, Chen MM, Escandon RD, Elliott L, Bee R, Habibzadeh MR, Goldman JH, Schiller NB, Malik FI, Wolff AA. Dose-dependent augmentation of cardiac systolic function with the selective cardiac myosin activator, omecamtiv mecarbil: a first-in-man study. *Lancet* 2011; 378:667–675.
61. Greenberg BH, Chou W, Saikali KG, Escandon R, Lee JH, Chen MM, Treshkur T, Megreladze I, Wasserman SM, Eisenberg P, Malik FI, Wolff AA, Shaburishvili T. Safety and tolerability of omecamtiv mecarbil during exercise in patients with ischemic cardiomyopathy and angina. *JACC Heart Fail* 2015; 3:22–29.
62. Vu T, Ma P, Xiao JJ, Wang YM, Malik FI, Chow AT. Population pharmacokinetic-pharmacodynamic modeling of omecamtiv mecarbil, a cardiac myosin activator, in healthy volunteers and patients with stable heart failure. *J Clin Pharmacol*. 2015 Nov;55(11):1236-47.
63. Chen PW, Trivedi A, Lee E, Dutta S, Ahamadi M. Population Pharmacokinetic Properties of Omecamtiv Mecarbil in Healthy Subjects and Patients with Heart Failure with Reduced Ejection Fraction. *J Cardiovasc Pharmacol*. 2022 Apr 1;79(4):539-548.

64. Shen YT, Malik FI, Zhao X, Depre C, Dhar SK, Abarzua P, Morgans DJ, Vatner SF. Improvement of cardiac function by a cardiac myosin activator in conscious dogs with systolic heart failure. *Circ Heart Fail* 2010; 3:522–527.
65. Bakkehaug JP, Kildal AB, Engstad ET, Boardman N, Næsheim T, Rønning L, Aasum E, Larsen TS, Myrmed T, How O-J. Myosin activator omecamtiv mecarbil increases myocardial oxygen consumption and impairs cardiac efficiency mediated by resting myosin ATPase activity. *Circ Heart Fail* 2015; 8:766–775.
66. Bakkehaug JP, Kildal AB, Engstad ET, Boardman N, Naesheim T, Ronning L, Aasum E, Larsen TS, Myrmed T, How O-J. Response to letter regarding article, “Myosin activator omecamtiv mecarbil increases myocardial oxygen consumption and impairs cardiac efficiency mediated by resting myosin ATPase activity”. *Circ Heart Fail* 2015; 8:1142.
67. Liu Y, White HD, Belknap B, Winkelmann DA, Forgacs E. omecamtiv mecarbil modulates the kinetic and motile properties of porcine  $\beta$ -cardiac myosin. *Biochemistry* 2015; 54:1963–1975.
68. Nagy L, Kovacs A, Bodi B, Pasztor ET, Fulop GA, Toth A, Edes I, Papp Z. The novel cardiac myosin activator omecamtiv mecarbil increases the calcium sensitivity of force production in isolated cardiomyocytes and skeletal muscle fibres of the rat. *Br J Pharmacol* 2015; 172:4506–4518.
69. Swenson AM, Tang W, Blair CA, Fetrow CM, Unrath WC, Previs MJ, Campbell KS, Yengo CM. Omecamtiv mecarbil enhances the duty ratio of human beta cardiac myosin resulting in increased calcium sensitivity and slowed force development in cardiac muscle. *J Biol Chem* 2017; 292:3768–3778.
70. Utter MS, Ryba DM, Li BH, Wolska BM, Solaro RJ. Omecamtiv mecarbil, a cardiac myosin activator, increases  $Ca^{2+}$  sensitivity in myofilaments with a dilated cardiomyopathy mutant tropomyosin E54K. *J Cardiovasc Pharmacol* 2015;66:347–353.
71. van der Velden J, Klein LJ, Zaremba R, Boontje NM, Huybregts MAJM, Stoker W, Eijnsman L, de Jong JW, Visser CA, Visser FC, Stienen GJM. Effects of calcium, inorganic phosphate, and pH on isometric force in single skinned cardiomyocytes from donor and failing human hearts. *Circulation* 2001; 104:1140–1146.
72. van der Velden J, Klein LJ, Zaremba R, Boontje NM, Huybregts MAJM, Stoker W, Eijnsman L, de Jong JW, Visser CA, Visser FC, Stienen GJM. Effects of calcium, inorganic phosphate, and pH on isometric force in single skinned cardiomyocytes from donor and failing human hearts. *Circulation* 2001; 104:1140–1146.
73. Messer AE, Jacques AM, Marston SB. Troponin phosphorylation and regulatory function in human heart muscle: dephosphorylation of Ser23/24 on troponin I could

- account for the contractile defect in end-stage heart failure. *J Mol Cell Cardiol* 2007; 42:247–259.
74. van der Velden J, Papp Z, Zaremba R, Boontje NM, de Jong JW, Owen VJ, Burton PBJ, Goldmann P, Jaquet K, Stienen GJM. Increased Ca<sup>2+</sup>-sensitivity of the contractile apparatus in end-stage human heart failure results from altered phosphorylation of contractile proteins. *Cardiovasc Res* 2003; 57:37–47.
75. Meyer M, Keweloh B, Guth K, Holmes JW, Pieske B, Lehnart SE, Just H, Hasenfuss G. Frequency-dependence of myocardial energetics in failing human myocardium as quantified by a new method for the measurement of oxygen consumption in muscle strip preparations. *J Mol Cell Cardiol* 1998; 30:1459–1470.
76. Teerlink JR, Felker GM, McMurray JJ, Ponikowski P, Metra M, Filippatos GS, Ezekowitz JA, Dickstein K, Cleland JG, Kim JB, Lei L, Knusel B, Wolff AA, Malik FI, Wasserman SM; ATOMIC-AHF Investigators. Acute treatment with omecamtiv mecarbil to increase contractility in acute heart failure: the ATOMIC-AHF study. *J Am Coll Cardiol* 2016; 67:1444–1455.
77. Teerlink JR, Felker GM, McMurray JJV, Solomon SD, Adams KF Jr, Cleland JGF, Ezekowitz JA, Goudev A, Macdonald P, Metra M, Mitrovic V, Ponikowski P, Serpytis P, Spinar J, Tomcsányi J, Vandekerckhove HJ, Voors AA, Monsalvo ML, Johnston J, Malik FI, Honarpour N. Chronic Oral Study of Myosin Activation to Increase Contractility in Heart Failure (COSMIC-HF): a phase 2, pharmacokinetic, randomised, placebo-controlled trial. *Lancet* 2016; 388:2895–2903.
78. Mann DL. Searching for the perfect agent to improve cardiac contractility. *Lancet* 2016; 388:2845–28.
79. Teerlink JR, Diaz R, Felker GM, McMurray JV, Metra M, Solomon SD, Legg JC, Büchele G, Varin C, Kurtz CE, Malik FI, Honarpour N. Omecamtiv Mecarbil in Chronic Heart Failure with Reduced Ejection Fraction: Rationale and Design of GALACTIC-HF. *JACC Heart Fail.* 2020 Apr;8(4):329-340.
80. Felker GM, Solomon SD, Claggett B, Diaz R, McMurray JV, Metra M, Anand I, Crespo-Leiro MG, Dahlström U, Goncalvesova E, Howlett JG, MacDonald P, Parkhomenko A, Tomcsányi J, Abbasi SA, Heitner SB, Hucko T, Kupfer S, Malik FI, Teerlink JR. Assessment of Omecamtiv Mecarbil for the Treatment of Patients With Severe Heart Failure: A Post Hoc Analysis of Data From the GALACTIC-HF Randomized Clinical Trial. *JAMA Cardiol.* 2022 Jan 1;7(1):26-34.
81. de Lemos JA, McGuire DK, Drazner MH: Btype natriuretic peptide in cardiovascular disease. *Lancet* 2003; 362:316–322.

82. Rubattu S, Sciarretta S, Valenti V, Stanzone R, Volpe M: Natriuretic peptides: an update on bioactivity, potential therapeutic use, and implication in cardiovascular diseases. *Am J Hypertens* 2008; 21:733–741.
83. Ikeda T, Matsuda K, Itoh H, Shirakami G, Miyamoto Y, Yoshimasa T, Nakao K, Ban T: Plasma levels of brain and atrial natriuretic peptides elevate in proportion to left ventricular end-systolic wall stress in patients with aortic stenosis. *Am Heart J* 1997; 133:307–314.
84. Choure A, Tang WH, Mills RM: Natriuretic peptides in valvular heart diseases. *Heart Fail Clin* 2006; 2:345–352.
85. Muders F, Kromer EP, Griese DP, Pfeifer M, Hense HW, Riegger GA, Elsner D. Evaluation of plasma natriuretic peptides as markers for left ventricular dysfunction *Am Heart J*, 134 (1997), pp. 442-449.
86. Anand IS, Fisher LD, Chiang YT, Latini R, Masson S, Maggioni A, Robert G, Cohn JN. Changes in brain natriuretic peptide and norepinephrine over time and mortality and morbidity in the Valsartan Heart Failure Trial (Val-HeFT) *Circulation*, 107 (2003), pp. 1278-1283.
87. de Lemos JA, Morrow DA, Bentley JH, Torbjorn O. The prognostic value of B-type natriuretic peptide in patients with acute coronary syndromes *N Engl J Med*, 345 (2001), pp. 1014-1021.
88. ten Wolde M, Tulevski II, Mulder JW, Söhne M, Boomsma F, Mulder BJM, Büller HR. Brain natriuretic peptide as a predictor of adverse outcome in patients with pulmonary embolism *Circulation*, 107 (2003), pp. 2082-2084.
89. Gerber IL, Stewart RA, French JK, Malcolm LE, Greaves SC, West TM, Kerr AJ, Mark AR, White H D. View full profile Associations between plasma natriuretic peptide levels, symptoms, and left ventricular function in patients with chronic aortic regurgitation *Am J Cardiol*, 92 (2003), pp. 755-758.
90. Weber M, Hausen M, Arnold R, Moellmann H, Nef H, Elsaesser A, Mitrovic V, Hamm C. Diagnostic and prognostic value of N-terminal pro B-type natriuretic peptide (NT-proBNP) in patients with chronic aortic regurgitation. *Int J Cardiol*. 2008 Jul 21;127(3):321-7.
91. Song BG, Park YH, Kang GH, Chun WJ, Oh JH, Choi JO, Lee SC, Park SW, Oh JK, Sung KI, Park P, Jeon ES. Preoperative, postoperative and one-year follow-up of N-terminal pro-B-type natriuretic peptide levels in volume overload of aortic regurgitation: comparison with pressure overload of aortic stenosis. *Cardiology*. 2010;116(4):286-91.



92. Tominaga S. A putative protein of a growth specific cDNA from BALB/ c-3T3 cells is highly similar to the extracellular portion of mouse interleukin 1 receptor. *FEBS Lett.* 1989;258(2):301–304.
93. Schmitz J, Owyang A, Oldham E, et al. IL-33, an interleukin-1-like cytokine that signals via the IL-1 receptor-related protein ST2 and induces T helper type 2-associated cytokines. *Immunity.* 2005;23(5): 479–490.
94. Tominaga S, Kuroiwa K, Tago K, Iwahana H, Yanagisawa K, Komatsu N. Presence and expression of a novel variant form of ST2 gene product in human leukemic cell line UT-7/GM. *Biochem Biophys Res Commun.* 1999;264(1):14–18.
95. Iwahana H, Hayakawa M, Kuroiwa K, et al. Molecular cloning of the chicken ST2 gene and a novel variant form of the ST2 gene product, ST2LV. *Biochim Biophys Acta.* 2004;1681(1):1–14.
96. Ciccone MM, Cortese F, Gesualdo M, et al. A novel cardiac bio-marker: ST2. A review. *Molecules.* 2013;18(12):15314–15328.
97. Mirchandani AS, Salmond RJ, Liew FY. Interleukin-33 and the function of innate lymphoid cells. *Trends Immunol.* 2012;33(8):389–396.
98. Liew FY, Pitman NI, McInnes IB. Disease-associated functions of IL-33: The new kid in the IL-1 family. *Nat Rev Immunol.* 2010;10(2):103–110.
99. Li R, Yang G, Yang R, Peng X, Li J. Interleukin-33 and receptor ST2 as indicators in patients with asthma: A meta-analysis. *Int J Clin Exp Med.* 2015;8(9):14935–14943.
100. Shi LJ, Liu C, Li JH, Zhu XY, Li YN, Li JT. Elevated levels of soluble ST2 were associated with rheumatoid arthritis disease activity and ameliorated inflammation in synovial fibroblasts. *Chin Med J (Engl).* 2018;131(3):316–322.
101. Boga S, Alkim H, Koksall AR, et al. Serum ST2 in inflammatory bowel disease: A potential biomarker for disease activity. *J Investig Med.* 2016;64(5):1016–1024.
102. Weinberg EO, Shimpo M, De Keulenaer GW, MacGillivray C, Tominaga S, Solomon SD, Rouleau JL, Lee RT. Expression and regulation of ST2, an interleukin-1 receptor family member, in cardiomyocytes and myocardial infarction. *Circulation.* 2002;106(23): 2961–2966.

103. Bartunek J, Delrue L, Van Durme F, et al. Nonmyocardial production of ST2 protein in human hypertrophy and failure is related to diastolic load. *J Am Coll Cardiol*. 2008;52(25):2166–2174.
104. Dudek M, Kałużna-Oleksy M, Migaj J, Straburzyńska-Migaj E. Clinical value of soluble ST2 in cardiology *Adv Clin Exp Med*. 2020 Oct;29(10):1205-1210.
105. Nuñez G, Clarke MF. The Bcl-2 family of proteins: regulators of cell death and survival. *Trends Cell Biol*. 1994; 4:399–403.
106. White E. Life, death and the pursuit of apoptosis. *Genes Dev*. 1996; 10:1–15.
107. Vekrellis K, McCarthy MJ, Watson A, Whitfield J, Rubin LL, Ham J. Bax promotes neuronal cell death and is downregulated during the development of the nervous system. *Development*. 1997; 124:1239–12.
108. Cory S, Huang DC, Adams JM. The Bcl-2 family: roles in cell survival and oncogenesis. *Oncogene*. 2003; 22:8590–8607.
109. Jarskog LF, Selinger ES, Lieberman JA, Gilmore JH. Apoptotic proteins in the temporal cortex in schizophrenia: high bax/bcl-2 ratio without caspase-3 activation. *Am J Psychiatry*. 2004; 161:109–115.
110. Oltvai ZN, Milliman CL, Korsmeyer SJ. Bcl-2 heterodimerizes in vivo with a conserved homolog, Bax, that accelerates programmed cell death. *Cell*. 1993; 74:609–619.
111. Aouacheri W, Saka S, Djafer R, Lefranc G. Protective effect of diclofenac towards the oxidative stress induced by paracetamol toxicity in rats. *Ann Biol Clin (Paris)* . 2009 Nov-Dec ;67(6) :619-27.
112. Mohora M, Greabu M, Muscurel C, et al. The sources and the targets of oxidative stress in the etiology of diabetes complications *Romanian J Biophys*, 17 (2007), pp. 63-84.
113. Small DM, Coombes JS, Bennett N, et al. Oxidative stress, anti-oxidant therapies and chronic kidney disease *Nephrology*, 17 (2012), pp. 311-321.
114. Kassab A, Piwowar A. Cell oxidant stress delivery and cell dysfunction onset in type 2 diabetes *Biochimie*, 94 (2012), pp. 1837-1848.
115. Karimi Galoughi K, Antoniadou C, Nicholls SJ, Channon KM, Figtree GA. Redox biomarkers in cardiovascular medicine. *Eur Heart J* 2015; 36:1576–1582.
116. Tsutsui H, Kinugawa S, Matsushima S. Oxidative stress and heart failure. *Am J Physiol Heart Circ Physiol* 2011;301:H2181-2190.

117. Ponikowski P, Voors AA, Anker SD, Bueno H, Cleland JG, Coats AJ, Falk V, González-Juanatey JR, Harjola VP, Jankowska EA, Jessup M, Linde C, Nihoyannopoulos P, Parissis JT, Pieske B, Riley JP, Rosano GM, Ruilope LM, Ruschitzka F, Rutten FH, van der Meer P. 2016. ESC Guidelines for the diagnosis and treatment of acute and chronic heart failure: The Task Force for the diagnosis and treatment of acute and chronic heart failure of the European Society of Cardiology (ESC). Developed with the special contribution of the Heart Failure Association (HFA) of the ESC. *Eur J Heart Fail* 2016; 18:891–975.
118. Muthukumar K, Nachiappan V. Cadmium-induced oxidative stress in *Saccharomyces cerevisiae*. *Indian Journal of Biochemistry & Biophysics*. December 2010;47 (6): 383–7.
119. Muthukumar K, Rajakumar S, Sarkar MN, Nachiappan V. Glutathione peroxidase3 of *Saccharomyces cerevisiae* protects phospholipids during cadmium-induced oxidative stress. *Antonie van Leeuwenhoek*. May 2011;99 (4): 761–71.
120. Borgstahl GE, Parge HE, Hickey MJ, Johnson MJ, Boissinot M, Hallewell RA. Human mitochondrial manganese superoxide dismutase polymorphic variant Ile58Thr reduces activity by destabilizing the tetrameric interface". *Biochemistry*. April 1996;35 (14): 4287–4297.
121. Hayyan M, Hashim MA, AlNashef IM. Superoxide Ion: Generation and Chemical Implications. *Chemical Reviews*. March 2016;116 (5): 3029–3085.
122. Meister A. Glutathione metabolism and its selective modification. *J. Biol. Chem*. November 1988;263 (33): 17205–8.
123. Deponate M. Glutathione catalysis and the reaction mechanisms of glutathione-dependent enzymes. *Biochim. Biophys. Acta*. May 2013;1830 (5): 3217–66.
124. Kim TT, Dyck JR. Is AMPK the savior of the failing heart? *Trends Endocrinol Metab* 2015; 26: 40-48.
125. Heidrich F, Schotola H, Popov AF, Sohns C, Schuenemann J, Friedrich M, Coskun KO, von Lewinski D, Hinz J, Bauer M, Mokashi SA, Sossalla S, Schmitto JD. AMPK - activated protein kinase and its role in energy metabolism of the heart. *Curr Cardiol Rev*2010; 6: 337-342.
126. Steinberg G.R., Carling D. AMP-activated protein kinase: The current landscape for drug development. *Nat. Rev. Drug Discov*. 2019; 18:527–551. doi: 10.1038/s41573-019-0019-2.

127. Sher T, Yi HF, McBride OW, Gonzalez FJ. "cDNA cloning, chromosomal mapping, and functional characterization of the human peroxisome proliferator activated receptor". *Biochemistry*. June 1993;32 (21): 5598–604.
128. Peeters A, Baes M. Role of PPAR $\alpha$  in Hepatic Carbohydrate Metabolism. *PPAR Research*. 2010: 572405.
129. Lemberger T, Saladin R, Vázquez M, Assimacopoulos F, Staels B, Desvergne B, Wahli W, Auwerx J. Expression of the peroxisome proliferator-activated receptor alpha gene is stimulated by stress and follows a diurnal rhythm. *J Biol Chem*. 1996 Jan 19;271(3):1764-9.
130. Kersten S. Integrated physiology and systems biology of PPAR $\alpha$ . *Molecular Metabolism*. 2014;3 (4): 354–371.
131. Michalik L, Auwerx J, Berger JP, Chatterjee VK, Glass CK, Gonzalez FJ. International Union of Pharmacology. LXI. Peroxisome proliferator-activated receptors. *Pharmacological Reviews*. December 2006;58 (4): 726–41.
132. Ahmadian M, Suh JM, Hah N, Liddle C, Atkins AR, Downes M, Evans RM. PPAR $\gamma$  signaling and metabolism: the good, the bad and the future. *Nature Medicine*. May 2013;19 (5): 557–66.
132. Naruhn S, Meissner W, Adhikary T, Kaddatz K, Klein T, Watzel B. 15-hydroxyeicosatetraenoic acid is a preferential peroxisome proliferator-activated receptor beta/delta agonist. *Molecular Pharmacology*. February 2010;77 (2): 171–84.
134. Kraegen, E. W., J. A. Sowden, M. B. Halstead, P. W. Clark, K. J. Rodnick, D. J. Chisolm & D. E. James. Glucose transporters and in vivo glucose uptake in skeletal and cardiac muscle: fasting, insulin stimulation and immunoisolation studies of GLUT1 and GLUT4. *Biochem. J*. 1993; 295, 287-293.
135. Abel ED. Glucose transport in the heart. *Front Biosci*. 2004 Jan 1; 9:201-15.
136. Takeuchi, K., F. X. McGowan, Jr., P. Glynn, A. M. Moran, C. M. Rader, H. Cao-Danh & P. J. del Nido. Glucose transporter upregulation improves ischemic tolerance in hypertrophied failing heart. *Circulation* 1998; II234-239; discussion II240-231.
137. Razeghi, P., M. E. Young, J. Ying, C. Depre, I. P. Uray, J. Kolesar, G. L. Shipley, C. S. Moravec, P. J. Davies, O. H. Frazier & H. Taegtmeyer. Downregulation of metabolic gene expression in failing human heart before and after mechanical unloading. *Cardiology* 2002; 97, 203-209.

138. Brosius, F. C., 3rd, Y. Liu, N. Nguyen, D. Sun, J. Bartlett & M. Schwaiger. Persistent myocardial ischemia increases GLUT1 glucose transporter expression in both ischemic and non-ischemic heart regions. *J Mol Cell Cardiol* 1997;29, 1675-1685.
139. Garvey, W. T., D. Hardin, M. Juhaszova & J. H. Dominguez. Effects of diabetes on myocardial glucose transport system in rats: implications for diabetic cardiomyopathy. *Am. J. Physiol.*1993; 264, H837-H844.
140. Jeong JY, Jeoung NH, Park KG, Lee IK. Transcriptional regulation of pyruvate dehydrogenase kinase. *Diabetes Metab J.* 2012 Oct;36(5):328-35.
141. Abbot EL, McCormack JG, Reynet C, Hassall DG, Buchan KW, Yeaman SJ. Diverging regulation of pyruvate dehydrogenase kinase isoform gene expression in cultured human muscle cells. *The FEBS Journal.* Jun 2005;272 (12): 3004–14.
142. Razeghi P, Young ME, Ying J, Depre C, Uray IP, Kolesar J, Shipley GL, Moravec CS, Davies PJ, Frazier OH, Taegtmeier H. Downregulation of metabolic gene expression in failing human heart before and after mechanical unloading. *Cardiology.* 2002;97 (4): 203–9.
143. Bonnefont JP, Djouadi F, Prip-Buus C, Gobin S, Munnich A, Bastin J. Carnitine palmitoyltransferases 1 and 2: biochemical, molecular and medical aspects. *Molecular Aspects of Medicine.* 2004;25 (5–6): 495–520.
144. Casals N, Zammit V, Herrero L, Fadó R, Rodríguez-Rodríguez R, Serra D. Carnitine palmitoyltransferase 1C: From cognition to cancer. *Prog Lipid Res.* 2016 Jan; 61:134-48.
145. Rasmussen BB, Holmbäck UC, Volpi E, Morio-Liondore B, Paddon-Jones D, Wolfe RR. Malonyl coenzyme A and the regulation of functional carnitine palmitoyltransferase-1 activity and fat oxidation in human skeletal muscle. *The Journal of Clinical Investigation.* Dec 2002;110 (11): 1687–93.
146. Abumrad NA, Davidson NO. Role of the Gut in Lipid Homeostasis. *Physiological Reviews.* 2012; 92:1061–85.
147. Nahle Z, Hsieh M, Pietka T, Coburn CT, Grimaldi PA, Zhang MQ, Das D, Abumrad NA. CD36-dependent regulation of muscle FoxO1 and PDK4 in the PPAR delta/beta-mediated adaptation to metabolic stress. *J Biol Chem.* 2008; 283:14317–26.
148. Glatz JF, Angin Y, Steinbusch LK, Schwenk RW, Luiken JJ. CD36 as a target to prevent cardiac lipotoxicity and insulin resistance. *Prostaglandins Leukot Essent Fatty Acids.* 2013; 88:71–7.

149. Pietka TA, Sulkin MS, Kuda O, Wang W, Zhou D, Yamada KA, Yang K, Su X, Gross RW, Nerbonne JM, Efimov IR, Abumrad NA. CD36 Protein Influences Myocardial Ca<sup>2+</sup> Homeostasis and Phospholipid Metabolism: CONDUCTION ANOMALIES IN CD36-DEFICIENT MICE DURING FASTING. *J Biol Chem*. 2012; 287:38901–12.
150. Sawamura T, Kume N, Aoyama T, Moriwaki H, Hoshikawa H, Aiba Y, et al. An endothelial receptor for oxidized low-density lipoprotein. *Nature* 1997; 386:73–7.
151. Chen J, Mehta JL, Haider N, Zhang X, Narula J, Li D. Role of caspases in Ox-LDL-induced apoptotic cascade in human coronary artery endothelial cells. *Circ Res* 2004; 94:370–6.
152. Lee JY, Chung J, Kim KH, An SH, Kim M, Park J, et al. Fluid shear stress regulates the expression of Lectin-like oxidized low density lipoprotein receptor-1 via KLF2-AP-1 pathway depending on its intensity and pattern in endothelial cells. *Atherosclerosis* 2018; 270:76–88.
153. Barreto J, Karathanasis SK, Remaley A, Sposito AC. Role of LOX-1 (Lectin-Like Oxidized Low-Density Lipoprotein Receptor 1) as a Cardiovascular Risk Predictor: Mechanistic Insight and Potential Clinical Use. *Arterioscler Thromb Vasc Biol*. 2021 Jan;41(1):153-166.
154. Kuhn H, Banthiya S, van Leyen K. Mammalian lipoxygenases and their biological relevance. *Biochim Biophys Acta* 1851: 308–330, 2015.
155. Singh NK, Rao GN. Emerging role of 12/15-Lipoxygenase (ALOX15) in human pathologies. *Prog Lipid Res*. 2019 Jan; 73:28-45.
156. Brewster UC, Perazella MA. The renin-angiotensin-aldosterone system and the kidney: effects on kidney disease. *Am J Med* .2004;116:263–272.
157. Timmermans PB, Wong PC, Chiu AT, Herblin WF, Benfield P, Carini DJ, Lee RJ, Wexler RR, Saye JA, Smith RD () Angiotensin II receptors and angiotensin II receptor antagonists. *Pharmacol Rev* .1993;45:205–251.
158. Ruster C, Wolf G. Renin-angiotensin-aldosterone system and progression of renal disease. *J Am Soc Nephrol* .2006;17:2985–2991.
159. Schulman IH, Raij L. The angiotensin II type 2 receptor: what is its clinical significance? *Curr Hypertens Rep* .2008;10:188–193.
160. Cassis P, Conti S, Remuzzi G, Benigni A. Angiotensin receptors as determinants of life span. *Pflugers Arch*. 2010 Jan;459(2):325-32.

161. Imig JD. ACE Inhibition and Bradykinin-Mediated Renal Vascular Responses: EDHF Involvement. *Hypertension*. 2004;43 (3): 533–535.
162. Delanghe JR, Speeckaert MM, De Buyzere ML. The host's angiotensin-converting enzyme polymorphism may explain epidemiological findings in COVID-19 infections. *Clinica Chimica Acta; International Journal of Clinical Chemistry*. 2020;505: 192–193.
163. Wang Y, Marsden PA. Nitric oxide synthases: gene structure and regulation. *Adv Pharmacol* 1995; 34:71–90.
164. Nathan C. Inducible nitric oxide synthase: what difference does it make? *J Clin Invest* 1997; 100:2417–2423.
165. Seddon M, Shah AM, Casadei B. Cardiomyocytes as effectors of nitric oxide signaling. *Cardiovasc Res* 2007; 75:315–326.
166. Paulus WJ, Vantrimpont PJ, Shah AM. Paracrine coronary endothelial control of left ventricular function in humans. *Circulation* 1995; 92:2119–2126.
167. Barouch LA, Harrison RW, Skaf MW. Nitric oxide regulates the heart by spatial confinement of nitric oxide synthase isoforms. *Nature* 2002; 416:337–340.
168. Vila-Petroff MG, Kim SH, Pepe S. Endogenous nitric oxide mechanisms mediate the stretch dependence of Ca<sup>2+</sup> release in cardiomyocytes. *Nat Cell Biol* 2001; 3:867–873.
169. Linz W, Wohlfart P, Schölkens BA. Interactions among ACE, kinins and NO. *Cardiovasc Res* 1999;43:549–561.
170. Piech A, Massart PE, Dessy C, Feron O, Havaux X, Morel N. Decreased expression of myocardial eNOS and caveolin in dogs with hypertrophic cardiomyopathy *Am J Physiol Heart Circ Physiol*, 282 (2002), pp. H219-H231.
171. Wildhirt SM, Weismueller S, Schulze C, Conrad N, Kornberg A, Reichart B. Inducible nitric oxide synthase activation after ischemia/reperfusion contributes to myocardial dysfunction and extent of infarct size in rabbits: Evidence for a late phase of nitric oxide-mediated reperfusion injury *Cardiovasc Res*, 43 (1999), pp. 698-711.
172. Yang B, Larson DF, Watson RR. Modulation of iNOS activity in age-related cardiac dysfunction *Life Sci*, 75 (2004), pp. 655-667.
173. Sam F, Sawyer DB, Xie Z, Chang DL, Ngoy S, Brenner DA. Mice lacking inducible nitric oxide synthase have improved left ventricular contractile function and reduced apoptotic cell death late after myocardial infarction *Circ Res*, 89 (2001), pp. 351-356.

174. Ziolo MT, Maier LS, Piacentino III V, Bossuyt J, Houser SR, Bers DM. Myocyte nitric oxide synthase 2 contributes to blunted beta-adrenergic response in failing human hearts by decreasing Ca<sup>2+</sup> transients. *Circulation*, 109 (2004), pp. 1886-189.
175. Paulus WJ. Beneficial effects of nitric oxide on cardiac diastolic function: 'The flip side of the coin' *Heart Fail Rev*, 5 (2000), pp. 337-344.
176. Tang L, Wang H, Ziolo MT. Targeting NOS as a therapeutic approach for heart failure. *Pharmacol Ther*. 2014 Jun;142(3):306-15.
177. Lundwall A, Brattsand M. Kallikrein-related peptidases. *Cell Mol Life Sci*. 2008;65, 2019–2038.
178. Chao J, Shen B, Gao L, Xia CF, Bledsoe G, Chao L. Tissue kallikrein in cardiovascular, cerebrovascular and renal diseases and skin wound healing. *Biol Chem*. 2010;391, 345–355.
179. Bergaya S., Matrougui K., Meneton P., Henrion D. & Boulanger C. M. Role of tissue kallikrein in response to flow in mouse resistance arteries. *J Hypertens*. 2004;22, 745–750.
180. Andrade S, Smaili S, Totarelli Monteforte P, Miranda A, Kouyoumdjian M, Sampaio MU, Lopes GS, Oliva M. A plant Kunitz-type inhibitor mimics bradykinin-induced cytosolic calcium increase and intestinal smooth muscle contraction. *Biol Chem*. 2012;393, 943–957.
181. Stadnicki A. Intestinal tissue kallikrein-kinin system in inflammatory bowel disease. *Inflamm Bowel Dis*. 2011;17, 645–654.
182. Yin H., Chao L. & Chao J. Nitric oxide mediates cardiac protection of tissue kallikrein by reducing inflammation and ventricular remodeling after myocardial ischemia/reperfusion. *Life Sci* 2008;82, 156–165.
183. Cao B, Yu Q, Zhao W, Tang Z, Cong B, Du J, Lu J, Zhu X, Ni X. Kallikrein-related peptidase 8 is expressed in myocardium and induces cardiac hypertrophy. *Sci Rep* 2016 Jan 29; 7:20024.
184. Leeb-Lundberg L.M.F., Marceau F., Müller-Esterl W., Pettibone D.J., Zuraw B.L. International union of pharmacology. XLV. Classification of the kinin receptor family: From molecular mechanisms to pathophysiological consequences. *Pharmacol. Rev*. 2005; 57:27–77.



185. Rocha E Silva M., Beraldo W.T., Rosenfeld G. Bradykinin, a hypotensive and smooth muscle stimulating factor released from plasma globulin by snake venoms and by trypsin. *Am. J. Physiol.* 1949; 156:261–273.
186. Da Costa P.L.N., Sirois P., Tannock I.F., Chammas R. The role of kinin receptors in cancer and therapeutic opportunities. *Cancer Lett.* 2014; 345:27–38.
187. Qadri F., Bader M. Kinin B1 receptors as a therapeutic target for inflammation. *Expert Opin. Ther. Targets.* 2018; 22:31–44.
188. Heitsch H. The therapeutic potential of bradykinin B2 receptor agonists in the treatment of cardiovascular disease. *Expert Opin. Investig. Drugs.* 2003; 12:759–770.
189. Duchene J., Ahluwalia A. The kinin B1 receptor and inflammation: New therapeutic target for cardiovascular disease. *Curr. Opin. Pharmacol.* 2009; 9:125–131.
190. Sriramula S. Kinin B1 receptor: A target for neuroinflammation in hypertension. *Pharmacol. Res.* 2020; 155:104715.
191. Jiao Q, Bai Y, Akaike T, Takeshima H, Ishikawa Y, Minamisawa S. Sarcalumenin is essential for maintaining cardiac function during endurance exercise training. *Am J Physiol Heart Circ Physiol.* 2009;297:H576–H582.
192. Clapham DE. Calcium signaling. *Cell.* 2007; 131:1047–1058.
193. Flavell SW, Greenberg ME. Signaling mechanisms linking neuronal activity to gene expression and plasticity of the nervous system. *Annu Rev Neurosci.* 2008; 31:563–590.
194. Dodd AN, Kudla J, Sanders D. The language of calcium signaling. *Annu Rev Plant Biol.* 2010; 61:593–620.
195. Qi H, Moran MM, Navarro B, Chong JA, Krapivinsky G, Krapivinsky L, Kirichok Y, Ramsey IS, Quill TA, Clapham DE. All four CatSper ion channel proteins are required for male fertility and sperm cell hyperactivated motility. *Proc Natl Acad Sci.* 2007; 104:1219–1223.
196. Voss J, Jones LR, Thomas DD. The physical mechanism of calcium pump regulation in the heart. *Biophys J.* 1994; 67:190–196.
197. Van Petegem F. Ryanodine receptors: Structure and function. *J Biol Chem.* 2012; 287:31624–31632.

198. Brady M, Koban MU, Dellow KA, Yacoub M, Boheler KR, Fuller SJ. Sp1 and Sp3 transcription factors are required for trans-activation of the human SERCA2 promoter in cardiomyocytes. *Cardiovasc Res.* 2003; 60:347–354.
199. Wehrens XHT, Marks AR. Altered function and regulation of cardiac ryanodine receptors in cardiac disease. *Trends Biochem Sci.* 2003; 28:671–678.
200. Priori SG, Napolitano C, Memmi M, Colombi B, Drago F, Gasparini M, Desimone L, Coltorti F, Bloise R, Keegan R, Cruz filho FES, Vignati G, Benatar A, Delogu A. Clinical and molecular characterization of patients with catecholaminergic polymorphic ventricular tachycardia. *Circulation.* 2002; 106:69–74.
201. Landstrom AP, Dobrev D, Wehrens XHT. Calcium signaling and cardiac arrhythmias. *Circ Res.* 2017; 120:1969–1993.
202. Lascano E, Negroni J, Vila Petroff M, Mattiazzi A. Impact of RyR2 potentiation on myocardial function. *Am J Physiol Heart Circ Physiol.* 2017;312:H1105–H1109.
203. Wescott AP, Jarfi MS, Lederer WJ, Williams GS. Ryanodine receptor sensitivity governs the stability and synchrony of local calcium release during cardiac excitation-contraction coupling. *Mol Cell Cardiol.* 2016; 92:82–92.
204. Yamaguchi N. Molecular insights into calcium dependent regulation of ryanodine receptor calcium release channels. *Adv Exp Med Biol.* 2020; 1131:321–336.
205. Ruiz-meana M, Minguet M, Bou-teen D, Miro-casas E, Castans C, Castellano J, Bonzon-kulichenko E, Igual A, Rodriguez-lecoq R, Vazquez J, Garcia-dorado D. Ryanodine receptor glycation favors mitochondrial damage in the senescent heart. *Circulation.* 2019; 139:949–964.
206. Zamponi GW, Striessnig J, Koschak A, Dolphin AC. The Physiology, Pathology, and Pharmacology of Voltage-Gated Calcium Channels and Their Future Therapeutic Potential. *Pharmacol Rev.* 2015 Oct;67(4):821-70.
207. Westhoff M, Dixon RE. Mechanisms and Regulation of Cardiac CaV1.2 Trafficking. *Int J Mol Sci.* 2021 May 31;22(11):5927.
208. Nicoll DA, Longoni S, Philipson KD. Molecular cloning and functional expression of the cardiac sarcolemmal Na<sup>+</sup>–Ca<sup>2+</sup> exchanger. *Science*, 250 ;1990, pp. 562-565.
209. Brini, M., Carafoli, E. The plasma membrane Ca<sup>2+</sup> ATPase and the plasma membrane sodium–calcium exchanger cooperates in the regulation of cell calcium. *Cold Spring Harbor Perspect Biol.* 2011;3(2), pii: a004168.

210. Blaustein MP, Lederer WJ. Sodium/calcium exchange: its physiological implications *Physiol. Rev.*, 79 (1999), pp. 763-854.
211. Sipido K.R., Varro A., Eisner D. Sodium calcium exchange as a target for antiarrhythmic therapy. *Handb Exp Pharmacol*, 2006;159–199.
212. Eisner D, Sipido K. Sodium calcium exchange in the heart-necessity or luxury? *Circ. Res.*, 95 (2004), pp. 549-551.
213. Stokke MK, Briston SJ, Jølle GF, Manzoor I, Louch WE, Øyehaug L, Christensen G, Eisner DA, Trafford AW, Sejersted OM, Sjaastad I. Ca<sup>2+</sup> wave probability is determined by the balance between SERCA2-dependent Ca<sup>2+</sup> reuptake and threshold SR Ca<sup>2+</sup> content. *Cardiovasc. Res.*, 90 (2011), pp. 503-512.
214. Maier LS. Role of CaMKII for signaling and regulation in the heart. *Front Biosci.* 2009; 14:486–496.
215. Kohlhaas M, Zhang T, Seidler T, Zibrova D, Dybkova N, Steen A, Wagner S, Chen L, Brown JH, Bers DM, Maier LS. Increased sarcoplasmic reticulum calcium leak but unaltered contractility by acute CaMKII overexpression in isolated rabbit cardiac myocytes. *Circ Res.* 2006; 98:235–244.
216. Zhang T, Brown JH. Role of Ca<sup>2+</sup>/calmodulin-dependent protein kinase II in cardiac hypertrophy and heart failure. *Cardiovasc Res.* 2004; 63:476–486.
217. Plante E, Couet J, Gaudreau M, Dumas MP, Drolet MC, Arsenault M. Left ventricular response to sustained volume overload from chronic aortic valve regurgitation in rats. *J Card Fail.* 2003;9(2):128–140.
218. Hoffman, J. E., & Buckberg, G. D. (2014). The myocardial oxygen supply: Demand index revisited. *Journal of the American Heart Association*, 3(1). 10.1161/JAHA.113.000285.
219. Strauer, BE. Myocardial oxygen consumption in chronic heart disease: Role of wall stress, hypertrophy and coronary reserve. *American Journal of Cardiology*, 1979;44, 730–740.
220. Champetier S, Bojmehrani A, Beaudoin J, Lachance D, Plante E, Roussel E, Couet J, Arsenault M. Gene profiling of left ventricle eccentric hypertrophy in aortic regurgitation in rats: rationale for targeting the beta-adrenergic and renin-angiotensin systems *Am J Physiol Heart Circ Physiol.* 2009 Mar;296(3):H669-77.
221. Roussel E, Drolet MC, Walsh-Wilkinson E, Dhahri W, Lachance D, Gascon S, Sarrhini O, Rousseau JA, Lecomte R, Couet J, Arsenault M. Transcriptional Changes Associated with Long-Term Left Ventricle Volume Overload in Rats: Impact on Enzymes Related to Myocardial Energy Metabolism *Biomed Res Int.* 2015;2015:949624.

222. Zoghbi WA, Enriquez-Sarano M, Foster E, Grayburn PA, Kraft CD, Levine RA, et al. Recommendations for evaluation of the severity of native valvular regurgitation with two-dimensional and Doppler echocardiography. *J Am Soc Echocardiogr.* 2003;16(7):777–802.
223. Lewis RP, Rittogers SE, Froester WF, Boudoulas H. A critical review of the systolic time intervals. *Circulation.* 1977;56(2):146–158.
224. Spodick DH, Doi YL, Bishop RL, Hashimoto T. Systolic time intervals reconsidered. Reevaluation of the preejection period: absence of relation to heart rate. *Am J Cardiol.* 1984;53(11):1667–1670.
225. Anderson, R. L., Sueoka, S. H., Rodriguez, H. M., Lee, K. H., Cox, D. R., Kawas, R., Morgan, B. P., Sakowicz, R., Morgans, D. J., Malik, F., & Elias, K. A. (2005). In vitro and in vivo efficacy of the cardiac myosin activator CK-1827452. *Molecular Biology of the Cell*, 16(abstract #1728). [https://cytokinetics.com/wp-content/uploads/2015/10/ASCB\\_1728.pdf](https://cytokinetics.com/wp-content/uploads/2015/10/ASCB_1728.pdf)
226. Pfaffla MW. A new mathematical model for relative quantification in real-time RT–PCR. *Nucleic Acids Res.* 2001 May 1 ; 29(9): e45.
227. El Oumeiri B, Dewachter L, Van de Borne P, Hubesch G, Melot C, Jaspers P, Stefanidis C, Mc Entee K, Vanden Eynden F. Altered Left Ventricular Rat Gene Expression Induced by the Myosin Activator Omecamtiv Mecarbil. *Genes (Basel).* 2023 Jan 1;14(1):122.
228. El Oumeiri B, Dewachter L, Van de Borne P, Hubesch G, Jaspers P, Stefanidis C, Mc Entee K, Vanden Eynden F. Gene profiling of left ventricle in experimental model of combined volume and pressure overload in rats (submitted manuscript)
229. El-Oumeiri B, Mc Entee K, Annoni F, Herpain A, Vanden Eynden F, Jaspers P, Van Nooten G, van de Borne P. Effects of the cardiac myosin activator Omecamtiv-mecarbil on severe chronic aortic regurgitation in Wistar rats. *BMC Cardiovasc Disord.* 2018 May 21;18(1):99.
230. El Oumeiri B, van de Borne P, Hubesch G, Herpain A, Annoni F, Jaspers P, Stefanidis C, Mc Entee K, Vanden Eynden F. The myosin activator omecamtiv mecarbil improves wall stress in a rat model of chronic aortic regurgitation. *Physiol Rep.* 2021 Aug;9(16): e14988.
231. El Oumeiri B, van de Borne P, Hubesch G, Jaspers P, Dewachter L, Stefanidis C, Mc Entee K, Vanden Eynden F. Detection of soluble suppression of tumorigenicity 2 and N-terminal B-type natriuretic peptide in a rat model of aortic regurgitation: differential

- responses to omecamtiv mecarbil. *J Basic Clin Physiol Pharmacol.* 2022 Oct 10;33(6):743-750.
232. Grossman, W. Cardiac hypertrophy: Useful adaptation or pathologic process. *American Journal of Medicine*, 69(4), 1980;576–584. 10.
233. Gaasch, W. H., & Zile, M. R. Left ventricular structural remodeling in health and disease: With special emphasis on volume, mass, and geometry. *Journal of the American College of Cardiology*, 58(17),2011; 1733–1740.
234. Taniguchi, K., Kawamaoto, T., Kuki, S., Masai, T., Mitsuno, M., Nakano, S., Kawashima, Y., & Matsuda, H. Left ventricular myocardial remodeling and contractile state in chronic aortic regurgitation. *Clinical Cardiology*, 23(8),2000; 608–614.
235. Percy, R. F., Miller, A. B., & Conetta, D. A. Usefulness of left ventricular wall stress at rest and after exercise for outcome prediction in asymptomatic aortic regurgitation. *American Heart Journal*, 125(1),1993; 151–155.
236. Greenberg, B., Massie, B., Thomas, D., Bristow, J. D., Cheitlin, M., Broudy, D., Szlachcic, J., & Krishnamurthy, G. Association between the exercise ejection fraction response and systolic wall stress in patients with chronic aortic insufficiency. *Circulation*, 71(3),1985; 458–465.
237. Petersen JW, Felker GM. Inotropes in the management of acute heart failure. *Crit Care Med.* 2008;36(1 Suppl): S106–S111.
238. Espinola-Zavaleta N, Gómez-Núñez N, Chávez PY, Sahagun-Sánchez G, Keirns C, Casanova JM, Romero-Cárdenas A, Roldán FJ, Vargas-Barrón J. Evaluation of the response to pharmacological stress in chronic aortic regurgitation. *Echocardiography.* 2001;18(6):491–496.
239. Rønning, L., Bakkehaug, J. P., Rødland, L., Kildal, A. B., Myrmel, T., & How, O. J. Opposite diastolic effects of omecamtiv mecarbil versus dobutamine and ivabradine co-treatment in pigs with acute ischemic heart failure. *Physiological Reports*, 2018;6(19).
240. Yin, F. C. Ventricular wall stress. *Circulation Research*, 1981;49(4), 829–842.
241. Grossman, W. Cardiac hypertrophy: Useful adaptation or pathologic process. *American Journal of Medicine.*1980;69(4), 576–584.
242. Hung, C. L., Verman, A., Uno, H., Shin, S. H., Bourgoun, M., Hassanein, A. H., McMurray, J. J., Velazquez, E. J., Kober, L., Pfeffer, M. A., & Solomon, S. D. VALIANT investigators. Longitudinal and circumferential strain rate, left ventricular

- remodeling, and prognosis after myocardial infarction. *Journal of the American College of Cardiology*, 2010; 56(22), 1812–1822.
243. Hoffman, J. E., & Buckberg, G. D. The myocardial oxygen supply: Demand index revisited. *Journal of the American Heart Association*, 2014;3(1).  
10.1161/JAHA.113.000285
244. Kolev, N., Huemer, G., & Zimpfer, M. *Transesophageal echocardiography. A new monitoring technique*. 1995; Springer Verlag.
245. Lang, R. M., Borow, K. M., Neumann, A., & Janzen, D. Systemic vascular resistance: An unreliable index of left ventricular afterload. *Circulation*. 1986;74, 1114–1118.
246. Levänen, J., Mäkelä, M. L., & Scheinin, H. Dexmedetomidine premedication attenuates ketamine-induced cardio-stimulatory effects and post-anesthetic delirium. *Anesthesiology*, 1995;82(5), 1117–1125.
247. Lee, K., Hwang, H. J., Kim, O. S., & Oh, Y. J. Assessment of dexmedetomidine effects on left ventricular function using pressure-volume loops in rats. *Journal of Anesthesia*, 2017;31(1), 18–24.
248. Davies, L. A., Hamilton, D. L., Hopkins, P. M., Boyett, M. R., & Harrison, S. M. Concentration-dependent inotropic effects of halothane, isoflurane, and sevoflurane on rat ventricular myocytes. *British Journal of Anaesthesia*, 1999;82(5), 723–730.
249. Heerdt, P. M., Gandhi, C. D., & Dickstein, M. L. Disparity of isoflurane effects on left and right ventricular afterload and hydraulic power generation in swine. *Anesthesia and Analgesia*, 1998;87, 511–521.
250. Song BG, Park YH, Kang GH, Chun WJ, Oh JH, Choi JO, Lee SC, Park SW, Oh JK, Sung KI, Park P, Jeon ES Preoperative, postoperative and one-year follow-up of N-terminal pro-B-type natriuretic peptide levels in volume overload of aortic regurgitation: comparison with pressure overload of aortic stenosis *Cardiology*. 2010;116(4):286-91.
251. Vanderheyden M, Goethals M, Verstreken S, De bruyne B, Muller K, Van Schuerbeeck E, Bartunek J. Wall stress modulates brain natriuretic peptide production in pressure overload cardiomyopathy. *J Am Coll Cardiol* 2004; 44:2349–54.
252. Najjar E, Faxén UL, Hage C, Donal E, Daubert JC, Linde C, Lund LH. ST2 in heart failure with preserved and reduced ejection fraction. *Scand Cardiovasc J*. 2019 Feb ;53(1):21-27.
253. Sugano A, Seo Y, Ishizu T, Sai S, Yamamoto M, Hamada-Harimura Y, Machino-Ohtsuka T, Obara K, Nishi I, Aonuma K, Nogami A. Soluble ST2 and brain natriuretic

- peptide predict different mode of death in patients with heart failure and preserved ejection fraction. *J Cardiol.* 2019 Apr;73(4):326-332.
254. Kakkar R, Lee RT. The IL-33/ST2 pathway: therapeutic target and novel biomarker. *Nat Rev Drug Discov.* 2008 Oct;7(10):827-40.
255. Letai A., Bassik M.C., Walensky L.D., Sorcinelli M.D., Weiler S., Korsmeyer S.J. Distinct BH3 domains either sensitize or activate mitochondrial apoptosis, serving as prototype cancer therapeutics. *Cancer Cell.* 2002; 2:183–192.
256. Machado A.R.T., Aissa A.F., Ribeiro D.L., Hernandes L.C., Machado C.S., Bianchi M.L.P., Sampaio S.V., Antunes L.M.G. The toxin B<sub>j</sub>ussuLAAO-II induces oxidative stress and DNA damage, upregulates the inflammatory cytokine genes TNF and IL6, and downregulates the apoptotic-related genes BAX, BCL2 and RELA in human Caco-2 cells. *Int. J. Biol. Macromol.* 2018;109:212–219.
257. Jarskog L.F., Selinger E.S., Lieberman J.A., Gilmore J.H. Apoptotic proteins in the temporal cortex in schizophrenia: High Bax/Bcl-2 ratio without caspase-3 activation. *Am. J. Psychiatry.* 2004; 161:109–115.
258. Dostanic S, Servant N, Wang C, Chalifour LE. Chronic  $\alpha$ -adrenoreceptor stimulation in vivo decreased Bcl-2 and increased Bax expression but did not activate apoptotic pathways in mouse heart. *Can. J. Physiol. Pharmacol.* 2004;82: 167–174.
259. Manoharan S, Kolanjiappan K, Suresh K, Panjamurthy K. Lipid peroxidation and antioxidants status in patients with oral squamous cell carcinoma. *Indian J Med Res.* 2005; 122:529–534.
260. Gozeler MS, Ekinçi Akdemir FN, Yildirim S, Sahin A, Eser G, Askin S. Levosimendan ameliorates cisplatin-induced ototoxicity: Rat model. *Int J Pediatr Otorhinolaryngol.* 2019 Jul; 122:70-75.
261. Rhoden A., Schulze T., Pietsch N., Christ T., Hansen A., Eschenhagen T. Comprehensive analyses of the inotropic compound omecamtiv mecarbil in rat and human cardiac preparations. *Am. J. Physiol. Circ. Physiol.* 2022;322:H373–H385.
262. Hu C., Dandapat A., Chen J., Fujita Y., Inoue N., Kawase Y., Jishage K., Suzuki H., Sawamura T., Mehta J.L. LOX-1 deletion alters signals of myocardial remodeling immediately after ischemia-reperfusion. *Cardiovasc. Res.* 2007; 76:292–302.
263. Egert S, Nguyen N and Schwaiger M. Contribution of  $\alpha$ -Adrenergic and  $\beta$ -Adrenergic Stimulation to Ischemia-Induced Glucose Transporter (GLUT) 4 and GLUT1 Translocation in the Isolated Perfused Rat Heart. *Circulation Research.* 1999; 84:1407–1415.

264. Hall JL, Stanley WC, Lopaschuk GD, Wisneski JA, Pizzurro RD, Hamilton CD, McCormack JG. Impaired pyruvate oxidation but normal glucose uptake in diabetic pig heart during dobutamine-induced work. *American Journal of Physiology-Heart and Circulatory Physiology*, 271(6), H2320–H2329.1996.
265. Sugden MC, Holness MJ. *FASEB J*. Interactive regulation of the pyruvate dehydrogenase complex and the carnitine palmitoyltransferase system. 1994 Jan;8(1):54-61.
266. Wu P, Sato J, Zhao Y, Jaskiewicz J, Popov KM, Harris RA. Starvation and diabetes increase the amount of pyruvate dehydrogenase kinase isoenzyme 4 in rat heart. *Biochem. J.* (1998) 329, 197–201.
267. Pettersen IK, Tusubira D, Ashrafi H, Dyrstad SE, Hansen L, Liu XZ, Nilsson LIH, Løvsletten NG, Berge K, Wergedahl H, Bjørndal B, Fluge Ø, Bruland O, Rustan AC, Halberg N, Røslund GV, Berge RK, Tronstad KJ. Upregulated PDK4 expression is a sensitive marker of increased fatty acid oxidation Mitochondrion. 2019 Nov; 49:97-110.
268. Sawamura T, Kume N, Aoyama T, et al. An endothelial receptor for oxidized low-density lipoprotein. *Nature*. 1997; 386: 73–77.
269. Li DY, Zhang YC, Philips MI, et al. Upregulation of endothelial receptor for oxidized low-density lipoprotein (LOX-1) in cultured human coronary artery endothelial cells by angiotensin II type-1 receptor activation. *Circ Res*. 1999; 84: 1043–1049.
270. Murase T, Kume N, Korenaga R, et al. Fluid shear stress transcriptionally induces lectin-like oxidized LDL receptor-1 in vascular endothelial cells. *Circ Res*. 1998; 83: 329–333.
271. Li D, Williams V, Liu L, Chen H, Sawamura T, Antakli T, Mehta JL. Mehta LOX-1 inhibition in myocardial ischemia-reperfusion injury: modulation of MMP-1 and inflammation. *Am J Physiol Heart Circ Physiol*. Nov; 283(5):H1795-8012002.
272. Kuhn H., O'Donnell V.B. 2006. Inflammation and immune regulation by 12/15-lipoxygenases. *Prog. Lipid Res.* 45:334–56.
273. Kayama Y, Minamino T, Toko H, Sakamoto M, Shimizu I, Takahashi H, Okada S, Tateno K, Moriya J, Yokoyama M, Nojima A, Yoshimura M, Egashira K, Aburatani H, Komuro I. Cardiac 12/15 lipoxygenase-induced inflammation is involved in heart failure. *J Exp Med*. 2009 Jul 6; 206(7): 1565–1574.
274. Takaya T, Wada H, Morimoto T, Sunagawa Y, Kawamura T, Takanabe-Mori R, Shimatsu A, Fujita Y, Sato Y, Fujita M, Kimura T, Sawamura T, Hasegawa K. Left



- ventricular expression of lectin-like oxidized low-density lipoprotein receptor-1 in failing rat hearts. *Circ J*. 2010 Apr;74(4):723-9.
275. Zendaoui A., Lachance D., Roussel E., Couet J., Arsenault M. Effects of spironolactone treatment on an experimental model of chronic aortic valve regurgitation. *J. Heart Valve Dis*. 2012;21:478–486.
276. Nánási P., Jr., Gaburjakova M., Gaburjakova J., Almássy J. Omecamtiv mecarbil activates ryanodine receptors from canine cardiac but not skeletal muscle. *Eur. J. Pharmacol*. 2017;809:73–79.
277. Fülöp G., Oláh A., Csipo T., Kovács Á., Pórszász R., Veress R., Horváth B., Nagy L., Bódi B., Fagyas M., et al. Omecamtiv mecarbil evokes diastolic dysfunction and leads to periodic electromechanical alternans. *Basic Res. Cardiol*. 2021;116:24.
278. Cassis P, Conti S, Remuzzi G, Benigni A. Angiotensin receptors as determinants of life span. *Pflugers Arch*. 2010 Jan;459(2):325-32.
279. Namsolleck P, Recarti C, Foulquier S, Steckelings UM, Unger T. AT (2) receptor and tissue injury: therapeutic implications. *Curr Hypertens Rep*. 2014 Feb;16(2):416.
280. Escobales N, Nuñez RE, Javadov S Mitochondrial angiotensin receptors and cardioprotective pathways. *Am J Physiol Heart Circ Physiol*. 2019 Jun 1;316(6):H1426-H1438.
281. Cho HJ, Xie QW, Calaycay J, Mumford RA, Swiderek KM, Lee TD, Nathan C. Calmodulin is a subunit of nitric oxide synthase from macrophages *J Exp Med*, 176 (1992), pp. 599-604.
282. Ziolo MT, Harshbarger CH, Roycroft KE, Smith JM, Romano FD, Sondgeroth KL, Wahler GM. Myocytes isolated from rejecting transplanted rat hearts exhibit a nitric oxide-mediated reduction in the calcium current *J Mol Cell Cardiol*, 33 (2001), pp. 1691-1699.
283. Wildhirt SM, Weismueller S, Schulze C, Conrad N, Kornberg A, Reichart B Inducible nitric oxide synthase activation after ischemia/reperfusion contributes to myocardial dysfunction and extent of infarct size in rabbits: Evidence for a late phase of nitric oxide-mediated reperfusion injury *Cardiovasc Res*, 43 (1999), pp. 698-711.
284. Ziolo MT, Maier LS, Piacentino V 3rd, Bossuyt J, Houser SR, Bers DM Myocyte nitric oxide synthase 2 contributes to blunted beta-adrenergic response in failing human hearts by decreasing Ca<sup>2+</sup> transients *Circulation*, 109 (2004), pp. 1886-1891.

285. Heymes C, Vanderheyden M, Bronzwaer JG, Shah AM, Paulus WJ. Endomyocardial nitric oxide synthase and left ventricular preload reserve in dilated cardiomyopathy *Circulation*, 99 (1999), pp. 3009-3016.
286. Paulus WJ. Beneficial effects of nitric oxide on cardiac diastolic function: 'The flip side of the coin' *Heart Fail Rev*, 5 (2000), pp. 337-344.
287. Cao B, Yu Q, Zhao W, Tang Z, Cong B, Du J, Lu J, Zhu X, Ni X. Kallikrein-related peptidase 8 is expressed in myocardium and induces cardiac hypertrophy *Sci Rep*. 2016 Jan 29; 7:20024.
288. Huang M, Du J, Wang Y, Ma S, Hu T, Shang J, Yu Q, Zhu X, Zhang G, Cong B. Tissue kallikrein-related peptidase 8 protects rat heart against acute ischemia reperfusion injury. *Int J Biol Macromol*. 2019 Nov 1; 140:1126-1133.
289. Rougeot C, Rosinski-Chupin I, Mathison R, Rougeon F. Rodent submandibular gland peptide hormones and other biologically active peptides *Peptides*, 21 (2000), pp. 443-455.
290. Borges JC, Silva JA Jr, Gomes MA, Lomez ES, Leite KM, Araujo RC, Bader M, Pesquero JB, Pesquero JL. Tonin in rat heart with experimental hypertrophy. *Am J Physiol Heart Circ Physiol*. 2003 Jun; 284(6):H2263-8.
291. Damasceno DD, Lima MP, Motta DF, Ferreira AJ, Quintão-Junior JF, Drummond LR, Natali AJ, Almeida AP, Pesquero JL. Cardiovascular and electrocardiographic parameters after tonin administration in Wistar rats. *Regul Pept*. 2013 Feb 10; 181: 30-6.
292. Chao J, Shen B, Gao L, Xia CF, Bledsoe G, Chao L. Tissue kallikrein in cardiovascular, cerebrovascular and renal diseases and skin wound healing. *Biol Chem*. 2010 Apr; 391(4):345-55.
293. Hamid S, Rhaleb IA, Kassem KM, Rhaleb NE. Role of Kinins in Hypertension and Heart Failure. *Pharmaceuticals (Basel)*. 2020 Oct 28;13(11):347.
294. Abadir PM, Periasamy A, Carey RM, Siragy HM. Angiotensin II type 2 receptor-bradykinin B2 receptor functional heterodimerization. *Hypertension*. 2006 Aug;48(2):316-22.
295. Levy RF, Serra AJ, Antonio EL, Dos Santos L, Bocalini DS, Pesquero JB, Bader M, Merino VF, de Oliveira HA, de Arruda Veiga EC, Silva JA Jr, Tucci PJ. Cardiac morphofunctional characteristics of transgenic rats with overexpression of the bradykinin B1 receptor in the endothelium. *Physiol Res*. 2017 Dec 20;66(6):925-932.

296. Duka A, Kintsurashvili E, Duka I, Ona D, Hopkins TA, Bader M, Gavras I, Gavras H. Angiotensin-converting enzyme inhibition after experimental myocardial infarct: role of the kinin B1 and B2 receptors. *Hypertension*. 2008 May;51(5):1352-7.
297. Zamponi GW, Striessnig J, Koschak A, Dolphin AC. The Physiology, Pathology, and Pharmacology of Voltage-Gated Calcium Channels and Their Future Therapeutic Potential. *Pharmacol Rev*. 2015 Oct;67(4):821-70.
298. Westhoff M, Dixon RE. Mechanisms and Regulation of Cardiac CaV1.2 Trafficking. *Int J Mol Sci*. 2021 May 31;22(11):5927.
299. Szentandrassy N, Horvath B, Vaczi K, Kistamas K, Masuda L, Magyar J, Banyasz T, Papp Z, Nanasi PP. Dose-dependent electrophysiological effects of the myosin activator omecantiv mecarbil in canine ventricular cardiomyocytes. *J Physiol Pharmacol*. 2016 Aug; 67(4):483-489.
300. Christel CJ, Cardona N, Mesirca P, Herrmann S, Hofmann F, Striessnig J, Ludwig A, Mangoni ME, Lee A. Distinct localization and modulation of Cav1.2 and Cav1.3 L-type Ca<sup>2+</sup> channels in mouse sinoatrial node. *J Physiol*. 2012 Dec 15; 590(24):6327-42.
301. Gavathiotis E, Suzuki M, Davis ML, Pitter K, Bird GH, Katz SG, Tu HC, Kim H, Cheng E, Tjandra N, Loren D, Walensky LD. BAX activation is initiated at a novel interaction site *Nature*, 2008; volume 455, pages 1076–1081.
302. Aouacheri W, Saka S, Djafer R, Lefranc G. Protective effect of diclofenac towards the oxidative stress induced by paracetamol toxicity in rats. *Ann Biol Clin (Paris)* . 2009 Nov-Dec;67(6):619-27.
303. Pias EK, Ekshyyan OY, Rhoads CA, Fuseler J, Harrison L, Aw TY (Apr 2003). "Differential effects of superoxide dismutase isoform expression on hydroperoxide-induced apoptosis in PC-12 cells". *The Journal of Biological Chemistry*. 278 (15): 13294–301.
304. Dhalla AK, Singal PK. Antioxidant changes in hypertrophied and failing guinea pig hearts. *Am J Physiol*. 1994; 266: H1280–H1285.
305. Cheng W, Li B, Kajstura J, Li P, Wolin MS, Sonnenblick EH, Hintze TH, Olivetti G, Anversa P. Stretch-induced programmed myocyte cell death. *J Clin Invest*. 1995; 96: 2247–2259.
306. Katz, E. B., A. E. Stenbit, K. Hatton, R. Depinho & M. J. Charron. Cardiac and adipose tissue abnormalities but not diabetes in mice deficient in GLUT4. *Nature* 1995 ;377, 151-155.

307. Lee SY, Ku HC, Kuo YH, Chiu HL, Su MJ. Pyrrolidinyl caffeamide against ischemia/reperfusion injury in cardiomyocytes through AMPK/AKT pathways. *J Biomed Sci.* 2015 ; 22 :18.
308. Zhuo XZ, Wu Y, Ni YJ, Liu JH, Gong M, Wang XH, Wei F, Wang TZ, Yuan Z, Ma AQ, et al. Isoproterenol instigates cardiomyocyte apoptosis and heart failure via AMPK inactivation-mediated endoplasmic reticulum stress. *Apoptosis.* 2013 ;18(7) :800–810.
309. Yeh CH, Chen TP, Wang YC, Lin YM, Fang SW. AMP-activated protein kinase activation during cardioplegia-induced hypoxia/reoxygenation injury attenuates cardiomyocytic apoptosis via reduction of endoplasmic reticulum stress. *Mediat Inflamm.* 2010; 2010 :130636.
310. Dong HW, Zhang LF, Bao SL. AMPK regulates energy metabolism through the SIRT1 signaling pathway to improve myocardial hypertrophy. *Eur Rev Med Pharmacol Sci.* 2018 May ;22(9) :2757-2766.
311. Ahmadian M, Suh JM, Hah N, Liddle C, Atkins AR, Downes M, Evans RM. "PPAR $\gamma$  signaling and metabolism: the good, the bad and the future". *Nature Medicine.* 2013;19 (5): 557–66.
312. Villa M, Cerda-Opazo P, Jimenez-Gallegos D, Garrido-Moreno V, Chiong M, Quest AF, et al. Pro-fibrotic effect of oxidized LDL in cardiac myofibroblasts. *Biochem Biophys Res Commun* 2020; 524:696–701.
313. Nusier M, Shah AK, Dhalla NS. Structure–function relationships and modifications of cardiac sarcoplasmic reticulum Ca<sup>2+</sup>-transport. *Physiol Res.* 2021 Dec 30;70(Suppl4): S443-S470.
314. Louch WE, Hougen K, Mork HK, Swift F, Aronsen JM, Sjaastad I, Reims HM, Roald B, Andersson KB, Christensen G, Sejersted OM. Sodium accumulation promotes diastolic dysfunction in end-stage heart failure following SERCA2 knockout. *J Physiol.* 2010; 588:465–478.
315. Nediani C, Formigli L, Perna AM, Ibba-Manneschi L, Zecchi-Orlandini S, Fiorillo C, Ponziani V, Cecchi C, Liguori P, Fratini G, Nassi P. Early changes induced in the left ventricle by pressure overload. An experimental study on swine heart. *J Mol Cell Cardiol.* 2000 Jan;32(1):131-42
316. Goyal J, Smith KM, Cowan JM, Wazer DE, Lee SW, Band V. The role for NES1 serine protease as a novel tumor suppressor. *Cancer Research.* 1998; 58:4782–4786.
317. Zhang Y, Song H, Miao Y, Wang R, Chen L. Frequent transcriptional inactivation of Kallikrein 10 gene by CpG island hypermethylation in non-small cell lung cancer. *Cancer*

Science. 2010; 101:934–940.

318. Wei CC, Chen Y, Powell LC, Zheng J, Shi K, Bradley WE, Powell PC, Ahmad S, Ferrario CM, Dell'Italia LJ. Cardiac kallikrein-kinin system is upregulated in chronic volume overload and mediates an inflammatory induced collagen loss. *PLoS One*. 2012;7(6): e40110.
319. Mueller T, Zimmermann M, Dieplinger B, Ankersmit HJ, Haltmayer M. Comparison of plasma concentrations of soluble ST2 measured by three different commercially available assays: the MBL ST2 assay, the Presage ST2 assay, and the R&D ST2 assay. *Clin Chim Acta*. 2012 Oct 9;413(19-20):1493-4.
320. Beaumont C, Walsh-Wilkinson É, Drolet MC, Roussel É, Melançon N, Fortier É, Harpin G, Beaudoin J, Arsenault M, Couet J. Testosterone deficiency reduces cardiac hypertrophy in a rat model of severe volume overload. *Physiol Rep*. 2019 May;7(9): e14088.
321. Uematsu T, Yamazaki T, Matsuno H, Hayashi Y, Nakashima M. A simple method for producing graded aortic insufficiencies in rats and subsequent development of cardiac hypertrophy. *J Pharmacol Methods*. 1989 Dec;22(4):249-57.
322. Plante E, Lachance D, Roussel E, Drolet MC, Arsenault M, Couet J. Impact of anesthesia on echocardiographic evaluation of systolic and diastolic function in rats. *J Am Soc Echocardiogr*. 2006 Dec;19(12):1520-5.

## RESEARCH ARTICLE

## Open Access



# Effects of the cardiac myosin activator Omecamtiv-mecarbil on severe chronic aortic regurgitation in Wistar rats

Bachar El-Oumeiri<sup>1\*</sup>, Kathleen Mc Entee<sup>2</sup>, Filippo Annoni<sup>3</sup>, Antoine Herpain<sup>3</sup>, Frédéric Vanden Eynden<sup>1</sup>, Pascal Jespers<sup>2</sup>, Guido Van Nooten<sup>1</sup> and Philippe van de Borne<sup>4</sup>

## Abstract

**Background:** Aortic regurgitation (AR) is a valvular disease that can lead to systolic heart failure. Treatment options besides cardiac surgery are limited and consequently severe AR is associated with higher mortality and morbidity when not operated. In this investigation, we examined the effects of a novel cardiac myosin activator, Omecamtiv-mecarbil (OM), in rats with chronic severe AR.

**Methods:** AR was created by retrograde puncture of the aortic valve leaflets in 20 adults Wistar rats. 12 animals survived the acute AR phase and were randomized 2 months thereafter into OM ( $n = 7$ ) or placebo groups ( $n = 5$ ). Two rats underwent a sham operation and served as controls. Equal volumes of OM or placebo (NaCl 0.9%) were perfused in the femoral vein by continuous infusion (1.2 mg/kg/hour) during 30 min. Doppler-echocardiography was performed before and at the end of the infusion periods.

**Results:** OM increased indices of global cardiac function (cardiac output, stroke volume), and increased systolic performance (fractional shortening, ejection fraction, left ventricular end systolic diameter) (all  $p < 0.05$ ). These effects concurred with decreases in indices of LV preload (left atrial size, left ventricular end diastolic diameter) as well in the aortic pre-ejection period / left ventricular ejection time ratio (all  $p < 0.05$ ). The severity score of the regurgitant AR jet did not change. Placebo infusion did not affect these parameters.

**Conclusion:** The cardiac myosin activator OM exerts favorable hemodynamic effects in rats with experimental chronic AR.

**Keywords:** Omecamtiv-mecarbil, Aortic regurgitation, Doppler-echocardiography, Wistar rat, Left ventricle

## Background

Aortic regurgitation (AR) is a valvular disease that affects men more than women, and whose incidence increases with age [1]. Severe AR is associated with higher morbidity and mortality compared to the general population [2]. Chronic AR secondary to rheumatic fever is a frequent condition in developing countries and in populations having no adequate access to health care [3]. Chronic severe AR imposes a combined left ventricular (LV) volume and pressure overload. Volume increase is a direct consequence of the regurgitant volume itself, while pressure overload results from increased parietal

stress and systolic hypertension [4]. AR is associated with a long asymptomatic period during which the LV progressively enlarges and hypertrophies in response to a chronic volume overload. The increased wall stress and LV volume/mass ratio can lead to impaired LV systolic function, clinical signs of heart failure and, finally, become irreversible and lethal [5]. So far, vasodilators are the only drugs indicated in asymptomatic AR, but their hemodynamic effects are inconsistent and their impact on clinical outcomes is largely uncertain [6, 7]. Rats are convenient animals to evaluate the response of the LV to severe AR as they develop LV abnormalities in a relatively short period of time (weeks). This is in contrast to humans, who can tolerate this condition without apparent LV dysfunction for decades [8]. The rats develop progressive LV dilatation and eccentric

\* Correspondence: Bachar.ElOumeiri@erasme.ulb.ac.be

<sup>1</sup>Department of Cardiac surgery, Erasme Hospital, ULB, 808 Lennik road, 1070, Brussels, Belgium

Full list of author information is available at the end of the article



© The Author(s). 2018 **Open Access** This article is distributed under the terms of the Creative Commons Attribution 4.0 International License (<http://creativecommons.org/licenses/by/4.0/>), which permits unrestricted use, distribution, and reproduction in any medium, provided you give appropriate credit to the original author(s) and the source, provide a link to the Creative Commons license, and indicate if changes were made. The Creative Commons Public Domain Dedication waiver (<http://creativecommons.org/publicdomain/zero/1.0/>) applies to the data made available in this article, unless otherwise stated.

hypertrophy, due to a chronic LV volume overload, as well as progressive irreversible LV systolic dysfunction, mimicking closely the evolution of the disease over a much larger time span in humans [9].

In chronic AR, indices of systolic function such as left ventricular ejection fraction (LVEF) are better prognostic indicators than indices of cardiac overload [2]. Moreover, markers of systolic function are useful for decision of a timely surgical valve replacement [10, 11]. Conventional medical treatment of congestive heart failure with altered ejection fraction is based on neuro-hormonal blockade, neuro-hormonal activation being considered responsible for aggravation of heart failure and loss of myocardial contractility [12]. Because of safety issues, conventional therapies that directly target cardiac contractility are sparsely used [13]. Heart failure (HF) remains a major public health problem worldwide. Existing drugs increase cardiac contractility indirectly through signaling cascades but are limited by their mechanism related adverse effects. To avoid this limitation Omecamtiv-mecarbil (OM) was developed. Omecamtiv-mecarbil, formerly called CK-1827452 (Cytokinetics Inc., San Francisco, CA, USA) is a novel drug which improves cardiac contractility by means of cardiac myosin activation. OM accelerated the transition of myosin from the weakly actin-bound to strongly actin-bound state measured by release of Hydrolyzed Phosphate (Pi). OM appeared to shift the equilibrium towards myosin adenosine triphosphate (ATP) hydrolysis without affecting the rate of hydrolysis, in addition to accelerating the rate of Pi release. OM decreased the rate of Pi release when actin was removed. This decrease in actin-independent ATP hydrolysis potentially increases the overall energetic efficiency of the system by diminishing ATP use not associated with mechanical work [14]. Consequently, OM increases systolic ejection duration without changing the rate of left ventricular pressure development [15, 16].

In two different canine models of pacing-induced systolic heart failure (after myocardial infarction [15] and in the presence of left ventricular hypertrophy [15]), OM increased systolic wall thickness and fractional shortening (FS), leading to an improved global cardiac function and lowered heart rate (HR), while myocardial energetics and loading conditions did not change. Cardiac morphology alterations in tachycardia-induced cardiomyopathy include chamber dilatation and normal or reduced ventricular wall thickness, with little or no change in myocardial mass. These changes, together with myocardial energy depletion and impaired energy utilization, are reversible once HR normalizes [17]. These characteristics differ completely from the chronic volume and pressure overload in severe AR, leading to LV dilatation and eccentric hypertrophy, an ultimately, to an irretrievably

compromised LV function. Favorable effects of OM in experimental pacing-induced cardiomyopathy may thus not apply to chronic severe AR. Consequently, the goal of the present study was to test the hypothesis that cardiac myosin activation with OM improved left ventricular function in a rat-model of chronic severe aortic regurgitation. The expanded goal of this study was to determine if OM affected AR severity.

## Methods

### Animals

Experiments were approved by the Institutional Animal Care and Use Committee of the Free University of Brussels. Studies were conducted in accordance with the Guide for the Care and Use of Laboratory Animals published by the National Institutes of Health (NIH Publication No. 85–23, revised 1996). Twenty-four male adult Wistar rats ( $401 \pm 90$  g body weight) were randomized to a sham intervention ( $n = 4$ ) or to AR creation ( $n = 20$ ). Rats that survived the acute phase ( $n = 12$ ) were randomized into an OM group ( $n = 7$ ) or a placebo group ( $n = 5$ ). The 4 rats (two in the OM group and two in the placebo group) who underwent a sham operation served as controls for the effect of time and measurement repetition on the parameters investigated in the study.

### Interventions

AR was created by retrograde puncture of the aortic valve leaflets under general anesthesia, as previously described [18]. Briefly, the animals were anesthetized with an intraperitoneal injection of 75 mg/kg of ketamine and 0.25 mg/kg of medetomidine. HR and rhythm were monitored via limb leads throughout the procedure. The right internal carotid artery was surgically exposed. A fixed core wire guide .025" (COOK incorporated, IN, 47404, USA) was advanced toward the aortic valve in a retrograde manner to tear valve leaflets and induce AR. The following echocardiographic criteria with popping sensation at the time of surgery were used to include animals in the study: a jet extent above 30% of the length of the LV and color-Doppler ratio of regurgitant jet width to LV outflow tract diameter above 50% [19]. The 2 sham-operated animals had their right carotid artery cannulated without puncturing the aortic valve. Animals were closely observed during the first hours and days after surgery for any sign of respiratory distress suggestive of acute heart failure.

### Measurements

Transthoracic 2D, M-mode and Doppler echocardiography were performed under general anesthesia with an ultrasound unit (Vivid-7, GE Healthcare, US) equipped with a 10Mhz surgical transducer. Rats were placed in the right and left lateral recumbent positions and their

electrocardiogram was monitored via limb leads throughout the procedure. All measurements were made according to the recommendations of the American Society of Echocardiography currently applied to humans [19]. Standard right parasternal (long and short axis) and left apical parasternal views were used for data acquisition. Left atrial size was assessed in right parasternal short axis at the level of the aorta. Diastolic (d) and systolic (s), septal wall thickness (SWT), posterior wall thickness (PWT) and LV diameters (LVEDD, LVESD) were measured in M-mode from a LV short axis view at the level of chordae tendinae and fractional shortening (FS) was calculated. Ejection fraction (EF) were derived using the Teicholz formula. Left ventricle mass was calculated using the American Society of Echocardiography recommended formula:  $LV\ mass = 0.8 \times \{1.04[(LVEDD + PWTd + SWTd)^3 - (LVEDD)^3]\} + 0.6\ g$ . Aortic diameter was measured from the right long axis parasternal view. Aortic flow was measured from the left apical view to calculate forward stroke volume (SV) and cardiac output and to measure pre-ejection period (PEP: delay from Q wave of QRS to aortic opening, ms), LV ejection time (LVET: interval from beginning to termination of aortic flow, ms), and inter-beat interval (RR). Systolic time was determined as PEP + LVET (ms). Diastolic time (ms) consists in RR interval (ms) - systolic time (ms). PEP/LVET ratio was also calculated. PEP/LVET is a more useful index of overall LV performance [20]. This ratio is better correlated with other LV performance measurements than either PEP or LVET, and is considered independent of HR [21]. Severity of the regurgitant aortic jet was subjectively graded (1 to 4).

#### Experimental design

Doppler-echocardiography was performed before AR creation, during surgery to confirm the presence and the severity of AR, and 2 months thereafter, both before and after OM (1.2 mg/kg/hour) or placebo (NaCl 0.9%) infusion for 30 min, by means of a femoral vein perfusion. All animals received equal volumes (12 ml/kg) of placebo or OM. This achieved plasma concentration of nearly 400 ng of OM/ml in a previous study [22]. Doppler-Echocardiography was performed after 30 min infusion. All animals remained alive during these experimental sessions which could thus be completed in 5 rats with placebo and 7 rats with OM.

#### Statistical analysis

Results are expressed as means  $\pm$  SD. A 2-factor ANOVA for repeated measures followed by post-hoc Bonferroni corrections for multiple comparisons was used to assess the effects of OM versus placebo, and any interaction between them, after 2 months of AR on the 16 animals. All other statistical analysis consisted

of paired-t tests between variables. Significance was set at a  $p$  value less than 0.05. (SPSS 23.0, IBM, Chicago, Ill, USA).

## Results

### AR and LV measurements (Fig. 1)

AR was achieved in all 20 animals and confirmed by the presence of a regurgitant jet quantified as severe in all animals. Eight animals died of congestive heart failure within 2 months and were not included in the final analysis. After 2 months AR (graduated from 0 to 4) was achieved at  $3.67 \pm 0.44$ , and echocardiographic signs of volume overload and eccentric hypertrophy were present with increased left atrial diameter, LVEDD, LVEDV and LV mass ( $n = 12$ , all  $p < 0.05$ , paired t tests). Load dependent indices of LV systolic function (FS and EF) were unchanged but LVESD were increased. SV and cardiac output were decreased ( $n = 12$ , both  $p < 0.01$ , paired t tests). As expected, no AR was detected in sham operated rats ( $n = 4$ ) with no modifications of LV function or dimension in the placebo group while only FS and EF increased after injection of OM ( $p = 0.011$  and  $p = 0.032$ , respectively) (Table 1).

### Effects of placebo in rats with AR (Table 2)

Before infusion, there was no difference in echocardiographic results between the 2 groups (placebo versus OM). NaCl infusion affected none of the echocardiographic parameters of global and systolic cardiac function neither the indices of LV preload ( $n = 5$ ,  $p > 0.06$ , paired t tests).

### Effects of OM in rats with AR (Table 3)

OM increased indices of global cardiac function (SV, cardiac output), decreased HR and increased systolic performance (FS, EF) ( $n = 7$ , all  $p < 0.05$ , paired t tests). These effects concurred with decreases in measures of LV preload (Left atrial diameter, LVEDD), and a decreased PEP/LVET ratio ( $n = 7$ , all  $p < 0.05$ , paired t tests). OM did not affect the severity score of the AR jet.

### Effects of OM versus placebo after 2 months of AR (Table 4)

Two-way ANOVA with Bonferroni corrections for multiple comparisons after 2 months of AR were done on the effects of placebo versus OM. Only FS and EF increased after OM as compared to placebo ( $p = 0.014$  and  $p = 0.012$ , respectively) (Fig. 2). None of the other hemodynamic changes investigated in this study achieved the level of significance in this analysis (none illustrated).



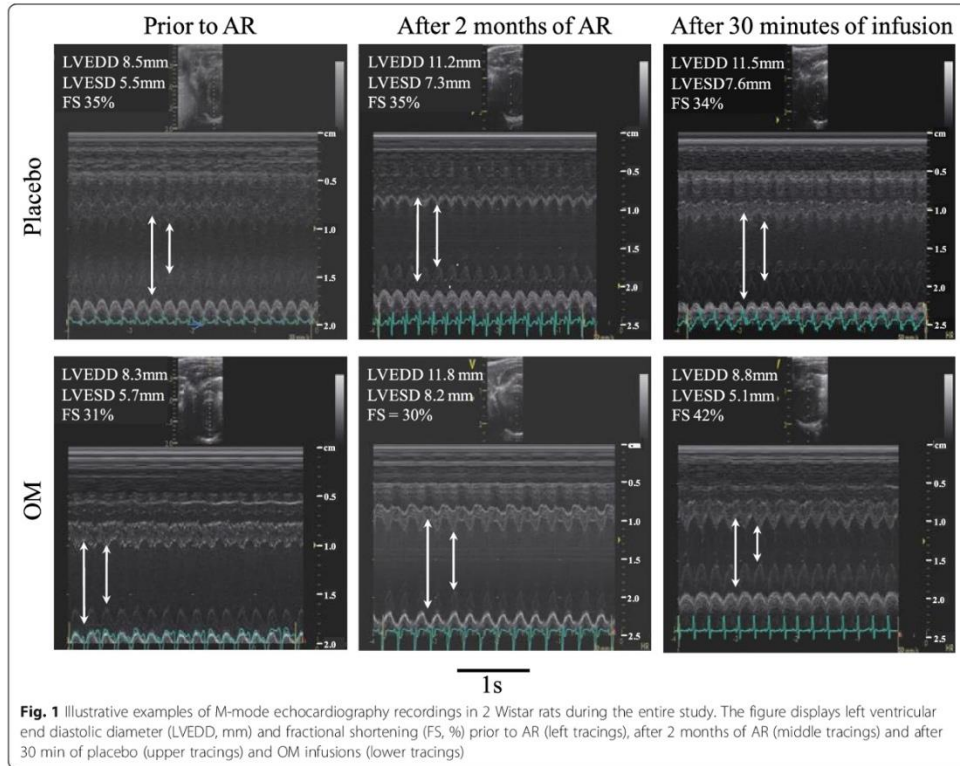


**Fig. 1** Illustrative examples of M-mode echocardiography recordings in 2 Wistar rats during the entire study. The figure displays left ventricular end diastolic diameter (LVEDD, mm) and fractional shortening (FS, %) prior to AR (left tracings), after 2 months of AR (middle tracings) and after 30 min of placebo (upper tracings) and OM infusions (lower tracings)

**Discussion**

We investigated the effect of the cardiac myosin activator OM on severe chronic AR in an experimental rat-model. The main findings of our study are that OM decreases volume overload induced by chronic AR. As OM lessened LVEDD and LVESD and increased SWTs, we can assume that OM markedly decreased LV wall stress in the presence of a severe chronic AR. We are not aware of a previous similar placebo-controlled study.

**Effects of OM on cardiac function**

The central hemodynamic feature of chronic AR is a combined volume and pressure overload of the LV [4, 23]. The LV responds to volume overload with a series of compensatory mechanisms, including a LV dilatation, an increase in chamber compliance and a combination of eccentric and concentric hypertrophy. The ejection phase indexes of LV systolic function at rest remain normal. However, an enlarged chamber size with the associated increase in wall stress also results in a stimulus for further hypertrophy

[24]. Despite the small number ( $n = 4$ ) of sham animals, OM increase EF and FS in sham OM group ( $n = 2$ ).

In our study OM decreased volume overload induced by AR during the whole cardiac cycle, by lowering LVEDD. Moreover, by decreasing LVEDD and LVESD and increasing SWTs, OM decreased wall stress in AR. This is of importance, since an increased wall stress may lead to overt LV systolic dysfunction [25]. Improving cardiac systolic function with a cardiac myosin activator could be favorable to ventricular remodeling [26].

In our study OM decreased the PEP/LVET ratio, a reliable index of LV performance. Acute reduction in afterload in patients with congestive heart failure improves LV systolic performance and decreases the PEP/LVET ratio, while an increase in preload will shorten PEP, prolong LVET and decrease PEP/LVET [27]. We found that despite preload reduction by OM, PEP was shortened and cardiac performance improved. This mechanism could explained the increase in stroke volume [28]. An improvement in cardiac function after infusion of OM in mongrel dogs, where heart failure was achieved by rapid ventricular

**Table 1** Two-way ANOVA statistics with Bonferroni correction at base (T1), before injection (T2) and after injection (T3) for all sham animals (n = 4)

	T1	T2	<i>p</i>	T3	<i>p</i>
Heart Rate (beats/min)	258 ± 11	270 ± 7	0,756	193 ± 15	0,251
Left Atrium (mm)	4.6 ± 0.2	6.2 ± 0.3	0,872	5.5 ± 0.2	0,118
LVEDD (mm)	7.9 ± 0.5	11.1 ± 0.4	0,938	10.1 ± 0.5	0,209
LVESD (mm)	5.5 ± 0.4	7.6 ± 0.3	0,736	6.1 ± 0.4	0,072
FS (%)	31.5 ± 1.4	30.5 ± 1.0	0,937	35.4 ± 1.5	0,011
EF (%)	64.1 ± 2.0	63.9 ± 1.4	0,630	68.8 ± 2.5	0,032
Stroke Volume (ml)	0.34 ± 0.03	0.22 ± 0.18	0,448	0.30 ± 0.04	0,762
Cardiac Output (ml/min)	79.5 ± 9.3	52.0 ± 4.5	0,890	61.6 ± 8.6	0,393
SWTs (mm)	2.1 ± 0.1	2.3 ± 0.2	0,671	2.7 ± 0.2	0,457
SWTd (mm)	1.4 ± 0.1	1.7 ± 0.2	0,971	2.1 ± 0.2	0,092
Systolic time (ms)	126 ± 3.7	134 ± 2.6	0,245	135 ± 2.6	0,153
Diastolic time (ms)	139 ± 8.4	135 ± 8.3	0,207	157 ± 14.5	0,138
PEP (ms)	15.0 ± 1.6	25.4 ± 1.3	0,413	21.8 ± 1.0	0,308
LVET (ms)	110 ± 4.4	109 ± 2.8	0,310	113 ± 3.9	0,268
PEP/LVET	0.13 ± 0.02	0.23 ± 0.02	0,800	0.19 ± 0.01	0,968
Systolic time/RR	0.48 ± 0.02	0.50 ± 0.02	0,344	0.47 ± 0.02	0,370

Values are mean ± SD. LVEDD Left ventricle end-diastolic diameter, LVEDV Left ventricle end-diastolic volume, LVESD Left ventricle end-systolic diameter, LVESD Left ventricle end-systolic volume, FS Fractional shortening, EF Ejection fraction, SV stroke volume, SWTs septal wall thickness at end-systole, SWTd septal wall thickness at end-diastole, PEP aortic pre-ejection period, LVET Left ventricular ejection time, RR inter-beat interval

**Table 2** Two-tailed T-test before and after Placebo infusion on LV function after 2 months of AR in a rat model (n = 5)

	Before infusion	After infusion	<i>p</i> -value
Heart Rate (beats/min)	249 ± 18	220 ± 41	0.437
Left Atrium (mm)	6.2 ± 0.8	5.8 ± 1.1	0.541
LVEDD (mm)	10.6 ± 0.8	12.24 ± 1.07	0.092
LVESD (mm)	7.5 ± 0.6	6.9 ± 0.84	0.341
FS (%)	28.8 ± 1.4	29.6 ± 5.2	0.706
EF (%)	60.8 ± 1.8	61.0 ± 8.4	0.968
Stroke Volume (ml)	0.24 ± 0.04	0.24 ± 0.08	0.890
Cardiac Output (ml/min)	60 ± 8	60 ± 12	0.369
SWTs (mm)	3.0 ± 0.16	2.9 ± 0.47	0.122
SWTd (mm)	1.6 ± 0.17	1.7 ± 0.29	0.281
Systolic time (ms)	136 ± 5	123 ± 17	0.340
Diastolic time (ms)	144 ± 24	173 ± 41	0.054
PEP (ms)	25.8 ± 4.6	21.2 ± 6.2	0.125
LVET (ms)	110 ± 8	102 ± 14	0.490
PEP/LVET	0.24 ± 0.05	0.20 ± 0.05	0.182
Systolic time/RR	0.49 ± 0.05	0.42 ± 0.05	0.047

Values are mean ± SD. Left ventricle end-diastolic diameter; LVEDV: Left ventricle end-diastolic volume; LVESD: Left ventricle end-systolic diameter; LVESD: Left ventricle end-systolic volume; FS: Fractional shortening; EF: Ejection fraction; SV: stroke volume; SWTs: septal wall thickness at end-systole; SWTd: septal wall thickness at end-diastole PEP: aortic pre-ejection period; LVET: Left ventricular ejection time; RR: inter-beat interval

**Table 3** Two-tailed T-test before and after OM infusion on LV function after 2 months of AR in a rat model (n = 7)

	Before infusion	After infusion	<i>p</i> -value
Heart Rate (beats/min)	253 ± 22	207 ± 35	0.091
Left Atrium (mm)	6.2 ± 0.8	5.5 ± 0.7	0.037
LVEDD (mm)	11.6 ± 1.09	9.0 ± 1.51	0.003
LVESD (mm)	7.8 ± 0.91	5.4 ± 1.30	0.009
FS (%)	32.1 ± 3.4	41.1 ± 5.3	0.004
EF (%)	65.0 ± 4.7	76.6 ± 5.8	0.002
Stroke Volume (ml)	0.19 ± 0.06	0.36 ± 0.11	0.011
Cardiac Output (ml/min)	44 ± 16	76 ± 14	0.027
SWTs (mm)	2.67 ± 0.48	3.33 ± 0.51	0.390
SWTd (mm)	1.6 ± 0.17	2.4 ± 0.39	0.274
Systolic time (ms)	133 ± 7	147 ± 8	0.003
Diastolic time (ms)	127 ± 16	141 ± 33	0.384
PEP (ms)	25.0 ± 2.3	22.4 ± 1.8	0.042
LVET (ms)	108 ± 6	125 ± 9	0.002
PEP/LVET	0.23 ± 0.02	0.18 ± 0.02	0.007
Systolic time/RR	0.51 ± 0.04	0.52 ± 0.06	0.735

Values are mean ± SD. LVEDD Left ventricle end-diastolic diameter, LVEDV Left ventricle end-diastolic volume, LVESD Left ventricle end-systolic diameter, LVESD Left ventricle end-systolic volume, FS Fractional shortening, EF Ejection fraction, SV stroke volume, SWTs septal wall thickness at end-systole, SWTd septal wall thickness at end-diastole, PEP aortic pre-ejection period, LVET Left ventricular ejection time, RR inter-beat interval

**Table 4** Two-way ANOVA statistics with Bonferroni correction at base (T1), before injection (T2) and after injection (T3) for all animals ( $n = 12$ )

	T1	T2	p	T3	p
Heart Rate (beats/min)	226 ± 23	228 ± 21	0.890	208 ± 28	0.113
Left Atrium (mm)	4.6 ± 0.2	6.2 ± 0.3	0.966	5.5 ± 0.2	0.277
LVEDD (mm)	7.9 ± 0.5	11.1 ± 0.4	0.235	10.1 ± 0.5	0.066
LVESD (mm)	5.5 ± 0.4	7.6 ± 0.3	0.871	6.1 ± 0.4	0.092
FS (%)	31.5 ± 1.4	30.5 ± 1.0	0.144	35.4 ± 1.5	0.014
EF (%)	64.1 ± 2.0	63.9 ± 1.4	0.173	68.8 ± 2.5	0.012
Stroke Volume (ml)	0.34 ± 0.03	0.22 ± 0.18	0.129	0.30 ± 0.04	0.135
Cardiac Output (ml/min)	79.5 ± 9.3	52.0 ± 4.5	0.098	61.6 ± 8.6	0.203
SWTs (mm)	2.1 ± 0.1	2.3 ± 0.2	0.597	2.7 ± 0.2	0.652
SWTd (mm)	1.4 ± 0.1	1.7 ± 0.2	0.439	2.1 ± 0.2	0.040
Systolic time (ms)	126 ± 3.7	134 ± 2.6	0.626	135 ± 2.6	0.293
Diastolic time (ms)	139 ± 8.4	135 ± 8.3	0.341	157 ± 14.5	0.293
PEP (ms)	15.0 ± 1.6	25.4 ± 1.3	0.771	21.8 ± 1.0	0.577
LVET (ms)	110 ± 4.4	109 ± 2.8	0.752	113 ± 3.9	0.180
PEP/LVET	0.13 ± 0.02	0.23 ± 0.02	0.811	0.19 ± 0.01	0.378
Systolic time/RR	0.48 ± 0.02	0.50 ± 0.02	0.567	0.47 ± 0.02	0.063

Values are mean ± SD. LVEDD Left ventricle end-diastolic diameter, LVEDV Left ventricle end-diastolic volume, LVESD Left ventricle end-systolic diameter, LVESV Left ventricle end-systolic volume, FS Fractional shortening, EF Ejection fraction, SV stroke volume, SWTs septal wall thickness at end-systole, SWTd septal wall thickness at end-diastole, PEP aortic pre-ejection period, LVET Left ventricular ejection time, RR inter-beat interval

pace-induced energy depletion, has also been reported, because OM decreased LV end-diastolic pressure without affecting LV systolic pressure [15].

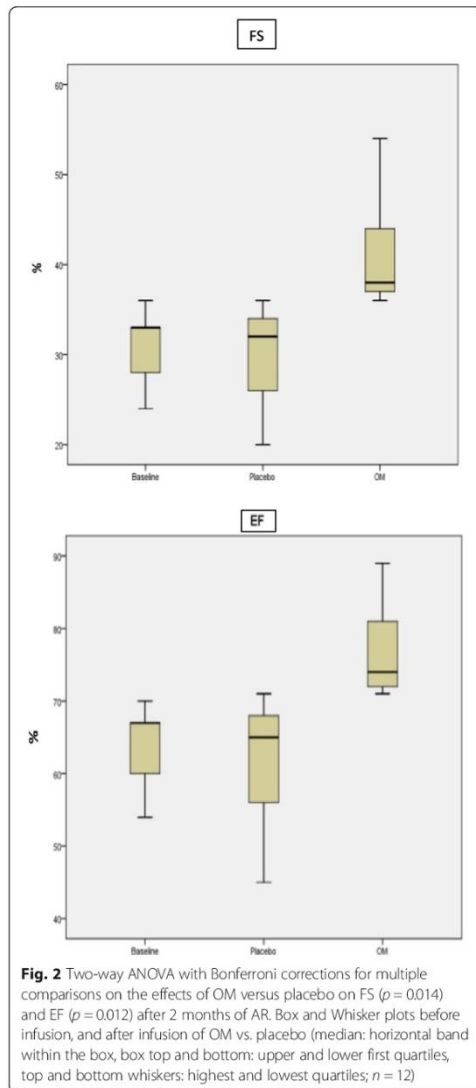
In contrast to our initial hypothesis, we found that OM did not affect the severity of the aortic leakage since the diastolic time-span remained unchanged, as a result of a reduction in HR. In mitigation, however, excessive prolongation the duration of systole might compromise myocardial blood flow, and thereby aggravate ischemia; even if studies with OM in patients with angina and ischemic cardiomyopathy seem reassuring in this regard [29]. This stands in contrast with inotropic drugs that enhance the risk of ischemia, arrhythmias and death. Hence forth those risks have limited their utility in treating acute and chronic heart failure [30].

Ketamine is a dissociative anesthetic agent that has cardiovascular effect resembling sympathetic nervous system stimulation, increase heart rate and cardiac output [31]. Medetomidine improves muscle relaxation, potentiates anesthetic action of ketamine and compensates the cardiac stimulating effect of ketamine by decreasing heart rate and cardiac output. Dexmedetomidine had no direct myocardial depressant effect in the rat heart in doses that are similar to those encountered under clinical conditions [32]. As animals were all anesthetized at the same regime, the decrease in heart rate observed in the OM group can be attributed to OM. However, we cannot predict if this bradycardic effect of OM had also been highlighted in conscious non-sedated animals.

#### Possible differential effects of OM as compared to other inotropic agents in AR

Dobutamine infusion, in patients with chronic aortic regurgitation and depressed LV ejection fraction, decreased LVEDD, LVEDV, LVESD and LVESV, while FS and EF improved [33]. In conscious dogs with heart failure, systemic and pulmonary systolic wall stress remained unchanged while HR, LV systolic pressure and LV dP/dt increased with Dobutamine [34]. Dobutamine also shortened LVET in healthy dogs [35]. On the opposite, in our study OM decreased HR and increased LVET, while others, in conscious dogs with systolic heart failure induced by rapid pacing, reported that OM did not affect LV dP/dt [15]. When a comparable concentration of OM than in our study was administered in normal humans (400 ng/ml) [36], blood pressure did not change. Thus OM and Dobutamine tend to enhance LV contractility by increasing wall thickening and fractional shortening, but in the presence of unchanged afterload conditions with OM [37], while arterial pressure and total vascular resistance increase with Dobutamine.

Currently available inotropes Dobutamin, Dopamin, Milrinone and Levosimendan have demonstrated proarrhythmic effects linked to increased mortality that can limit their clinical utility [38]. Most inotropic agents modify calcium cellular homeostasis. This is important, as intracellular calcium plays an important role in myocardial oxygen demand [39]. The well-known and widely used sympathomimetic drug dobutamine increases calcium



channels accessibility [40]. Other medications, such as levosimendan, enhance the sensitivity of troponin-c towards calcium, not at the expense of an increase in intracellular calcium concentration [22]. Levosimendan increases contractility by enhancing cross-bridge formation between actin and myosin [22, 41]. The side effect of these increases in contractility is that they raise also

myocardial oxygen consumption which is also pro arrhythmic. The molecules may also alter the expression of genes and promote the apoptosis of myocardial cells elicited by the increased intracellular calcium [39, 41]. OM inhibits non-actin dependent cardiac myosin adenosine triphosphate [16] and does not raise myocardial oxygen consumption [15]. A recent study in anesthetized animals suggested the opposite, namely that OM increased myocardial oxygen consumption [42], and however this was apparently undermined by methodological limitations [43]. These favorable characteristics of OM could prove useful in patients with AR.

**Effects of OM dose on the observed changes**

In our study we administrated 1.2 mg/kg/h of OM during 30 min. This was expected to raise plasma concentrations of OM to nearly 400 ng/ml [44]. In rats with heart failure induced by a ligation of the left coronary artery, infusion of OM resulted in comparable increases in FS than in our study, starting at plasma concentrations of approximately 200 ng/ml [44]. Administration of less than 0.48 mg/kg/h of OM yield plasma levels < 160 ng/ml, where no LV functional improvements were observed [36]. In healthy human improvements in EF began at a dose of 0.5 mg/kg/h, while improvements in FS, LVET and SV began at an infusion rate of 0.125 mg/kg/h [36]. No change in orthostatic vital signs was noted in this study [45]. In patients with heart failure [45], LVET increased at OM concentrations > 100 ng/ml, while SV and FS raised at plasma levels > 200 ng/ml. EF increased only beginning concentrations > 300 ng/ml. Supine and standing systolic blood pressure decreased at > 400 and > 500 ng/ml, respectively. Last, in the ATOMIC-AHF study [46], patients with acute heart failure treated with OM disclosed a concentration-dependent reduction in HR at a concentration > 200 ng/ml while blood pressure increased at a concentration > 300 ng/ml, as compared to placebo. There was also a concentration-related decrease in LVESD and increase in LVET. OM concentrations > 400 ng/ml achieved a better dyspnea response. Thus the dose administered in our study seems in the upper range of the concentrations where favorable hemodynamic modifications of OM are clear-cut, without being harmful. Adverse effects of OM consist in an excessive prolongation of systolic ejection time > 110 ms [36]. This was observed with supra therapeutic concentrations of OM (~1200 ng/ml) which may induce myocardial ischemia by reducing the time during which diastolic coronary blood flow can occur [46]. A drug overdose in a patient with heart failure, with a predicted concentration of 1750 ng/ml at the time of infusion termination, resulted in chest pain, sweating, hypotension, and ECG changes suggestive of ischemia [45]. It is not known,

however, that the angina symptoms, observed at supra-therapeutic concentrations of OM, are related - or not - to the presently recognized ryanodine receptors activating effect of OM [47].

#### Study limitations

The tested animal group was small because many rats did not recover from the acute AR procedure. Another striking limitation of our study resides in the fact that we could not achieve ventricular blood pressure measurement during the study. As such, our assessment of ventricular loading conditions remains incomplete. Several studies suggest however that systemic blood pressure is not affected at the OM concentrations we achieved in our study [36, 37]. Our study did also not assess whether OM has dose-dependent hemodynamic effects in our model of AR. Lower doses of OM may still exert favorable hemodynamic effects, while even further reducing the risk of excessive prolongations in LVET. This will require additional studies. Moreover, as already discussed, a direct comparison of the effects of different inotropic agents in AR-related heart failure would also provide further insights in the differential hemodynamic effects of OM, as compared to other inotropic agents. Last, the effects of OM on animals who might otherwise not survive the decompensation period after an acute AR should be also studied. This is a very poorly tolerated condition in humans [48], which could benefit from further studies on the best hemodynamic support while awaiting cardiac surgery [48]. Last, the sham group in our study comprised only 2 animals in the OM group and 2 animals in the placebo group.

Another limitation of the study, the possible fistula with left atrium created during aortic valve leaflets puncture, this fistula can explain the decrease of stroke volume and cardiac output after the creation of the aortic regurgitation.

#### Conclusion

The present placebo-controlled study shows improvements in cardiac function after infusion of OM. Our investigations demonstrate these effects for the first time in the rat-model with chronic severe AR. We observed a decrease in volume overload and an increase in cardiac output and wall thickness. Moreover OM enhanced EF and FS, while coincidentally lowering the HR and wall stress. On the other hand, OM did not affect the duration of diastole and the severity of AR.

#### Abbreviations

AR: Aortic regurgitation; ATP: Adenosin triphosphate; EF: Ejection fraction; FS: Fractional shortening; HR: Heart rate; LV: Left ventricle; LVEDD: Left ventricle end-diastolic diameter; LVESD: Left ventricle end-systolic diameter; LVET: Left ventricular ejection time; OM: Omecamtiv-mecarbil; PEP: Pre-ejection period; Pi: Hydrolyzed phosphate; RR: Inter-beat interval; SV: Stroke volume

#### Funding

This study was supported and funded by the for Cardiac Surgery Foundation of the Free University of Brussels (B. El Oumeiri), the Sauciez-Van Pouke Foundation (B. El Oumeiri, K. Mc Entee, and P. Van de Borne).

#### Availability of data and materials

All materials and data are available at request at the Laboratory of Physiology of the University of Brussels.

#### Authors' contributions

BE carried out the experiments, performed the statistical analysis and drafted the manuscript and participated in the design of the study. KME coordinated the study and participated in its design. FA and AH carried out the echocardiography. FVD participated in the coordination of the study, PJ did the technical assistance GVN performed the statistical analysis and reviewed the manuscript. PVB conceived the study and participated in the drafting of the manuscript. All authors read and approved the final manuscript.

#### Ethics approval

Experiments were approved by the Institutional Animal Care and Use Committee of the Free University of Brussels under N° 461 N. Studies were conducted at the Laboratory of Physiology of the University of Brussels (LA 1230334) in accordance with the Guide for the Care and Use of Laboratory Animals published by the National Institutes of Health (NIH Publication No. 85-23, revised 1996).

#### Competing interests

The authors declare that they have no competing interests.

#### Publisher's Note

Springer Nature remains neutral with regard to jurisdictional claims in published maps and institutional affiliations.

#### Author details

<sup>1</sup>Department of Cardiac surgery, Erasme Hospital, ULB, 808 Lennik road, 1070, Brussels, Belgium. <sup>2</sup>Laboratory of Physiology and Pharmacology, ULB, Brussels, Belgium. <sup>3</sup>Department of intensive care, Erasme Hospital, ULB, Brussels, Belgium. <sup>4</sup>Department of Cardiology, Erasme Hospital, ULB, Brussels, Belgium.

Received: 9 February 2017 Accepted: 7 May 2018

Published online: 21 May 2018

#### References

- Maurer G. Aortic regurgitation. *Heart*. 2006 Jul;92(7):994–1000.
- Dujardin KS, Enriquez-Sarano M, Schaff HV, Bailey KR, Seward JB, Tajik AJ. Mortality and morbidity of aortic regurgitation in clinical practice. A long-term follow-up study. *Circulation*. 1999 Apr 13;99(14):1851–7.
- Chockalingam A, Gnanavelu G, Elangovan S, Chockalingam V. Current profile of acute rheumatic fever and valvulitis in southern India. *J Heart Valve Dis*. 2003 Sep;12(5):573–6.
- Carabello BA. Aortic regurgitation. A lesion with similarities to both aortic stenosis and mitral regurgitation. *Circulation*. 1990 Sep;82(3):1051–3.
- Bonow RO. Aortic Regurgitation. *Curr Treat Options Cardiovasc Med*. 2000 Apr;2(2):125–32.
- Evangelista A, Tornos P, Sambola A, Permyer-Miralda G, Soler-Soler J. Long-term vasodilator therapy in patients with severe aortic regurgitation. *N Engl J Med*. 2005 Sep 29;353(13):1342–9.
- Mahajerin A, Gurm HS, Tsai TT, Chan PS, Nallamothu BK. Vasodilator therapy in patients with aortic insufficiency: a systematic review. *Am Heart J*. 2007 Apr;153(4):454–61.
- Magid NM, Opio G, Wallerson DC, Young MS, Borer JS. Heart failure due to chronic experimental aortic regurgitation. *Am J Physiol*. 1994 Aug;267(2 Pt 2):H556–62.
- Plante E, Couet J, Gaudreau M, Dumas MP, Drolet MC, Arsenault M. Left ventricular response to sustained volume overload from chronic aortic valve regurgitation in rats. *J Card Fail*. 2003 Apr;9(2):128–40.
- Borer JS, Hochreiter C, Herrold EM, et al. Prediction of indications for valve replacement among asymptomatic or minimally symptomatic patients with chronic aortic regurgitation and normal left ventricular performance. *Circulation*. 1998;97:525–34.

11. Borow KM. Surgical outcome in chronic aortic regurgitation: a physiologic framework for assessing preoperative predictors. *J Am Coll Cardiol*. 1987 Nov;10(5):165–70.
12. Weber KT, Brilla CG. Pathological hypertrophy and cardiac interstitium. Fibrosis and renin-angiotensin-aldosterone system. *Circulation*. 1991 Jun;83(6):1849–65.
13. Krum H, Teerlink JR. Medical therapy for chronic heart failure. *Lancet*. 2011 Aug 20;378(9792):713–21.
14. Psotka MA, Teerlink JR. Direct myosin activation by Omecamtiv Mecarbil for heart failure with reduced ejection fraction. *Handb Exp Pharmacol*. 2017; 243:465–90.
15. Shen YT, Malik FI, Zhao X, Depre C, Dhar SK, Abarzúa P, Morgans DJ, Vatner SF. Improvement of cardiac function by a cardiac myosin activator in conscious dogs with systolic heart failure. *Circ Heart Fail*. 2010 Jul;3(4):522–7.
16. Malik FI, Hartman JJ, Elias KA, Morgan BP, Rodriguez H, Brejc K, et al. Cardiac myosin activation: a potential therapeutic approach for systolic heart failure. *Science*. 2011 Mar 18;331(6023):1439–43.
17. Umana E, Solares CA, Alpert MA. Tachycardia-induced cardiomyopathy. *Am J Med*. 2003 Jan;114(1):51–5.
18. Arsenaault M, Plante E, Drolet MC, Couet J. Experimental aortic regurgitation in rats under echocardiographic guidance. *J Heart Valve Dis*. 2002 Jan;11(1): 128–34.
19. Zoghbi WA, Enriquez-Sarano M, Foster E, Grayburn PA, Kraft CD, Levine RA, et al. Recommendations for evaluation of the severity of native valvular regurgitation with two-dimensional and Doppler echocardiography. *J Am Soc Echocardiogr*. 2003 Jul;16(7):777–802.
20. Lewis RP, Rittogers SE, Froester WF, Boudoulas H. A critical review of the systolic time intervals. *Circulation*. 1977 Aug;56(2):146–58.
21. Spodick DH, Doi YL, Bishop RL, Hashimoto T. Systolic time intervals reconsidered. Reevaluation of the prejection period: absence of relation to heart rate. *Am J Cardiol*. 1984 Jun 1;53(11):1667–70.
22. Stevenson LW. Clinical use of inotropic therapy for heart failure: looking backward or forward? Part II: chronic inotropic therapy. *Circulation*. 2003 Jul 29;108(4):492–7.
23. Wisenbaugh T, Allen P, Cooper G 4th, O'Connor WN, Mezaros L, Streter F, Bahinski A, Houser S, Spann JF. Hypertrophy without contractile dysfunction after reversal of pressure overload in the cat. *Am J Phys*. 1984 Jul;247(1 Pt 2): H146–54.
24. Bekeredjian R, Grayburn PA. Valvular heart disease: aortic regurgitation. *Circulation*. 2005 Jul 5;112(1):125–34.
25. Boudoulas H. Systolic time intervals. *Eur Heart J*. 1990 Dec;11 Suppl 1:93–104.
26. Teerlink JR, Felker GM, McMurray JJ, Solomon SD, Adams KF Jr, Cleland JG, Ezekowitz JA, Goudev A, Macdonald P, Metra M, Mitrovic V, Ponikowski P, Serpytis P, Spinar J, Tomcsányi J, Vandekerckhove HJ, Voors AA, Monsalvo ML, Johnston J, Malik FI, Honarpour N; COSMIC-HF investigators. Chronic oral study of myosin activation to increase contractility in heart failure (COSMIC-HF): a phase 2, pharmacokinetic, randomised, placebo-controlled trial. *Lancet*. 2016 Dec 10;388(10062):2895–903.
27. Wallace AG, Mitchell JH, Skinner NS, Sarnoff SJ. Duration of the phases of left ventricular systole. *Circ Res*. 1963 Jun;12:611–9.
28. Greenberg BH, Chou W, Saikali KG, Escandón R, Lee JH, Chen MM, Treshkur T, Megreladze I, Wasserman SM, Eisenberg P, Malik FI, Wolff AA, Shaburishvili T. Safety and tolerability of omecamtiv mecarbil during exercise in patients with ischemic cardiomyopathy and angina. *JACC Heart Fail*. 2015 Jan;3(1):22–9.
29. Petersen JW, Felker GM. Inotropes in the management of acute heart failure. *Crit Care Med*. 2008 Jan;36(1 Suppl):S106–11.
30. Espinola-Zavaleta N, Gómez-Núñez N, Chávez PY, Sahagún-Sánchez G, Keirns C, Casanova JM, Romero-Cárdenas A, Roldán FJ, Vargas-Barrón J. Evaluation of the response to pharmacological stress in chronic aortic regurgitation. *Echocardiography*. 2001 Aug;18(6):491–6.
31. Levänen J, Mäkelä ML, Scheinin H. Dexmedetomidine premedication attenuates ketamine-induced cardio-stimulatory effects and post-anesthetic delirium. *Anesthesiology*. 1995 May;82(5):1117–25.
32. Lee K, Hwang HJ, Kim OS, Oh YJ. Assessment of dexmedetomidine effects on left ventricular function using pressure-volume loops in rats. *J Anesth*. 2017 Feb;31(1):18–24.
33. Asai K, Uechi M, Sato N, Shen W, Meguro T, Mathier MA, Shannon RP, Vatner SF. Lack of desensitization and enhanced efficiency of calcium channel promoter in conscious dogs with heart failure. *Am J Phys*. 1998 Dec;275(6 Pt 2):H2219–26.
34. Banfor PN, Preusser LC, Campbell TJ, Marsh KC, Polakowski JS, Reinhart GA, Cox BF, Fryer RM. Comparative effects of levosimendan, OR-1896, OR-1855, dobutamine, and milrinone on vascular resistance, indexes of cardiac function, and O<sub>2</sub> consumption in dogs. *Am J Physiol Heart Circ Physiol*. 2008 Jan;294(1):H238–48.
35. Anderson RL, Sueoka SH, Lee KH, Rodriguez HM, Kawas RF, Godinez G, Morgan BP, Sakowicz R, Morgans DJ, Malik F, Elias KA. In vitro and in vivo characterization of CK-1827452, a selective cardiac myosin activator. *J Card Fail*. 2006;12:586.
36. Teerlink JR, Clarke CP, Saikali KG, Lee JH, Chen MM, Escandón RD, Elliott L, Bee R, Habibzadeh MR, Goldman JH, Schiller NB, Malik FI, Wolff AA. Dose-dependent augmentation of cardiac systolic function with the selective cardiac myosin activator, omecamtiv mecarbil: a first-in-man study. *Lancet*. 2011 Aug 20;378(9792):667–75.
37. Tariq S, Aronow WS. Use of inotropic agents in treatment of systolic heart failure. *Int J Mol Sci*. 2015 Dec 4;16(12):29060–8.
38. Kojima S, Wu ST, Parnley WW, Wikman-Coffelt J. Relationship between intracellular calcium and oxygen consumption: effects of perfusion pressure, extracellular calcium, dobutamine, and nifedipine. *Am Heart J*. 1994 Feb; 127(2):386–91.
39. Tsien RW, Bean BP, Hess P, Lansman JB, Nilius B, Nowycky MC. Mechanisms of calcium channel modulation by beta-adrenergic agents and dihydropyridine calcium agonists. *J Mol Cell Cardiol*. 1986 Jul;18(7):691–710.
40. Vhasenfass G, Pieske B, Castell M, Kretschmann B, Maier LS, Just H. Influence of the novel inotropic agent levosimendan on isometric tension and calcium cycling in failing human myocardium. *Circulation*. 1998 Nov 17;98(20):2141–7.
41. Moin DS, Sackheim J, Hamo CE, Butler J. Cardiac Myosin Activators in Systolic Heart Failure: More Friend than Foe? *Curr Cardiol Rep*. 2016 Oct;18(10):100.
42. Bakkehaug JP, Kildal AB, Engstad ET, Boardman N, Naesheim T, Rønning L, Aasum E, Larsen TS, Myrnes T, How OJ. Myosin Activator Omecamtiv Mecarbil Increases Myocardial Oxygen Consumption and Impairs Cardiac Efficiency Mediated by Resting Myosin ATPase Activity. *Circ Heart Fail*. 2015 Jul;8(4):766–75.
43. Teerlink JR, Malik FI, Kass DA. Letter by Teerlink et al regarding article, "myosin activator Omecamtiv Mecarbil increases myocardial oxygen consumption and impairs cardiac efficiency mediated by resting myosin ATPase activity". *Circ Heart Fail*. 2015 Nov;8(6):1141.
44. Anderson RL, Sueoka SH, Rodriguez HM, Lee KH, Cox DR, Kawas R, Morgan BP, Sakowicz R, Morgans DJ, Malik F, Elias KA. In vitro and in vivo efficacy of the cardiac myosin activator CK-1827452. *Mol bio cell*. 2005;16(abstract #1728). [https://cytokinetics.com/wp-content/uploads/2015/10/ASCB\\_1728.pdf](https://cytokinetics.com/wp-content/uploads/2015/10/ASCB_1728.pdf).
45. Cleland JG, Teerlink JR, Senior R, Nifontov EM, Mc Murray JJ, Lang CC, et al. The effects of the cardiac myosin activator, omecamtiv mecarbil, on cardiac function in systolic heart failure: a double-blind, placebo-controlled, crossover, dose-ranging phase 2 trial. *Lancet*. 2011 Aug 20;378(9792):676–83.
46. Teerlink JR, Felker GM, McMurray JJ, Ponikowski P, Metra M, Filipatos GS. ATOMIC-AHF investigators. Acute treatment with Omecamtiv Mecarbil to increase contractility in acute heart failure: the ATOMIC-AHF study. *J Am Coll Cardiol*. 2016 Mar 29;67(12):1444–55.
47. Nánási P Jr, Gaburjakova M, Gaburjakova J, Almássy J. Omecamtiv mecarbil activates ryanodine receptors from canine cardiac but not skeletal muscle. *Eur J Pharmacol*. 2017 Aug 15;809:73–9.
48. Dervan J, Goldberg S. Acute aortic regurgitation: pathophysiology and management. *Cardiovasc Clin*. 1986;16(2):281–8.

**Ready to submit your research? Choose BMC and benefit from:**


- fast, convenient online submission
- thorough peer review by experienced researchers in your field
- rapid publication on acceptance
- support for research data, including large and complex data types
- gold Open Access which fosters wider collaboration and increased citations
- maximum visibility for your research: over 100M website views per year

**At BMC, research is always in progress.**

Learn more [biomedcentral.com/submissions](https://biomedcentral.com/submissions)



## The myosin activator omecamtiv mecarbil improves wall stress in a rat model of chronic aortic regurgitation

Bachar El Oumeiri<sup>1</sup>  | Philippe van de Borne<sup>2</sup> | Géraldine Hubesch<sup>3</sup> | Antoine Herpain<sup>4</sup> | Filippo Annoni<sup>4</sup> | Pascale Jespers<sup>3</sup> | Constantin Stefanidis<sup>1</sup> | Kathleen Mc Entee<sup>3</sup> | Frédéric Vanden Eynden<sup>1</sup>

<sup>1</sup>Department of Cardiac Surgery, ULB Erasme University Hospital, Brussels, Belgium

<sup>2</sup>Department of Cardiology, ULB Erasme University Hospital, Brussels, Belgium

<sup>3</sup>Laboratory of Physiology and Pharmacology, ULB, Brussels, Belgium

<sup>4</sup>Department of Intensive Care, ULB Erasme University Hospital, Brussels, Belgium

### Correspondence

Bachar El Oumeiri, Department of Cardiac Surgery, ULB Hospital Universitaire Erasme, Route de Lennik, 808 Brussels, Belgium.  
Email: Bachar.el.oumeiri@erasme.ulb.ac.be

### Funding information

This study was supported and funded by the Fonds pour la Chirurgie Cardiaque, Brussels, Belgium, grant number 489639.

### Abstract

In patients with chronic aortic regurgitation (AR), excessive preload and afterload increase left ventricle wall stress, leading to left ventricular systolic dysfunction. Thus, the objective of the present study was to evaluate the effects of the myosin activator omecamtiv mecarbil (OM) on left ventricle wall stress in an experimental rat model of severe chronic AR. Forty adult male Wistar rats were randomized into two experimental groups: induction of AR (acute phase) by retrograde puncture ( $n = 34$ ) or a sham intervention ( $n = 6$ ). Rats that survived the acute phase ( $n = 18$ ) were randomized into an OM group ( $n = 8$ ) or a placebo group ( $n = 10$ ). Equal volumes of OM (1.2 mg/kg/h) or placebo (0.9% NaCl) were continuously infused into the femoral vein over 30 min. OM significantly decreased end-systolic and end-diastolic and maximum wall stress in this experimental rat model of chronic severe AR ( $p < 0.001$ ) and increased systolic performance assessed by fractional shortening and left ventricle end-systolic diameter; both  $p < 0.05$ ). These effects were correlated with decreased indices of global cardiac function (cardiac output and stroke volume;  $p < 0.05$ ) but were not inferior to baseline pump indices. Infusion with placebo did not affect global cardiac function but decreased end-systolic wall stress ( $p < 0.05$ ) and increased systolic performance (all  $p < 0.001$ ). In the sham-operated (control) group, OM decreased diastolic wall stress ( $p < 0.05$ ). Based on these results, OM had a favorable effect on left ventricle wall stress in an experimental rat model of severe chronic AR.

### KEYWORDS

aortic regurgitation, omecamtiv mecarbil, overload, wall stress

## 1 | INTRODUCTION

Aortic regurgitation (AR) is characterized by diastolic reflux of blood from the aorta into the left ventricle (LV) due

to incomplete closure of the aortic cusps. The prevalence of chronic AR is not precisely known. The Framingham Offspring study (Singh et al., 1999) reported that the overall prevalence of AR was 13% in men and 8.5% in women.

This is an open access article under the terms of the Creative Commons Attribution License, which permits use, distribution and reproduction in any medium, provided the original work is properly cited.

© 2021 The Authors. *Physiological Reports* published by Wiley Periodicals LLC on behalf of The Physiological Society and the American Physiological Society

The central hemodynamic feature of chronic AR is the combined volume and pressure overload of the LV (Carabello, 1990). This results in a series of compensatory mechanisms, including an increase in end-diastolic volume, an increase in chamber compliance to accommodate the increased volume without an increase in filling pressure, and a combination of eccentric and concentric hypertrophy (Otto & Bonow, 2009). In early compensated severe AR, the LV adapts to the volume overload by eccentric hypertrophy (Ricci, 1982). Over time, progressive LV dilation and systolic hypertension increase wall stress and the volume/mass ratio of the LV (Bekeredjian & Grayburn, 2005). The increase in wall stress leads to overt LV systolic dysfunction, which manifests as a decline in the left ventricle ejection fraction (LVEF; Bekeredjian & Grayburn, 2005), followed by irreversible heart failure and death. Increased LV wall stress has generally been associated with worse clinical outcomes (Greenberg et al., 1985; Kumpuris et al., 1982).

Vasodilator therapy is designed to reduce regurgitant volume, LV volume, and wall stress (Otto & Bonow, 2009). However, in asymptomatic patients with severe AR and normal LV function, vasodilators failed to demonstrate any significant benefit, did not delay the need for surgery, did not reduce regurgitant volume, and had no beneficial effect on LV size or function (Evangelista et al., 2005).

As rats develop LV abnormalities in response to severe AR in a relatively short period (weeks) in contrast to humans (who can tolerate this condition for decades without apparent LV dysfunction), rats make an ideal model to investigate chronic AR (Magid et al., 1984).

Heart failure continues to be a major leading public health problem that is estimated to affect more than 26 million people worldwide; the incidence is steadily increasing, primarily owing to the aging of the population (Ambrosy et al., 2014). The progression of heart failure leads to myocardial contractility deficiency, eventually resulting in a decrease in cardiac output (CO). Although inotropic agents have been shown to improve cardiac contractility, their use has been associated with increased morbidity and mortality caused by intracellular calcium overload, which is associated with ventricular arrhythmia, atrial fibrillation, hypotension, induced myocardial ischemia, increased myocardial oxygen consumption, and direct myocyte toxicity (Tariq & Aronow, 2015; Teerlink et al., 2009). Omecamtiv mecarbil (OM), formerly known as CK-1827452, is a cardiac myosin activator that increases the proportion of myosin heads bound to actin, creating a force-producing state that is not associated with cytosolic calcium accumulation (Malik et al., 2011). As the total number of myosin heads bound to actin filaments increases, force production is boosted (Malik et al., 2011). As a result, OM prolongs the duration of total systole

by enhancing the rate of entry of myosin into the force-generating state, which implies increased formation of active cross-bridges, ultimately leading to stronger cardiac contractions (Liu et al., 2015).

OM increased systolic ejection time and cardiac myocyte fractional shortening in two experimental canine models of heart failure, with no significant increase in LV myocardial oxygen consumption or myocyte intracellular calcium (Shen et al., 2010). One of the main determinants of myocardial oxygen consumption is peak systolic wall stress (Hoffman & Buckberg, 2014). Resting LV myocardial oxygen consumption and wall stress also exhibit a linear relationship, in which doubling wall tension approximately doubles LV oxygen consumption (Strauer, 1979).

In our previous study (El Oumeiri et al., 2018), we showed that OM significantly decreased both LV end-systolic diameter (LVESD) and LV end-diastolic diameter (LVEDD) in rats with severe chronic AR. However, we lacked information on preload and afterload, and the anesthesia procedure included intraperitoneal ketamine. Ketamine has a cardiovascular effect resembling sympathetic nervous system stimulation, increasing heart rate and CO (Levänen et al., 1995). In addition, the number of animals in all groups was small, and AR was assessed subjectively using a 1 to 4 scale to classify the severity of regurgitation.

The present study aimed to evaluate the immediate (acute) effects of a single dose of OM on AR and cardiac contractile parameters in an experimental rat model of AR induced by a retrograde puncture. Our model combined the effects of pressure and volume overload on the LV. To determine whether OM affected LV wall stress, the experimental design incorporated both placebo and sham control groups.

## 2 | MATERIALS AND METHODS

### 2.1 | Experimental animals

The experimental protocol was approved by the Institutional Animal Care and Use Committee of the Free University of Brussels. Studies were conducted in accordance with the *Guide for the Care and Use of Laboratory Animals* published by the National Institutes of Health (NIH Publication No. 85-23; revised 1996). Forty male adult Wistar rats ( $486 \pm 49$  g body weight) were separated into two groups: sham intervention ( $n = 6$ ) or AR induction ( $n = 34$ ). Rats that survived AR induction or the acute phase ( $n = 18$ ) were randomized into the OM ( $n = 8$ ) or placebo ( $n = 10$ ) groups. Rats that underwent the sham intervention ( $n = 6$ ) also received OM and served as controls



to assess the effect of time and repeated measurements on the variables investigated in the study.

## 2.2 | Anesthesia and surgical procedure

Animals were anesthetized using 1.5% inhaled isoflurane. AR was induced by retrograde puncture of the aortic valve leaflet, as previously described (El Oumeiri et al., 2018). Heart rate (HR) and rhythm were monitored via limb leads throughout the procedure. The right internal carotid artery was surgically exposed and ligated distally; subsequently, a transverse arteriotomy was performed, through which a fixed-core wire guide (0.025 inch diameter; Cook Inc.) was advanced toward the aortic valve in a retrograde manner to tear the valve leaflets and induce AR. The following echocardiographic criteria after achieving a popping sensation at the time of surgery were used to include animals in the study: (1) a jet extent greater than 30% of the length of the LV, and (2) a color-Doppler ratio of regurgitant jet width to LV outflow tract diameter greater than 50% (Zoghbi et al., 2003). The six sham-operated animals underwent cannulation of the right carotid artery without aortic valve puncture. Animals were closely observed during the first hours and days after surgery for any sign of respiratory distress suggestive of acute heart failure. Pre- and post-surgery analgesia were administered.

## 2.3 | Cardiac measurements

Transthoracic 2D, M-mode, and Doppler echocardiography were performed under general anesthesia (1.5% isoflurane) using an ultrasound scanner (Vivid-E90, GE Healthcare) equipped with a 12-MHz phased-array transducer (GE 12S-D, GE Healthcare). Rats were placed in the right and left lateral recumbent positions, and electrocardiography was conducted via limb leads throughout the procedure. All measurements were made according to the recommendations of the Society of Echocardiography for human subjects (Zoghbi et al., 2003). Standard right parasternal (long- and short-axis) and left apical parasternal views were used for data acquisition. Fractional shortening (FS) was calculated using the formula  $FS = LVEDD - LVESD / LVEDD \times 100$ , in M-mode from an LV short-axis view at the level of the chordae tendineae using the following measured parameters: diastolic (d) and systolic (s) septal wall thickness (SWTd and SWTs, respectively), posterior wall thickness (PWTd and PWTs, respectively), and LV end-systolic and end-diastolic diameters (LVEDD and LVESD, respectively). Ejection fraction (EF) was derived using the Teicholz formula. Left ventricle mass was calculated using the American

Society of Echocardiography recommended formula:  $LV \text{ mass} = 0.8 \times \{1.04[(LVEDD + PWTd + SWTd)^3 - (LVEDD)^3]\} + 0.6 \text{ g}$ . The aortic diameter was measured from the right long-axis parasternal view. The aortic flow was measured from the left apical view to calculate forward stroke volume (SV) and CO, and to measure pre-ejection period (PEP: delay from Q wave of QRS to aortic opening; ms), LV ejection time (LVET: interval from beginning to termination of aortic flow; ms), and interbeat interval (RR; ms). Systolic time (ST; ms) was determined as PEP + LVET (ms), and diastolic time (ms) was calculated as RR interval – systolic time. We also calculated the PEP/LVET ratio, a more useful index of overall LV systolic performance (Lewis et al., 1977), which is better correlated with other LV performance measurements than either PEP or LVET alone and is considered independent of HR (Spodick et al., 1984). The severity of the regurgitated aortic jet was objectively evaluated by measuring the pressure half-time (PHT) of the AR jet using a continuous-wave Doppler. A PHT of <200 ms was considered indicative of severe AR. Relative wall thickness (RWT) was calculated using the formula  $RWT = 2 \cdot PWTd / LVEDD$ , where PWTd is the posterior wall thickness at end-diastole (mm).

## 2.4 | Calculation of wall stress variables

Wall stress was calculated based on Laplace's law ( $\sigma = P \times r / 2w$ , where  $\sigma$  is the wall stress,  $P$  is the left intraventricular pressure,  $r$  is the LV diameter, and  $w$  is the wall thickness.) Wall stress—the true measure of LV afterload—decreases during ejection and is twice as high in protosystole as in telesystole. The calculation of maximum stress ( $\sigma_{\max}$ ) must be performed at maximum systolic pressure using the telediastolic diameter, which is that of protosystole before it shortens during ejection as follows:  $\sigma_{\max} = (P_{\max} \cdot Dtd) / 2w$ , where  $P$  is the maximum systolic pressure,  $D$  is the LVEDD, and  $w$  is the end-diastolic wall thickness. End-systolic wall stress ( $\sigma_{\text{es}}$ ) is calculated using the formula  $\sigma_{\text{es}} = P_{\text{es}} \cdot Dts / 2w$ , where  $P_{\text{es}}$  is the end-systolic pressure,  $Dts$  is the LVESD, and  $w$  is the end-systolic wall thickness. Wall stress on diastole ( $\sigma_d$ ) was also calculated:  $\sigma_d = Pd \cdot Dtd / 2w$ , where  $Pd$  is the diastolic pressure.

## 2.5 | Invasive blood pressure measurement

Invasive arterial pressures were measured with a micro manometer (rodent catheter 1.6 F, Transonic Systems Inc.) inserted in the right common carotid artery before and after the induction of AR (only once in sham-operated

rats) and the left femoral artery for all rats before and after injection of OM or placebo (2 months after induction of AR). The micro manometer was connected to a data acquisition system (ADV500PV system, Transonic Systems Inc.).

## 2.6 | Experimental design

Doppler echocardiography was performed before AR induction (baseline) during surgery to confirm the presence and severity of AR. Doppler echocardiography was performed again 2 months after the induction of AR, both before and after the infusion of OM (1.2 mg/kg/h) or placebo (0.9% NaCl). In the treatment groups, animals received equal volumes (12 ml/kg) of placebo ( $n = 10$ ) or OM ( $n = 8$ ) employing femoral vein perfusion for 30 min. This procedure achieved a plasma concentration of nearly 400 ng of OM/ml in a previous study (Anderson et al., 2005). Doppler echocardiography was performed immediately after the 30-min infusion. All animals remained alive during these experimental sessions.

## 2.7 | Statistical analyses

Results are expressed as means  $\pm$  standard deviation (SD). Data were analyzed using a two-factor analysis of variance (ANOVA) for repeated measures. Inter-group differences were tested using two-way ANOVA. If the  $F$  ratio of the ANOVA reached the threshold  $p$ -value of  $<0.05$ , further comparisons were made using the parametric Student's  $t$  test. A  $p$ -value of  $<0.05$  was considered to be significant (SPSS 23.0, IBM Corp.).

## 3 | RESULTS

### 3.1 | LV and AR measurements

AR was achieved in all 34 rats, as confirmed by the presence of a regurgitant jet quantified as severe (PHT  $<200$  ms). Sixteen rats died during induction surgery or from congestive heart failure before the end of the 2-month follow-up and were thus excluded from the final analysis. After 2 months, AR (PHT  $<200$  ms) was confirmed, and the presence of volume overload and eccentric hypertrophy were established echocardiographically by significant increases in LVEDD, LVESD, and LV mass ( $n = 18$ , all  $p < 0.001$ , Figure 2). Load-dependent indices of LV systolic function (FS and EF) and RWT were significantly lower than baseline ( $p < 0.05$ ,  $n = 18$ ), whereas SV and CO were significantly higher than baseline

( $n = 18$ , both  $p < 0.001$ ). As expected, signs of AR were not present in the sham-operated rats ( $n = 6$ ), and thus no changes in LV functions or dimensions were observed in this group.

### 3.2 | Measures of wall stress and blood pressure

Diastolic arterial blood pressure was significantly lower after the induction of AR ( $n = 18$ ,  $p < 0.001$ ). End-systolic and maximum wall stress were significantly higher in all rats with AR after induction ( $n = 18$ ,  $p < 0.05$ ). We detected no changes in  $\sigma_{\max}$  or arterial blood pressure in sham-operated rats ( $n = 6$ ).

### 3.3 | Effects of placebo in rats with AR

Infusion with 0.9% NaCl (placebo group,  $n = 10$ ; Figure 1) affected some echocardiographic parameters in rats with AR. FS was significantly higher ( $p < 0.05$ ), whereas LVESD, LVESDD, and end-systolic wall stress were significantly lower ( $p < 0.05$ ). Hemodynamically, NaCl infusion significantly increased systolic and diastolic blood pressures ( $p < 0.05$ ), as well as PWTs and the PEP/LVET ratio ( $p < 0.05$ ).

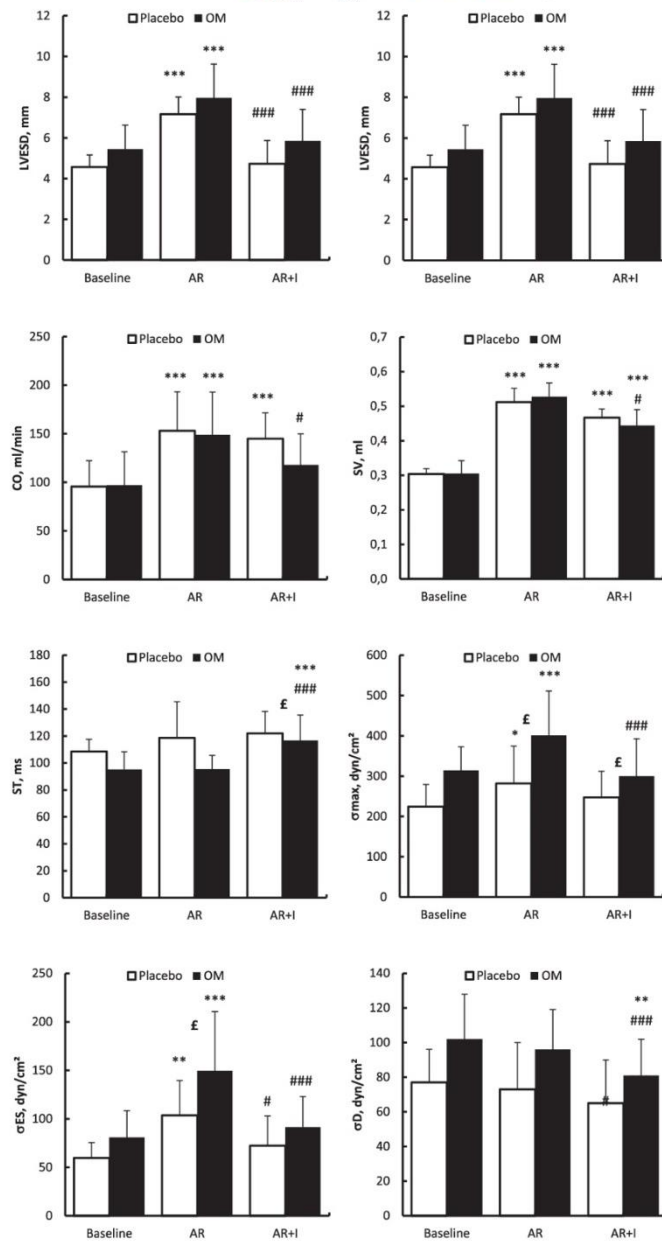
### 3.4 | Effects of OM in rats with AR

Infusion with OM (treatment group,  $n = 8$ ; Figure 1; supplement files) significantly increased FS, ST, and LVET ( $p < 0.05$ ) and significantly decreased LVEDD and LVESD ( $p < 0.05$ ). In addition, OM treatment resulted in a significant decrease in the wall stress parameters  $\sigma_{\max}$ ,  $\sigma_{es}$ , and  $\sigma_d$  ( $p < 0.05$ ). OM infusion also affected indices of global cardiac function, including significant decreases in SV and CO ( $p < 0.05$ ), but did not affect the severity of AR (PHT  $110 \pm 12$  ms vs.  $89 \pm 10$  ms before OM injection,  $P$  ns).

### 3.5 | Effects of OM compared with placebo in rats with AR

The effects of OM and placebo treatments in AR rats were compared by using two-way ANOVA (Figure 1, see supplement files). In the comparison of OM versus placebo, values for PEP ( $p < 0.01$ ), the PEP/LVET ratio ( $p < 0.001$ ), the ST/RR ratio ( $p < 0.01$ ), and SWTs ( $p < 0.01$ ) were lower in rats infused with OM than those in the placebo group. Similarly, diastolic time (DT) was greater in rats of the OM group than in rats of the

**FIGURE 1** Hemodynamic effects of aortic regurgitation (AR) induced in rats at baseline, 2 months after induction of AR (pre-infusion), and following infusion (I) of omecamtiv mecarbil (OM) or placebo (0.9% NaCl)<sup>1</sup>. Values are expressed as mean  $\pm$  SD. \* $p < 0.05$ ; \*\* $p < 0.01$ ; \*\*\* $p < 0.001$  (or other symbols; two-way analysis of variance). Comparisons: \* = within a group compared with baseline; # = within a group compared with 2 months (pre-infusion); £ = compared with placebo group at the same time point; # within the same group (placebo (n=10) or OM (n=8) before and after infusion, the 2 group had a AR; ### is  $p < 0.001$  (in the same group placebo after 2 months before and after infusion of placebo n=10, or for the OM group (n=8) after 2 months before and after OM infusion). CO, cardiac output; LVEDD, left ventricle end-diastolic diameter; LVESD, left ventricle end-systolic diameter; ST, systolic time; SV, stroke volume;  $\sigma$ , max wall stress;  $\sigma_{di}$ , diastolic wall stress;  $\sigma_{es}$ , end-systolic wall stress



placebo group ( $p < 0.05$ ). No other echocardiographic or hemodynamic parameters investigated in this study exhibited significant differences between the OM and placebo groups.

### 3.6 | Effects of OM in sham-operated rats

The effects of OM treatments in AR rats and sham-operated rats were compared by two-way ANOVA (see

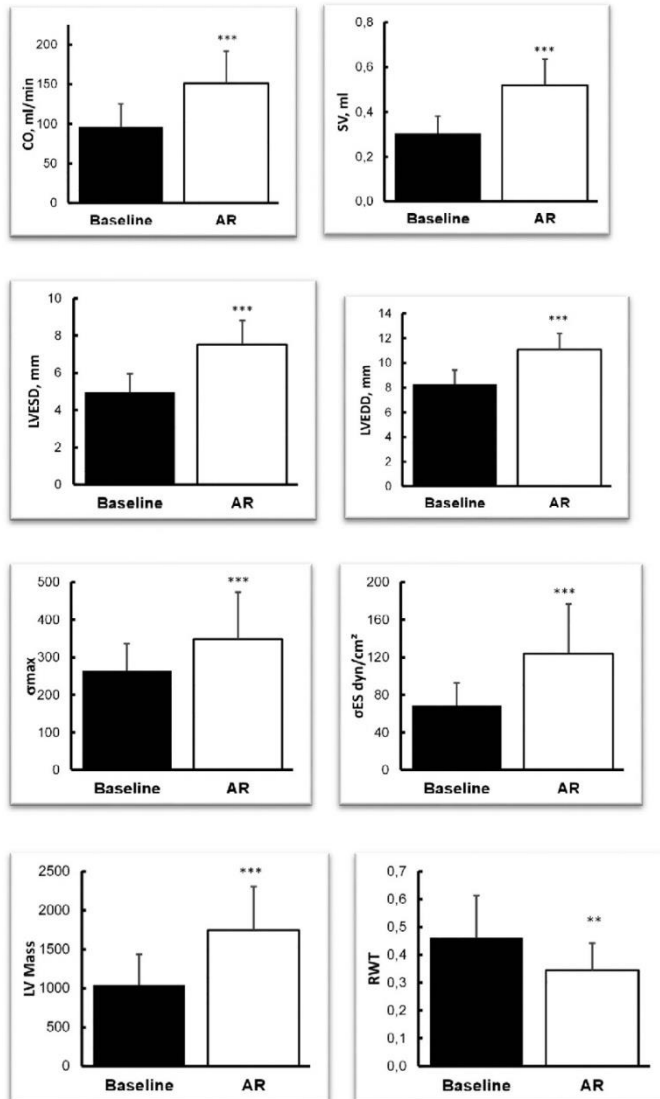


**FIGURE 2** Hemodynamic effects of aortic regurgitation (AR) induced in rats ( $n = 18$ ) at baseline and 2 months after induction of AR. Values are expressed as mean  $\pm$  SD. \* $p < 0.05$ ; \*\* $p < 0.01$ ; \*\*\* $p < 0.001$  (or other symbols; two-way analysis of variance). Comparisons: \* = within a group compared with baseline; \* between the same rats that had an AR 2 months before ( $n=18$ ), before AR and 2 months after induction of AR. CO, cardiac output; LVEDD, left ventricle end-diastolic diameter; LVESD, left ventricle end-systolic diameter; RWT, relative wall thickness; SV, stroke volume;  $\sigma$ , max wall stress;  $\sigma_d$ , diastolic wall stress;  $\sigma_{es}$ , end-systolic wall stress

supplement files). Infusion of OM in sham-operated rats ( $n = 6$ ) resulted in significant decreases in  $\sigma_d$ , the PEP/LVET ratio, and PEP (all  $p < 0.05$ ).

#### 4 | DISCUSSION

The main findings of our study are that OM decreased LV wall stress parameters associated with the prolongation of ejection time without improvement of indices of global

cardiac function (SV, CO), but with maintenance of baseline global cardiac function in rats with severe chronic AR.

##### 4.1 | Effect of AR on cardiac function and wall stress

Chronic severe AR imposes a combined volume and pressure overload on the LV. The volume overload is a consequence of the regurgitant volume itself (Bekeredjian &

Grayburn, 2005), whereas the pressure overload results from systolic hypertension, which occurs as a result of an increase in total aortic SV from both the regurgitant volume and the forward stroke volume that is ejected into the aorta during systole (Bekeredjian & Grayburn, 2005). This effect was observed in the 18 rats with successful induction of AR (Figure 2). In compensated severe AR, eccentric hypertrophy with combined concentric hypertrophy of the LV is an essential adaptive response to volume overload, which itself is a compensatory mechanism that permits the ventricle to normalize its afterload and maintain normal ejection performance (physiologic hypertrophy; Grossman, 1980). This effect was observed in our rat model, as demonstrated by an RWT value of  $0.34 \pm 0.02$  ( $n = 18$ ), with LV dilation, corresponding to physiologic hypertrophy (Gaasch et al., 2011), in agreement with the LV structural remodeling previously described (Gaasch et al., 2011) in humans. Sarcomeres are laid down in series, and myofibers are elongated (Ricci, 1982), and eccentric hypertrophy preserves LV diastolic compliance and increases LV mass, such that the volume/mass ratio is normal, and LVEF is maintained by increased preload (Bekeredjian & Grayburn, 2005). Again, these effects were observed in our model (Figure 2).

LV dilatation and systolic hypertension increase wall stress and volume/mass ratio. In the present study, LV wall stress was elevated in rats with AR, and EF was significantly lower than baseline, 2 months after the induction of AR (Figure 2). Taniguchi et al. (2000) reported an abnormal relationship between EF (depressed contractility) and LV wall stress in patients with chronic AR and advanced cellular hypertrophy which worsened with LV enlargement. Percy et al. (1993) addressed the prognostic significance of LV wall stress in asymptomatic patients with AR, and concluded that elevated wall stress in chronic AR predicts a faster deterioration of LV function. Greenberg et al. (1985) demonstrated associations between EF response and systolic wall stress and concluded that patients with EF decreased during exercise had elevated resting LV systolic wall stress. The groups studied had similar near-normal LV end-systolic dimensions and abnormal LV wall stress, suggesting that elevated wall stress in chronic AR predicts a poorer mechanical and clinical prognosis that may be independent of classical parameters such as LV dimensions and LV function.

#### 4.2 | Effect of OM on wall stress and AR

Our results showed that treatment with OM decreased maximum wall stress, end-systolic wall stress, and diastolic wall stress of the LV (Figure 1) in our rat model of AR. In our model, this effect was related to a decrease in LVEDD

and a decrease in average maximum systolic pressure. End-systolic wall stress was significantly lower ( $p < 0.05$ ) in the placebo group ( $n = 10$ ), but to a lesser extent than in the OM group ( $n = 8$ ;  $p < 0.001$ ). Furthermore, decreases in LVEDD and end-diastolic pressure following OM have been reported in animal models of ischemia (Bakkehaug et al., 2015; Rønning et al., 2018). Reducing ventricular wall stress is considered a cornerstone in treating heart failure (Yin, 1981). In its simplest form, as described by Laplace's law, ventricular wall stress is directly proportional to the diameter of the ventricle and ventricular pressure and is inversely proportional to the wall thickness of the ventricle. It is widely believed that increased ventricular wall stress is responsible for the adverse remodeling process that eventually leads to heart failure (Grossman, 1980). Increased wall stress is an independent predictor of subsequent LV remodeling (Hung et al., 2010). One of the main determinants of myocardial oxygen usage is peak systolic wall stress (Hoffman & Buckberg, 2014). Because the cavity decreases in size and the wall thickens during ejection, protosystolic stress is twice the telesystolic stress (Kolev et al., 1995). This variation is greater than that of the pressures during systole; therefore, peripheral vascular resistance overestimates the overload losses secondary to vasodilatation but underestimates increases caused by vasoconstriction (Lang et al., 1986).

In the present study, OM extended LVET and ST, as reported previously (Liu et al., 2015), without changes in DT. OM did not affect the severity of AR, as measured by AR PHT  $< 200$  ms. This finding agrees with the results of our previous study (El-Oumeiri et al., 2018). However, in our previous study, we subjectively graded the severity of the AR jet on a scale from 1 to 4, whereas in this study, we used an objective quantification of AR to measure the effect of OM on AR more precisely.

#### 4.3 | Effect of OM on cardiac function

OM decreased SV and CO without an effect on HR but with prolongation of LVET and ST (Tables S1–S3). In contrast, OM increased FS in a similar manner to classic inotropes by improved emptying in systole. Furthermore, we did not observe any SV, CO, or HR changes in our placebo group. The extended myocardial systole could have caused the reduced contractile efficiency observed in the OM group. The fact that LVEDD, and consequently the LV volume, decreased despite unchanged preload and HR suggests that OM induces myocardial constraint in late diastole. This is in line with a previous study that reported that OM slows relaxation and increases passive tension at rest in isolated rat cardiomyocytes (Nagy et al., 2015).

Shen et al. (2010) reported that OM significantly increases CO and SV. However, their study differed in several aspects from the present study. They used a canine model of ischemia, the animals were conscious, and the dose of OM and duration of infusion were different. All these factors could explain the difference in the effect of OM on cardiac function compared with our study. Nevertheless, OM significantly extended LVET in both studies.

Because our AR model did not exhibit characteristics of diastolic dysfunction, the interpretation that OM impairs diastolic performance warrants caution. The impairment of diastolic function by OM was reported by Rønning et al. (2018) in pigs with acute ischemic heart failure. OM failed to restore general pump indices such as SV, CO, and EF in the pig model. Likewise, they found no significant changes in SV and CO in the pig model of ischemia in response to OM treatment.

In our previous study (El Oumeiri et al., 2018), OM increased SV and CO in rats with AR. In that study, the animals were anesthetized with an intraperitoneal injection of ketamine/medetomidine. Ketamine is a dissociative anesthetic agent with a cardiovascular effect resembling sympathetic nervous system stimulation, increasing HR and CO (Levanen et al., 1995). Medetomidine improves muscle relaxation, potentiates the anesthetic action of ketamine, and compensates for the cardiac-stimulating effect of ketamine by decreasing HR and CO. Dexmedetomidine had no direct myocardial depressant effect in the rat heart in doses like those encountered in clinical conditions (Lee et al., 2017). Because the different animal groups were all anesthetized using the same regimen, the decrease in HR we observed can be attributed to OM in our previous study. However, we cannot predict whether this bradycardic effect of OM would also have occurred in conscious, non-sedated animals. In the current study, animals were anesthetized using 1.5% inhaled isoflurane. Current evidence suggests that isoflurane exerts a negative inotropic effect (Davies et al., 1999). This in contrast with the increase in SV during isoflurane anesthesia we observed in this study, possibly because the negative inotropic effects of isoflurane can be overridden by a decrease in systemic vascular resistance (Heerdt et al., 1998).

## 5 | STUDY LIMITATIONS

This study was performed with a limited number of rats with chronic AR and thus represented a narrow observational window into the natural course of this disease. Further investigations with a larger sample size will be necessary for a more robust evaluation, interpretation, and corroboration of our findings. We also did not assess whether OM has dose-dependent hemodynamic effects

in our model of AR. Another limitation is that, although measurements of RWT are applicable in human models, it is unclear whether the same is true of the rat model used in the present study.

## 6 | CONCLUSIONS

Our data demonstrate that OM significantly decreased LV wall stress in rats with induced chronic severe AR. In terms of cardiac function, we observed a decrease in SV and CO, but no inferior general pump indices or (in other words) baseline values of SV and CO. Although OM significantly increased the duration of LVET and ST, it did not affect the duration of DT or the severity of AR. The observed effects of OM in the current study reflect the acute (immediate) effect of a single dose; we did not evaluate effects in either the short or medium term.

## CONFLICT OF INTEREST

None declared.

## AUTHOR CONTRIBUTIONS

All experiments were conducted in the Physiology and Pharmacology Laboratory of the University of Brussels. BE conceived the study, participated in its design, carried out the experiments, performed the statistical analysis, and drafted the manuscript. KME conceived and coordinated the study, participated in its design, and carried out the echocardiography. FA and AH read the echocardiography. GH participated in the coordination of the study and carried out the experiments. PJ and CS provided technical assistance, performed the statistical analysis, and reviewed the manuscript. PVB and FV conceived the study and participated in the drafting of the manuscript. All authors read and approved the final manuscript.

## ORCID

Bachar El Oumeiri  <https://orcid.org/0000-0002-5955-0547>

## REFERENCES

- Ambrosy, A. P., Fonarow, G. C., Butler, J., Chioncel, O., Greene, S. J., Vaduganathan, M., Nodari, S., Lam, C. S. P., Sato, N., Shah, A. N., & Gheorghiade, M. (2014). The global health and economic burden of hospitalizations for heart failure: Lessons learned from hospitalized heart failure registries. *Journal of the American College of Cardiology*, 63(12), 1123–1133.
- Anderson, R. L., Sueoka, S. H., Rodriguez, H. M., Lee, K. H., Cox, D. R., Kawas, R., Morgan, B. P., Sakowicz, R., Morgans, D. J., Malik, F., & Elias, K. A. (2005). In vitro and in vivo efficacy of the cardiac myosin activator CK-1827452. *Molecular Biology of the Cell*, 16(abstract #1728). [https://cytokinetics.com/wp-content/uploads/2015/10/ASCB\\_1728.pdf](https://cytokinetics.com/wp-content/uploads/2015/10/ASCB_1728.pdf)

- Bakkehaug, P. J., Kildal, A. B., Engstad, E. T., Boardman, N., Næsheim, T., Rønning, L., Aasum, E., Larsen, T. S., Myrmet, T., & Jakob, O. (2015). How myosin activator omecamtiv mecarbil increases myocardial oxygen consumption and impairs cardiac efficiency mediated by resting myosin ATPase activity. *Circulation: Heart Failure*, 8(4), 766–775. <https://doi.org/10.1161/CIRCHEARTFAILURE.114.002152>
- Bekeredjian, R., & Grayburn, P. A. (2005). Valvular heart disease: Aortic regurgitation. *Circulation*, 112(1), 125–134. <https://doi.org/10.1161/CIRCULATIONAHA.104.488825>
- Carabello, B. A. (1990). Aortic regurgitation. A lesion with similarities to both aortic stenosis and mitral regurgitation. *Circulation*, 82(3), 1051–1053. <https://doi.org/10.1161/01.CIR.82.3.1051>
- Davies, L. A., Hamilton, D. L., Hopkins, P. M., Boyett, M. R., & Harrison, S. M. (1999). Concentration-dependent inotropic effects of halothane, isoflurane, and sevoflurane on rat ventricular myocytes. *British Journal of Anaesthesia*, 82(5), 723–730. <https://doi.org/10.1093/bja/82.5.723>
- El-Oumeiri, B., Mc Entee, K., Annoni, F., Herpain, A., Vanden Eynden, F., Jespers, P., Van Nooten, G., & Van de Borne, P. (2018). Effects of the cardiac myosin activator Omecamtiv-mecarbil on severe chronic aortic regurgitation in Wistar rats. *BMC Cardiovascular Disorders*, 18(1), 99. <https://doi.org/10.1186/s12872-018-0831-3>
- Evangelista, A., Tornos, P., Sambola, A., Permyer-Miralda, G., & Soler-Soler, J. (2005). Long-term vasodilator therapy in patients with severe aortic regurgitation. *New England Journal of Medicine*, 353(13), 1342–1349. <https://doi.org/10.1056/NEJMoA050666>
- Gaasch, W. H., & Zile, M. R. (2011). Left ventricular structural remodeling in health and disease: With special emphasis on volume, mass, and geometry. *Journal of the American College of Cardiology*, 58(17), 1733–1740. <https://doi.org/10.1016/j.jacc.2011.07.022>
- Greenberg, B., Massie, B., Thomas, D., Bristow, J. D., Cheitlin, M., Broudy, D., Szlachcic, J., & Krishnamurthy, G. (1985). Association between the exercise ejection fraction response and systolic wall stress in patients with chronic aortic insufficiency. *Circulation*, 71(3), 458–465. <https://doi.org/10.1161/01.CIR.71.3.458>
- Grossman, W. (1980). Cardiac hypertrophy: Useful adaptation or pathologic process. *American Journal of Medicine*, 69(4), 576–584. [https://doi.org/10.1016/0002-9343\(80\)90471-4](https://doi.org/10.1016/0002-9343(80)90471-4)
- Heerdt, P. M., Gandhi, C. D., & Dickstein, M. L. (1998). Disparity of isoflurane effects on left and right ventricular afterload and hydraulic power generation in swine. *Anesthesia and Analgesia*, 87, 511–521.
- Hoffman, J. E., & Buckberg, G. D. (2014). The myocardial oxygen supply: Demand index revisited. *Journal of the American Heart Association*, 3(1). <https://doi.org/10.1161/JAHA.113.000285>
- Hung, C. L., Verman, A., Uno, H., Shin, S. H., Bourgoun, M., Hassanein, A. H., McMurray, J. J., Velazquez, E. J., Kober, L., Pfeffer, M. A., & Solomon, S. D. (2010). VALIANT investigators. Longitudinal and circumferential strain rate, left ventricular remodeling, and prognosis after myocardial infarction. *Journal of the American College of Cardiology*, 56(22), 1812–1822.
- Kolev, N., Huemer, G., & Zimpfer, M. (1995). *Transesophageal echocardiography. A new monitoring technique*. Springer Verlag.
- Kumpuris, A. G., Quinones, M. A., Waggoner, A. D., Kanon, D. J., Nelson, J. G., & Miller, R. R. (1982). Importance of preoperative hypertrophy, wall stress and end-systolic dimension as echocardiographic predictors of normalization of left ventricular dilatation after valve replacement in chronic aortic insufficiency. *The American Journal of Cardiology*, 49(5), 1091–1100. [https://doi.org/10.1016/0002-9149\(82\)90032-7](https://doi.org/10.1016/0002-9149(82)90032-7)
- Lang, R. M., Borow, K. M., Neumann, A., & Janzen, D. (1986). Systemic vascular resistance: An unreliable index of left ventricular afterload. *Circulation*, 74, 1114–1118. <https://doi.org/10.1161/01.CIR.74.5.1114>
- Lee, K., Hwang, H. J., Kim, O. S., & Oh, Y. J. (2017). Assessment of dexmedetomidine effects on left ventricular function using pressure-volume loops in rats. *Journal of Anesthesia*, 31(1), 18–24. <https://doi.org/10.1007/s00540-016-2278-y>
- Levänen, J., Mäkelä, M. L., & Scheinin, H. (1995). Dexmedetomidine premedication attenuates ketamine-induced cardio-stimulatory effects and post-anesthetic delirium. *Anesthesiology*, 82(5), 1117–1125. <https://doi.org/10.1097/0000542-199505000-00005>
- Lewis, R. P., Rittogers, S. E., Froester, W. F., & Boudoulas, H. (1977). A critical review of the systolic time intervals. *Circulation*, 56(2), 146–158. <https://doi.org/10.1161/01.CIR.56.2.146>
- Liu, Y., White, H. D., Belknap, B., Winkelmann, D. A., & Forgacs, E. (2015). Omecamtiv mecarbil modulates the kinetic and motile properties of porcine  $\beta$ -cardiac myosin. *Biochemistry*, 54, 1963–1975. <https://doi.org/10.1021/bi5015166>
- Magid, N. M., Opio, G., Wallerson, D. C., Young, M. S., & Borer, J. S. (1994). Heart failure due to chronic experimental aortic regurgitation. *American Journal of Physiology-Heart and Circulatory Physiology*, 267(2 Pt 2), H556–H562. <https://doi.org/10.1152/ajpheart.1994.267.2.H556>
- Malik, F. I., Hartman, J. J., Elias, K. A., Morgan, B. P., Rodriguez, H., Brejc, K., Anderson, R. L., Sueoka, S. H., Lee, K. H., Finer, J. T., Sakowicz, R., Baliga, R., Cox, D. R., Garard, M., Godinez, G., Kawas, R., Kraynack, E., Lenzi, D., Lu, P. P., ... Morgans, D. J. (2011). Cardiac myosin activation: A potential therapeutic approach for systolic heart failure. *Science*, 331, 1439–1443. <https://doi.org/10.1126/science.1200113>
- Nagy, L., Kovács, Á., Bódi, B., Pásztor, E. T., Fülöp, G. Á., Tóth, A., Édes, I., & Papp, Z. (2015). The novel cardiac myosin activator omecamtiv mecarbil increases the calcium sensitivity of force production in isolated cardiomyocytes and skeletal muscle fibres of the rat. *British Journal of Pharmacology*, 172(18), 4506–4518. <https://doi.org/10.1111/bph.13235>
- Otto and Bonow. (2009). *Valvular heart disease* (3rd ed.). Saunders.
- Percy, R. F., Miller, A. B., & Conetta, D. A. (1993). Usefulness of left ventricular wall stress at rest and after exercise for outcome prediction in asymptomatic aortic regurgitation. *American Heart Journal*, 125(1), 151–155. [https://doi.org/10.1016/0002-8703\(93\)90068-K](https://doi.org/10.1016/0002-8703(93)90068-K)
- Ricci, D. R. (1982). Afterload mismatch and preload reserve in chronic aortic regurgitation. *Circulation*, 66(4), 826–834. <https://doi.org/10.1161/01.CIR.66.4.826>
- Rønning, L., Bakkehaug, J. P., Rodland, L., Kildal, A. B., Myrmet, T., & How, O. J. (2018). Opposite diastolic effects of omecamtiv mecarbil versus dobutamine and ivabradine co-treatment in pigs with acute ischemic heart failure. *Physiological Reports*, 6(19). <https://doi.org/10.14814/phy2.13879>
- Shen, Y., Malik, F. I., Zhao, X., Depre, C., Dhar, S. K., Abarzúa, P., Morgans, D. J., & Vatner, S. F. (2010). Improvement of cardiac function by a cardiac myosin activator in conscious

- dogs with systolic heart failure. *Circulation: Heart Failure*, 3, 522–527. <https://doi.org/10.1161/CIRCHEARTF.A1LURE.109.930321>
- Singh, J. P., Evans, J. C., Levy, D., Larson, M. G., Freed, L. A., Fuller, D. L., Lehman, B., & Benjamin, E. J. (1999). Prevalence and clinical determinants of mitral, tricuspid, and aortic regurgitation (the Framingham Heart Study). *American Journal of Cardiology*, 83(6), 897–902. [https://doi.org/10.1016/S0002-9149\(98\)01064-9](https://doi.org/10.1016/S0002-9149(98)01064-9)
- Spodick, D. H., Doi, Y. L., Bishop, R. L., & Hashimoto, T. (1984). Systolic time intervals reconsidered. *The American Journal of Cardiology*, 53(11), 1667–1670. [https://doi.org/10.1016/0002-9149\(84\)90599-X](https://doi.org/10.1016/0002-9149(84)90599-X)
- Strauer, B.-E. (1979). Myocardial oxygen consumption in chronic heart disease: Role of wall stress, hypertrophy and coronary reserve. *American Journal of Cardiology*, 44, 730–740. [https://doi.org/10.1016/0002-9149\(79\)90295-9](https://doi.org/10.1016/0002-9149(79)90295-9)
- Taniguchi, K., Kawamaoto, T., Kuki, S., Masai, T., Mitsuno, M., Nakano, S., Kawashima, Y., & Matsuda, H. (2000). Left ventricular myocardial remodeling and contractile state in chronic aortic regurgitation. *Clinical Cardiology*, 23(8), 608–614. <https://doi.org/10.1002/clc.4960230812>
- Tariq, S., & Aronow, W. S. (2015). Use of inotropic agents in treatment of systolic heart failure. *International Journal of Molecular Sciences*, 16, 29060–29068. <https://doi.org/10.3390/ijms161226147>
- Teerlink, J. R., Metra, M., Zacà, V., Sabbah, H. N., Cotter, G., Gheorghide, M., & Cas, L. D. (2009). Agents with inotropic properties for the management of acute heart failure syndromes. Traditional agents and beyond. *Heart Failure Reviews*, 14, 243–253. <https://doi.org/10.1007/s10741-009-9153-y>
- Yin, F. C. (1981). Ventricular wall stress. *Circulation Research*, 49(4), 829–842.
- Zoghbi, W. A., Enriquez-Sarano, M., Foster, E., Grayburn, P. A., Kraft, C. D., Levine, R. A., Nihoyannopoulos, P., Otto, C. M., Quinones, M. A., Rakowski, H., Stewart, W. J., Waggoner, A., & Weissman, N. J. (2003). American Society of Echocardiography. Recommendations for evaluation of the severity of native valvular regurgitation with two-dimensional and Doppler echocardiography. *Journal of the American Society of Echocardiography*, 16(7), 777–802. [https://doi.org/10.1016/S0894-7317\(03\)00335-3](https://doi.org/10.1016/S0894-7317(03)00335-3)

## SUPPORTING INFORMATION

Additional supporting information may be found online in the Supporting Information section.

**How to cite this article:** El Oumeiri, B., van de Borne, P., Hubesch, G., Herpain, A., Annoni, F., Jespers, P., Stefanidis, C., Mc Entee, K., & Vanden Eynden, F. (2021). The myosin activator omecamtiv mecarbil improves wall stress in a rat model of chronic aortic regurgitation. *Physiological Reports*, 9, e14988. <https://doi.org/10.14814/phy2.14988>



Bachar El Oumeiri\*, Philippe van de Borne, Géraldine Hubesch, Pascale Jespers, Laurence Dewachter, Constantin Stefanidis, Kathleen Mc Entee and Frédéric Vanden Eynden

## Detection of soluble suppression of tumorigenicity 2 and N-terminal B-type natriuretic peptide in a rat model of aortic regurgitation: differential responses to omecamtiv mecarbil

<https://doi.org/10.1515/jbcpp-2022-0215>

Received August 5, 2022; accepted September 21, 2022;  
published online October 10, 2022

### Abstract

**Objectives:** Both N-terminal fragment of B-type natriuretic peptide (NT-proBNP) and soluble isoform of ST2 (sST2) have been identified as biomarkers of heart failure. We evaluated the plasma levels of NT-proBNP and sST2 in a rat model of severe aortic valve regurgitation (AR) and correlated these findings with echocardiographic measurements. We also examined the impact of omecamtiv mecarbil (OM) on these parameters.

**Methods:** The plasma levels of NT-proBNP and sST2 were measured in 18 rats both before and 2 months after surgical induction of AR, and at these same time points, in six rats assigned to a sham-procedure control group. Plasma biomarkers were then measured again after infusion of OM or placebo in rats with AR (n=8 and 10, respectively) and OM alone in the sham control rats (n=6). Echocardiographic measurements were collected before and 2 months after induction of AR.

**Results:** Our results revealed increased levels of plasma NT-proBNP ( $219 \pm 34$  pg/mL vs.  $429 \pm 374$  pg/mL;  $p < 0.001$ ) in rats with AR at day 7 after infusion of placebo, whereas plasma levels of sST2 were higher in this cohort after infusion of either OM or placebo. We identified a significant positive correlation between plasma sST2 with posterior

wall thickness in diastole ( $r = 0.34$ ,  $p < 0.05$ ) and total body weight ( $r = 0.45$ ,  $p < 0.01$ ) in rats with surgically induced AR. **Conclusions:** Because sST2 increased markedly, whereas NT-proBNP remained unchanged, when OM was administered, we hypothesize that sST2 has a distinct capability to detect deleterious effects of passive muscle tension, not reliably assessed by NT-proBNP, in the setting of AR.

**Keywords:** aortic regurgitation; biomarkers; heart failure; omecamtiv mecarbil; overload.

### Introduction

First described in 1989 [1], the soluble isoform of suppression of tumorigenicity 2 (ST2) has been identified as a biomarker that can be used to monitor the progression and prognosis of acute and chronic heart failure (HF) [2]. ST2 is a member of the interleukin (IL)-1 receptor family and is the major receptor for IL-33, a proinflammatory cytokine that is secreted by numerous cells and cell types in response to damage [3] and is part of the cardioprotective signaling system. IL-33 binds to membrane-localized ST2 and exerts both antihypertrophic and antifibrotic effects. The soluble isoform of ST2 (sST2) can also interact with IL-33 and thereby, inhibit its cardioprotective effects [4]. Cardiac fibroblasts and cardiomyocytes release sST2 in response to stress and overload; the circulating levels of this protein reflect the degree of myocardial stress, ventricular remodeling, and fibrosis [5]. Interestingly, the main source of sST2 in HF may be the vascular endothelium rather than myocardial cells [6].

By contrast, a B-type natriuretic peptide (BNP) and its N-terminal fragment (NT-proBNP) are neurohormones synthesized by the ventricular myocardium. Increases in ventricular wall stress and myocardial hypertrophy in states of pressure and/or volume overload signal the release of these peptides [7]. Plasma BNP levels have been incorporated into clinical practice for prognostic stratification and management of HF [8]. Circulating levels of sST2

\*Corresponding author: Bachar El Oumeiri, Department of Cardiac Surgery, ULB Hôpital Universitaire Erasme, Route de Lennik, 808, Brussels, Belgium, E-mail: Bachar.el.oumeiri@erasme.ulb.ac.be

Philippe van de Borne, Department of Cardiology, ULB Erasme University Hospital, Brussels, Belgium

Géraldine Hubesch, Pascale Jespers, Laurence Dewachter and Kathleen Mc Entee, Laboratory of Physiology and Pharmacology, ULB, Brussels, Belgium

Constantin Stefanidis and Frédéric Vanden Eynden, Department of Cardiac Surgery, Université Libre de Bruxelles (ULB) Erasme University Hospital, Brussels, Belgium

serve as an independent predictor of this condition that can be added to those determined for BNP [9]. Omecamtiv mecarbil (OM) is an inotropic drug targeting sacromeres [10], binds specifically to the catalytic S1 domain of cardiac myosin, and thus has no significant impact on the forms of myosin found in smooth or skeletal muscle [10]. Mechanistically, OM activates cardiac myosin and accelerates the hydrolysis of ATP, thereby increasing the binding to actin and enhancing force generation and the strength of cardiac contractions [10]. In an experimental model of canine HF, the administration of OM increased the systolic ejection time, cardiac myocyte fractional shortening (FS), stroke volume (SV), and cardiac output (CO) and reduced left ventricular (LV) end-diastolic pressure and peripheral vascular resistance [11].

Aortic valve regurgitation (AR) is a common heart disease; chronic severe AR imposes a combined volume and pressure overload; and myocardial remodeling in AR leads to an alteration of LV function and wall stress.

Effects of AR on sST2 and NT-proBNP are unknown in rodents, and those of OM-mediated cardiac contraction strength increases on these parameters. We tested the hypothesis that severe chronic AR increases NT-proBNP and sST2 in rats in relation to changes in LV morphology and function. In addition, we anticipated that OM administration in AR could exert differential effects on sST2 and NT-proBNP, given the importance of myocardial stress in sST2 release.

## Methods

### Animals

The experimental protocol was approved by the Institutional Animal Care and Use Committee of the "Université Libre de Bruxelles". Studies were conducted in accordance with the Guide for the Care and Use of Laboratory Animals published by the National Institutes of Health (NIH Publication No. 85-23; revised 1996). Our study included 24 male adult Wistar rats ( $482 \pm 57$  g body weight). Six rats were assigned to the sham intervention group and 18 rats underwent the induction of AR. The 18 rats that were subjected to AR induction were divided at random into the OM (n=8) or placebo, a physiologic saline solution (0.9% NaCl), (n=10) treatment groups. AR was induced under general anesthesia (1.5% inhaled isoflurane) by retrograde puncture of the aortic valve leaflet, as previously described [12]. The six rats assigned to the sham (control) group underwent cannulation of the right carotid artery under general anesthesia without aortic valve puncture. Heart rate and rhythm were monitored via limb leads throughout the procedure. Invasive arterial pressures were measured with a micro-manometer (rodent catheter 1.6 F, Transonic Systems BV, Elstree, the Netherlands) inserted in the right common carotid artery. The clinical condition of each rat was monitored daily throughout the experiment with a particular focus on the respiratory function.

### Echocardiography

All rats were assessed by echocardiography performed by experienced cardiologists who were blinded to the group assignments and treatments. Transthoracic 2D, M-mode, and Doppler echocardiography were performed under general anesthesia (1.5% isoflurane) using an ultrasound scanner (Vivid-E90, GE Healthcare, Wauwatosa, WI, USA) equipped with a 12-MHz phased-array transducer (GE 12S-D, GE Healthcare). Echocardiographic measurements were obtained according to the American Society of Echocardiography guidelines [13, 14]. Standard right parasternal (long and short axis) and left apical parasternal views were used for data acquisition. FS was calculated using the formula  $FS = (LV \text{ end-diastolic diameter [LVEDD]} - LV \text{ end-systolic diameter [LVESD]}) / LVEDD \times 100$  in M-mode from a short-axis view of the LV at the level of the chordae tendineae using measured parameters including (a) diastolic (d) and systolic (s) septal wall thickness (SWTd and SWTs, respectively), (b) posterior wall thickness (PWTd and PWTs, respectively), and (c) LVEDD and LVESD, as defined above. Ejection fraction (EF) was derived using the Teicholz formula. LV mass was calculated using the formula recommended by the American Society of Echocardiography, i.e.,  $LV \text{ mass} = 0.8 \times [1.04 \{ (LVEDD + PWTd + SWTd)^3 - (LVESD)^3 \}] + 0.6 \text{ g}$ . The aortic diameter was measured from the right long-axis parasternal view. The aortic flow was measured from the left apical view to calculate the forward SV and CO. A pressure half-time (PHT) of <200 ms was considered to be indicative of severe AR. The relative wall thickness (RWT) was calculated using the formula  $RWT = 2 \times PWTd / LVEDD$ , with PWTd measured at end-diastole (in mm).

### Experimental design

Doppler echocardiography was performed before the induction of AR (baseline) and during the surgical procedure to confirm the presence and severity of the lesion. It was performed again 60 days after the experimental induction of AR in these rats. Rats with AR in the OM treatment (n=8) and placebo, a physiologic saline solution, (0.9% NaCl) (n=10) groups received equal volumes (12 mL/kg body weight) of OM (1.2 mg/kg/h) or placebo, respectively, via a 30 min infusion through the femoral vein. Rats that underwent the sham intervention (n=6) received the same dose of OM.

### Plasma levels of sST2 and NT-proBNP

Blood samples were obtained from each rat by venipuncture under general anesthesia (1.5% inhaled isoflurane) on the day of the surgery, immediately before (baseline), and 2 months after the induction of AR (or sham procedure, i.e., before infusion of OM or placebo), and 1, 2, and 7 days thereafter. The samples were collected into vacuum blood collection tubes (BD Vacutainer, Plymouth, UK) with ethylenediaminetetraacetic acid as the anticoagulant. The tubes were centrifuged immediately after collection at 3,000 rpm and 4 °C for 15 min to obtain plasma, which was separated in multiple aliquots and stored at -80 °C until analysis. The plasma levels of sST2 were measured using a rat ST2 ELISA Kit (MYBIOSOURCE, San Diego, CA, USA). The detection range for sST2 assay kit was 62.5 pg/mL–2000 pg/mL. The plasma levels of NT-proBNP were measured using a rat NT-proBNP ELISA Kit (MYBIOSOURCE, San Diego, CA, USA). The plasma levels of sST2 and NT-proBNP were measured using

electrochemiluminescence immunoassay GLOMAX multidetection system (Promega Corporation, Madison, WI, USA). The lower limit of detection for the NT-proBNP assay kit was 5 pg/mL, with a functional sensitivity of <50 pg/mL, and a working range (imprecision profile  $\leq 10\%$  coefficient of variation) that extended to ~35,000 pg/mL. The assays were carried out as per the manufacturer's instructions. The results were presented as the mean value of duplicated experiments. Laboratory technicians were blinded as to the specific characteristics of each sample.

### Statistical analysis

Results are presented as means  $\pm$  standard deviation (SD). Data were analyzed using a two-factor analysis of variance (ANOVA) for repeated measures. Intergroup differences were tested using a two-way ANOVA. If the F ratio of the ANOVA reached the threshold p-value of <0.05, further comparisons were made using the parametric Student's t-test. A p-value of <0.05 was considered to be significant (SPSS 23.0, IBM Corp., Armonk, NY). Correlations were analyzed parametrically by Pearson's rank correlation.

## Results

### Impact of surgically induced AR on echocardiographic findings

The impact of surgically induced AR was evaluated 60 days after the completion of the procedure. Values obtained from these rats are shown in Table 1. Our findings were consistent with the diagnosis of severe AR (e.g., PHT <200 ms) in each of the 18 rats that underwent this procedure. By contrast, no AR was detected in the six rats in the sham control group.

### Plasma NT-proBNP levels detected in response to surgically induced AR

The baseline levels of plasma NT-proBNP were  $244 \pm 48$  pg/mL in the 18 rats that were designated to undergo surgical induction of AR. About 60 days after the induction of AR, the plasma levels of NT-proBNP were not significantly different, i.e.,  $231 \pm 35$  pg/mL in this experimental cohort (Figure 1). We also detected no significant differences in plasma NT-proBNP levels among the six rats in the sham control group ( $235 \pm 37$  pg/mL at baseline vs.  $280 \pm 66$  pg/mL measured 60 days later). We identified no correlations between plasma NT-proBNP levels and echocardiographic parameters, blood pressure, or body weight.

**Table 1:** Echocardiographic measurements in rats (n=18) at baseline and 60 days after induction of AR. Correlations of plasma NT-proBNP and sST2 levels with echocardiographic variables and invasive arterial pressure measurements at baseline and 2 months (60 days) after the induction of AR.

Parameter <sup>d</sup>	Baseline	2 Months	r (NT-proBNP)	r (sST2)
FS, %	40 $\pm$ 6	32 $\pm$ 7 <sup>c</sup>	0.014	0.12
EF, %	75 $\pm$ 10	64 $\pm$ 12 <sup>c</sup>	0.08	0.13
SWTs, mm	2.72 $\pm$ 0.57	2.64 $\pm$ 0.59	0.017	0.04
SWTd, mm	1.94 $\pm$ 0.53	2.11 $\pm$ 0.64	0.08	-0.065
LVESD, mm	5.0 $\pm$ 1.0	7.5 $\pm$ 1.3 <sup>c</sup>	-0.02	-0.06
LVEDD, mm	8.3 $\pm$ 1.1	11.1 $\pm$ 1.3 <sup>c</sup>	-0.033	-0.028
HR, BPM	309 $\pm$ 50	291 $\pm$ 43	-0.096	-0.14
LVOT, mm	2.48 $\pm$ 0.18	2.76 $\pm$ 0.18 <sup>c</sup>	-0.14	0.12
PWTs, mm	2.86 $\pm$ 0.46	2.87 $\pm$ 0.69	-0.083	0.21
PWTd, mm	1.85 $\pm$ 0.45	1.87 $\pm$ 0.41	0.17	0.34 <sup>a</sup>
PEP, ms	24 $\pm$ 9	23 $\pm$ 13	0.014	0.08
LVET, ms	78 $\pm$ 5	86 $\pm$ 8	0.08	0.2
ST, ms	103 $\pm$ 13	108 $\pm$ 17	0.05	0.017
DT, ms	99 $\pm$ 28	101 $\pm$ 30	0.06	0.1
RR, ms	201 $\pm$ 30	208 $\pm$ 28	0.08	0.12
PEP/LVET	0.30 $\pm$ 0.10	0.26 $\pm$ 0.15	-0.25	0.11
ST/RR	0.53 $\pm$ 0.11	0.52 $\pm$ 0.10	0.03	-0.08
ARPht, ms		91 $\pm$ 25		
SV, mL	0.30 $\pm$ 0.08	0.52 $\pm$ 0.12 <sup>c</sup>	-0.1	0.03
CO, mL/min	96 $\pm$ 29	151 $\pm$ 41 <sup>c</sup>	-0.08	0.02
LVOT VTI, mm	65 $\pm$ 13	87 $\pm$ 15 <sup>c</sup>	-0.081	-0.03
BP sys, mmHg	116 $\pm$ 6	122 $\pm$ 15	-0.09	-0.05
BP dia, mmHg	78 $\pm$ 7	60 $\pm$ 10 <sup>c</sup>	0.05	-0.12
Weight, g	486 $\pm$ 76	562 $\pm$ 66 <sup>c</sup>	-0.004	0.45 <sup>b</sup>
LV mass	1,042 $\pm$ 394	1,747 $\pm$ 558 <sup>c</sup>	0.047	0.02
$\sigma$ d, dyn/cm <sup>2</sup>	88 $\pm$ 25	87 $\pm$ 30	-0.06	0.18
$\sigma$ max, dyn/cm <sup>2</sup>	264 $\pm$ 72	348 $\pm$ 125 <sup>c</sup>	-0.15	-0.014
$\sigma$ Es, dyn/cm <sup>2</sup>	69 $\pm$ 24	124 $\pm$ 52 <sup>c</sup>	-0.02	-0.02
RWT	0.46 $\pm$ 0.15	0.34 $\pm$ 0.10 <sup>c</sup>	0.08	0.24

Values presented are means  $\pm$  SD; <sup>a</sup>p<0.05; <sup>b</sup>p<0.01; <sup>c</sup>p<0.001; <sup>d</sup>FS, fractional shortening; EF, ejection fraction; SWTs, septal wall thickness in systole; SWTd, septal wall thickness in diastole; LVESD, left ventricle end-systolic diameter; LVEDD, left ventricle end-diastolic diameter; HR, heart rate; LVOT, left ventricle outflow tract diameter; PWTs, posterior wall thickness in systole; PWTd, posterior wall thickness in diastole; PEP, pre-ejection period; LVET, left ventricular ejection time; ST, systolic time; DT, diastolic time; RR, interval between successive R waves; ARPht, aortic regurgitation pressure half-time; SV, stroke volume; CO, cardiac output; VTI, velocity-time integral; BP, blood pressure;  $\sigma$ , wall stress;  $\sigma$ max, maximum wall stress;  $\sigma$ d, end-diastolic wall stress;  $\sigma$ Es, end-systolic wall stress; RWT, relative wall thickness.

### Plasma NT-proBNP levels detected in response to administration of OM or placebo

The plasma NT-proBNP levels were measured on day 0 as well as on days 1, 2, and 7 after OM or placebo treatment (i.e., days 60, 61, 62, and 67 post-procedure) of rats with

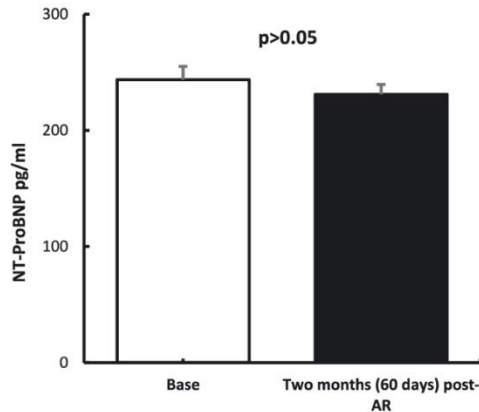


**Figure 1:** Plasma NT-proBNP levels in adult male rats (n=18) at baseline and 60 days after induction of AR (day 60). Values shown (pg/mL) are means  $\pm$  SDs.

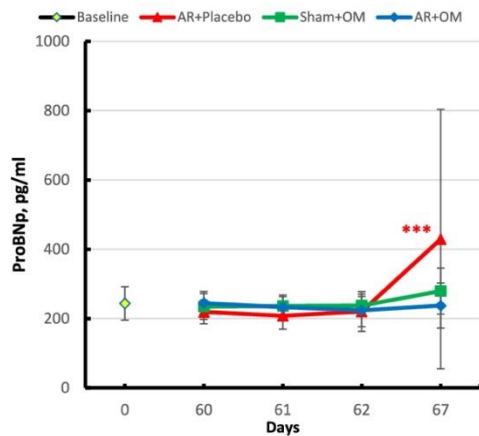


**Figure 2:** Plasma NT-proBNP levels. Shown are values at baseline (day 0) and at days 60, 61, 62, and 67 after induction of AR or sham procedure in response to administration of OM or placebo in rats with AR (n=8 or 10, respectively) and OM infusion only in rats in the sham control group (n=6). Values shown are means  $\pm$  SDs; \*\*\*p<0.001.

experimentally induced AR and sham control rats treated with OM (Figure 2). Interestingly, the plasma NT-proBNP levels increased significantly in the rats with surgically induced AR on day 7 after infusion of placebo ( $219 \pm 34$  pg/mL

on day 0 vs.  $429 \pm 374$  pg/mL on day 7; p<0.001). We also observed significant increases in plasma NT-proBNP when comparing levels detected on day 1 and day 2 vs. day 7 ( $208 \pm 39$  pg/mL and  $220 \pm 57$  pg/mL, respectively vs.  $429 \pm 374$  pg/mL on day 7; p<0.001). We observed no significant changes when comparing levels detected on days 0, 1, and 2 (days 60, 61, and 62 post-procedure) to one another. Likewise, we observed no significant changes in plasma levels of NT-proBNP in either the sham (n=6) or surgically induced AR group (n=8) when comparing levels detected at day 0 to those on 1, 2, and 7 after infusion with OM.

### Plasma sST2 levels detected in rats with surgically induced AR

As shown in Figure 3, we detected no significant differences in plasma sST2 in rats when comparing levels detected before and 2 months after surgical induction of AR ( $583 \pm 514$  pg/mL vs.  $543 \pm 340$  pg/mL). We also detected no significant changes in the levels of plasma sST2 in rats in the sham group at these time points. However, we did identify significant correlations between plasma levels of sST2 and PWTd as determined by echocardiography ( $r=0.34$ , p<0.05). We also identified a significant correlation between plasma sST2 and body weight ( $r=0.45$ , p<0.01), as shown in Figure 4.

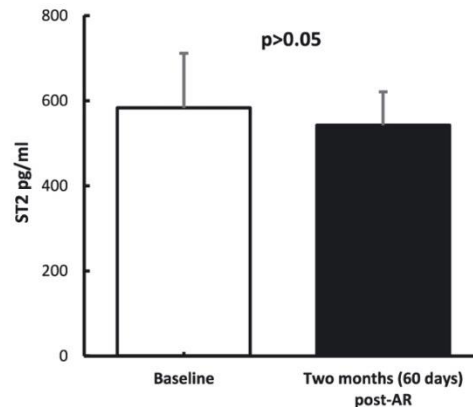


**Figure 3:** Plasma sST2 levels in adult male rats (n=18) at baseline and 60 days after the induction of AR. Values shown (pg/mL) are means  $\pm$  SDs.

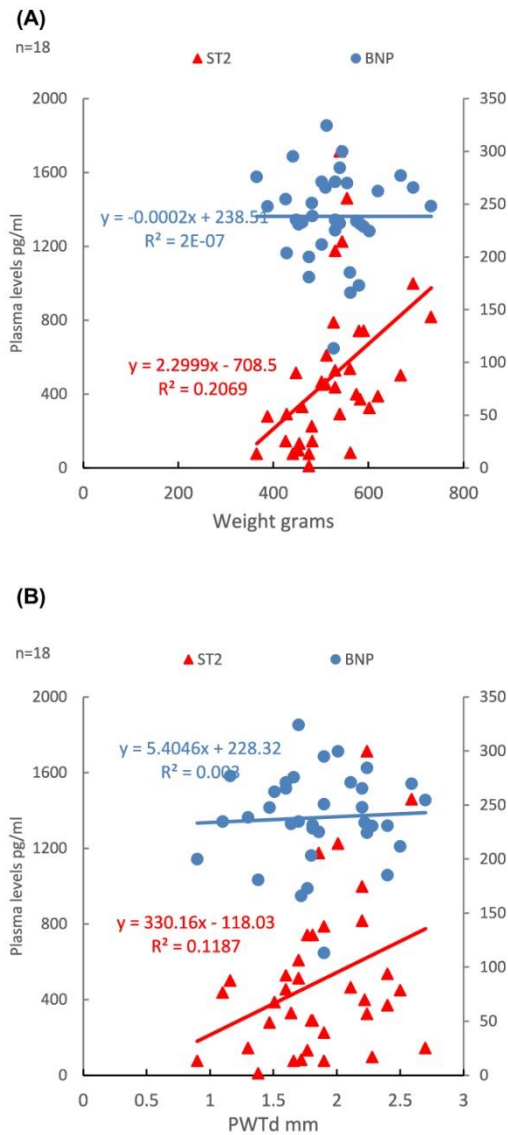


**Figure 4:** (A) Correlations between plasma NT-proBNP and sST2 levels and body weight (n=18 rats) at baseline and 60 days after the induction of AR (p<0.01); (B) correlations between plasma NT-proBNP and sST2 levels and PWTd (n=18 rats) at baseline and 60 days after the induction of AR; \*p<0.05.

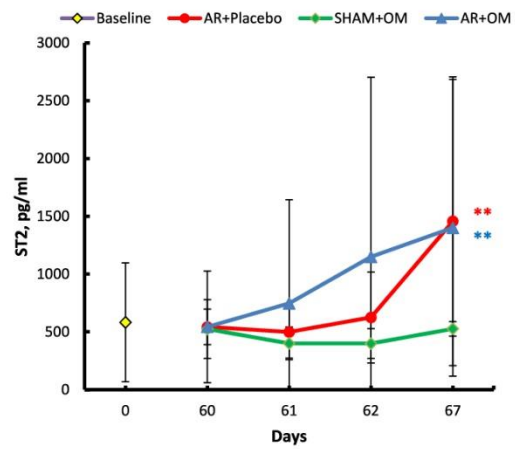


**Figure 5:** Plasma sST2 levels. Shown are values at baseline (day 0) and at days 60, 61, 62, and 67 after induction of AR or sham procedure in response to administration of OM or placebo in rats with AR (n=8 or 10, respectively) and OM infusion only in rats in the sham control group (n=6). Values shown are means  $\pm$  SDs; \*\*p<0.01.

### Plasma sST2 levels detected in response to administration of OM or placebo

The plasma sST2 levels measured on day 0 and days 1, 2, and 7 after OM or placebo treatment (i.e., days 60, 61, 62, and 67 post-procedure) of rats with experimentally induced AR and sham control rats treated with OM were assessed (Figure 5). The plasma sST2 levels increased significantly on day 7 when compared to that on day 0 in rats with AR after infusion of placebo (543  $\pm$  154 pg/mL vs. 1,457  $\pm$  1,248 pg/mL, p<0.01). Significant increases in plasma sST2 were also observed when comparing results obtained on day 1 (day 61) and day 2 (day 62) vs. day 7 (day 67; 498  $\pm$  225 pg/mL and 625  $\pm$  393 pg/mL, respectively, vs. 1,457  $\pm$  1,248 pg/mL, p<0.01). Among the rats with AR who were treated with OM, we detected significant increases in sST2 on day 7 after the infusion (543  $\pm$  483 pg/mL at day 0 vs. 1,401  $\pm$  1,284 pg/mL, p<0.01). However, we observed no significant differences in plasma sST2 when comparing levels detected on days 1 and 2 vs. day 7. No significant differences in plasma sST2 levels were detected in any of these comparisons in the sham group.

## Discussion

Our findings included several notable results. First, contrary to our initial hypothesis and despite the severity of cardiac dysfunction revealed by the echocardiographic findings (particularly, those documenting changes in LV parameters), we detected no significant changes in plasma levels of NT-proBNP at 2 months after surgical induction of AR when compared to that in baseline. As might be anticipated from these results, we detected no significant correlations between echocardiographic parameters and plasma NT-proBNP levels. As one explanation for this finding, we consider the possibility that compensatory mechanisms might develop in the LV in response to chronic severe AR. For example, the LV can adapt to the volume overload by developing eccentric hypertrophy and increased mass. In this situation, the LV volume/mass ratio remains within normal limits. Likewise, the LVEF is maintained by increased preload, and, despite an increase in the end-systolic diameter and pressure early in the course of the disease, the end-systolic wall stress is maintained within the normal range by a compensatory increase in wall thickness [15]. In a previous study, Song et al. [16] reported that NT-proBNP levels may reflect time-dependent structural and/or functional changes in the LV. Similarly, Weber and colleagues [17] found that NT-proBNP levels were associated with clinical symptoms in patients with chronic AR, notably with dyspnea. Interestingly, none of the rats in our study developed dyspnea. Another possible explanation considers the long time span between the induction of AR and the first biochemical assessment. Given the biological half-life of NT-proBNP, the plasma levels detected at 2 months after induction of AR may be significantly influenced by the number of cardiomyocytes available for and engaged in its production.

It is unlikely that the significant increase in NT-proBNP in the rats with AR treated with a placebo infusion can be explained by an increase in wall stress as a result of volume overload *per se* because the two groups of rats (AR and sham) that were treated with OM received the same volume of liquid, yet no modification of the plasma NT-proBNP levels were observed in the latter group. However, the volume overload not counteracted by concomitant OM administration in the presence of AR could explain this observation. This result is consistent with an OM-mediated reduction in myocardial wall stress in AR, as reported by a previous study [18]. Of note, NT-proBNP expression is promoted not only by mechanical stretch, but also by proinflammatory, oxidative, and trophic stimuli [19].

Our results also revealed that plasma sST2 levels underwent no significant change from baseline levels at

60 days after induction of AR, despite the impact of this procedure on LV function to the opposite of our working hypothesis. Najjar et al. [20] reported that there were no significant differences in sST2 levels when comparing healthy controls to subjects with HF with a preserved EF. This is in contrast to Weinberg et al. [5] who reported that sST2 levels increased significantly as early as 1 day after experimentally induced myocardial infarction (MI). Interestingly, 3 days after MI, serum sST2 levels were similar to those of the unmanipulated control mice. This group also reported a significant increase in ST2 levels detected in human subjects 1 day after experiencing an MI when compared to values obtained at 2 weeks and 3 months thereafter. Collectively, these results suggest that elevations in circulating sST2 levels may represent a transient response to acute myocardial stress that diminishes over time and ultimately returns to baseline levels after several weeks to months. Such mechanisms could, thus, account for observations.

In this study, we identified significant positive correlations between sST2 levels with body weight and PWTd. Interestingly, we observed no significant increases in PWTd at 2 months after the induction of AR. The explanation for this observation is unclear given the overall absence of changes in sST2 after AR induction. We can only speculate that the stress imposed on cardiomyocytes during diastole secondary to the overload linked to AR as described in human subjects may have played a role [21]. The gene encoding sST2 is induced under conditions of myocardial overload associated with MI, because the myocardial tissue that remains viable is required to bear more stress.

In our model, no associations were identified between plasma sST2 levels with LV function and geometry, including LV volume and mass. This finding is consistent with the results reported in other recent studies that also demonstrated no specific associations between sST2 levels and LV function or geometry, as assessed by echocardiography in human subjects [9, 20]. Likewise, we observed a correlation between sST2 levels and weight only in the rats with surgically induced AR. This correlation may reflect the impact of myocardial stress, ventricular remodeling, and/or fibrosis [5]. It is also possible that the surgical induction of AR results in a chronic inflammatory response. Of note, sST2 has been implicated in numerous inflammatory diseases [22] and in cardiovascular pathophysiology. No correlations between these parameters were detected in the sham control group despite the significant weight gain.

The significant increase in plasma sST2 levels observed in rats with AR in response to administration of the placebo may be directly related to acute cardiomyocyte stretch due to volume overload and mechanical stress [21]. Volume overload in a setting of a fragilized hemodynamic status as

a result of AR could conceivably induce similar changes in sST2 than those already discussed with NT-proBNP. By contrast, no changes in plasma sST2 levels were detected in the sham control rats at days 1, 2, and 7 after OM administration, possibly since cardiomyocytes in the control rats can support this acute volume overload.

Changes in sST2 levels in rats with AR who received volume overload and OM differ completely from those already discussed with NT-proBNP. We believe that this is an important finding of our study as it highlights a differential regulation of NT-proBNP and sST2 in AR. Rønning et al. [23] reported that the administration of OM prolonged the systolic ejection time in LVs that were dilated due to AR. This effect may be associated with limitations on LV distensibility observed in diastole. Interestingly, OM had an opposite effect in animal models of cardiac ischemia. This is consistent with the previous findings that OM reduces the rate of relaxation and increases passive tension in isolated cardiomyocytes while at rest [24]. This will limit the extent to which the cardiomyocytes can undergo additional stretch or distension, including that required to compensate for AR. In such circumstances, NT-proBNP remained unchanged, whereas sST2 increased markedly in our study suggesting that passive muscle tension with OM has distinct and subtle deleterious effects in the setting of AR, not reliably assessed by modifications in NT-proBNP. Furthermore the effects of OM are concentration, time, and species-dependent [25].

## Limitations

This study has several limitations. First, our analysis included only a small number of rats. Second, we did not measure plasma NT-proBNP and sST2 at any time between the induction of AR and the initiation of experimental infusions 2 months later. Thus, we do not have a clear sense of events that may have taken place during this interval. Third, we did not perform echocardiographic or any invasive hemodynamic measurements on days 1, 2, and 7 after the OM or placebo infusions. Thus, we were unable to evaluate the relationships between these parameters and the changes in plasma sST2 and NT-proBNP concentrations observed. Finally, we used an ELISA kit marked “research use only” to assay plasma sST2 levels. There may be considerable differences between the results from this commercial assay and others that are currently in wide use [26].

## Conclusions

Among our findings, we noted that plasma levels of sST2 correlated positively with both PWTd and body weight in

rats with chronic severe AR. Interestingly, NT-proBNP and sST2 levels were significantly higher in these rats after infusion of placebo, a finding that may be linked to pressure overload. Importantly, plasma sST2 to the opposite of NT-proBNP increased after therapeutic infusion with OM. These results may reflect LV dysfunction associated with the administration of OM in the presence of AR, a drug whose mechanism of action has not been fully determined.

**Research funding:** This study was supported and funded by the Fonds pour la Chirurgie Cardiaque, Brussels, Belgium, grant number 489639 and Fondation Emile Saucez –RenÃ© Van Poucke, Brussels, Belgium.

**Author contributions:** All authors have accepted responsibility for the entire content of this manuscript and approved its submission.

**Competing interest:** The authors declare that they have no competing interests.

**Ethics approval:** The experimental protocol was approved by the Institutional Animal Care and Use Committee of the ‘Université Libre de Bruxelles’. Studies were conducted in accordance with the Guide for the Care and Use of Laboratory Animals published by the National Institutes of Health (NIH Publication No. 85–23; revised 1996).

**Availability and data materials:** All materials and data are available at request at the laboratory of physiology of the University of Brussels.

## References

1. Tominaga S. A putative protein of a growth specific cDNA from BALB/c-3T3 cells is highly similar to the extracellular portion of mouse interleukin 1 receptor. *FEBS Lett* 1989;258:301–4.
2. Yancy CW, Jessup M, Bozkurt B, Butler J, Casey DE Jr., Colvin MM, et al. 2017 ACC/AHA/HFSA focused update of the 2013 ACCF/AHA guideline for the management of heart failure: a report of the American college of cardiology/American heart association task force on clinical practice guidelines and the heart failure society of America. *J Am Coll Cardiol* 2017;70:776–803.
3. Kakkar R, Hei H, Dobner S, Lee RT. Interleukin 33 as a mechanically responsive cytokine secreted by living cells. *J Biol Chem* 2012;287:6941–8.
4. Sanada S, Hakuno D, Higgins LJ, Schreiter ER, McKenzie AN, Lee RT. IL-33 and ST2 comprise a critical biomechanically induced and cardioprotective signaling system. *J Clin Invest* 2007;117:1538–49.
5. Weinberg EO, Shimpo M, Keulenaer GWD, MacGillivray C, Tominaga S, Solomon SD, et al. Expression and regulation of ST2, an interleukin-1 receptor family member, in cardiomyocytes and myocardial infarction. *Circulation* 2002;106:2961–6.
6. Bartunek J, Delrue L, Van Durme F, Muller O, Casselman F, Wiest BD, et al. Nonmyocardial production of ST2 protein in human hypertrophy and failure is related to diastolic load. *J Am Coll Cardiol* 2008;52:2166–74.

7. Ikeda T, Matsuda K, Itoh H, Shirakami G, Miyamoto Y, Yoshimasa T, et al. Plasma levels of brain and atrial natriuretic peptides elevate in proportion to left ventricular end-systolic wall stress in patients with aortic stenosis. *Am Heart J* 1997;133:307–14.
8. Miller WL, Hartman KA, Burritt MF, Grill DE, Rodeheffer RJ, Burnett JC Jr., et al. Serial biomarker measurements in ambulatory patients with chronic heart failure: the importance of change over time. *Circulation* 2007;116:249–57.
9. Sugano A, Seo Y, Ishizu T, Sai S, Yamamoto M, Hamada-Harimura Y, et al. Soluble ST2 and brain natriuretic peptide predict different mode of death in patients with heart failure and preserved ejection fraction. *J Cardiol* 2019;73:326–32.
10. Malik FI, Hartman JJ, Elias KA, Morgan BP, Rodríguez H, Brejc K, et al. Cardiac myosin activation: a potential therapeutic approach for systolic heart failure. *Science* 2011;331:1439–43.
11. Shen Y, Malik FI, Zhao X, Depre C, Dhar SK, Abarzúa P, et al. Improvement of cardiac function by a cardiac myosin activator in conscious dogs with systolic heart failure. *Circ Heart Fail* 2010;3:522–7.
12. El-Oumeiri B, Entee KM, Annoni F, Herpain A, Eynden FV, Jespers P, et al. Effects of the cardiac myosin activator Omecamtiv-mecarbil on severe chronic aortic regurgitation in Wistar rats. *BMC Cardiovasc Disord* 2018;18:99.
13. Zoghbi WA, Enriquez-Sarano M, Foster E, Grayburn PA, Kraft CD, Levine RA, et al. American Society of Echocardiography. Recommendations for evaluation of the severity of native valvular regurgitation with two-dimensional and Doppler echocardiography. *J Am Soc Echocardiogr* 2003;16:777–802.
14. Nagueh SF, Smiseth OA, Appleton CP, Byrd BF 3rd, Dokainish H, Edvardsen T, et al. Recommendations for the evaluation of left ventricular diastolic function by echocardiography: an update from the American society of echocardiography and the European association of cardiovascular imaging. *J Am Soc Echocardiogr* 2016;29:277–314.
15. Bekeredjian R, Grayburn PA. Valvular heart disease: aortic regurgitation. *Circulation* 2005;112:125–34.
16. Song BG, Park YH, Kang GH, Chun WJ, Oh JH, Choi JO, et al. Preoperative, postoperative and one-year follow-up of N-terminal pro-B-type natriuretic peptide levels in volume overload of aortic regurgitation: comparison with pressure overload of aortic stenosis. *Cardiol* 2010;116:286–91.
17. Weber M, Hausen M, Arnold R, Moellmann H, Nef H, Elsaesser A, et al. Diagnostic and prognostic value of N-terminal pro B-type natriuretic peptide (NT-proBNP) in patients with chronic aortic regurgitation. *Int J Cardiol* 2008;127:321–7.
18. El Oumeiri B, van de Borne P, Hubesch G, Herpain A, Annoni F, Jespers P, et al. The myosin activator omecamtiv mecarbil improves wall stress in a rat model of chronic aortic regurgitation. *Phys Rep* 2021;9:e14988.
19. Vanderheyden M, Goethals M, Verstreken S, De bruyne B, Muller K, Van Schuerbeeck E, et al. Wall stress modulates brain natriuretic peptide production in pressure overload cardiomyopathy. *J Am Coll Cardiol* 2004;44:2349–54.
20. Najjar E, Faxén UL, Hage C, Donal E, Daubert JC, Linde C, et al. ST2 in heart failure with preserved and reduced ejection fraction. *Scand Cardiovasc J* 2019;53:21–7.
21. Kakkar R, Lee RT. The IL-33/ST2 pathway: therapeutic target and novel biomarker. *Nat Rev Drug Discov* 2008;7:827–40.
22. Boga S, Alkim H, Koksal AR, Ozagari AA, Bayram M, Tekin N, et al. Serum ST2 in inflammatory bowel disease: a potential biomarker for disease activity. *J Invest Med* 2016;64:1016–24.
23. Rønning L, Bakkehaug JP, Rødland L, Kildal AB, Myrmet T, How OL. Opposite diastolic effects of omecamtiv mecarbil versus dobutamine and ivabradine co-treatment in pigs with acute ischemic heart failure. *Phys Rep* 2018;6:e13879.
24. Nagy L, Kovács Á, Bódi B, Pásztor ET, Fülöp GÁ, Tóth A, et al. The novel cardiac myosin activator omecamtiv mecarbil increases the calcium sensitivity of force production in isolated cardiomyocytes and skeletal muscle fibres of the rat. *Br J Pharmacol* 2015;172:4506–18.
25. Rhoden A, Schulze T, Pietsch N, Christ T, Hansen A, Eschenhagen T. Comprehensive analyzes of the inotropic compound omecamtiv mecarbil in rat and human cardiac preparations. *Am J Physiol Heart Circ Physiol* 2022;322:H373–8.
26. Mueller T, Zimmermann M, Dieplinger B, Ankersmit HJ, Haltmayer M. Comparison of plasma concentrations of soluble ST2 measured by three different commercially available assays: the MBL ST2 assay, the presage ST2 assay, and the R&D ST2 assay. *Clin Chim Acta* 2012;413:1493–4.



Article

## Altered Left Ventricular Rat Gene Expression Induced by the Myosin Activator Omecamtiv Mecarbil

Bachar El Oumeiri <sup>1,\*</sup>, Laurence Dewachter <sup>2</sup>, Philippe Van de Borne <sup>3</sup>, Géraldine Hubsch <sup>2</sup>, Christian Melot <sup>2</sup>, Pascale Jespers <sup>2</sup>, Constantin Stefanidis <sup>1</sup>, Kathleen Mc Entee <sup>2</sup> and Frédéric Vanden Eynden <sup>1</sup>

<sup>1</sup> Department of Cardiac Surgery, Université Libre de Bruxelles (ULB) Erasme University Hospital, 1070 Brussels, Belgium

<sup>2</sup> Laboratory of Physiology and Pharmacology, Faculty of Medicine, Université Libre de Bruxelles (ULB), 1070 Brussels, Belgium

<sup>3</sup> Department of Cardiology, Université Libre de Bruxelles (ULB) Erasme University Hospital, 1070 Brussels, Belgium

\* Correspondence: bachar.el.oumeiri@erasme.ulb.ac.be

**Abstract:** To explore the impact of omecamtiv mecarbil (OM) on the gene expression profile in adult male rats. Fourteen male Wistar rats were randomly assigned to a single OM (1.2 mg/kg/h; n = 6) or placebo (n = 8) 30-min infusion. Echocardiography was performed before and after OM infusion. Seven days after infusion, rats were euthanized, and left ventricular (LV) tissues were removed for *real-time* quantitative polymerase chain reaction (RTq-PCR) experiments. After OM infusion, pro-apoptotic *Bax*-to-*Bcl2* ratio was decreased, with increased *Bcl2* and similar *Bax* gene expression. The gene expression of molecules regulating oxidative stress, including glutathione disulfide reductase (*Gsr*) and superoxide dismutases (*Sod1/Sod2*), remained unchanged, whereas the expression of antioxidant glutathione peroxidase (*Gpx*) increased. While LV gene expression of key energy sensors, peroxisome proliferator activator (*Ppar*)  $\alpha$  and  $\gamma$ , AMP-activated protein kinase (*Ampk*), and carnitine palmitoyltransferase 1 (*Cpt1*) remained unchanged after OM infusion, and the expression of pyruvate dehydrogenase kinase 4 (*Pdk4*) increased. The LV expression of the major myocardial glucose transporter *Glut1* decreased, with no changes in *Glut4* expression, whereas the LV expression of oxidized low-density lipoprotein receptor 1 (*Olr1*) and arachidonate 15-lipoxygenase (*Alox15*) increased, with no changes in fatty acid transporter *Cd36*. An increased LV expression of angiotensin II receptors *AT1* and *AT2* was observed, with no changes in angiotensin I-converting enzyme expression. The Kalikrein-bradykinin system was upregulated with increased LV expression of kallikrein-related peptidases *Klk8*, *Klk1c2*, and *Klk1c12* and bradykinin receptors B1 and B2 (*Bdkrb1* and *Bdkrb2*), whereas the LV expression of inducible nitric oxide synthase 2 (*Nos2*) increased. LV expression in major molecular determinants involved in calcium-dependent myocardial contraction remained unchanged, except for an increased LV expression of calcium/calmodulin-dependent protein kinase II delta (*Cacna1c*) in response to OM. A single intravenous infusion of OM, in adult healthy rats, resulted in significant changes in the LV expression of genes regulating apoptosis, oxidative stress, metabolism, and cardiac contractility.

**Keywords:** left ventricle; omecamtiv mecarbil; gene expression; apoptosis; metabolism; oxidative stress



**Citation:** El Oumeiri, B.; Dewachter, L.; Van de Borne, P.; Hubsch, G.; Melot, C.; Jespers, P.; Stefanidis, C.; Mc Entee, K.; Vanden Eynden, F. Altered Left Ventricular Rat Gene Expression Induced by the Myosin Activator Omecamtiv Mecarbil. *Genes* **2023**, *14*, 122. <https://doi.org/10.3390/genes14010122>

Academic Editor: Andrzej Ciechanowicz

Received: 21 November 2022

Revised: 20 December 2022

Accepted: 27 December 2022

Published: 1 January 2023



**Copyright:** © 2023 by the authors. Licensee MDPI, Basel, Switzerland. This article is an open access article distributed under the terms and conditions of the Creative Commons Attribution (CC BY) license (<https://creativecommons.org/licenses/by/4.0/>).

### 1. Introduction

Heart failure (HF) is a major cause of morbidity and mortality and remains a public health problem worldwide [1,2]. Current therapies used to treat HF, including  $\beta$ -blockers, diuretics, and angiotensin-converting enzyme (ACE) inhibitors, are not completely effective. Similarly, while inotropic drugs, including  $\beta$ -adrenergic agonists (e.g., dobutamine) and phosphodiesterase inhibitors (e.g., levosimendan and milrinone) increase cardiac output (CO), their ongoing use results in increased myocardial oxygen consumption, high levels

of intracellular calcium ( $\text{Ca}^{2+}$ ), elevated heart rate, arrhythmias, and mortality [3]. Indeed, these drugs are known to increase the rate of  $\text{Ca}^{2+}$  cycling and ATP utilization in the myocardium because more  $\text{Ca}^{2+}$  needs to be removed from the cytoplasm and sequestered in the sarcoplasmic reticulum [4]. The adverse long-term effects of these drugs may be related to the actions of  $\text{Ca}^{2+}$ /calmodulin-dependent protein kinase II (CaMKII) and other protein kinases that induce myocardial apoptosis, hypertrophy, and fibrosis [5]. Similarly,  $\beta$ -adrenergic activation alters myocardial metabolic substrate use and may trigger energy deficits and oxidative stress [6].

Omecamtiv mecarbil (OM) is a novel small molecule that directly activates cardiac myosin. The sarcomere contains both thin and thick filaments and is the fundamental unit of cardiac muscle contractility. Cardiac myosin, which is the main component of the thick filament, uses chemical energy derived from ATP hydrolysis to generate contractile force. OM selectively activates the S1 domain of cardiac myosin, but has no impact on myosin filaments from any other muscle [7]. The administration of OM increases the rate of ATP turnover and improves contractility by increasing the number of myosin heads capable of interacting with actin filaments, albeit with no impact on  $\text{Ca}^{2+}$  homeostasis [7]. In a canine model of systolic HF, OM increased the systolic ejection time, stroke volume (SV), and CO [8]. In vitro and in vivo studies confirmed that OM selectively inhibits cardiac myosin ATPase and, thus, has the potential to decrease myocardial oxygen consumption [9]. Contrarily, the administration of OM increased myocardial oxygen consumption in a pig model of HF [10] and resulted in impaired myocardial efficiency by increasing  $\text{O}_2$  consumption both at baseline and during work in an isolated mouse heart model; these responses were abolished by the addition of a myosin-ATPase inhibitor [10]. While these data suggested that the administration of OM may result in increased  $\text{O}_2$  consumption, these findings were not fully consistent with the OM-mediated inhibition of baseline myosin ATPase activity observed in vitro [9]. Similarly, Nagy et al. [11] reported that OM-treated myofilaments were sensitized to  $\text{Ca}^{2+}$  in an exposed rat myocyte model, while Utter et al. [12] found that OM re-sensitized myofilaments exhibited decreased  $\text{Ca}^{2+}$  sensitivity in a mouse model of dilated cardiomyopathy.

In this context, the objective of this study was to examine the OM-mediated changes in gene expression in adult rat myocardium, with a particular emphasis on the pathways associated with apoptosis, oxidative stress, energy substrate metabolism, and  $\text{Ca}^{2+}$ -mediated cardiac contractility.

## 2. Methods

### 2.1. Animal Model and Experimental Design

The experimental protocol was approved by the Institutional Animal Care and Use Committee of the Faculty of Medicine of the Université Libre de Bruxelles (ULB; Brussels, Belgium; protocol acceptance number: 644N). Experiments were conducted in accordance with the Guide for the Care and Use of Laboratory Animals published by the United States National Institutes of Health (NIH Publication No. 85-23; revised 1996).

Fourteen adult male Wistar rats (Janvier, Le Genest-Saint-Isle, France) were randomly assigned for intravenous administration of OM (1.2 mg/kg/h for 30 min via the femoral vein;  $n = 6$ ; mean body weight:  $553 \pm 38$  g) or placebo ( $n = 8$ ; mean body weight:  $536 \pm 39$  g) on day 0. Dose of OM was chosen to achieve peak plasma concentrations of  $\sim 400$  ng/mL, as previously reported [13]. Seven days after OM infusion, OM- and placebo-treated rats were sacrificed by exsanguination via section of the abdominal aorta. The hearts were rapidly harvested and dissected to isolate the LV, which was snap-frozen in liquid nitrogen and stored at  $-80$  °C for further biological analysis.

### 2.2. Echocardiography and Cardiac Measurements

Transthoracic 2D, M-mode, and Doppler echocardiography were performed using an ultrasound scanner (Vivid-E90, GE Healthcare, Wauwatosa, WI, USA) equipped with a 12-MHz phased-array transducer (GE 12S-D, GE Healthcare) in anesthetized rats (with

inhaled 1.5% isoflurane). All echocardiographic measurements were obtained by the same observer, according to the American Society of Echocardiography guidelines [14]. Standard right parasternal (long and short axis) and left apical parasternal views were used for data acquisition. Fractional shortening (FS) was calculated using the formula  $(FS = LVEDD - LVESD / LVEDD \times 100)$  in M-mode from a LV short-axis view. Ejection fraction (EF) was derived using the Teicholz formula. Electrocardiogram was monitored via limb leads throughout the procedure. Aortic flow was measured from the left apical view to calculate forward stroke volume (SV) and cardiac output (CO) and to measure pre-ejection period (PEP: delay from Q wave of QRS to aortic opening; ms), LV ejection time (LVET: interval from beginning to termination of aortic flow; ms), and inter-beat interval (RR; ms). Systolic time (ms) was determined as PEP + LVET (ms), and diastolic time (ms) was calculated as RR interval – systolic time. Echocardiography was performed before and 30-min after OM/placebo administration.

### 2.3. Real-Time Quantitative Polymerase Chain Reaction (RTq-PCR)

Total RNA was extracted from snap-frozen LV myocardial tissue using TRIzol reagent (Invitrogen, Merelbeke, Belgium), followed by a chloroform/ethanol extraction and a final purification using QIAGEN RNeasy<sup>®</sup> Mini kit (QIAGEN, Hilden, Germany), according to manufacturer's instructions. RNA concentration was determined by standard spectrophotometric techniques, using a spectrophotometer Nanodrop<sup>®</sup> (ND-1000; Isogen Life Sciences, De Meern, The Netherlands), and RNA integrity was assessed by visual inspection of GelRed (Biotium, Hayward, California)-stained agarose gels. Reverse transcription was performed using random hexamer primers and Superscript II Reverse Transcriptase (Invitrogen, Merelbeke, Belgium), according to the manufacturer's instructions. Gene-specific sense and antisense primers for RTq-PCR (Table 1) were designed using the Primer3 program for *rattus norvegicus* gene sequences, including those for B-cell lymphoma 2 (*Bcl2*), Bcl2 associated X apoptosis regulator (*Bax*), glutathione peroxidase (*Gpx*), glutathione-disulfide reductase (*Gsr*), superoxide dismutases 1 and 2 (*Sod1* and *Sod2*), AMP-activated protein kinase (*Ampk*), peroxisome proliferator-activated receptors  $\alpha$  and  $\gamma$  (*Ppar*  $\alpha$  and  $\gamma$ ), solute carrier family 2 members 1 (*Slc2a1*, also known as *Glut1*) and 4 (*Slc2a4* or *Glut4*), pyruvate dehydrogenase kinase (*Pdk4*), carnitine palmitoyltransferase1 (*Cpt1*), fatty acid transporter *Cd36*, oxidized low-density lipoprotein receptor 1 (*Olr1*, also known as *Lox1*), arachidonate 15-lipoxygenase (*Alox15*), angiotensin II receptor type 1a (*Agtr1a*, also known as *AT1*), angiotensin II receptor type 2 (*Agtr2*, also known as *AT2*), angiotensin-converting enzymes 1 and 2 (*ACE1* and *ACE2*), nitric oxide synthases 2 and 3 (*Nos2*, also called *inducible NOS* or *iNOS* and *Nos3*, also called *endothelial NOS* or *eNOS*), kallikrein-related peptidases 8 and 10 (*Klk8* and *Klk10*), kallikrein 1-related peptidases C2 and C12 (*Klk1c2* and *Klk1c12*), bradykinin receptors B1 and B2 (*Bdkrb1* and *Bdkrb2*), ATPase sarcoplasmic/endoplasmic reticulum  $Ca^{2+}$  transporting 2 (*Atp2a2*, also called *Serca2*), ryanodine receptor 2 (*Ryr2*), calcium voltage-gated channel subunit alpha1C (*Cacna1c*), solute carrier family 8 member A1 (*Slc8a1*),  $Ca^{2+}$ /calmodulin-dependent protein kinase II delta (*Camk2d*), glyceraldehyde-3-phosphate dehydrogenase (*Gapdh*), and hypoxanthine phosphoribosyltransferase 1 (*Hprt1*) used as housekeeping genes. Intron-spanning primers were selected whenever possible to avoid inappropriate amplification of contaminant genomic DNA. Amplification reactions were performed in duplicate using SYBRGreen PCR Master Mix (Quanta Biosciences, Gaithersburg, MD, USA), specific primers, and diluted template cDNA. Analysis of the results was performed using an iCycler System (BioRad Laboratories, Hercules, CA, USA). Relative quantification was achieved using the Pfaffl method [15] by normalization with the housekeeping genes, *Gapdh* and *Hprt1*.

**Table 1.** Primers used for real-time quantitative polymerase chain reaction (RTq-PCR) in rat left ventricular (LV) myocardial tissue.

Genes		Primer Sequences
Glycerol-3-phosphate dehydrogenase ( <i>GAPDH</i> )	Sense	5'-AAGATGGTGAAGGTCGGTGT-3'
	Antisense	5'-ATGAAGGGGTCGTTGATGG-3'
Hypoxanthine guanine phosphoribosyl transferase ( <i>HPRT</i> )	Sense	5'-ACAGGCCAGACTTTGTGGA-3'
	Antisense	5'-ATCCACTTTCGCTGATGACAC-3'
AMP-activated protein kinase ( <i>Ampk</i> )	Sense	5'-TTCGGGAAAGTGAAGGTGGG-3'
	Antisense	5'-TCTCTGCGGATTTCCCGAC-3'
Angiotensin-converting enzyme 1 ( <i>ACE1</i> )	Sense	5'-AGTGGGTGCTGCTCTTCCTA-3'
	Antisense	5'-GGAGGCTGTGATGGTTATGG-3'
Angiotensin-converting enzyme 2 ( <i>ACE2</i> )	Sense	5'-GCCTTGGAAAATGTGGTAGG-3'
	Antisense	5'-TTCAGCCAGACAAACAATGG-3'
Angiotensin II receptor type 1a ( <i>Agtr1a</i> or <i>AT1</i> )	Sense	5'-ACATTCCTGGGCTTCGTGTC-3'
	Antisense	5'-CATCATTTCCTGGCGTGTTC-3'
Angiotensin II receptor type 2 ( <i>Agtr2</i> or <i>AT2</i> )	Sense	5'-TGCTCTGACCTGGATGGGA-3'
	Antisense	5'-AGCTGTTTGGTGAATCCAGG-3'
Arachidonate 15-lipoxygenase ( <i>Alox15</i> )	Sense	5'-GCACTCTCCGTCATCTTG-3'
	Antisense	5'-GCTTCTCCATTGTGCTTCCT-3'
ATPase sarcoplasmic/endoplasmic reticulum Ca <sup>2+</sup> transporting 2 ( <i>Atp2a2</i> or <i>Serca2</i> )	Sense	5'-GCAGGTCAAGAAGCTCAAGG-3'
	Antisense	5'-TCTCTGCGGATTTCCCGAC-3'
Bcl2 associated X apoptosis regulator ( <i>Bax</i> )	Sense	5'-CGTGGTTGCCCTCTTCTACT-3'
	Antisense	5'-TCACGGAGGAAGTCCAGTGT-3'
B-cell lymphoma 2 ( <i>Bcl2</i> )	Sense	5'-TTTCTCCTGGCTGTCTCTGAA-3'
	Antisense	5'-CATATTTGTTTGGGGCAGGT-3'
Bradykinin receptor B1 ( <i>Bdkrb1</i> )	Sense	5'-AAGCTACGTGCCCTGCTCATC-3'
	Antisense	5'-CGGGGACGACTTTAACAGAG-3'
Bradykinin receptor B2 ( <i>Bdkrb2</i> )	Sense	5'-GCTGTCGTGGAAGTGGCTAT-3'
	Antisense	5'-AAGTCCCGTTATGAGCAGA-3'
Ca <sup>2+</sup> /calmodulin-dependent protein kinase II delta ( <i>Camk2d</i> )	Sense	5'-ATCCACAACCCTGATGAAA-3'
	Antisense	5'-GCTTTCGTGTTTACGTCT-3'
Ca <sup>2+</sup> voltage-gated channel subunit alpha1 C ( <i>Cacna1c</i> )	Sense	5'-CCTATTTCCGTGACCTGTGG-3'
	Antisense	5'-GGAGGGACTTGATGGTGTG-3'
Carnitine palmitoyltransferase 1 ( <i>Cpt1</i> )	Sense	5'-AAGAACACGAGCCAACAAGC-3'
	Antisense	5'-ACCATACCCAGTGCCATCAC-3'
CD36 fatty acid transporter ( <i>Cd36</i> )	Sense	5'-TTTCTGCTTCTCATCGCCG-3'
	Antisense	5'-GGATGTGGAACCCATAACTGG-3'
Glutathione peroxidase ( <i>Gpx</i> )	Sense	5'-CCGACCCCAAGTACATCATT-3'
	Antisense	5'-AACACCGTCTGGACCTACCA-3'
Glutathione-disulfide reductase ( <i>Gsr</i> )	Sense	5'-GCCGCCTGAACAACATCTAC-3'
	Antisense	5'-CTTTTCCCGTTGACTTCCA-3'
Kallikrein-related peptidase 8 ( <i>Klk8</i> )	Sense	5'-CGGAGACAGATGGGTCTTAA-3'
	Antisense	5'-ATCTCTTGCTCGGGCTCAT-3'
Kallikrein-related peptidase 10 ( <i>Klk10</i> )	Sense	5'-GCAGGTCTCCCTCTTCCATA-3'
	Antisense	5'-CAGTGGCTATTCTCCAGCA-3'
Kallikrein 1-related peptidase C2 ( <i>Klk1c2</i> )	Sense	5'-CAGGAGAGATGGAAGGAGGA-3'
	Antisense	5'-CGGTGTTTGGGTTTAGCAC-3'
Kallikrein 1-related peptidase C12 ( <i>Klk1c12</i> )	Sense	5'-CATCAAAGCCACACACAGAT-3'
	Antisense	5'-AAGCACACCATCACAGAGGAG-3'

Table 1. Cont.

Genes		Primer Sequences
Nitric oxide synthase 2 ( <i>NOS2</i> or <i>iNOS</i> )	Sense	5'-GTTTCCCCCAGATCCTCACT-3'
	Antisense	5'-CTCTCCATTGCCCCAGTTT-3'
Nitric oxide synthase 3 ( <i>NOS3</i> or <i>eNOS</i> )	Sense	5'-GGTATTGATGCTCGGGACT-3'
	Antisense	5'-TGATGGCTGAACGAAGATTG-3'
Oxidized low density lipoprotein receptor 1 ( <i>Olr1</i> or <i>Lox1</i> )	Sense	5'-CATTACCTCCCCATTTT-3'
	Antisense	5'-GTAAAGAAACGCCCTGGT-3'
Peroxisome proliferator-activated receptor $\alpha$ ( <i>Ppar <math>\alpha</math></i> )	Sense	5'-TTAGAGGCGAGCCAAGACTG-3'
	Antisense	5'-CAGAGCACCAATCTGTGATGA-3'
Peroxisome proliferator-activated receptor $\gamma$ ( <i>Ppar <math>\gamma</math></i> )	Sense	5'-GCGCTAAATTCATCTTAACTC-3'
	Antisense	5'-CTGTGTCAACCATGGTAAATTT-3'
Pyruvate dehydrogenase kinase 4 ( <i>Pdk4</i> )	Sense	5'-GAGCCTGATGGATTTAGTGA-3'
	Antisense	5'-CGAACTTTGACCAGCGTGT-3'
Ryanodine receptor 2 ( <i>Ryr2</i> )	Sense	5'-GGAAGTACGGAGGAAAGTG-3'
	Antisense	5'-GAGACCAGCATTTGGGTTGT-3'
Solute carrier family 2 member 1 ( <i>Slc2a1</i> or <i>Glut1</i> )	Sense	5'-TCTTCGAGAAGGCAGGTGTG-3'
	Antisense	5'-TCCACGACGAACAGCGAC-3'
Solute carrier family 2 member 4 ( <i>Slc2a4</i> or <i>Glut4</i> )	Sense	5'-AGGCCGGGACACTATACCC-3'
	Antisense	5'-TCCCCATCTTCAGAGCCGAT-5'
Solute carrier family 8 member A1 ( <i>Slc8a1</i> )	Sense	5'-GAGATTGGAGAACCCTCT-3'
	Antisense	5'-AGTGGCTGCTGTGCATCGTA-3'
Superoxide dismutase 1 ( <i>Sod1</i> )	Sense	5'-GGTCCACGAGAAAACAAGATGA-3'
	Antisense	5'-CAATCACACCACAAGCCAAG-3'
Superoxide dismutase 2 ( <i>Sod2</i> )	Sense	5'-AAGGAGCAAGGTCGCTTACA-3'
	Antisense	5'-ACACATCAATCCCCAGCAGT-3'

#### 2.4. Statistical Analysis

Results are presented as mean  $\pm$  standard deviation (SD), with "n" representing the number of individual data points. The echocardiographic data were compared using Student's *t*-test for repeated measures ( $n = 6$ ) before and after OM perfusion. The RTq-PCR data evaluating LV gene expression were compared using Student's *t*-test for independent samples (with  $n = 8$  in the control group and  $n = 6$  in the treated group). Statistical analyses were performed using StatView 5.0 software. A *p*-value  $< 0.05$  was considered statistically significant.

### 3. Results

#### 3.1. Effect of OM on Cardiac Function in Rats

As illustrated in Table 2, the infusion of OM increased the fractional shortening (FS) and the LV ejection time (LVET) and decreased the aortic pre-ejection period (PEP), which resulted in a reduction in the PEP/LVET ratio. No other investigated echocardiographic parameters were significantly altered by OM infusion (Table 2).

Table 2. Echocardiographic measurements in rats ( $n = 6$ ) at baseline and 30 min after OM infusion.

Parameters	Before OM Infusion	After OM Infusion
FS (%)	38.8 $\pm$ 3.6	44.1 $\pm$ 4.4 *
EF (%)	76.0 $\pm$ 4.4	80.6 $\pm$ 5.2
LVESD (mm)	5.5 $\pm$ 0.5	4.6 $\pm$ 0.9
LVEDD (mm)	9.0 $\pm$ 0.4	8.3 $\pm$ 0.9
HR (beats/min)	283 $\pm$ 57	303 $\pm$ 68

Table 2. Cont.

Parameters	Before OM Infusion	After OM Infusion
SBP (mmHg)	128 ± 9	128 ± 21
DBP (mmHg)	90 ± 10	88 ± 20
LVET (ms)	79 ± 6	89 ± 8 *
PEP (ms)	21 ± 5	14 ± 7 *
PEP/LVET	0.26 ± 0.06	0.15 ± 0.07 *
CO (mL/min)	90 ± 21	106 ± 22
SV (mL)	0.32 ± 0.06	0.35 ± 0.04
LA (mm)	5.8 ± 0.8	5.7 ± 0.5

Values presented are means ± SD; \*  $p < 0.05$ . FS, fractional shortening; EF, ejection fraction; LVESD, left ventricle end-systolic diameter; LVESD, left ventricle end-systolic diameter; LVEDD, left ventricle end-diastolic diameter; HR, heart rate; PEP, pre-ejection period; LVET, left ventricular ejection time; SV, stroke volume; CO, cardiac output; SBP, systolic blood pressure; DBP, diastolic blood pressure; LA, left atrial diameter.

### 3.2. OM Altered Myocardial LV Expression of Genes Regulating Apoptosis and Oxidative Stress

Myocardial LV gene expression of anti-apoptotic *Bcl2* was significantly higher in rats treated with OM, compared to placebo, whereas no difference in gene expression of pro-apoptotic *Bax* was observed (Figure 1A). The resulting pro-apoptotic *Bax*-to-*Bcl2* ratio was reduced in the LV of rats that underwent OM infusion (Figure 1A). We also examined the differential expression of genes involved in oxidative stress regulation. The myocardial expression of *Gpx*, an antioxidant enzyme, increased in the LV after OM infusion, whereas no changes in *Gsr*, *Sod1*, or *Sod2* gene expression were observed (Figure 1B).

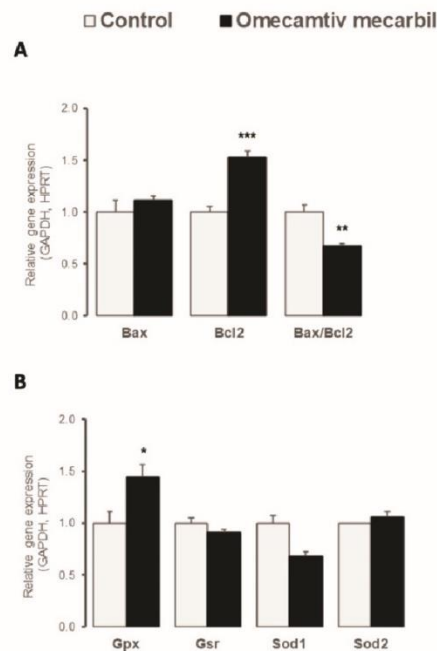


**Figure 1.** Myocardial left ventricular relative expression of genes implicated in (A) apoptosis (*Bax*, *Bcl2*) and (B) oxidative stress (*Gpx*, *Gsr*, *Sod1*, *Sod2*) processes seven days after omecamtiv mecarbil (OM;  $n = 6$ ; black bars) versus placebo ( $n = 8$ ; grey bars) infusion. Values are presented as mean ± SD; \*  $0.01 < p < 0.05$ , \*\*  $0.001 < p < 0.01$ , \*\*\*  $p < 0.001$ .

### 3.3. OM Impacted LV Expression Profile of Key Determinants of Cardiac Energy Substrate Use

To assess the effects of OM infusion on basal myocardial energy metabolism, we evaluated the gene expression profile of the transcription factors and molecules regulating cardiac glucose and fatty acid metabolism. As illustrated in Figure 2A, myocardial LV gene expression of key energy sensors *Ppar α* and  $\gamma$  and *Ampk* remained unchanged. Myocardial LV expression of *Slc2a1* (*Glut1*), the major myocardial glucose transporter, decreased after OM infusion, while gene expression of *Slc2a4* (*Glut4*) remained unchanged (Figure 2B). In contrast, myocardial LV expression of *Pdk4*, a mitochondrial pyruvate dehydrogenase (PDH) regulator overarching metabolic shift between fatty acid oxidation and glycolysis as energy fuel, increased after OM infusion (Figure 2C), whereas the carnitine palmitoyl-transferase1 (*Cpt1*) remained unchanged (Figure 2D). As illustrated in Figure 2E, the OM infusion increased the LV expression of *Alox15* encoding the 12/15 lipoxygenase enzyme implicated in polyunsaturated fatty acid metabolism and of oxidized low-density lipoprotein receptor 1 (*Olr1*, also known as *Lox1*) encoding for a scavenger receptor mediating the uptake of oxidized lipoproteins into cells, whereas the gene expression of fatty acid transporter *Cd36* remained unchanged.

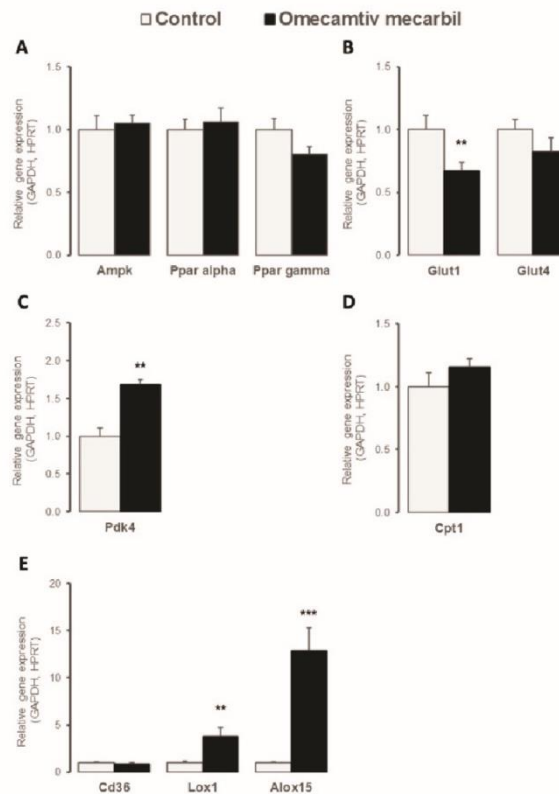


**Figure 2.** Myocardial left ventricular relative expression of genes implicated in cardiac metabolism, including (A) cellular energy sensors such as *Ampk*, *Ppar α*, and *Ppar γ*; (B) glucose transporters *Glut1* and *Glut4*; (C) mitochondrial metabolic regulators contributing to glucose to fatty acids shift as cardiac major energy fuel, such as *Pdk4* and (D) *Cpt1*; and (E) fatty acid metabolism regulators such as *Cd36*, *Lox-1*, and *Alox-15*, seven days after omecamtiv mecarbil (OM; n = 6; black bars) versus placebo (n = 8; grey bars) infusion. Values are presented as mean ± SD; \*\* 0.001 < p < 0.01, \*\*\* p < 0.001.

### 3.4. OM Altered LV Expression of Genes Implicated in Cardiac Contractility

Because OM is a myosin-specific activator that increases myocardial contractility independently of  $Ca^{2+}$  fluxes, we evaluated the OM-induced myocardial expression of different regulators of cardiac contraction. As illustrated in Figure 3A, OM infusion increased the myocardial LV gene expression of both angiotensin receptors *AT1* and *AT2*, while the gene expression of angiotensin-converting enzymes *ACE1* and *ACE2* remained unchanged (Figure 3B). Myocardial LV expression of NO-synthase catalyzing the production of NO, was increased by OM infusion for the inducible *iNOS* isoform, while it remained stable for the constitutive *eNOS* isoform (Figure 3C). The kallikrein-bradykinin system was upregulated in the LV of rats after OM infusion, with the increased myocardial LV expression of genes encoding the serine proteases *Klk8*, *Klk1c2*, and *Klk1c12* (Figure 3D), as well as the bradykinin receptors (*Bdkr*) *B1* and *B2* (Figure 3E), which are G-protein-coupled receptors mediating kinin actions. No change in myocardial gene expression in *Klk10* was observed (Figure 3D). Finally, OM infusion did not induce any changes in the gene expression of major players involved in  $Ca^{2+}$ -dependent cardiac contraction, except for an increase in LV gene expression of *Cacna1c* in response to OM (Figure 3F).

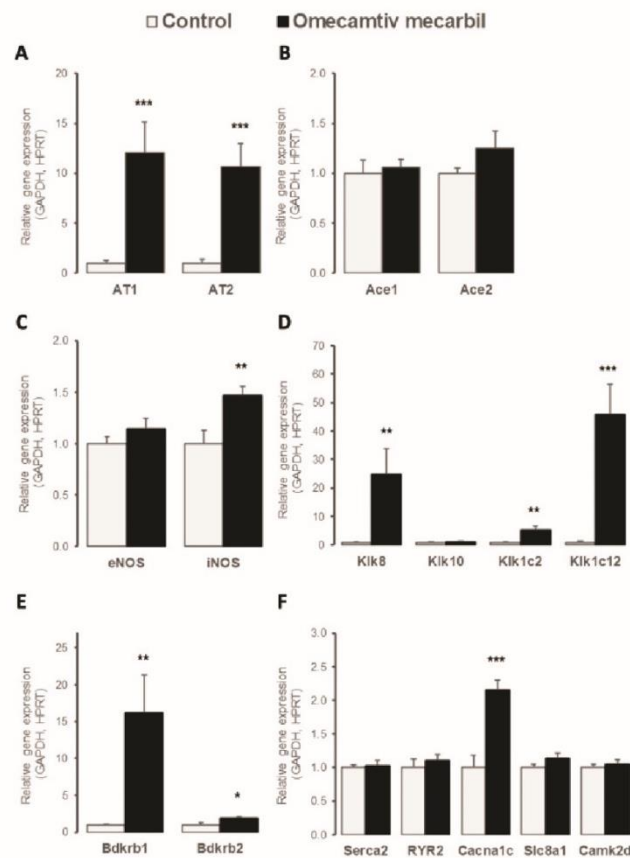


**Figure 3.** Myocardial left ventricular relative expression of genes controlling myocardial contractility including (A) *AT1* and *AT2* angiotensin II receptors; (B) *ACE1* and *ACE2* angiotensin-converting



enzymes; (C) endothelial (*eNos* or *Nos3*) and inducible (*iNos* or *Nos2*) nitric oxide synthases; (D) major cardiac actors of kallikrein (*Klk8*, *Klk10*, *Klk1c2*, and *Klk1c12*)-(E) bradykinin (*Bdkrb1* and *Bdkrb2*) system and of (F)  $\text{Ca}^{2+}$ -dependent excitation–contraction *Atp2a*, *Ryr2*, *Cacna1c*, *Slc8a1*, and *Camk2d* seven days after omecamtiv mecarbil (OM;  $n = 6$ ; black bars) versus placebo ( $n = 8$ ; grey bars) infusion. Values are presented as mean  $\pm$  SD; \*  $0.01 < p < 0.05$ , \*\*  $0.001 < p < 0.01$ , \*\*\*  $p < 0.001$ .

#### 4. Discussion

The present results show that a single 30-min infusion of myosin activator OM induced significant LV expression alterations in genes regulating apoptosis (with decreased pro-apoptotic *Bax-to-Bcl2* ratio), oxidative stress (with increased antioxidant *Gpx*), cardiac metabolism (with decreased *Glut1* and increased *Lox1*, *Alox15*, and *Pdk4*), and contraction (with increased *AT1* and *AT2*, upregulation of kallikrein-bradykinin system, but no changes in molecules involved in  $\text{Ca}^{2+}$ -dependent myocardial contraction) 7 weeks after OM infusion.

In the present study, we evaluated the echocardiographic parameters and gene expression in the LV of rats after OM infusion, compared to placebo-infused rats. As previously reported [8,16], the administration of OM resulted in increases in both the ejection time and the FS. Our findings did not achieve statistical significance for the ejection fraction, potentially because of the limited number of rats and/or the concentration of drug used. However, we did not observe significant increases in CO and SV in OM-treated rats.

The first set of gene expression profile focuses on the differential expression of the genes regulating apoptosis. Specifically, we examined the OM-induced gene expression of mitochondrial anti-apoptotic *Bcl2*, and pro-apoptotic *Bax* [17]. *Bcl2* is known to control the release of cytochrome c, preserve mitochondrial integrity, and protect against apoptosis [18]. Our findings revealed a significant increase in *Bcl2* expression, leading to a down-regulation of the *Bax-to-Bcl2* ratio, in response to OM infusion. The *Bax-to-Bcl2* ratio reflects an overall vulnerability to apoptosis; increases in the *Bax-to-Bcl2* ratio suggest higher levels of apoptotic activity [19]. In contrast to the response to the inotropic agent dobutamine, which partially activates the apoptosis processes in vivo [20], our results suggested that OM did not activate apoptotic processes and was even able to protect the LV against apoptosis. *Gpx* is one of three main antioxidant enzymes [21]. Our findings revealed that OM infusion resulted in increased expression of *Gpx*, but had no impact on any other tested antioxidant genes. Interestingly, these findings are contrasted with those reported for other inotropic drugs. Indeed, levosimendan was shown to reduce oxidative stress through increased expression of genes encoding *Sod* and *Gpx* [22]. In a recent publication, Rhoden et al. [23] reported that OM promoted the accumulation of mitochondrial reactive oxygen species (ROS) in both rat and human cardiac tissues. As ROS are known to promote the expression of *Gpx* [24], our results suggested a link between OM and this critical antioxidant pathway.

We also evaluated the effects of OM on cardiac metabolism via the evaluation of genes involved in the metabolism of fatty acids, glucose, and lactate and the production of high-energy phosphates [25]. *Glut1* is the major determinant of homeostatic glucose transport in cardiac muscle [25]. Administration of OM resulted in decreased expression of *Glut1* in rat LV, which may result in decreased glucose uptake. In contrast to the findings reported for dobutamine [26], the present results suggest that OM promoted a shift from glycolytic to oxidative metabolism [26]. Fatty acid catabolism is coordinately regulated with glucose pathways to support homeostasis in response to changes in energy supply or demand. Reciprocal regulation in fatty acid and glucose metabolism involves both the PDH complex and the *Cpt* [27]. PDH converts the pyruvate generated by glycolysis to acetyl-CoA and  $\text{CO}_2$  via oxidative decarboxylation, while the *Cpt* contributes to fatty acid transport into mitochondria, where they undergo oxidation to generate acetyl-CoA [27]. *Pdk4* is an important regulator of PDH activity [28]. Increased levels of *Pdk4* promote the inactivation of PDH and, thus, act on the metabolic shift from glucose to fatty acid oxidation [28]. In the present study, the administration of OM resulted in increased expression in *Pdk4*, which may be a marker of increased fatty acid oxidation in the LV [29].

Decreased glucose uptake and increased fatty acid oxidation may result in the production of higher levels of ATP and higher O<sub>2</sub> consumption. These findings are consistent with those reported by Bakkehaug et al. [10], who reported that the administration of OM resulted in increased myocardial oxygen consumption. Similarly, Lox1, which was originally identified as a receptor for oxidatively-modified LDL [30], can be induced by numerous stimuli, including angiotensin II [31], shear stress [32], and ischemia-reperfusion injury [33]. Alox15, which is a lipid-peroxidizing enzyme [34], has been implicated in the pathogenesis of atherosclerosis [30,31,35], diabetes, and neurodegenerative disease [34]. The expression levels of both *Lox1* and *Alox15* were markedly increased in HF [35,36], and increased expression of *Lox1* was detected in cases of diastolic dysfunction [24,37]. OM-associated diastolic dysfunction and stiffness have also been reported [38,39]. Here, we found increased LV expression in *Lox1* and *Alox15* in OM-infused rats. Because *Lox1* expression has been related to diastolic dysfunction, the link between OM infusion, specific molecular determinants, and diastolic dysfunction should be further studied in future studies.

Angiotensin II binding to AT1 induces vasoconstriction and promotes oxidative stress by activating NADPH oxidase and inducing eNOS uncoupling. This results in a switch from NO to the production of ROS, including superoxide. In contrast, binding to AT2 promotes vasorelaxation, protection against ischemia-reperfusion injury and myocardial infarction, and decreased inflammation [40]. Thus, the activation of AT2-mediated pathways may counter-regulate those resulting from AT1 activation [41]. Here, we found increased gene expression of both *AT1* and *AT2* in response to OM, with an observed *AT2*-to-*AT1* ratio of 1.15. A high *AT2*-to-*AT1* ratio has been associated with increased oxidative stress and cardiac cell apoptosis [42]. The relatively low ratio observed in the present study is consistent with the absence of activation of apoptosis and oxidative stress. Nitric oxide synthase (NOS) catalyzes the conversion of L-arginine to L-citrulline and NO, which is a free radical involved in both homeostatic and immunological functions. iNOS is a Ca<sup>2+</sup>-independent enzyme that is expressed in cardiomyocytes, in response to environmental perturbation (e.g., cytokine release) [43]. The activation of iNOS results in substantially higher levels of NO, compared to other forms of NOS [44]. In the heart, iNOS contributes to a contractile dysfunction characteristic of ischemia-reperfusion injury, infarction, and HF [45,46]. In contrast, several studies have shown beneficial effects of iNOS in the normal, hypertrophied, transplanted, or cardiomyopathic human heart [47,48]. Here, we found that the administration of OM resulted in increased *iNOS* expression, whose significance to OM mechanism of action has to be further determined.

KLK8 has been previously detected in the rat myocardium [49]. Although its physiologic substrates remain largely unknown, the expression of *Klk8* protects against acute ischemia-reperfusion injury and induces cardiac hypertrophy in rats [49,50], in response to pressure overload [49]. *Klk1c2* (also known as tonin) can catalyze the release of angiotensin II directly from angiotensinogen; thus, the activation of this enzyme may result in increased production of angiotensin II, independently of ACE activity [51]. *Klk1c2* may also induce cardiac hypertrophy [52]. *Klk1c2* perfusion in Wistar rats induced coronary vasoconstriction and simultaneously depressed myocardial contractility; the time to peak for cell shortening and half relaxation was significantly reduced. All these results suggest that Ca<sup>2+</sup> handling is significantly accelerated by *Klk1c2* [53]. Direct interactions between *Klk1c2* or *Klk1* and the Kinin B2 receptor are critical factors responsible for cardioprotective responses. The activation of this pathway is known to inhibit oxidative stress, apoptosis, and inflammation, as well as cardiac hypertrophy and fibrosis [54]. These ligand-receptor interactions result in improved cardiac function and lead to reduced blood pressure [54]. In our study, OM administration resulted in an increased expression of *Klk1*, *Klk1c2*, and *Klk8*. In the present study, increases in all these three proteases may allow the heart to develop a combined adaptive response to OM [50]. The bradykinin receptor family includes two G protein-coupled receptors (*Bdkrb1* and *Bkrbr2*) that also mediate the biological effects of kinins [55]. *Bdkrb1* is expressed and synthesized *de novo*, in response to tissue injury and inflammation [56]. *Bdkrb2* is the main receptor for bradykinin; it interacts

directly with AT2 [56], as well as other receptors [55]. While signaling, both *Bdkrb1* and *Bdkrb2* induce NO production [55], and their overall physiological and pathophysiological significance remain unknown [55]. Cardioprotective effects mediated by *Bdkrb1* or *Bdkrb2* alone via ACE-inhibition have been reported [55]. Endothelial overexpression of *Bdkrb1* in rat models has resulted in an expanded LV cavity and reduced function [57]. Bradykinin-mediated upregulation of *Bdkrb2* in the absence of *Bdkrb1* did not provide full cardioprotection. Interestingly, the upregulation of *Bdkrb1*, in the absence of *Bdkrb2*, results in further tissue damage [58]. In the present study, the administration of OM resulted in increased expression of both *Bdkrb1* and *Bdkrb2* and could, therefore, suggest potential cardioprotective effects.

The L-type  $\text{Ca}^{2+}$  channel  $\alpha 1\text{C}$ -subunit gene (*Cacna1c*) plays an essential role in cardiac excitation–contraction coupling [59]. This protein is localized in the T-tubule sarcolemma, adjacent to RYR2, where it controls  $\text{Ca}^{2+}$  influx from the extracellular milieu into the cytosol and, thus, serves as a major determinant of cardiac function.  $\beta$ -adrenergic receptor stimulation increases the number of L-type channels at the sarcolemma, which results in enhanced  $\text{Ca}^{2+}$  influx and amplification of excitation–contraction coupling [60]. Prolonged AT1 signaling via reduced L-type  $\text{Ca}^{2+}$  channels results in a negative inotropic effect [60].  $\text{Ca}^{2+}$ -calmodulin-dependent protein kinase II (CaMKII) activity controls the expression of *Cacna1c* in isolated rat neonatal ventricular cardiomyocytes [38]. In the present study, the administration of OM increased the expression of *Cacna1c*, although this resulted in no modification of the *Serca2*, *RYR2*, *GLUT1*, or *CamkII* expressions; these have been all implicated in maintaining  $\text{Ca}^{2+}$  homeostasis. In canine LV monocytes, OM has been recently shown to affect intracellular  $\text{Ca}^{2+}$  homeostasis by increasing the capacity of RYR2 to remain open, therefore impacting cardiomyocyte repolarization [61]. However, it seems that *Cacna1c* would provide only minor contributions to intracellular  $\text{Ca}^{2+}$  release. Administration of OM did not result in a significant increase in the concentration of cytosolic  $\text{Ca}^{2+}$ . The increase in *Cacna1c* expression in response to OM might, instead, be related to a diastolic  $\text{Ca}^{2+}$  leak from the sarcoplasmic reticulum [38]. Low-level  $\text{Ca}^{2+}$  release induced by Cav1.2  $\alpha 1$  may serve to restore and maintain  $\text{Ca}^{2+}$  levels that resulted from the leak in the SR [62]. As previously reported [39], permeabilized human cardiomyocytes exhibited a marked reduction in the rate of force generation and relaxation once the  $\text{Ca}^{2+}$  concentration reached a steady state in permeabilized human cardiomyocytes. Collectively, these findings suggest the existence of a previously unidentified action of OM in promoting  $\text{Ca}^{2+}$  regulation at the actin-myosin complex.

The present study has several limitations. Although the effects of OM are concentration-, time-, and species-dependent [23], only one set of experimental conditions was examined here. Furthermore, the experimental data were obtained in healthy rats. Thus, caution is appropriate when extrapolating these data to humans. In addition, the evaluation was performed at gene level and may not correspond directly with protein levels *in vivo*. Future studies should be performed in experimental models with LV pathology to better understand the effects of OM in this context.

In conclusion, OM infusion in rats resulted in a gene expression profile suggesting myocardial LV preservation against apoptosis and oxidative stress, together with an increased fatty acid oxidation that may be compatible with an increased  $\text{O}_2$  consumption rate. Interestingly, the administration of OM did not induce any changes in the LV expression of the genes involved in  $\text{Ca}^{2+}$  homeostasis and its associated contraction. It will be critical to design future studies built on these findings to understand the precise mechanisms of action underlying OM.

**Author Contributions:** B.E.O. Conceptualization, methodology, writing—original draft, writing—review and editing, investigation. L.D. validation, writing—review and editing. P.V.d.B. funding acquisition, writing—review and editing, supervision, validation. G.H. data curation, resources. C.M. formal analysis, software. P.J. data curation, investigation. C.S. software, visualization. K.M.E. Conceptualization, methodology, project administration, supervision. F.V.E. funding acquisition, resources, supervision, validation. All authors have read and agreed to the published version of the manuscript.

**Funding:** This study was supported and funded by the Fonds pour la Chirurgie Cardiaque, Brussels, Belgium grant number 489639.

**Institutional Review Board Statement:** The experimental protocol was approved by the Institutional Animal Care and Use Committee of the Université Libre de Bruxelles (Brussels, Belgium). Studies were conducted in accordance with the Guide for the Care and Use of Laboratory Animals published by the National Institutes of Health (NIH Publication No. 85-23; revised 1996).

**Informed Consent Statement:** Not applicable.

**Data Availability Statement:** All experiments were conducted in the Physiology and Pharmacology Laboratory of the Université Libre de Bruxelles (Brussels, Belgium). All data are available and accessible upon request.

**Conflicts of Interest:** The authors declare no conflict of interest.

## References

1. Mozaffarian, D.; Benjamin, E.J.; Go, A.S.; Arnett, D.K.; Blaha, M.J.; Cushman, M.; de Ferranti, S.; Després, J.P.; Fullerton, H.J.; Howard, V.J.; et al. Heart disease and stroke statistics—2015 update: A report from the American Heart Association. *Circulation* **2015**, *131*, e29–e322. [CrossRef] [PubMed]
2. Adams, K.F., Jr.; Fonarow, G.C.; Emerman, C.L.; LeJemtel, T.H.; Costanzo, M.R.; Abraham, W.T.; Berkowitz, R.L.; Galvao, M.; Horton, D.P.; ADHERE Scientific Advisory Committee and Investigators. Characteristics and outcomes of patients hospitalized for heart failure in the United States: Rationale, design, and preliminary observations from the first 100,000 cases in the Acute Decompensated Heart Failure National Registry (ADHERE). *Am. Heart J.* **2005**, *149*, 209–216. [CrossRef] [PubMed]
3. Follath, F.; Cleland, J.G.; Just, H.; Papp, J.G.; Scholz, H.; Peuhkurinen, K.; Harjola, V.P.; Mitrovic, V.; Abdalla, M.; Sandell, E.P.; et al. Efficacy and safety of intravenous levosimendan compared with dobutamine in severe low-output heart failure (the LIDO study): A randomised double-blind trial. Steering Committee and Investigators of the Levosimendan Infusion versus Dobutamine (LIDO) Study. *Lancet* **2002**, *360*, 196–202. [CrossRef]
4. Song, L.S.; Wang, S.Q.; Xiao, R.P.; Spurgeon, H.; Lakatta, E.G.; Cheng, H. beta-Adrenergic stimulation synchronizes intracellular Ca(2+) release during excitation-contraction coupling in cardiac myocytes. *Circ. Res.* **2001**, *88*, 794–801. [CrossRef] [PubMed]
5. Bristow, M.R. Treatment of chronic heart failure with beta-adrenergic receptor antagonists: A convergence of receptor pharmacology and clinical cardiology. *Circ. Res.* **2011**, *109*, 1176–1194. [CrossRef] [PubMed]
6. Stapel, B.; Kohlhaas, M.; Ricke-Hoch, M.; Haghikia, A.; Erschow, S.; Knuuti, J.; Silvola, J.M.U.; Roivainen, A.; Saraste, A.; Nickel, A.G.; et al. Low STAT3 expression sensitizes to toxic effects of  $\beta$ -adrenergic receptor stimulation in peripartum cardiomyopathy. *Eur. Heart J.* **2017**, *38*, 349–361. [CrossRef]
7. Malik, F.I.; Hartman, J.J.; Elias, K.A.; Morgan, B.P.; Rodriguez, H.; Brejc, K.; Anderson, R.L.; Sueoka, S.H.; Lee, K.H.; Finer, J.T.; et al. Cardiac Myosin Activation: A Potential Therapeutic Approach for Systolic Heart Failure. *Science* **2011**, *331*, 1439–1443. [CrossRef]
8. Shen, Y.-T.; Malik, F.I.; Zhao, X.; Depre, C.; Dhar, S.K.; Abarzúa, P.; Morgans, D.J.; Vatner, S.F. Improvement of Cardiac Function by a Cardiac Myosin Activator in Conscious Dogs With Systolic Heart Failure. *Circ. Heart Fail.* **2010**, *3*, 522–527. [CrossRef]
9. Liu, Y.; White, H.D.; Belknap, B.; Winkelmann, D.A.; Forgacs, E. Omecamtiv Mecarbil Modulates the Kinetic and Motile Properties of Porcine  $\beta$ -Cardiac Myosin. *Biochemistry* **2015**, *54*, 1963–1975. [CrossRef]
10. Bakkehaug, J.P.; Kildal, A.B.; Engstad, E.T.; Boardman, N.; Næsheim, T.; Rønning, L.; Aasum, E.; Larsen, T.S.; Myrmet, T.; How, O.-J. Myosin Activator Omecamtiv Mecarbil Increases Myocardial Oxygen Consumption and Impairs Cardiac Efficiency Mediated by Resting Myosin ATPase Activity. *Circ. Heart Fail.* **2015**, *8*, 766–775. [CrossRef]
11. Nagy, L.; Kovács, A.; Bódi, B.; Pásztor, E.T.; Fülöp, G.; Tóth, A.; Édes, I.; Papp, Z. The novel cardiac myosin activator omecamtiv mecarbil increases the calcium sensitivity of force production in isolated cardiomyocytes and skeletal muscle fibres of the rat. *Br. J. Pharmacol.* **2015**, *172*, 4506–4518. [CrossRef] [PubMed]
12. Utter, M.S.; Ryba, D.; Li, B.H.; Wolska, B.M.; Solaro, R.J. Omecamtiv Mecarbil, a Cardiac Myosin Activator, Increases Ca<sup>2+</sup> Sensitivity in Myofilaments With a Dilated Cardiomyopathy Mutant Tropomyosin E54K. *J. Cardiovasc. Pharmacol.* **2015**, *66*, 347–353. [CrossRef]
13. Anderson, R.L.; Sueoka, S.H.; Rodriguez, H.M.; Lee, K.H.; Cox, D.R.; Kawas, R.; Morgan, B.P.; Sakowicz, R.; Morgans, D.J.; Malik, F.; et al. In vitro and in vivo efficacy of the cardiac myosin activator CK-1827452. *Mol. Bio. Cell* **2005**, *16*. Available online: [https://cytokinetics.com/wp-content/uploads/2015/10/ASCB\\_1728.pdf](https://cytokinetics.com/wp-content/uploads/2015/10/ASCB_1728.pdf) (accessed on 19 December 2022).
14. Nagueh, S.F.; Smiseth, O.A.; Appleton, C.P.; Byrd, B.F., 3rd; Dokainish, H.; Edvardsen, T.; Flachskampf, F.A.; Gillebert, T.C.; Klein, A.L.; Lancellotti, P.; et al. Recommendations for the Evaluation of Left Ventricular Diastolic Function by Echocardiography: An Update from the American Society of Echocardiography and the European Association of Cardiovascular Imaging. *J. Am. Soc. Echocardiogr.* **2016**, *29*, 277–314. [CrossRef] [PubMed]

15. Pfaffla, M.W. A new mathematical model for relative quantification in real-time RT-PCR. *Nucleic Acids Res.* **2001**, *29*, e45. [CrossRef] [PubMed]
16. El-Oumeiri, B.; Mc Entee, K.; Annoni, F.; Herpain, A.; Eynden, F.V.; Jespers, P.; Van Nooten, G.; Van De Borne, P. Effects of the cardiac myosin activator Omecamtiv-mecarbil on severe chronic aortic regurgitation in Wistar rats. *BMC Cardiovasc. Disord.* **2018**, *18*, 99. [CrossRef] [PubMed]
17. Letai, A.; Bassik, M.C.; Walensky, L.D.; Sorcinelli, M.D.; Weiler, S.; Korsmeyer, S.J. Distinct BH3 domains either sensitize or activate mitochondrial apoptosis, serving as prototype cancer therapeutics. *Cancer Cell* **2002**, *2*, 183–192. [CrossRef]
18. Machado, A.R.T.; Aissa, A.F.; Ribeiro, D.L.; Hernandez, L.C.; Machado, C.S.; Bianchi, M.L.P.; Sampaio, S.V.; Antunes, L.M.G. The toxin BjuuuLAAO-II induces oxidative stress and DNA damage, upregulates the inflammatory cytokine genes TNF and IL6, and downregulates the apoptotic-related genes BAX, BCL2 and RELA in human Caco-2 cells. *Int. J. Biol. Macromol.* **2018**, *109*, 212–219. [CrossRef]
19. Jarskog, L.F.; Selinger, E.S.; Lieberman, J.A.; Gilmore, J.H. Apoptotic proteins in the temporal cortex in schizophrenia: High Bax/Bcl-2 ratio without caspase-3 activation. *Am. J. Psychiatry* **2004**, *161*, 109–115. [CrossRef]
20. Dostanic, S.; Servant, N.; Wang, C.; E Chalifour, L. Chronic  $\beta$ -adrenoreceptor stimulation in vivo decreased Bcl-2 and increased Bax expression but did not activate apoptotic pathways in mouse heart. *Can. J. Physiol. Pharmacol.* **2004**, *82*, 167–174. [CrossRef]
21. Manoharan, S.; Kolanjiappan, K.; Suresh, K.; Panjamurthy, K. Lipid peroxidation & antioxidants status in patients with oral squamous cell carcinoma. *Indian J. Med. Res.* **2005**, *122*, 529–534.
22. Gozeler, M.S.; Akdemir, F.N.E.; Yildirim, S.; Sahin, A.; Eser, G.; Askin, S. Levosimendan ameliorates cisplatin-induced ototoxicity: Rat model. *Int. J. Pediatr. Otorhinolaryngol.* **2019**, *122*, 70–75. [CrossRef] [PubMed]
23. Rhoden, A.; Schulze, T.; Pietsch, N.; Christ, T.; Hansen, A.; Eschenhagen, T. Comprehensive analyses of the inotropic compound omecamtiv mecarbil in rat and human cardiac preparations. *Am. J. Physiol. Circ. Physiol.* **2022**, *322*, H373–H385. [CrossRef] [PubMed]
24. Hu, C.; Dandapat, A.; Chen, J.; Fujita, Y.; Inoue, N.; Kawase, Y.; Jishage, K.; Suzuki, H.; Sawamura, T.; Mehta, J.L. LOX-1 deletion alters signals of myocardial remodeling immediately after ischemia-reperfusion. *Cardiovasc. Res.* **2007**, *76*, 292–302. [CrossRef] [PubMed]
25. Egert, S.; Nguyen, N.; Schwaiger, M. Contribution of  $\alpha$ -Adrenergic and  $\beta$ -Adrenergic Stimulation to Ischemia-Induced Glucose Transporter (GLUT) 4 and GLUT1 Translocation in the Isolated Perfused Rat Heart. *Circ. Res.* **1999**, *84*, 1407–1415. [CrossRef] [PubMed]
26. Hall, J.L.; Stanley, W.C.; Lopaschuk, G.D.; Wisneski, J.A.; Pizzurro, R.D.; Hamilton, C.D.; McCormack, J.G. Impaired pyruvate oxidation but normal glucose uptake in diabetic pig heart during dobutamine-induced work. *Am. J. Physiol. Circ. Physiol.* **1996**, *271*, H2320–H2329. [CrossRef]
27. Sugden, M.C.; Holness, M.J. Interactive regulation of the pyruvate dehydrogenase complex and the carnitine palmitoyltransferase system. *FASEB J.* **1994**, *8*, 54–61. [CrossRef]
28. Wu, P.; Sato, J.; Zhao, Y.; Jaskiewicz, J.; Popov, M.K.; Harris, A.R. Starvation and diabetes increase the amount of pyruvate dehydrogenase kinase isoenzyme 4 in rat heart. *Biochem. J.* **1998**, *329*, 197–201. [CrossRef]
29. Pettersen, I.K.N.; Tusubira, D.; Ashrafi, H.; Dyrstad, S.E.; Hansen, L.; Liu, X.Z.; Nilsson, L.I.H.; Løvsetten, N.G.; Berge, K.; Wergedahl, H.; et al. Upregulated PDK4 expression is a sensitive marker of increased fatty acid oxidation. *Mitochondrion* **2019**, *49*, 97–110. [CrossRef]
30. Sawamura, T.; Kume, N.; Aoyama, T.; Moriwaki, H.; Hoshikawa, H.; Aiba, Y.; Tanaka, T.; Miwa, S.; Katsura, Y.; Kita, T.; et al. An endothelial receptor for oxidized low-density lipoprotein. *Nature* **1997**, *386*, 73–77. [CrossRef]
31. Li, D.Y.; Zhang, Y.C.; Philips, M.I.; Sawamura, T.; Mehta, J.L. Upregulation of Endothelial Receptor for Oxidized Low-Density Lipoprotein (LOX-1) in Cultured Human Coronary Artery Endothelial Cells by Angiotensin II Type 1 Receptor Activation. *Circ. Res.* **1999**, *84*, 1043–1049. [CrossRef]
32. Murase, T.; Kume, N.; Korenaga, R.; Ando, J.; Sawamura, T.; Masaki, T.; Kita, T. Fluid Shear Stress Transcriptionally Induces Lectin-like Oxidized LDL Receptor-1 in Vascular Endothelial Cells. *Circ. Res.* **1998**, *83*, 328–333. [CrossRef] [PubMed]
33. Li, D.; Williams, V.; Liu, L.; Chen, H.; Sawamura, T.; Antakli, T.; Mehta, J.L. Mehta LOX-1 inhibition in myocardial ischemia-reperfusion injury: Modulation of MMP-1 and inflammation. *Am. J. Physiol. Heart Circ. Physiol.* **2002**, *283*, H1795–H1801. [CrossRef] [PubMed]
34. Kuhn, H.; O'Donnell, V.B. Inflammation and immune regulation by 12/15-lipoxygenases. *Prog. Lipid Res.* **2006**, *45*, 334–356. [CrossRef] [PubMed]
35. Kayama, Y.; Minamino, T.; Toko, H.; Sakamoto, M.; Shimizu, I.; Takahashi, H.; Okada, S.; Tateno, K.; Moriya, J.; Yokoyama, M.; et al. Cardiac 12/15 lipoxygenase-induced inflammation is involved in heart failure. *J. Exp. Med.* **2009**, *206*, 1565–1574. [CrossRef]
36. Takaya, T.; Wada, H.; Morimoto, T.; Sunagawa, Y.; Kawamura, T.; Takanabe-Mori, R.; Shimatsu, A.; Fujita, Y.; Sato, Y.; Fujita, M.; et al. Left Ventricular Expression of Lectin-Like Oxidized Low-Density Lipoprotein Receptor-1 in Failing Rat Hearts. *Circ. J.* **2010**, *74*, 723–729. [CrossRef]

37. Zendaoui, A.; Lachance, D.; Roussel, E.; Couet, J.; Arsenault, M. Effects of spironolactone treatment on an experimental model of chronic aortic valve regurgitation. *J. Heart Valve Dis.* **2012**, *21*, 478–486.
38. Nánási, P., Jr.; Gaburjakova, M.; Gaburjakova, J.; Almássy, J. Omecamtiv mecarbil activates ryanodine receptors from canine cardiac but not skeletal muscle. *Eur. J. Pharmacol.* **2017**, *809*, 73–79. [[CrossRef](#)]
39. Fülöp, G.; Oláh, A.; Csipo, T.; Kovács, Á.; Pórszász, R.; Veress, R.; Horváth, B.; Nagy, L.; Bódi, B.; Fagyas, M.; et al. Omecamtiv mecarbil evokes diastolic dysfunction and leads to periodic electromechanical alternans. *Basic Res. Cardiol.* **2021**, *116*, 24. [[CrossRef](#)]
40. Cassis, P.; Conti, S.; Remuzzi, G.; Benigni, A. Angiotensin receptors as determinants of life span. *Pflügers Arch.-Eur. J. Physiol.* **2010**, *459*, 325–332. [[CrossRef](#)]
41. Namsolleck, P.; Recarti, C.; Foulquier, S.; Steckelings, U.M.; Unger, T. AT(2) receptor and tissue injury: Therapeutic implications. *Curr. Hypertens. Rep.* **2014**, *16*, 416. [[CrossRef](#)] [[PubMed](#)]
42. Escobales, N.; Nuñez, R.E.; Javadov, S. Mitochondrial angiotensin receptors and cardioprotective pathways. *Am. J. Physiol. Heart Circ. Physiol.* **2019**, *316*, H1426–H1438. [[CrossRef](#)]
43. Cho, H.J.; Xie, Q.W.; Calaycay, J.; Mumford, R.A.; Swiderek, K.M.; Lee, T.D.; Nathan, C. Calmodulin is a subunit of nitric oxide synthase from macrophages. *J. Exp. Med.* **1992**, *176*, 599–604. [[CrossRef](#)] [[PubMed](#)]
44. Ziolo, M.T.; Harshbarger, C.H.; Roycroft, K.E.; Smith, J.M.; Romano, F.D.; Sondgeroth, K.L.; Wahler, G.M. Myocytes Isolated from Rejecting Transplanted Rat Hearts Exhibit a Nitric Oxide-mediated Reduction in the Calcium Current. *J. Mol. Cell. Cardiol.* **2001**, *33*, 1691–1699. [[CrossRef](#)] [[PubMed](#)]
45. Wildhirt, S.M.; Weismueller, S.; Schulze, C.; Conrad, N.; Kornberg, A.; Reichart, B. Inducible nitric oxide synthase activation after ischemia/reperfusion contributes to myocardial dysfunction and extent of infarct size in rabbits: Evidence for a late phase of nitric oxide-mediated reperfusion injury. *Cardiovasc. Res.* **1999**, *43*, 698–711. [[CrossRef](#)]
46. Ziolo, M.T.; Maier, L.S.; Piacentino, V., 3rd; Bossuyt, J.; Houser, S.R.; Bers, D.M. Myocyte nitric oxide synthase 2 contributes to blunted beta-adrenergic response in failing human hearts by decreasing Ca<sup>2+</sup> transients. *Circulation* **2004**, *109*, 1886–1891. [[CrossRef](#)]
47. Heymes, C.; Vanderheyden, M.; Bronzwaer, J.G.; Shah, A.M.; Paulus, W.J. Endomyocardial nitric oxide synthase and left ventricular preload reserve in dilated cardiomyopathy. *Circulation* **1999**, *99*, 3009–3016. [[CrossRef](#)]
48. Paulus, W.J. Beneficial effects of nitric oxide on cardiac diastolic function: ‘The flip side of the coin’. *Heart Fail. Rev.* **2000**, *5*, 337–344. [[CrossRef](#)]
49. Cao, B.; Yu, Q.; Zhao, W.; Tang, Z.; Cong, B.; Du, J.; Lu, J.; Zhu, X.; Ni, X. Kallikrein-related peptidase 8 is expressed in myocardium and induces cardiac hypertrophy. *Sci. Rep.* **2016**, *7*, 20024. [[CrossRef](#)]
50. Huang, M.; Du, J.; Wang, Y.; Ma, S.; Hu, T.; Shang, J.; Yu, Q.; Zhu, X.; Zhang, G.; Cong, B. Tissue kallikrein-related peptidase8 protects rat heart against acute ischemia reperfusion injury. *Int. J. Biol. Macromol.* **2019**, *140*, 1126–1133. [[CrossRef](#)]
51. Rougeot, C.; Rosinski-Chupin, I.; Mathison, R.; Rougeon, F. Rodent submandibular gland peptide hormones and other biologically active peptides. *Peptides* **2000**, *21*, 443–455. [[CrossRef](#)]
52. Borges, J.C.; Silva, J.; Gomes, M.A.; Lomez, E.S.L.; Leite, K.M.; Araujo, R.C.; Bader, M.; Pesquero, J.B.; Pesquero, J.L. Tonin in rat heart with experimental hypertrophy. *Am. J. Physiol. Circ. Physiol.* **2003**, *284*, H2263–H2268. [[CrossRef](#)] [[PubMed](#)]
53. Damasceno, D.D.; Lima, M.P.; Motta, D.F.; Ferreira, A.J.; Quintão-Junior, J.F.; Drummond, L.R.; Natali, A.J.; Almeida, A.P.; Pesquero, J.L. Cardiovascular and electrocardiographic parameters after tonin administration in Wistar rats. *Regul. Pept.* **2013**, *181*, 30–36. [[CrossRef](#)] [[PubMed](#)]
54. Chao, J.; Shen, B.; Gao, L.; Xia, C.-F.; Bledsoe, G.; Chao, L. Tissue kallikrein in cardiovascular, cerebrovascular and renal diseases and skin wound healing. *Biol. Chem.* **2010**, *391*, 345–355. [[CrossRef](#)] [[PubMed](#)]
55. Hamid, S.; Rhaleb, I.; Kassem, K.; Rhaleb, N.-E. Role of Kinins in Hypertension and Heart Failure. *Pharmaceuticals* **2020**, *13*, 347. [[CrossRef](#)] [[PubMed](#)]
56. Abadir, P.M.; Periasamy, A.; Carey, R.M.; Siragy, H.M. Angiotensin II type 2 receptor-bradykinin B2 receptor functional heterodimerization. *Hypertension* **2006**, *48*, 316–322. [[CrossRef](#)]
57. Levy, R.F.; Serra, A.J.; Antonio, E.L.; Dos Santos, L.; Bocalini, D.S.; Pesquero, J.B.; Bader, M.; Merino, V.F.; De Oliveira, H.A.; Veiga, E.C.D.A.; et al. Cardiac Morphofunctional Characteristics of Transgenic Rats with Overexpression of the Bradykinin B1 Receptor in the Endothelium. *Physiol. Res.* **2017**, *925*–932. [[CrossRef](#)] [[PubMed](#)]
58. Duka, A.; Kintsurashvili, E.; Duka, I.; Ona, D.; Hopkins, T.A.; Bader, M.; Gavras, I.; Gavras, H. Angiotensin-converting enzyme inhibition after experimental myocardial infarct: Role of the kinin B1 and B2 receptors. *Hypertension* **2008**, *51*, 1352–1357. [[CrossRef](#)]
59. Zamponi, G.; Striessnig, J.; Koschak, A.; Dolphin, A.C. The Physiology, Pathology, and Pharmacology of Voltage-Gated Calcium Channels and Their Future Therapeutic Potential. *Pharmacol. Rev.* **2015**, *67*, 821–870. [[CrossRef](#)]
60. Westhoff, M.; Dixon, R.E. Mechanisms and Regulation of Cardiac CaV1.2 Trafficking. *Int. J. Mol. Sci.* **2021**, *22*, 5927. [[CrossRef](#)]

61. Szentandrassy, N.; Horvath, B.; Vaczi, K.; Kistamas, K.; Masuda, L.; Magyar, J.; Banyasz, T.; Papp, Z.; Nanasi, P.P. Dose-dependent electrophysiological effects of the myosin activator omecamtiv mecarbil in canine ventricular cardiomyocytes. *J. Physiol. Pharmacol. Off. J. Pol. Physiol. Soc.* **2016**, *67*, 483–489.
62. Christel, C.J.; Cardona, N.; Mesirca, P.; Herrmann, S.; Hofmann, F.; Striessnig, J.; Ludwig, A.; Mangoni, M.E.; Lee, A. Distinct localization and modulation of Cav1.2 and Cav1.3 L-type Ca<sup>2+</sup> channels in mouse sinoatrial node. *J. Physiol.* **2012**, *590*, 6327–6342. [[CrossRef](#)] [[PubMed](#)]

**Disclaimer/Publisher’s Note:** The statements, opinions and data contained in all publications are solely those of the individual author(s) and contributor(s) and not of MDPI and/or the editor(s). MDPI and/or the editor(s) disclaim responsibility for any injury to people or property resulting from any ideas, methods, instructions or products referred to in the content.

## 12. APPENDIX E

### **Gene profiling of left ventricle in experimental model of combined volume and pressure overload in rats (Submitted manuscripts)**

Bachar El Oumeiri<sup>1</sup>, Laurence Dewachter<sup>2</sup>, Philippe van de Borne<sup>3</sup>, Géraldine Hubesch<sup>2</sup>, Pascale Jaspers<sup>2</sup>, Constantin Stefanidis<sup>1</sup>, Kathleen Mc Entee<sup>2</sup>, Frédéric Vanden Eynden<sup>1</sup>

<sup>1</sup> Department of Cardiac Surgery, Université Libre de Bruxelles (ULB) Erasme University Hospital, Brussels, Belgium

<sup>2</sup> Laboratory of Physiology and Pharmacology, Faculty of Medicine, Université Libre de Bruxelles, Brussels, Belgium

<sup>3</sup> Department of Cardiology, ULB Erasme University Hospital, Brussels, Belgium

Corresponding author: Bachar El Oumeiri, MD

Department of Cardiac Surgery

ULB Hopital Universitaire Erasme

Route de Lennik, 808

1070-Brussels

Belgium

Email : Bachar.el.oumeiri@hubruxelles.be



## ***Abstract***

To explore the impact of combined volume and pressure overload on the gene expression profile in adult male rats. Eighteen male Wistar rats were included in our study. Ten rats have aortic regurgitation (AR) created two months before and eight rats served as control group. Rats with AR and the group control received equal volumes (12 ml/kg body weight) of 0.9% NaCl, respectively, via a 30 min infusion through the femoral vein. Echocardiography was performed before and after saline infusion. Seven days after infusion, rats were euthanized, and left ventricular (LV) tissues were removed for *real-time* quantitative polymerase chain reaction (RTq-PCR) experiments. After saline infusion, pro-apoptotic *Bax*-to-*Bcl2* ratio was increased, with increased *Bax* gene expression. The gene expression of molecules regulating oxidative stress, including glutathione superoxide dismutases (*Sod1*) remained unchanged, (*Sod2*) decreased whereas the expression of antioxidant glutathione peroxidase (*Gpx*) increased. While LV gene expression of key energy sensors, peroxisome proliferator activator (*Ppar*)  $\alpha$  remained unchanged, (*Ppar*)  $\gamma$ , AMP-activated protein kinase (*Ampk*), decreased after saline infusion. The LV expression of the major myocardial glucose transporter *Glut1* and *Glut4* expression remained unchanged, whereas the LV expression of oxidized low-density lipoprotein receptor 1 (*Olr1*) and arachidonate 15-lipoxygenase (*Alox15*) increased, with no changes in fatty acid transporter *Cd36*. The Kalikrein-bradykinin system, LV expression of kallikrein-related peptidases *Klk8* and bradykinin receptors B1 and B2 (*Bdkrb1* and *Bdkrb2*) remained unchanged, whereas the LV expression of *Klk10* increased. LV expression in major molecular determinants involved in calcium-dependent myocardial contraction remained unchanged, except for a decreased LV expression of ATPase sarcoplasmic/endoplasmic reticulum  $\text{Ca}^{2+}$  transporting 2 (*Serca2a*) in response to saline infusion. A single intravenous infusion of saline solution, in adult rats with chronic severe aortic regurgitation, resulted in significant changes in the LV expression of genes regulating apoptosis, oxidative stress, metabolism, and cardiac contractility.

**Keywords:** left ventricle, gene expression, apoptosis, metabolism, oxidative stress

## Introduction

Chronic severe Aortic regurgitation (AR) imposes a combined volume and pressure overload on the left ventricle (LV) (1). The volume overload is a consequence of the regurgitant volume itself and is therefore directly related to the severity of the leak. The pressure overload results from systolic hypertension, which occurs as a result of increased total aortic stroke volume because both the regurgitant volume and the forward stroke volume are ejected into the aorta during systole (2). In early, compensated severe AR, the LV adapts to the volume overload by eccentric hypertrophy, in which sarcomeres are laid down in series and myofibers are elongated (3), in addition eccentric hypertrophy increases LV mass, such that the LV volume/mass ratio is normal, and LV ejection fraction (LVEF) is maintained by increased preload (1). AR is associated with a long asymptomatic period during which the LV progressively dilates and hypertrophies in response to chronic volume overload, this process is accompanied by a decrease in LV function, occurrence of symptoms, and eventually heart failure (4). No medical therapy has yet been clearly shown to be effective to slow dilation, hypertrophy, and loss of function or to have any impact on morbidity or mortality (5), the role of medical, particularly vasodilators are primarily to decrease systolic hypertension and delay the onset of LV dysfunction in asymptomatic patients. The Framingham heart study reported that the overall prevalence of AR was 13% in men and 8.5% in women (6). It's anticipated that the prevalence of AR will increase even further due to the rapidly growing aged population worldwide (7). The pathophysiological mechanisms involved in chronic AR remain not fully elucidated (8). Gene expression profiles have been established in several animals' models of LV eccentric hypertrophy, including by us in a rat model after short (2-weeks) and late stage of the disease (9 months) (8,9,10).

Considering that AR is a chronic condition often evolving over decades in human, the study of animals are of great interest. We present here the study of LV gene expression profiling in a combined model of pressure and volume overload caused by severe aortic valve regurgitation in male Wistar rats. We examine gene expression in the rat myocardium, with a

particular emphasis on pathways associated with apoptosis, oxidative stress, metabolism, and calcium- mediated cardiac contractility.

## **Methods**

### **Animal model and experimental design**

The experimental protocol was approved by the Institutional Animal Care and Use Committee of the Faculty of Medicine of the Université Libre de Bruxelles (ULB; Brussels, Belgium; protocol acceptance number: 644N). Experiments were conducted in accordance with the Guide for the Care and Use of Laboratory Animals published by the United States National Institutes of Health (NIH Publication No. 85-23; revised 1996). Our study included 18 males adult Wistar rats (Janvier, Le Genest-Saint-Isle, France). Ten rats (mean body weight:  $577 \pm 24$  g) has aortic regurgitation (AR) created two months before AR was induced under general anesthesia (1.5% inhaled isoflurane) by retrograde puncture of the aortic valve leaflet as previously described (11). The other group (n=8) served as control group (mean body weight:  $536 \pm 39$  g). Rats with AR (n = 10) and the group control (n = 8) received equal volumes (12 ml/kg body weight) of 0.9% NaCl, respectively, via a 30 min infusion through the femoral vein. Seven days after saline infusion rats were sacrificed by exsanguination via section of the abdominal aorta. The hearts were rapidly harvested and dissected to isolate the LV, which was snap-frozen in liquid nitrogen and stored at  $-80^{\circ}\text{C}$  for further biological analysis.

### **Echocardiography and cardiac measurements**

Transthoracic 2D, M-mode, and Doppler echocardiography was performed using an ultrasound scanner (Vivid-E90, GE Healthcare, Wauwatosa, WI, USA) equipped with a 12-MHz phased-array transducer (GE 12S-D, GE Healthcare) in anesthetized rats (with inhaled 1.5% isoflurane). All echocardiographic measurements were obtained by the same observer according to the American Society of Echocardiography guidelines (12). Standard right parasternal (long and short axis) and left apical parasternal views were used for data acquisition. Fractional shortening (FS) was calculated using the formula (FS = LVEDD –

LVESD/LVEDD x 100) in M-mode from a LV short-axis view. Ejection fraction (EF) was derived using the Teicholz formula. Electrocardiogram was monitored via limb leads throughout the procedure. Aortic flow was measured from the left apical view to calculate forward stroke volume (SV) and cardiac output (CO), and to measure pre-ejection period (PEP: delay from Q wave of QRS to aortic opening; msec), LV ejection time (LVET: interval from beginning to termination of aortic flow; msec), and inter-beat interval (RR; msec). Systolic time (msec) was determined as PEP + LVET (msec), and diastolic time (msec) was calculated as RR interval – systolic time. Echocardiography was performed before and 30-min after saline administration.

### **Real-time quantitative polymerase chain reaction (RTq-PCR)**

Total RNA was extracted from snap-frozen LV myocardial tissue using TRIzol reagent (Invitrogen, Merelbeke, Belgium) followed by a chloroform/ethanol extraction and a final purification using QIAGEN RNeasy® Mini kit (QIAGEN, Hilden, Germany), according to manufacturer's instructions. RNA concentration was determined by standard spectrophotometric techniques, using a spectrophotometer Nanodrop® (ND-1000; Isogen Life Sciences, De Meern, The Netherlands) and RNA integrity was assessed by visual inspection of GelRed (Biotium, Hayward, California)-stained agarose gels. Reverse transcription was performed using random hexamer primers and Superscript II Reverse Transcriptase (Invitrogen, Merelbeke, Belgium) according to the manufacturer's instructions. Gene-specific sense and antisense primers for RTq-PCR (Table 1) were designed using the Primer3 program for *rattus norvegicus* gene sequences, including those for B-cell lymphoma 2 (Bcl2), Bcl2 associated X apoptosis regulator (Bax), glutathione peroxidase (Gpx), glutathione-disulfide reductase (Gsr), superoxide dismutases 1 and 2 (Sod1 and Sod2), AMP-activated protein kinase (Ampk), peroxisome proliferator-activated receptors alpha and gamma (Ppar alpha and gamma), solute carrier family 2 members 1 (Slc2a1, also known as Glut1) and 4 (Slc2a4 or Glut4), fatty acid transporter Cd36, oxidized low-density lipoprotein

receptor 1 (Olr1, also known as Lox1), arachidonate 15-lipoxygenase (Alox15), kallikrein related-peptidases 8 and 10 (Klk8 and Klk10), bradykinin receptors B1 and B2 (Bdkrb1 and Bdkrb2), ATPase sarcoplasmic/endoplasmic reticulum Ca<sup>2+</sup> transporting 2 (Atp2a2, also called Serca2), ryanodine receptor 2 (Ryr2), calcium voltage-gated channel subunit alpha1C (Cacna1c), glyceraldehyde-3-phosphate dehydrogenase (Gapdh) and hypoxanthine phosphoribosyltransferase 1 (Hprt1) used as housekeeping genes.

Intron-spanning primers were selected whenever possible to avoid inappropriate amplification of contaminant genomic DNA. Amplification reactions were performed in duplicate using SYBRGreen PCR Master Mix (Quanta Biosciences, Gaithersburg, MD, USA), specific primers, and diluted template cDNA. Analysis of the results was performed using an iCycler System (BioRad Laboratories, Hercules, CA, USA). Relative quantification was achieved using the Pfaffl method (13) by normalization with the housekeeping genes, Gapdh and Hprt1.

### **Statistical analysis**

Results are presented as mean ± standard deviation (SD) with “n” representing the number of individual data points. The echocardiographic data were compared using Student’s t-test for repeated measures (n = 10) before and after saline perfusion. The RTq-PCR data evaluating LV gene expression, were compared using Student’s t-test for independent samples (with n = 8 in the control group and n=10 in the AR group). Statistical analyses were performed using StatView 5.0 Software. A p-value < 0.05 was considered statistically significant.

## **Results**

### **Effects of AR on LV measurements in rats**

As illustrated in Table 2 AR as confirmed by the presence of a regurgitant jet quantified as severe (PHT <200 ms).

After 2 months, AR (PHT <200 ms) was confirmed, and the presence of volume overload and eccentric hypertrophy was established echocardiographically by significant increases in LVEDD, LVESD, and LV mass (n = 10, all p < 0.001, Table.1). Load-dependent indices of LV systolic function (FS and EF) and RWT were significantly lower than baseline (p < 0.05, n = 10), whereas SV and CO were significantly higher than baseline (n = 10, both p < 0.001), wall stress was significantly higher than baseline (n=10, p <0.05)

### **Effects of saline infusion in rats with AR**

As illustrated in Table 2, infusion of saline 0.9% affected some echocardiographic parameters in rats with AR. FS was significantly higher (p < 0.05), whereas LVESD, LVESDD, and end-systolic wall stress was significantly lower (p < 0.05). Hemodynamically, NaCl infusion significantly increased systolic and diastolic blood pressures (p < 0.05), as well as PWTs and the PEP/LVET ratio (p < 0.05).

### **AR altered myocardial LV expression of genes regulating apoptosis and oxidative stress**

Myocardial LV gene expression of pro-apoptotic Bax was significantly higher in rats with AR compared to control group, whereas no difference in gene expression of anti-apoptotic Bcl2 was observed (Fig. 1A). The resulting pro-apoptotic Bax-to-Bcl2 ratio was increase in the LV of rats with AR (Fig. 1A). We also examined differential expression of genes involved in oxidative stress regulation. Myocardial expression of Gpx, an anti-oxidant enzyme, increased in the LV rats with AR, decreased Sod2 gene expression whereas no changes in Sod1 gene expression were observed (Fig. 1B).

### **AR impacted LV expression profile of key determinants of cardiac energy substrate use**

To assess the effects of AR on basal myocardial energy metabolism, we evaluated gene expression profile of transcription factors and molecules regulating cardiac glucose and fatty acid metabolism. As illustrated in Fig. 2A, myocardial LV gene expression of key energy sensors Ppar gamma and Ampk decreased. Myocardial LV expression of Slc2a1 (Glut1), the major myocardial glucose transporter remained unchanged in rats with AR, while gene expression of Slc2a4 (Glut4) decreased with AR (Fig. 2B). As illustrated in Fig. 2C, AR increased LV expression of Alox15 encoding the 12/15 lipoxygenase enzyme implicated in polyunsaturated fatty acid metabolism, and of oxidized low-density lipoprotein receptor 1 (Olr1, also known as Lox1) encoding for a scavenger receptor mediating the uptake of oxidized lipoproteins into cells, whereas gene expression of fatty acid transporter Cd36 remained unchanged.

### **AR altered LV expression of genes implicated in cardiac contractility**

As illustrated in Fig. 3A, AR did not induce a major change in LV gene expression in Kallikrein-bradykinin system except an increase in LV gene expression of KIK10. Again, after 2 months chronic severe AR did not induce major changes in gene expression of Cacna1c and RYR , except an decrease in LV gene expression of Serca2 in response to AR (Fig. 3B).



## Discussion

Induction of AR in experimental rats led to combined LV volume and pressure overload as well as significant changes in gene expression. Collectively, our findings revealed differential expression of genes that promote apoptosis (an increased *Bax/Bcl2* ratio), oxidative stress (decreased expression of *Sod2*), cardiac metabolism (decreased expression of *Glut4*, *Ampk4*, and *Ppar $\gamma$* , and increased expression of *Lox1* and *Alox15*), and Ca<sup>2+</sup>-dependent myocardial contraction (increased expression of *Klk10* and decreased expression of *Serca2a*) at t = 7 days after placebo infusion in rats with AR.

As previously reported (230), the administration of the placebo to rats with AR resulted in increases in fractional shortening (FS), cardiac output (CO), and stroke volume (SV) accompanied by decreases in LV end-systolic dimension (ESD), end-diastolic diameter (EDD), and end-systolic wall stress. Hemodynamically, placebo (saline) infusion resulted in significant increases in both systolic and diastolic blood pressures. However, we observed no significant increases in maximum wall stress, end-diastolic wall stress, or ejection fraction (EF).

The first set of profiles focused on the differential expression of the genes involved in the regulation of apoptosis. Specifically, we examined AR-induced expression of the mitochondrial anti-apoptotic protein, Bcl2, and pro-apoptotic protein, Bax (254). Bax is a well-characterized member of the Bcl-2 gene family; this protein resides in the cytosol until it has been activated by stress stimuli, whereupon it induces cell death (300). Our findings revealed a significant increase in *Bax* expression and a concomitant increase in the *Bax/Bcl2* ratio in response to AR. An elevated *Bax/Bcl2* ratio reflects a higher level of pro-apoptotic activity and an overall increased vulnerability to apoptosis (256). Our findings revealed that AR led to differential expression of the critical antioxidants *Gpx* and *Sod2* which both function to protect cells against hydroperoxide-mediated injury associated with the scavenging of reactive oxygen species (ROS) (301). As exposure to ROS can promote *Gpx* expression (298), the function of *Sod2* was to eliminate ROS and thus confer protection

against cell death (302). Animal models of hemodynamic overload exhibit chronic increases in myocardial oxidative stress which can lead to myocardial remodeling and HF (303).

Furthermore, tonic mechanical stretch of rat papillary muscle increases ROS production and thus may mediate myocyte apoptosis in this model (304). Taken together, our results suggest a link between AR and apoptotic activity at the level of gene expression.

We also evaluated the effects of AR on cardiac metabolism via the evaluation of genes involved in FA and glucose metabolism. In this study, we found that rats with AR exhibited decreased myocardial expression of *Glut4*; interestingly, *Glut1* expression remained unchanged. Both GLUT1 and GLUT4 are critical glucose transporters in the heart. Germ-line disruption of the gene encoding GLUT4 resulted in striking cardiac hypertrophy and impaired function. *Glut4* gene-deleted animals were hyper-insulinemic and exhibited profound changes in cardiac substrate delivery. Thus, it was not clear whether the observed cardiac hypertrophy was a primary or secondary consequence of *GLUT4* ablation (305). We also evaluated the differential expression of several key energy sensors, including PPARs and AMPK. AMPK detects the intracellular ATP/AMP ratio and plays a pivotal role in promoting intracellular adaptation to energy stress. Our findings revealed decreased expression of *Ampk* in rats with AR. Previous studies highlighted the contributions of local AMPK activation to cardiac protection, notably its role in accelerating ATP generation and attenuating ATP depletion to protect against cardiac dysfunction and cardiomyocyte apoptosis (306). While AMPK inactivation has been linked to the activation of apoptotic processes in cardiomyocytes (307), AMPK activation reduced cardiomyocyte apoptosis, reversed diabetic cardiomyopathy, and inhibited the development of myocardial hypertrophy (308, 309). Furthermore, AMPK regulates FA metabolism by promoting FA uptake and oxidation; it can also regulate glucose metabolism by promoting glucose uptake and glycolysis (309). Similarly, PPAR $\gamma$  regulates FA storage by stimulating lipid uptake and adipogenesis by fat cells and regulates glucose metabolism by increasing insulin sensitivity (132). Decreases in *Glut4*, *Ampk*, and *Ppar $\gamma$*  expression with no changes in the levels of *Glut1* suggest that LV tissues from rats with AR

use glucose rather than FAs as a primary source of oxidative energy.

Lox1 is a membrane scavenger receptor that contributes to endothelial cell internalization of oxidized low-density lipoprotein (ox-LDL) (150). Myocardial ischemia enhances the expression of *Lox1*, thereby promoting cardiomyocyte apoptosis, local inflammation, and fibroblast activation, thus favoring myocardial fibrosis and loss of function (310). Similar results were obtained when endothelial cells were exposed to shear stress, thus supporting a role for disrupted blood flow on Lox1-mediated mechano-transduction (152). As described in a previous report, increased expression of *Lox1* was detected in cases of diastolic dysfunction (299). Similarly, Alox15, which is a lipid-peroxidizing enzyme (269), has been implicated in the pathogenesis of atherosclerosis (150), diabetes, and neurodegenerative disease (269). The expression levels of both *Lox1* and *Alox15* were markedly increased in HF (270, 271). AR-associated diastolic dysfunction and shear stress may thus explain at least some of our results. Sarcoplasmic reticulum (SR) Ca<sup>2+</sup> pump ATPase (SERCA) plays a major role in Ca<sup>2+</sup> signaling and is involved in a significant range of cell functions including transcription, apoptosis, exocytosis, signal transduction, and cell motility (311). SERCA is responsible for the movement of Ca<sup>2+</sup> against the concentration gradient between the SR and the cytosol. SERCA 2 gene-deleted mice exhibit disrupted SR function that was associated with HF (312). Decreased SERCA2a expression was reported in both pressure (313) and chronically volume-overloaded mice (314). In this study, decreased expression of *Serca2a* observed in rats with AR correlated with findings reported in the literature.

Klk10 is a member of the kallikrein-related peptidase (KLK) family. This enzyme was initially discovered as a potential tumor suppressor that was downregulated in breast, prostate, testicular, and lung cancer (315, 316). Administration of Klk10 inhibits endothelial inflammation and the development of barrier dysfunction. It also reduces endothelial cell migration and tube formation but has no impact on apoptosis or proliferation, among other potential anti-atherogenic therapeutic targets (316).

Our results highlight an increase in *Klk10* expression in AR rats. Interestingly, results from a

previous study revealed increased expression of *Klk10* in a model volume of overload secondary to an aorta-cava fistula (317) but not in AR. This may be related to the onset of the compensatory phase of AR which includes compensatory/defense mechanisms used to prevent ventricular dysfunction.

#### Study limitations

The results of this study have to be viewed in the light of some limitations. Rodent left ventricle may differ in some aspect from humans, all the rats in our study are male or in the expression of genes in the left ventricle related to AR can be different depending on the sex (46), In addition, the evaluation was performed at gene level and may not correspond directly with protein levels in vivo. The role of various signaling pathways controlling the gene expression in the AR will need to be explored more in details

In conclusion combined pressure and volume overload in rats resulted in a gene expression profile suggesting increasing myocardial LV apoptosis and oxidative stress with an increased glucose oxidation and other gene expression suggesting left ventricle dysfunction, *klk10* augmentation maybe related to a defense mechanism.

## References

1. Bekeredjian R, Grayburn PA. Valvular heart disease: aortic regurgitation. *Circulation*. 2005 Jul 5;112(1):125-34.
2. Carabello BA. Aortic regurgitation. A lesion with similarities to both aortic stenosis and mitral regurgitation. *Circulation*. 1990 Sep;82(3):1051-3.
3. Ricci DR. Afterload mismatch and preload reserve in chronic aortic regurgitation. *Circulation*. 1982 Oct;66(4):826-34.
4. Bonow R. O. Chronic mitral regurgitation and aortic regurgitation: have indications for surgery changed? *Journal of the American College of Cardiology*. 2013;61(7):693–701.
5. Nishimura R. A., Otto C. M., Bonow R. O., et al. 2014 AHA/ACC guideline for the management of patients with valvular heart disease: a report of the American College of Cardiology/American Heart Association Task Force on Practice Guidelines. *Journal of the American College of Cardiology*. 2014;63(22):e57–e185.
6. Coffey S, Cairns BJ, Iung B. The modern epidemiology of heart valve disease. *Heart* 2016;102:75-85.
7. Kodali SK, Velagapudi P, Hahn RT, et al. Valvular Heart Disease in Patients  $\geq$ 80 Years of Age. *J Am Coll Cardiol* 2018;71:2058-72.
8. Ponikowski P, Voors AA, Anker SD, et al. 2016 ESC Guidelines for the diagnosis and treatment of acute and chronic heart failure: The Task Force for the diagnosis and treatment of acute and chronic heart failure of the European Society of Cardiology (ESC) Developed with the special contribution of the Heart Failure Association (HFA) of the ESC. *Eur Heart J* 2016;37:2129-200.
9. Champetier S, Bojmehrani A, Beaudoin J, Lachance D, Plante E, Roussel E, Couet J, Arsenault M. Gene profiling of left ventricle eccentric hypertrophy in aortic regurgitation in rats: rationale for targeting the beta-adrenergic and renin-angiotensin systems *Am J Physiol Heart Circ Physiol*. 2009 Mar;296(3):H669-77.
10. Roussel E, Drolet MC, Walsh-Wilkinson E, Dhahri W, Lachance D, Gascon S, Sarrhini O, Rousseau JA, Lecomte R, Couet J, Arsenault M. Transcriptional Changes Associated with Long-Term Left Ventricle Volume Overload in Rats: Impact on Enzymes Related to Myocardial Energy Metabolism *Biomed Res Int*. 2015;2015:949624.
11. El-Oumeiri B, McEntee K, Annoni F, Herpain A, Vanden Eynden F, Jespers P, Van Nooten G, van de Borne P. Effects of the cardiac myosin activator Omecamtiv-mecarbil on severe chronic aortic regurgitation in Wistar rats. *BMC Cardiovasc Disord*. 2018 May 21;18(1):99.
12. Nagueh SF, Smiseth OA, Appleton CP, Byrd BF 3rd, Dokainish H, Edvardsen T, Flachskampf FA, Gillebert TC, Klein AL, Lancellotti P, Marino P, Oh JK, Popescu BA,

- Waggoner AD. Recommendations for the Evaluation of Left Ventricular Diastolic Function by Echocardiography: An Update from the American Society of Echocardiography and the European Association of Cardiovascular Imaging. *J Am Soc Echocardiogr.* 2016 Apr;29(4):277-314.
13. Pfaffla MW. A new mathematical model for relative quantification in real-time RT-PCR. *Nucleic Acids Res.* 2001 May 1; 29(9): e45.
14. El Oumeiri B, van de Borne P, Hubesch G, Herpain A, Annoni F, Jespers P, Stefanidis C, Mc Entee K, Vanden Eynden F. The myosin activator omecamtiv mecarbil improves wall stress in a rat model of chronic aortic regurgitation. *Physiol Rep.* 2021 Aug;9(16): e14988
15. . Letai A., Bassik M.C., Walensky L.D., Sorcinelli M.D., Weiler S., Korsmeyer S.J. Distinct BH3 domains either sensitize or activate mitochondrial apoptosis, serving as prototype cancer therapeutics. *Cancer Cell.* 2002;2:183–192.
16. Evripidis Gavathiotis, Motoshi Suzuki, Marguerite L. Davis, Kenneth Pitter, Gregory H. Bird, Samuel G. Katz, Ho-Chou Tu, Hyungjin Kim, Emily H.-Y. Cheng, Nico Tjandra & Loren D. Walensky BAX activation is initiated at a novel interaction site *Nature* volume 455, pages1076–1081 (2008)
17. Jarskog L.F., Selinger E.S., Lieberman J.A., Gilmore J.H. Apoptotic proteins in the temporal cortex in schizophrenia: High Bax/Bcl-2 ratio without caspase-3 activation. *Am. J. Psychiatry.* 2004;161:109–115.
18. Aouacheri W, Saka S, Djafer R, Lefranc G. Protective effect of diclofenac towards the oxidative stress induced by paracetamol toxicity in rats. *Ann Biol Clin (Paris)* . 2009 Nov-Dec;67(6):619-27.
19. Hu C., Dandapat A., Chen J., Fujita Y., Inoue N., Kawase Y., Jishage K., Suzuki H., Sawamura T., Mehta J.L. LOX-1 deletion alters signals of myocardial remodeling immediately after ischemia-reperfusion. *Cardiovasc. Res.* 2007; 76:292–302.
20. Pias EK, Ekshyyan OY, Rhoads CA, Fuseler J, Harrison L, Aw TY (Apr 2003). "Differential effects of superoxide dismutase isoform expression on hydroperoxide-induced apoptosis in PC-12 cells". *The Journal of Biological Chemistry.* 278 (15): 13294–301.
21. Dhalla AK, Singal PK. Antioxidant changes in hypertrophied and failing guinea pig hearts. *Am J Physiol.* 1994; 266: H1280–H1285.
22. Cheng W, Li B, Kajstura J, Li P, Wolin MS, Sonnenblick EH, Hintze TH, Olivetti G, Anversa P. Stretch-induced programmed myocyte cell death. *J Clin Invest.* 1995; 96: 2247–2259.
23. Katz, E. B., A. E. Stenbit, K. Hatton, R. Depinho & M. J. Charron. Cardiac and adipose tissue abnormalities but not diabetes in mice deficient in GLUT4. *Nature* 377, 151-155. (1995)

24. Lee SY, Ku HC, Kuo YH, Chiu HL, Su MJ. Pyrrolidinyl caffeamide against ischemia/reperfusion injury in cardiomyocytes through AMPK/AKT pathways. *J Biomed Sci.* 2015; 22:18.
25. Zhuo XZ, Wu Y, Ni YJ, Liu JH, Gong M, Wang XH, Wei F, Wang TZ, Yuan Z, Ma AQ, et al. Isoproterenol instigates cardiomyocyte apoptosis and heart failure via AMPK inactivation-mediated endoplasmic reticulum stress. *Apoptosis.* 2013;18(7):800–810.
26. Yeh CH, Chen TP, Wang YC, Lin YM, Fang SW. AMP-activated protein kinase activation during cardioplegia-induced hypoxia/reoxygenation injury attenuates cardiomyocytic apoptosis via reduction of endoplasmic reticulum stress. *Mediat Inflamm.* 2010; 2010:130636.
27. Dong HW, Zhang LF, Bao SL. AMPK regulates energy metabolism through the SIRT1 signaling pathway to improve myocardial hypertrophy. *Eur Rev Med Pharmacol Sci.* 2018 May;22(9):2757-2766.
28. Ahmadian M, Suh JM, Hah N, Liddle C, Atkins AR, Downes M, Evans RM (May 2013). "PPAR $\gamma$  signaling and metabolism: the good, the bad and the future". *Nature Medicine.* 19 (5): 557–66.
29. Sawamura T, Kume N, Aoyama T, Moriwaki H, Hoshikawa H, Aiba Y, et al. An endothelial receptor for oxidized low-density lipoprotein. *Nature* 1997; 386:73–7
30. Villa M, Cerda-Opazo P, Jimenez-Gallegos D, Garrido-Moreno V, Chiong M, Quest AF, et al. Pro-fibrotic effect of oxidized LDL in cardiac myofibroblasts. *Biochem Biophys Res Commun* 2020; 524:696–701.
31. Lee JY, Chung J, Kim KH, An SH, Kim M, Park J, et al. Fluid shear stress regulates the expression of Lectin-like oxidized low density lipoprotein receptor-1 via KLF2-AP-1 pathway depending on its intensity and pattern in endothelial cells. *Atherosclerosis* 2018; 270:76–88.
32. Zendaoui A., Lachance D., Roussel E., Couet J., Arsenault M. Effects of spironolactone treatment on an experimental model of chronic aortic valve regurgitation. *J. Heart Valve Dis.* 2012; 21:478–486.
33. Kuhn H., O'Donnell V.B. Inflammation and immune regulation by 12/15-lipoxygenases. *Prog. Lipid Res.* 2006; 45:334–356.
34. Sawamura T., Kume N., Aoyama T., Moriwaki H., Hoshikawa H., Aiba Y., Tanaka T., Miwa S., Katsura Y., Kita T., et al. An endothelial receptor for oxidized low-density lipoprotein. *Nature.* 1997;386:73–77.
35. Kuhn H., O'Donnell V.B. Inflammation and immune regulation by 12/15-lipoxygenases. *Prog. Lipid Res.* 2006;45:334–356.

36. Kayama Y., Minamino T., Toko H., Sakamoto M., Shimizu I., Takahashi H., Okada S., Tateno K., Moriya J., Yokoyama M., et al. Cardiac 12/15 lipoxygenase-induced inflammation is involved in heart failure. *J. Exp. Med.* 2009;206:1565–1574.
37. Takaya T., Wada H., Morimoto T., Sunagawa Y., Kawamura T., Takanabe-Mori R., Shimatsu A., Fujita Y., Sato Y., Fujita M., et al. Left Ventricular Expression of Lectin-Like Oxidized Low-Density Lipoprotein Receptor-1 in Failing Rat Hearts. *Circ. J.* 2010;74:723–729.
38. Nusier M, Shah AK, Dhalla NS. Structure-function relationships and modifications of cardiac sarcoplasmic reticulum Ca<sup>2+</sup>-transport. *Physiol Res.* 2021 Dec 30;70(Suppl4):S443-S470.
39. Louch WE, Hougen K, Mork HK, Swift F, Aronsen JM, Sjaastad I, ReimS HM, Roald B, Andersson KB, Christensen G, Sejersted OM. Sodium accumulation promotes diastolic dysfunction in end-stage heart failure following SERCA2 knockout. *J Physiol.* 2010;588:465–478.
40. Feldman AM, Weinberg EO, Ray PE, Lorell BH. Selective changes in cardiac gene expression during compensated hypertrophy and the transition to cardiac decompensation in rats with chronic aortic banding. *Circ Res.* 1993 Jul;73(1):184-92.
41. Nediani C, Formigli L, Perna AM, Ibba-Manneschi L, Zecchi-Orlandini S, Fiorillo C, Ponziani V, Cecchi C, Liguori P, Fratini G, Nassi P. Early changes induced in the left ventricle by pressure overload. An experimental study on swine heart. *J Mol Cell Cardiol.* 2000 Jan;32(1):131-42
42. Goyal J, Smith KM, Cowan JM, Wazer DE, Lee SW, Band V. The role for NES1 serine protease as a novel tumor suppressor. *Cancer Research.* 1998;58:4782–4786.
43. Zhang Y, Song H, Miao Y, Wang R, Chen L. Frequent transcriptional inactivation of Kallikrein 10 gene by CpG island hypermethylation in non-small cell lung cancer. *Cancer Science.* 2010;101:934–940.
44. Wei CC, Chen Y, Powell LC, Zheng J, Shi K, Bradley WE, Powell PC, Ahmad S, Ferrario CM, Dell'Italia LJ. Cardiac kallikrein-kinin system is upregulated in chronic volume overload and mediates an inflammatory induced collagen loss. *PLoS One.* 2012;7(6):e40110.
45. Beaumont C, Walsh-Wilkinson É, Drolet MC, Roussel É, Melançon N, Fortier É, Harpin G, Beaudoin J, Arsénault M, Couet J. Testosterone deficiency reduces cardiac hypertrophy in a rat model of severe volume overload. *Physiol Rep.* 2019 May;7(9):e14088.



## Figure legends

Fig. 1 Myocardial left ventricular relative expression of genes implicated in (A) apoptosis (Bax, Bcl2) and (B) oxidative stress (Gpx, Sod1, Sod2) processes seven days after placebo infusion in rats with AR (AR; n=10; black bars) versus placebo (n=8; grey bars) infusion. Values are presented as mean  $\pm$  SD; \*0.01 < p < 0.05, \*\*0.001 < p < 0.01, \*\*\* p < 0.001.

Fig. 2 Myocardial left ventricular relative expression of genes implicated in cardiac metabolism including (A) cellular energy sensors such as Ampk, Ppar alpha, and Ppar gamma; (B) glucose transporters Glut1 and Glut4; (C) fatty acid metabolism regulators such as Cd36, Lox-1, and Alox-15, seven days after placebo infusion in rats with AR (AR; n=10; black bars) versus placebo (n=8; grey bars) infusion. Values are presented as mean  $\pm$  SD; \*\*0.001 < p < 0.01.

Fig. 3 Myocardial left ventricular relative expression of genes controlling myocardial contractility including (A) cardiac actors of kallikrein (klk8,klk10) - bradykinin (Bdkrb1 and Bdkrb2) system and (B) Ca<sup>2+</sup>-dependent excitation-contraction Serca2a, Ryr2, Cacna1c seven days after placebo infusion in rats with AR (OM; n=10; black bars) versus placebo (n=8; grey bars) infusion. Values are presented as mean  $\pm$  SD; \*0.01 < p < 0.05, \*\*0.001 < p < 0.01, \*\*\*p < 0.001.

Table 1. Primers used for real-time quantitative polymerase chain reaction (RTq-PCR) in rat left ventricular (LV) myocardial tissue.

Genes		Primer Sequences
<b>Glycerol-3-phosphate dehydrogenase (<i>GAPDH</i>)</b>	<i>Sense</i>	5' – AAGATGGTGAAGGTCGGTGT – 3'
	<i>Antisense</i>	5' – ATGAAGGGGTCGTTGATGG – 3'
<b>Hypoxanthine guanine phosphoribosyl transferase (<i>HPRT</i>)</b>	<i>Sense</i>	5' – ACAGGCCAGACTTTGTTGGA – 3'
	<i>Antisense</i>	5' – ATCCACTTTCGCTGATGACAC – 3'
<b>AMP-activated protein kinase (<i>Ampk</i>)</b>	<i>Sense</i>	5' – TTCGGGAAAGTGAAGGTGGG – 3'
	<i>Antisense</i>	5' – TCTCTGCGGATTTTCCCGAC – 3'
<b>Arachidonate 15-lipoxygenase (<i>Alox15</i>)</b>	<i>Sense</i>	5' - GCACTCTCCGTCCATCTTG - 3'
	<i>Antisense</i>	5' - GCTTCTCCATTGTTGCTTCCCT - 3'
<b>ATPase sarcoplasmic/endoplasmic reticulum Ca<sup>2+</sup> transporting 2 (<i>Atp2a2</i> or <i>Serca2</i>)</b>	<i>Sense</i>	5' – GCAGGTCAAGAAGCTCAAGG – 3'
	<i>Antisense</i>	5' – TCTCTGCGGATTTTCCCGAC – 3'
<b>Bcl2 associated X apoptosis regulator (<i>Bax</i>)</b>	<i>Sense</i>	5' - CGTGGTTGCCCTCTTCTACT - 3'
	<i>Antisense</i>	5' - TCACGGAGGAAGTCCAGTGT - 3'
<b>B-cell lymphoma 2 (<i>Bcl2</i>)</b>	<i>Sense</i>	5' - TTTCTCCTGGCTGTCTCTGAA - 3'
	<i>Antisense</i>	5' - CATATTTGTTTGGGGCAGGT - 3'
<b>Bradykinin receptor B1 (<i>Bdkrb1</i>)</b>	<i>Sense</i>	5' -AAGCTACGTGCCTGCTCATC - 3'
	<i>Antisense</i>	5' - CGGGGACGACTTTAACAGAG - 3'
<b>Bradykinin receptor B2 (<i>Bdkrb2</i>)</b>	<i>Sense</i>	5' - GCTGTCGTGGAAGTGGCTAT - 3'
	<i>Antisense</i>	5' - AAGGTCCCCTTATGAGCAGA - 3'
<b>Ca<sup>2+</sup> voltage-gated channel subunit alpha1 C (<i>Cacna1c</i>)</b>	<i>Sense</i>	5' – CCTATTTCCGTGACCTGTGG – 3'
	<i>Antisense</i>	5' – GGAGGGACTTGATGGTGTG – 3'
<b>CD36 fatty acid transporter (<i>Cd36</i>)</b>	<i>Sense</i>	5' - TTTCTGCTTCTCATCGCCG - 3'
	<i>Antisense</i>	5' - GGATGTGGAACCCATAACTGG - 3'
<b>Glutathione peroxidase (<i>Gpx</i>)</b>	<i>Sense</i>	5' - CCGACCCCAAGTACATCATT - 3'
	<i>Antisense</i>	5' - AACACCGTCTGGACCTACCA - 3'
<b>Kallikrein-related-peptidase 8 (<i>Klk8</i>)</b>	<i>Sense</i>	5' -CGGAGACAGATGGGTCTCTAA - 3'
	<i>Antisense</i>	5' - ATCTCTTGCTCGGGCTCAT - 3'
<b>Kallikrein-related-peptidase 10 (<i>Klk10</i>)</b>	<i>Sense</i>	5' - GCAGGTCTCCCTCTTCCATA - 3'
	<i>Antisense</i>	5' - CAGTGGCTTATTTCTCCAGCA - 3'
<b>Oxidized low density lipoprotein receptor 1 (<i>Olr1</i> or <i>Lox1</i>)</b>	<i>Sense</i>	5' -CATTACCTCCCCATTTT - 3'
	<i>Antisense</i>	5' - GTAAAGAAACGCCCTGGT - 3'
<b>Peroxisome proliferator-activated receptor alpha (<i>Ppar alpha</i>)</b>	<i>Sense</i>	5' – TTAGAGGCGAGCCAAGACTG – 3'
	<i>Antisense</i>	5' – CAGAGCACCAATCTGTGATGA – 3'
<b>Peroxisome proliferator-activated receptor gamma (<i>Ppar gamma</i>)</b>	<i>Sense</i>	5' – GCGCTAAATTCATCTTAACTC – 3'
	<i>Antisense</i>	5' – CTGTGTCAACCATGGTAATTT – 3'
<b>Ryanodine receptor 2 (<i>Ryr2</i>)</b>	<i>Sense</i>	5' – GGAAGTACGGAGGAAAGTG – 3'
	<i>Antisense</i>	5' – GAGACCAGCATTGGGTTGT – 3'
<b>Solute carrier family 2 member 1 (<i>Slc2a1</i> or <i>Glut1</i>)</b>	<i>Sense</i>	5' - TCTTCGAGAAGGCAGGTGTG - 3'
	<i>Antisense</i>	5' - TCCACGACGAACAGCGAC - 3'
<b>Solute carrier family 2 member 4 (<i>Slc2a4</i> or <i>Glut4</i>)</b>	<i>Sense</i>	5' - AGGCCGGGACACTATACCC - 3'

	<i>Antisense</i>	5' - TCCCCATCTTCAGAGCCGAT -5'
<b>Superoxide dismutase 1 (<i>Sod1</i>)</b>	<i>Sense</i>	5' - GGTCCACGAGAAACAAGATGA - 3'
	<i>Antisense</i>	5' - CAATCACACCACAAGCCAAG - 3'
<b>Superoxide dismutase 2 (<i>Sod2</i>)</b>	<i>Sense</i>	5' -AAGGAGCAAGGTCGCTTACA - 3'
	<i>Antisense</i>	5' - ACACATCAATCCCCAGCAGT - 3'

Table 2 Hemodynamic effects of aortic regurgitation (AR) induced in rats at baseline, 2 months after induction of AR (pre-infusion), and following infusion of placebo (0.9% NaCl)<sup>1</sup>

Parameters	Placebo (n=10)		
	Base	2 Months	2Months+placabo
FR, %	42 ± 2	33 ± 1 *	44 ± 4 ###
FE, %	76 ± 3	65 ± 4 **	70 ± 3
SIVs, mm	3.03 ± 0.18	2.85 ± 0.22	3.20 ± 0.25
SIVd, mm	2.20 ± 0.18	2.38 ± 0.24 \$	2.42 ± 0.15 \$
LVESD, mm	4.6 ± 0.2	7.2 ± 0.3 \$\$***	4.7 ± 0.4 ###
LVEDD, mm	7.9 ± 0.2	10.7 ± 0.3 \$***	8.5 ± 0.2 ###
FC, BPM	315 ± 19	301 ± 15	313 ± 13
LVOT, mm	2.41 ± 0.06	2.82 ± 0.06 ***	2.85 ± 0.05 ***
PVGs, mm	3.00 ± 0.14	2.89 ± 0.24	3.45 ± 0.19 \$*#
PVGd, mm	1.88 ± 0.17	1.76 ± 0.15	2.35 ± 0.16
PEP, ms	28 ± 2	31 ± 3	34 ± 3 \$\$**
LVET, ms	81 ± 1	87 ± 3	88 ± 4
ST, ms	109 ± 3	119 ± 4	122 ± 6
DT, ms	88 ± 9	85 ± 8	72 ± 5 \$
RR, ms	197 ± 11	202 ± 9	194 ± 8
PEP/LVET	0.34 ± 0.02	0.36 ± 0.03	0.38 ± 0.03 ##
ST/RR	0.58 ± 0.04 \$	0.59 ± 0.02 \$\$	0.63 ± 0.02 \$\$
ARPhT, ms		92 ± 7	123 ± 15 #
SV, ml	0.30 ± 0.02	0.51 ± 0.04 \$\$***	0.47 ± 0.03 ***
CO, ml/min	96 ± 8	153 ± 12 \$***	145 ± 8 ***
LVOT VTI, mm	66 ± 4	81 ± 3	74 ± 4
TA Sys Pré, mmHg	119 ± 2	115 ± 2	135 ± 4 **###
TA Dia Pré, mmHg	82 ± 1	59 ± 3 \$\$\$***	69 ± 4 \$*#
TA Sys Post, mmHg	106 ± 3		
TA Dia Post, mmHg	63 ± 3		
Poids, g	502 ± 27	577 ± 24 ***	
LV Mass	1094 ± 140	1750 ± 209 \$***	1453 ± 122 #
Laplace s	46 ± 4	76 ± 7 **	53 ± 6 #
Laplace d	77 ± 6 \$	73 ± 9 \$\$	65 ± 8 \$
σmax	224 ± 18 \$	282 ± 29 *	248 ± 20
Sigma Es	60 ± 5 \$	104 ± 11 **	73 ± 10 #
RWT	0.49 ± 0.05	0.33 ± 0.03 **	0.56 ± 0.05 ##

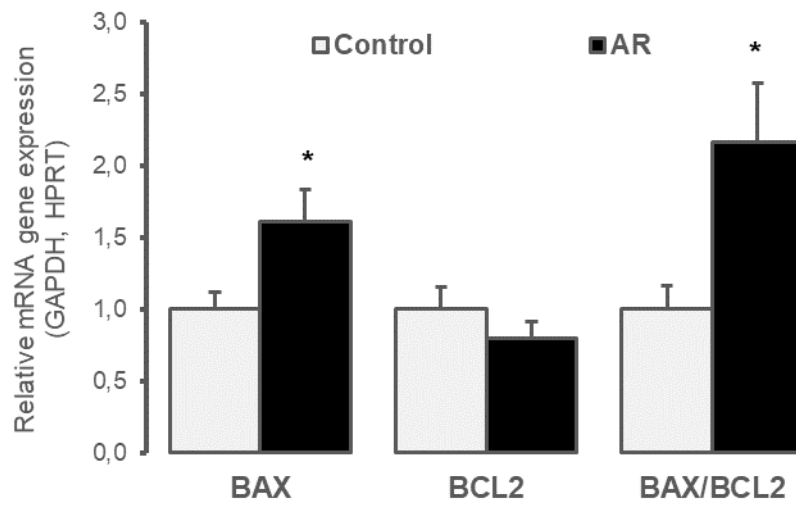
<sup>1</sup>Values are expressed as mean ± SD. \*p < 0.05; \*\*p < 0.01; \*\*\*p < 0.001 (or other symbols; two-way ANOVA). Comparisons: \* = within a group compared with baseline; \$ = compared with sham-operated rats at the same time point.

<sup>2</sup>FS, fractional shortening; EF, ejection fraction; SWTs, septal wall thickness in systole; SWTd, septal wall thickness in diastole; LVESD, left ventricle end-systolic diameter; LVEDD, left ventricle end-diastolic diameter; HR, heart rate; LVOT, left ventricle outflow tract diameter; PWTs, posterior wall thickness in systole; PWTd, posterior wall thickness in

diastole; PEP, pre-ejection period; LVET, left ventricle ejection time; ST, systolic time; DT, diastolic time; RR, interval between successive R; ARPht, aortic regurgitation pressure half-time; SV, stroke volume; CO, cardiac output; VTI, velocity-time integral; BP, blood pressure;  $\sigma_d$ , diastolic wall stress;  $\sigma$ , max wall stress;  $\sigma_{Es}$ , end-systolic wall stress; RWT, relative wall thickness.

**Figure 1**

**A.**



**B.**

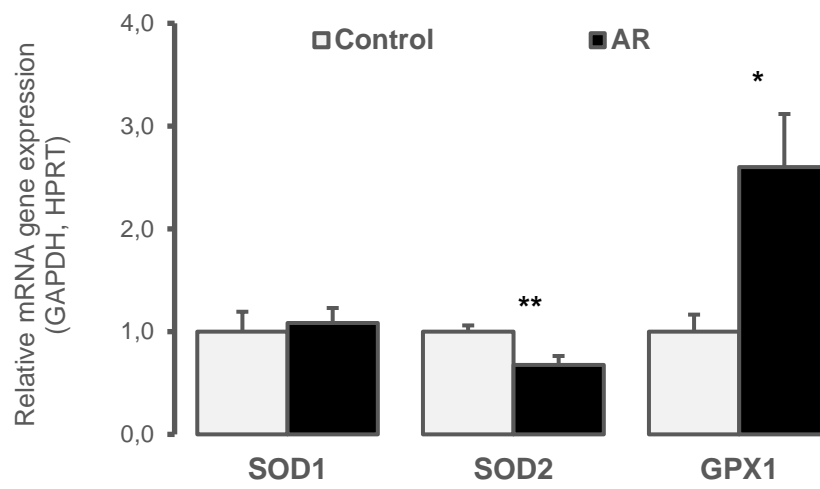
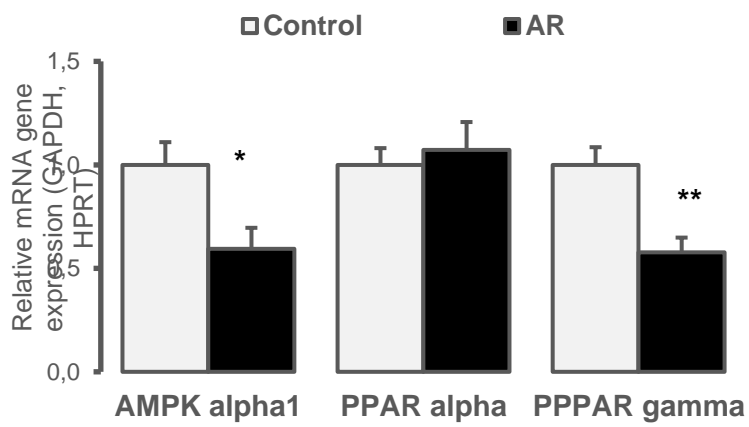
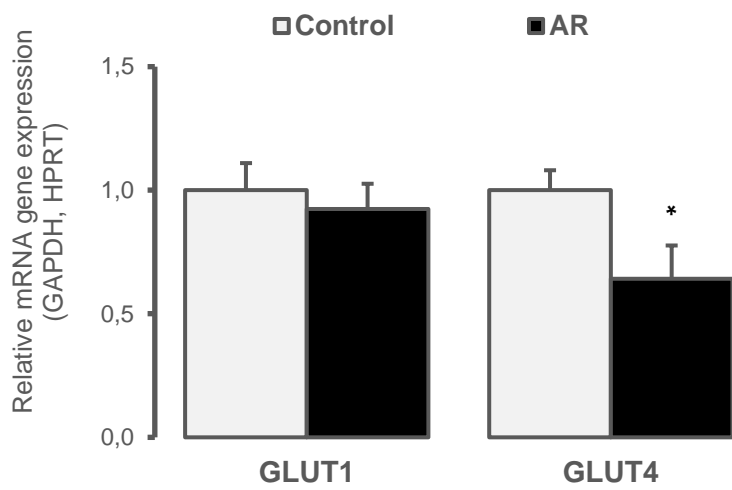


**Figure 2**

**A.**



**B.**



**C.**

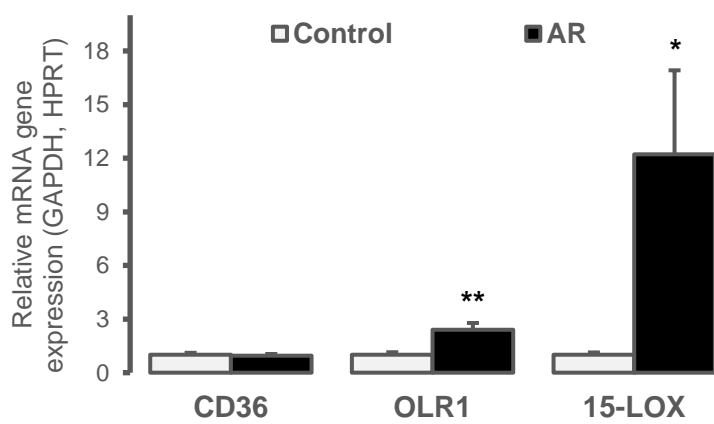
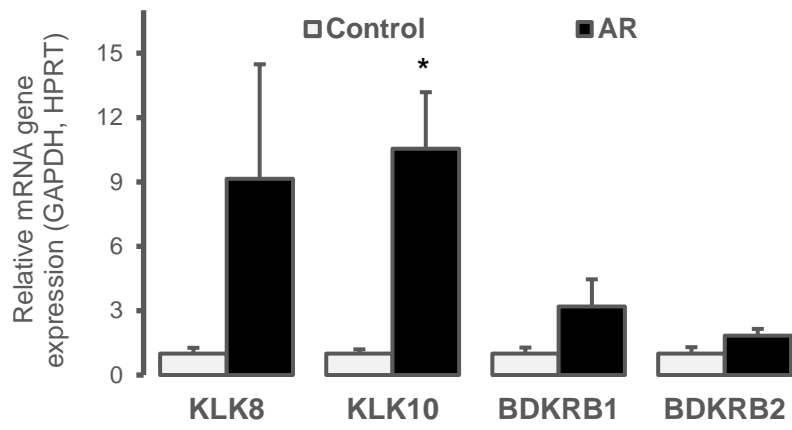
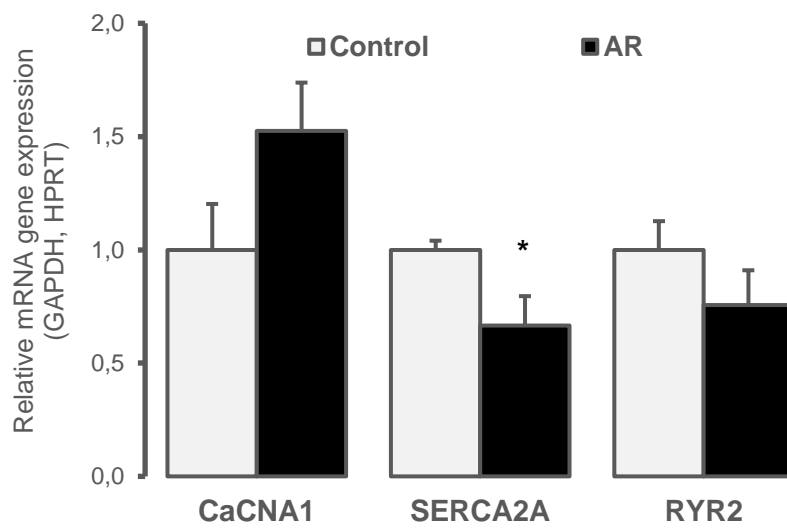


**Figure 3**

**A.**



**B.**





## LIST of PUBLICATIONS

**El Oumeiri B**, Dewachter L, Van de Borne P, Hubesch G, Jespers P, Stefanidis C, Mc Entee K, Vanden Eynden F. Gene profiling of left ventricle in experimental model of combined volume and pressure overload in rats (Submitted manuscripts)

**El Oumeiri B**, Dewachter L, Van de Borne P, Hubesch G, Melot C, Jespers P, Stefanidis C, Mc Entee K, Vanden Eynden F. Altered Left Ventricular Rat Gene Expression Induced by the Myosin Activator Omecamtiv Mecarbil. *Genes (Basel)*. 2023 Jan 1;14(1):122.

**El Oumeiri B**, van de Borne P, Hubesch G, Jespers P, Dewachter L, Stefanidis C, Mc Entee K, Vanden Eynden F. Detection of soluble suppression of tumorigenicity 2 and N-terminal B-type natriuretic peptide in a rat model of aortic regurgitation: differential responses to omecamtiv mecarbil. *J Basic Clin Physiol Pharmacol*. 2022 Oct 10;33(6):743-750.

**El Oumeiri B**, van de Borne P, Hubesch G, Herpain A, Annoni F, Jespers P, Stefanidis C, Mc Entee K, Vanden Eynden F. The myosin activator omecamtiv mecarbil improves wall stress in a rat model of chronic aortic regurgitation. *Physiol Rep*. 2021 Aug;9(16): e14988.

C. Stefanidis, E Engelman, M El Mourad, A Roussoulières, J Vachiery, **B El Oumeiri**, M Chirade, F Vanden Eynden. Pharmacological Treatment of Pump-Related Thrombosis in Patients with Left Ventricular Assist Device (HeartWare HVAD). *The Journal of Heart and Lung Transplantation* 39 (4), S393-S394.

Coeckelenbergh S, Valente F, Mortier J, Engelman E, Roussoulières A, **El Oumeiri B**, Antoine M, Van Obbergh L, Taccone FS, Vanden Eynden F, Stefanidis C. Long-Term Outcome After Venoarterial Extracorporeal Membrane Oxygenation as Bridge to Left Ventricular Assist Device Preceding Heart Transplantation. *J Cardiothorac Vasc Anesth*. 2022 Jun;36(6):1694-1702

Vanden Eynden F, **El Oumeiri B**, Bové T, Van Nooten G, Segers P Proximal pressure reducing effect of wave reflection in the pulmonary circulation disappear in obstructive disease: insight from a rabbit model. *Am J Physiol Heart Circ Physiol*. 2019 May 1;316(5):H992-H1004.

Vanden Eynden F, Segers P, Bové T, De Somer F, **El Oumeiri B**, Van Nooten G. Use of a right ventricular continuous flow pump to validate the distensible model of the pulmonary vasculature. *Physiol Res*. 2019 Apr 30;68(2):233-243.

**El Oumeiri B**, Mc Entee K, Annoni F, Herpain A, Vanden Eynden F, Jespers P, Van Nooten G, van de Borne P. Effects of the cardiac myosin activator Omecamtiv-mecarbil on severe chronic aortic regurgitation in Wistar rats. *BMC Cardiovasc Disord*. 2018 May 21;18(1):99.

Nguyen T, Antoine M, Vanden Eynden F, Van Nooten G, **El Oumeiri B**. A bullet through the aortic arch. *Acta Cardiol*. 2018 Jun;73(3):303-304.

Vanden Eynden F, Bol Alima M, Racape J, **El Oumeiri B**, Vachiéry JL, Van Nooten G. Composite indices of upstream pulmonary vascular impedance and capacitance do not help in

identifying patients who should undergo pulmonary endarterectomy in chronic thromboembolic pulmonary hypertension. *Acta Cardiol.* 2016 Jun;71(3):281-90.

Hougardy JM, Revercez P, Pourcelet A, EL **Oumeiri B**, Racapé J, Le Moine A, Vanden Eynden F, De Backer D. Chronic kidney disease as major determinant of the renal risk related to on-pump cardiac surgery: a single-center cohort study. *Acta Chir Belg.* 2016 Aug;116(4):217-224.

Vanden Eynden F, Antoine M, **El Oumeiri B**, Chirade ML, Vachiéry JL, Van Nooten G. How to cope with a temporarily aborted transplant program: solutions for a prolonged waiting period. *Ann Transl Med.* 2015 Nov;3(20):306.

**EL Oumeiri B**, Vanden Eynden F, Van Nooten G. Unusual 30-year durability of Hancock II porcine bioprosthesis in tricuspid position. *Int J Surg Case Rep.* 2015;8C:158-60.

**EL Oumeiri B**, Vanden Eynden F, Stefanidis C, Antoine M, Nooten GV. Gonococcal ascending aortic aneurysm with penetrating ulcer and bovine arch. *Asian Cardiovasc Thorac Ann.* 2015 Sep;23(7):861-3.

**El Oumeiri B**, Vanden Eynden F, Van Nooten G. The modified maze procedure as concomitant surgery: the impact of left atrial size. *Interact Cardiovasc Thorac Surg.* 2013 Feb;16(2):156.

**El-Oumeiri B**, Louagie Y, Buche M. Reoperation for ascending aorta false aneurysm using deep hypothermia and circulatory arrest. *Interact Cardio Vasc Thoracic Surgery.* 2011 Apr;12(4):605-8.

Mathieu M, **El Oumeiri B**, Touihri K, Hadad I, Mahmoudabady M, Bartunek J, Heyndrickx G, Brimiouille S, Naeije R, Mc Entee K. Left ventricular-arterial uncoupling in Heart failure with preserved ejection fraction after myocardial infarction in dogs-invasive versus echocardiographic evaluation. *BMC Cardiovasc Disord.* 2010 Jun 29;10(1):32.

**El Oumeiri B**, Glineur D, Boodhwani M, Etienne PY, Poncelet A, De Kerchove L, Papadatos S, Noirhomme P, El Khoury G. Recycling of Internal Thoracic Arteries in Reoperative Coronary Surgery: In Hospital and Long Term Results *Ann Thorac Surg* 2011 Apr;91(4):1165-8.

Ramadan A, Stefanidis C, N'Gatchou W, **El Oumeiri B**, Jansens JL, De Smet JM, Antoine A, De Canniere D. Five years follow-up after Y-graft arterial revascularization: on pump versus off pump; prospective clinical trial. *Interact CardioVasc Thorac Surg* 2010 ;10 :423-427.

Mathieu M, Bartunek J, **El Oumeiri B**, Touihri K, Hadad I, Thoma P, Metens T, Mendes da Costa A, Mahmoudabady M, Egrise D, Blocklet D, Mazouz N, Naeije R, Heyndrickx G, Mc Entee K. Cell therapy with autologous bone-marrow mononuclear stem cells is associated with superior cardiac recovery as compared to non-modified mesenchymal stem cells in the canine model of chronic myocardial infarction. *J Thorac Cardiovasc Surg.* 2009 Sep;138(3):646-53.

**El Oumeiri B**, Boodhwani M, Glineur D, De kherchove L, Poncelet A, Astarci P, Lacroix V, Verhelst R, Rubay J, Noirhomme P, El khoury G .Extending the Scope of Mitral Valve Repair in Rheumatic Disease. *Ann Thorac Surg*. 2009 Jun;87(6):1735-40.

**El Oumeiri B**, Poncelet A, El Khoury Why freedom from atrial fibrillation is still lower with endoscopic pulmonary vein isolation than the Cox-Maze III procedure? *J Thorac Cardiovasc Surg*. 2009 Apr;137(4):1036.

**El Oumeiri B**, Lacroix V, Astarci P. Bilateral atrial appendage excision should be performed routinely in the surgical treatment of atrial fibrillation. *Interact Cardiovasc Thorac Surg*. 2008 Apr;7(2):205-6.

**El Oumeiri B**. The possible reasons of limited rate freedom from atrial fibrillation after thoracoscopic microwave. *Interact Cardiovasc Thorac Surg*. 2007 Dec;6(6):698-9.

**El Oumeiri B**, Casselman F, Vanermen H. Video-assisted left ventricle mass removal Eur J Cardiothorac Surg. 2007 Aug;32(2):383.

**El Oumeiri B**, Casselman F, Geelen P, Wellens F, Degrieck I, Van Praet F, Camu G, Vanermen H. Surgical Treatment of Atrial Fibrillation (Review). *Minerva Cardioangiol*. 2007 Jun;55(3):369-78.

**El Oumeiri B**, Stefanidis C, Sabry A, Antoine M, De met JM, De Canniere D, Jansens JL. Long-term follow-up after endocardial radiofrequency modified Nitta procedure for concomitant atrial fibrillation treatment. *Interact CardioVasc Thorac Surg* 2007; 6:319-322

**El Oumeiri B**, Jansens JL. Surgical repair of residual shunt after transcatheter closure of secundum atrial septal defect with an amplatzer septal occluder: a case report. *Acta Chir Belg*, 2006; 106: 86-88.

**El Oumeiri B**, Lipski A, De Smet JM. Off-pump treatment of coronary artery perforation after percutaneous intervention with pericardial patch. *Int Cardiovasc Thorac Surg*, 2005;4: 509-510.